frontiers | Research Topics

Beyond traditional culture: New approaches for a rapid detection and identification of microorganisms and their antimicrobial resistance

Edited by
Elena Jordana-Lluch, Nicasio Mancini, John W. A. Rossen and Onya Opota

Published in
Frontiers in Cellular and Infection Microbiology

ISSN 1664-8714
ISBN 978-2-83251-763-5
DOI 10.3389/978-2-83251-763-5

About Frontiers

Frontiers is more than just an open access publisher of scholarly articles: it is a pioneering approach to the world of academia, radically improving the way scholarly research is managed. The grand vision of Frontiers is a world where all people have an equal opportunity to seek, share and generate knowledge. Frontiers provides immediate and permanent online open access to all its publications, but this alone is not enough to realize our grand goals.

Frontiers journal series

The Frontiers journal series is a multi-tier and interdisciplinary set of open-access, online journals, promising a paradigm shift from the current review, selection and dissemination processes in academic publishing. All Frontiers journals are driven by researchers for researchers; therefore, they constitute a service to the scholarly community. At the same time, the *Frontiers journal series* operates on a revolutionary invention, the tiered publishing system, initially addressing specific communities of scholars, and gradually climbing up to broader public understanding, thus serving the interests of the lay society, too.

Dedication to quality

Each Frontiers article is a landmark of the highest quality, thanks to genuinely collaborative interactions between authors and review editors, who include some of the world's best academicians. Research must be certified by peers before entering a stream of knowledge that may eventually reach the public - and shape society; therefore, Frontiers only applies the most rigorous and unbiased reviews. Frontiers revolutionizes research publishing by freely delivering the most outstanding research, evaluated with no bias from both the academic and social point of view. By applying the most advanced information technologies, Frontiers is catapulting scholarly publishing into a new generation.

What are Frontiers Research Topics?

Frontiers Research Topics are very popular trademarks of the *Frontiers journals series*: they are collections of at least ten articles, all centered on a particular subject. With their unique mix of varied contributions from Original Research to Review Articles, Frontiers Research Topics unify the most influential researchers, the latest key findings and historical advances in a hot research area.

Find out more on how to host your own Frontiers Research Topic or contribute to one as an author by contacting the Frontiers editorial office: frontiersin.org/about/contact

Beyond traditional culture: New approaches for a rapid detection and identification of microorganisms and their antimicrobial resistance

Topic editors

Elena Jordana-Lluch — Balearic Islands Health Research Institute (IdISBa), Spain
Nicasio Mancini — Vita-Salute San Raffaele University, Italy
John W. A. Rossen — IDbyDNA Inc, United States
Onya Opota — Université de Lausanne, Switzerland

Citation

Jordana-Lluch, E., Mancini, N., Rossen, J. W. A., Opota, O., eds. (2023). *Beyond traditional culture: New approaches for a rapid detection and identification of microorganisms and their antimicrobial resistance*. Lausanne: Frontiers Media SA. doi: 10.3389/978-2-83251-763-5

Table of contents

frontiers in Cellular and Infection Microbiology

ORIGINAL RESEARCH
published: 02 December 2021
doi: 10.3389/fcimb.2021.772966

Rapid Detection of *bla*$_{KPC}$, *bla*$_{NDM}$, *bla*$_{OXA-48-like}$ and *bla*$_{IMP}$ Carbapenemases in *Enterobacterales* Using Recombinase Polymerase Amplification Combined With Lateral Flow Strip

Fang Wang[1†], *Lei Wang*[1,2†], *Huimin Chen*[1], *Na Li*[1], *Yan Wang*[1*], *Yan Li*[1*] *and Wei Liang*[1*]

[1] Department of Central Laboratory, The Second People's Hospital of Lianyungang City (Cancer Hospital of Lianyungang), Lianyungang, China, [2] School of Biotechnology, Jiangsu University of Science and Technology, Zhenjiang, China

OPEN ACCESS

Edited by:
John W. A. Rossen,
IDbyDNA Inc., United States

Reviewed by:
Fupin Hu,
Fudan University, China
Marina Oviaño,
A Coruña University Hospital Complex (CHUAC), Spain

***Correspondence:**
Yan Wang
wangyan1358@163.com
Yan Li
1325188199@qq.com
Wei Liang
hslwys@163.com

†These authors have contributed equally to this work and share first authorship

Specialty section:
This article was submitted to Clinical Microbiology, a section of the journal Frontiers in Cellular and Infection Microbiology

Received: 09 September 2021
Accepted: 15 November 2021
Published: 02 December 2021

Citation:
Wang F, Wang L, Chen H, Li N, Wang Y, Li Y and Liang W (2021) Rapid Detection of bla$_{KPC}$, bla$_{NDM}$, bla$_{OXA-48-like}$ and bla$_{IMP}$ Carbapenemases in Enterobacterales Using Recombinase Polymerase Amplification Combined With Lateral Flow Strip. Front. Cell. Infect. Microbiol. 11:772966. doi: 10.3389/fcimb.2021.772966

The emergence of carbapenemase-producing *Enterobacterales* (CPE) infections is a major global public health threat. Rapid and accurate detection of pathogenic bacteria is essential to optimize treatment and timely avoid further transmission of these bacteria. Here, we aimed to develop a rapid on site visualization detection method for CPE using improved recombinase polymerase amplification (RPA) combined with lateral flow strip (LFS) method, based on four most popular carbapenemase genes: *bla*$_{KPC}$, *bla*$_{NDM}$, *bla*$_{OXA-48-like}$, and *bla*$_{IMP}$. All available allelic variants of the above carbapenemases were downloaded from the β-lactamase database, and the conserved regions were used as targets for RPA assay. Five primer sets were designed targeting to each carbapenemase gene and the RPA amplification products were analyzed by agarose gel electrophoresis. FITC-labeled specific probes were selected, combined with the best performance primer set (Biotin-labeled on the reverse primer), and detected by RPA-LFS. Mismatches were made to exclude the false positive signals interference. This assay was evaluated in 207 clinically validated carbapenem-resistant *Enterobacterales* (CRE) isolates and made a comparison with conventional PCR. Results showed that the established RPA-LFS assay for CPE could be realized within 30 min at a constant temperature of 37°C and visually detected amplification products without the need for special equipment. This assay could specifically differentiate the four classes of carbapenemases without cross-reactivity and shared a minimum detection limit of 100 fg/reaction (for *bla*$_{KPC}$, *bla*$_{NDM}$, and *bla*$_{OXA-48-like}$) or 1000 fg/reaction (for *bla*$_{IMP}$), which is ten times more sensitive than PCR. Furthermore, the detection of 207 pre-validated clinically CRE strains using the RPA-LFS method resulted in 134 *bla*$_{KPC}$, 69 *bla*$_{NDM}$, 3 *bla*$_{OXA-48-like}$, and 1 *bla*$_{IMP}$. The results of the RPA-LFS

assay were in consistent with PCR, indicating that this method shared high sensitivity and specificity. Therefore, the RPA-LFS method for CPE may be a simple, specific, and sensitive method for the rapid diagnosis of carbapenemase *Enterobacterales*.

Keywords: Carbapenemase, *Enterobacterales*, recombinase polymerase amplification, rapid detection, false positive

INTRODUCTION

Enterobacterales are conditionally pathogenic bacteria that cause serious hospital-acquired infections (Feil, 2017). The spread of carbapenemase-producing *Enterobacterales* (CPE) has become a major global public health threat. Carbapenems have traditionally been used to treat infections caused by broad-spectrum beta-lactamase-producing *Escherichia coli* and *Klebsiella pneumoniae* and are still considered antibiotics to be used as a last resort (Nordmann et al., 2012; van Duin and Doi, 2017; Rochford et al., 2018; Lin et al., 2020). Carbapenemase-producing enzymes in these bacteria, which are capable of hydrolyzing all carbapenems, cephalosporins, and beta-lactams are the main cause of resistance to carbapenem antibiotics (Khan et al., 2017; Segagni Lusignani et al., 2020). Most carbapenemase genes are located on the metastable genetic elements, such as plasmids and integrons; thus, carbapenem resistance is easily transferred horizontally leading to rapid spread wordwide (Conlan et al., 2014; Bengtsson-Palme et al., 2018; Paveenkittiporn et al., 2021). Among these, *Klebsiella pneumoniae* carbapenemase (KPC), New Delhi metallo-β-lactamase (NDM), oxacillinase (OXA-48-like), and imipenemase (IMP) are the most prevalent carbapenemases in CPE (Han et al., 2020).

Rapid and accurate detection of carbapenemase genes is extremely important for preventing and monitoring infections and avoiding large-scale carbapenem-resistant bacterial infections outbreak. Currently, in clinical microbiology laboratories, the detection of carbapenemase-producing bacteria is primarily performed using phenotypic methods, such as Carba-NP test, combined disk test, and carbapenem inactivation method (Aguirre-Quiñonero and Martínez-Martínez, 2017; Nordmann et al., 2020; Tsai et al., 2020). These methods generally have disadvantages of a prolonged testing time, being complex to perform, and being prone to false negatives, whereby some clinical isolates only show low levels of resistance (Hansen, 2021). Rapid assays have been developed based on carbapenemases, including immunochromatographic NG-Test Carba5, RESIST-5 O.O.K.N.V., IMP K-SeT, MALDI-TOF, polymerase chain reaction (PCR), and quantitative PCR (Glupczynski et al., 2016; Foudraine et al., 2019; Vergara et al., 2020; Kanahashi et al., 2021). These methods reduce the detection time to a few minutes; however, they rely on sophisticated instrumentation and trained personnel, which limit widespread application, especially in source-limited area.

Recombinase polymerase amplification (RPA) was first proposed by Piepenburg et al. (Piepenburg et al., 2006) and uses recombinase activity to open the double strand of a DNA molecule and amplifies the DNA target using strand-displacing enzyme activity. Amplification can be completed within approximately 30–40 min at a temperature range of 37°C–42°C. The use of lateral flow strips (LFS) as endpoint visual readouts of the amplified DNA targets makes the method less device-dependent. The colored signal can be observed semi-quantitatively by the naked eye on the LFS using gold nanoparticles (AuNPs) that interact with the labeled isothermal amplification product (Wang et al., 2019; Xie et al., 2021). RPA-LFS has been successfully used for the molecular diagnosis of diseases caused by pathogenic bacteria, such as methicillin-resistant *Staphylococcus aureus*, *Mycobacterium tuberculosis* and *neo-cryptococcosis* (Yang et al., 2013; Law et al., 2018; Ma et al., 2019).

In this study, the false-positive signals from primer dimers were thoroughly eliminated by the introduction of specific probes and base substitutions with specific guidance in the primer and probe sequences. As a result, a rapid and accurate RPA-LFS method was established for the detection of four (bla_{KPC}, bla_{NDM}, $bla_{\mathrm{OXA\text{-}48\text{-}like}}$, and bla_{IMP}) important carbapenemase genes in clinical CPE of CRE strains. The assay could be completed within 30 min under 37°C isothermal condition. The rapid identification of carbapenemase genes from 207 pre-validated clinical CRE isolates demonstrated the high specificity and sensitivity of the method. Thus, a simple, specific, and sensitive assay was established to provide a technical reference for the rapid detection of clinical carbapenemases.

MATERIALS AND METHODS

Ethics Statement

This study was approved by the Medical Ethics Committee of the Second People's Hospital of Lianyungang City (Permit Number: 2020005). The clinical strains were collected from 2020 to 2021 and isolated from sputum, urine, drainage fluid, or secretion samples. All the isolate samples were obtained written consent, on an institutionally approved document, from every patient.

Source of the Strain

Four PCR-amplified and sequenced 'standard strains,' including bla_{KPC}, bla_{NDM}, $bla_{\mathrm{OXA\text{-}48\text{-}like}}$, and bla_{IMP} from *Klebsiella pneumoniae* were used to establish the RPA-LFS assay for carbapenemases. Seven other common pathogenic bacteria, including *Klebsiella pneumoniae*, *Escherichia coli*, *Pseudomonas aeruginosa*, *Acinetobacter baumannii*, *Streptococcus pneumoniae*, *Staphylococcus aureus*, and *Enterococcus faecalis* were used to validate the specificity of the RPA-LFS method. A total of 207 clinical strains with carbapenem resistance validated by the paper diffusion method were collected from 2020 to 2021 and verified that

no duplicate isolates were from the same patient. These clinical isolates, including *K. pneumoniae*, *Escherichia coli*, *Enterobacter cloacae*, *Citrobacter freundii*, and *Serratia marcescens*, were used to validate the practical application of the RPA-LFS technology for the rapid detection of carbapenemases in *Enterobacterales* (**Table 1**). All strains were collected from the microbiology laboratory of the Second People's Hospital of Lianyungang City and identified by MALDI-TOF mass spectrometer.

Genomic DNA Extraction

For reactions using purified genomic DNA as a template, genomic DNA was extracted using the Bacterial Genomic DNA Extraction Kit (Tiangen Biochemical Technology Co., Ltd., Beijing, China) and stored at −20°C for backup. If bacterial cultures were used as templates, bacterial DNA was extracted using the heated boiling method. The individual colonies were suspended in 50 μL Tris-EDTA buffers, boiled for 10 min, and centrifuged at 12000 × g for 10 min, after which the supernatant was used as the DNA template.

Design of Primers for RPA Reactions

For the primer design method, sequences of all the isoforms of bla_{KPC}, bla_{NDM}, $bla_{OXA\text{-}48\text{-}like}$ and bla_{IMP} genes were downloaded from GeneBank. Five pairs of primers for each carbapenemase gene detection were designed separately using Primer Premier 5.0 to capture all the variants based on the regions conserved among the isoforms. The primer design parameters were: size setting of 30–35, product size of 100–500 bp, GC content of 20%–80%, and Tm value setting of 50–100. Default settings were used for all other parameters. Five pairs of primers were selected for testing according to their scores from the highest to the lowest.

RPA Procedure

For the RPA experiments, we used the TwistAmp Liquid DNA Amplification Kit (TwistDx Inc., Maidenhead, United Kingdom). A total of 50 μL of the reaction system was added to the tubes in the following order: 25 μL 2 × reaction buffer, 5 μL 10 × base mix, 2.5 μL 20 × core mix, 2.1 μL upstream primer (10 μM) and 2.1 μL downstream primer (10 μM; General Biosystems Co., Ltd., Anhui, China), 9.8 μL ddH_2O, and 1 μL template. To ensure that all reaction systems reacted simultaneously, 2.5 μL of 280 mM magnesium acetate was added to the PCR tube caps, and the template and 280 mM magnesium acetate were added to the reaction system simultaneously using transient centrifugation. The reaction system was vortex-centrifuged and immediately incubated in a heater at 37°C for 30 min. No genomic DNA template reaction system was used as negative control. Each sample has two tubes of reaction, one for the sample itself and the other for the control. Amplification of primers was detected using 1.5% agarose gel electrophoresis.

RPA-LFS Probe Design

Primer Premier 5 software was used to design specific probes between forward and reverse primer targeting sequences, and the formation of dimers, hairpin structures, mismatches, etc. between the probe and the reverse primer should be theoretically avoided as much as possible. The design principles are: (1) The probe size is 46-51 bp, GC content is 20-80%, and Tm is 57-80°C; (2) The maximum hairpin score is 9, and the maximum primer-dimer score is set to 9. The maximum poly-X is set to 5, and other parameters are set to default values; (3) The 5' end of the probe is labeled with FITC, and the 3' end was blocked with SpC3, the base at the middle of the probe was replaced with tetrahydrofuran (THF), and there was at least 30 bp of base before the THF site, while at least 15 bp of base followed; (4) The 5' end of the reverse primer was labeled with biotin.

RPA-LFS Procedure

The RPA-LFS experiment was performed using the TwistAmp DNA Amplification nfo Kit (TwistDx Inc., Maidenhead, United Kingdom) in 50 μL of the reaction system. The following systems were added sequentially to the lyophilized powder tubes that contained the enzyme components: 29.5 μL rehydration buffer, 2.1 μL forward primer (10 μM), 2.1 μL reverse primer (10 μM), 0.6 μL probe (10 μM), 12.2 μL ddH_2O and 1 μL template. To ensure that all reaction systems began simultaneously, 2.5 μL of 280 mM magnesium acetate was added to the tube cap, transiently centrifuged, and immediately incubated in a

TABLE 1 | Information of bacteria strains used in this study.

Species	Strain amount	Source	Sample type	Carbapenase gene
K. pneumoniae	1	Sputum isolated strain	Reference Strain	bla_{KPC}
K. pneumoniae	1	Sputum isolated strain	Reference Strain	bla_{NDM}
K. pneumoniae	1	Sputum isolated strain	Reference Strain	bla_{IMP}
K. pneumoniae	1	Sputum isolated strain	Reference Strain	$bla_{OXA\text{-}48\text{-}like}$
K. pneumoniae	1	Sputum isolated strain	Reference Strain	/
E. coli	1	Sputum isolated strain	Reference Strain	/
P. aeruginosa	1	Sputum isolated strain	Reference Strain	/
A. baumannii	1	Sputum isolated strain	Reference Strain	/
S. pneumoniae	1	Sputum isolated strain	Reference Strain	/
S. aureus	1	Sputum isolated strain	Reference Strain	/
E. faecalis	1	Sputum isolated strain	Reference Strain	/
K. pneumoniae	159	Sputum, urine, drainage fluid	Validations Strain	131 bla_{KPC}, 24 bla_{NDM}, 3 $bla_{OXA\text{-}48\text{-}like}$, and 1 bla_{IMP}
E. coli	33	Urine, Sputum, drainage fluid	Validations Strain	33 bla_{NDM}
E. cloacae	8	Sputum, urine, secretion	Validations Strain	8 bla_{NDM}
C. freundii	5	Urine, drainage fluid	Validations Strain	1 bla_{KPC}, 4 bla_{NDM},
S. marcescens	2	Sputum	Validations Strain	2 bla_{KPC}

thermostatic heater at 37°C for 30 min. Then, 5 μL of amplification product was used for LFS (Ustar Biotechnologies Ltd., Hangzhou, China) visual detection within 3 min. There are two red lines displayed on the LFS, namely the control line (top) and the test line (bottom). The control line exists in every test to ensure the validity of the LFS, while the test line could only be observed for positive reactions. Each sample has two strips, one for the sample itself and the other for the control.

Examination of Clinical Specimens

To evaluate the detection compliance of the RPA-LFS method, parallel PCR experiments were carried out to calculate the compliance rates of the results of the two methods. A total of 207 pre-validated CRE clinical strains were collected and bacteria were treated using the heated boiling method. One microliter of the boiled resuspension was taken and used as a template for the RPA-LFS and PCR assays. The compliance rate was calculated as:{(number of positive samples for both methods + number of negative samples for both methods)/total number of samples} × 100%.

RESULTS

Design and Screening of Prime Sets for the RPA System

The bla_{KPC}, bla_{NDM}, $bla_{OXA\text{-}48\text{-}like}$, and bla_{IMP} genes were used as target sequences, and five pairs of primer sets were designed for each gene targeting to the highly conserved area (**Supplementary Table 1**). The genome DNA of four standard strains of *K. pneumoniae* were used as templates to verify the amplification of each of the five primer pairs. As shown in **Figure 1**, all designed primers amplified the target bands as expected. Primer pairs with brighter target bands, fewer primer-dimers, without non-specific amplification are of better choice. Therefore, bla_{KPC}-4, bla_{NDM}-1, $bla_{OXA\text{-}48\text{-}like}$-2 and bla_{IMP}-4 were selected for subsequent detection.

Adding Probes to the RPA-LFS Reaction

The use of probes in the RPA reaction increases the amplification specificity and reduces primer-dependent artifacts. Specific probes were designed within the targeting fragments of the four primer pairs that were screened for better performance (**Supplementary Table 1**). The amplification performance and false positives of the primer-probe-needle set were verified. The combination of the four primer-probe pairs provided correct positive signals (two visible red bands both on the test lines and control lines) when tested using RPA-LFS, which indicated that the four primer-probe pairs had good amplification performance. However, they also showed a visible weaken red band on the test line in the no template control, which indicated there are false-positive signals for all these five primer-probe combinations (**Figure 2**).

Elimination of False-Positive Signals Using Base Mismatches

RPA can tolerate some base mismatches between the primer/probe and template, which provides some flexibility in primer/

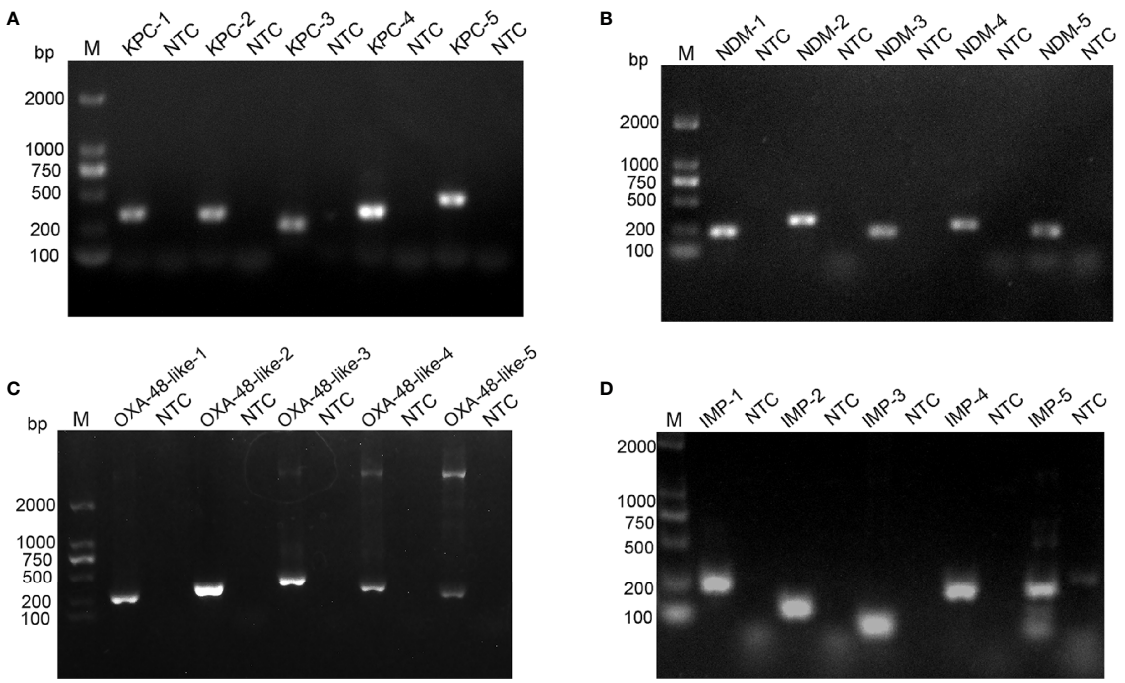

FIGURE 1 | Screening of optimal primer pairs using RPA amplification reactions. Agarose gel images show the amplification results of five primer pairs designed for bla_{KPC} **(A)**, bla_{NDM} **(B)**, $bla_{OXA\text{-}48\text{-}like}$ **(C)** and bla_{IMP} **(D)** genes. The name of each primer pair is above each lane: Lane M is DNA ladder. NTC lanes are template-free controls for the respective primer pairs. Band sizes of the DNA ladders are shown on the left.

probe design and screening (Daher et al., 2015). Analysis using the Primer Premier 5 software revealed that the probe had multiple consecutively matching bases to the reverse primer, which could result in a false-positive signal. Therefore, base substitutions were introduced to eliminate false-positive signals, and the principles of substitution were (1) Breaks were performed on sites with more than four contiguous matching bases or two or more contiguous matching bases at the 3 ' end; (2) no substitution of three bases near the 3' end; (3) no consecutive two-base substitutions; (4) substitution of preferably no more than three bases, otherwise, the sensitivity of the assay may be affected, and (5) A-G and T-C swaps were used preferentially. The sequences of the modified reverse primer (mR) and probe (mP) are listed in **Table 2**, and the replacement bases are indicated in red. Using this modified primer-probe device, false-positive signals were eliminated without affecting amplification performance (**Figure 3A**). The primer-probe sets were used for all subsequent RPA-LFS reactions. Meanwhile, analysis of the RPA amplification products using 1.5% agarose gel electrophoresis showed that the amplification products of bla_{KPC}, bla_{IMP}, and $bla_{OXA\text{-}48\text{-}like}$ primer-probe sets all showed two clear bands, which represented the amplification products of the forward-reverse and probe-reverse primers, respectively, whereas the two amplification products of bla_{NDM} were of similar size and, thus, could not be distinguished from each other, so they were shown as a single band (**Figure 3B**).

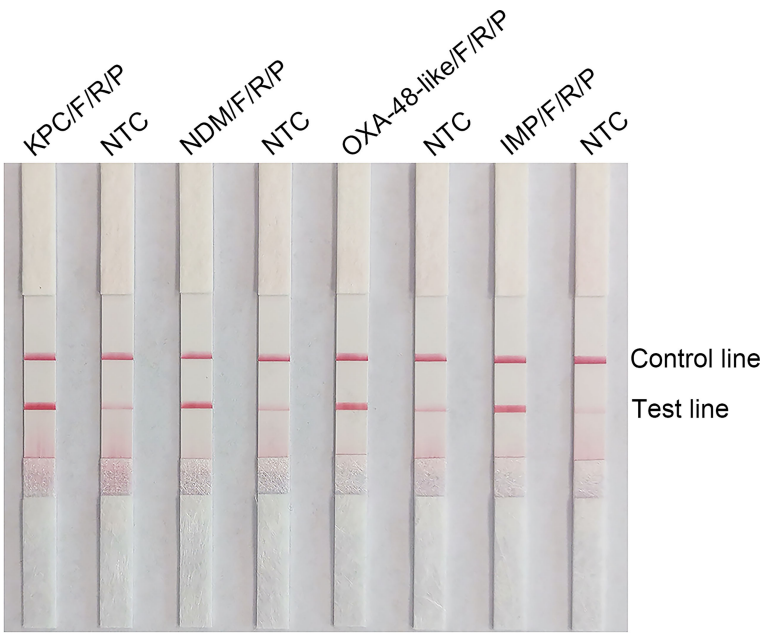

FIGURE 2 | Testing the performance of the primer-probe sets using the RPA-LFS reaction. Results of the LFS detection of the RPA amplification products are shown. The name of each primer-probe set is labeled above the corresponding strip. The NTC strip is the template-free control for the corresponding RPA reaction on the immediate left strip. The positions of the test and control lines are marked to the right of the bars. The image represents the results of three independent experiments.

TABLE 2 | Primer-probe sets after base substitution.

Name	Sequence (5'-3')	Length (bp)	Amplicon size (bp)
KPC-4-F	AACGCCGCCGCCAATTTGTTGCTGAAGGAG	30	269
KPC-4-mR	5'-Biotin-ATGCGGTGGTTGCCGGTCGTGTTTGCCTTT	30	
KPC-mP	5'-FITC-GCGATACTACGTTCCGTCTGGATCGCTGGG [THF]GCTGGAGCTGAACTC-/C3-spacer/-3'	46	196
NDM-1-F	ATGCTGAATAAAAGGAAAACTTGATGGAAT	30	238
NDM-1-mR	5'-Biotin-GCCCCGAAACCCGTCATGTCGAGACAGGAA	30	
NDM-mP	5'-FITC-AATAAAAGGAAAACTTGATGGAATTGCCCA A[THF]ATTATGCACCCGATC-/C3-spacer/-3'	47	232
OXA-2	GTAGACAGTTTCTGGCTCGACGGTGGTATT	30	327
OXA-2-R	5'-Biotin-TTCCTGTTTGAGCACTTCTTTTGTGATGGC	30	
OXA-mP	5'-FITC-TCGAACCTATGATTGGCTGGTGGGTCGGTT [THF]GGTTGAACTTGATGA-/C3-spacer/-3'	46	140
VIM-4-F	TTCATAGTGACAGCACGGGCGGAATAGAGT	30	258
VIM-4-R	5'-Biotin-CGTACGGTTTAATAAAACAACCACCGAATA	30	
VIM-mP	5'-FITC-CAATCCATCCCCACGAATGCGTCTGACTTA [THF]CTAATGAGCTGCTGA-/C3-spacer/-3'	46	217

Modified bases are in red. F represents forward primer, R signifies reverse primer, P means probe and m indicates modified.

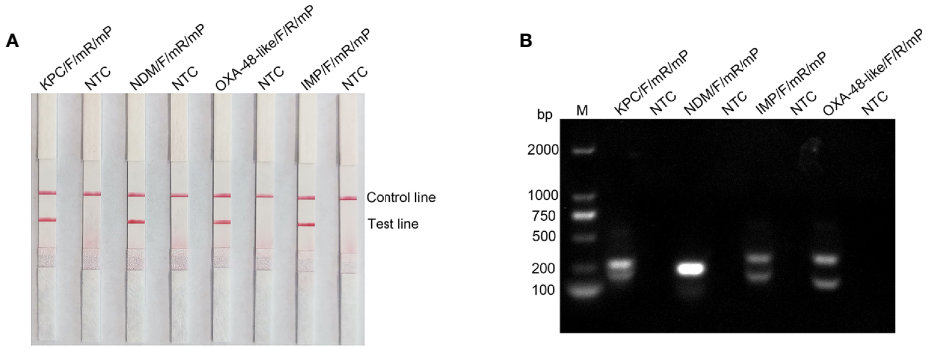

FIGURE 3 | Testing the modified primer-probe set using the RPA-LFS reaction. **(A)** Results of the LFS detection of the RPA amplification products. The name of each primer-probe set is labeled above the corresponding band. **(B)** RPA amplification products were analyzed using agarose gel electrophoresis. The name of each primer-probe set is above each lane: Lane M is DNA ladder. NTC lanes are template-free controls for the respective primer-probe sets. Band sizes of the DNA ladders are shown on the left.

Specificity of the RPA-LFS Assay

K. pneumoniae genomes carrying bla_{KPC}, bla_{NDM}, $bla_{OXA\text{-}48\text{-}like}$, and bla_{IMP} genes as well as seven other common pathogenic bacteria were used as templates to detect the specificity of primer-probe combinations. Results are shown in **Figure 4**, all four primer-probe sets could only detect strains containing the corresponding genes, and no bands were present at the test lines when using genomic DNA from other respiratory bacterial pathogens. Overall, these results illustrated that the established RPA-LFS detection system had good specificity towards the four classes of carbapenemases and no cross-reactivity with other pathogenic bacteria.

Detection Limits of the RPA-LFS Method

To assess the detection limit of RPA-LFS, purified genomes of bacteria carrying the four carbapenemases were subjected to 10-fold serial dilutions, ranging from 10^6 to 10 fg (50 μL/reaction volume with 1 μL of diluted genome added to each reaction). Results are shown in **Figure 5**. bla_{KPC}, bla_{NDM}, and $bla_{OXA\text{-}48\text{-}like}$ all had a minimum detection line of 10^2 fg/reaction; moreover, bla_{IMP} had a 10^3 fg/reaction. The lowest line for bla_{KPC}, bla_{NDM}, and $bla_{OXA\text{-}48\text{-}like}$ was 10^3/reaction by PCR and 10^4/reaction for bla_{IMP}. Our established RPA-LFS reaction system was more sensitive than the PCR reaction.

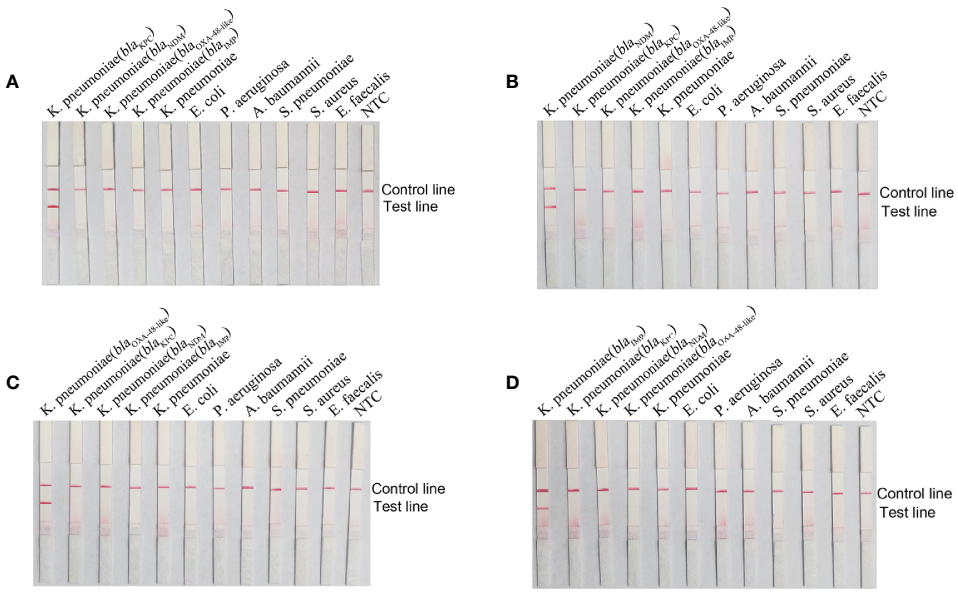

FIGURE 4 | Specificity of the RPA-LFS reaction system. The name of the template added to each reaction is labeled above the corresponding band. Primer-probe combinations of bla_{KPC} **(A)**, bla_{NDM} **(B)**, $bla_{OXA\text{-}48\text{-}like}$ **(C)** and bla_{IMP} **(D)** were added to the reactions. The NTC strip was used as a control reaction without a template.

Examination of Clinical Strains

The four carbapenemase families of the 207 clinically validated CRE isolates were examined using the RPA-LFS method and conventional PCR. A total of 134 CPE containing the bla_{KPC} gene, 69 bla_{NDM}, 3 $bla_{OXA-48-like}$, and 1 bla_{IMP} strain (**Table 3**). There was 100% compliance with the two methods of testing. Notably, the RPA-LFS method was simple and rapid and showed a higher proficiency in detecting carbapenemase genotypes in clinical isolates compared with that of conventional PCR and subsequent sequencing.

DISCUSSION

The emergence of rapid and global spread of carbapenem-resistant *Enterobacterales* (CRE) poses a great threat to human health. Since different types of antimicrobial drugs have different antimicrobial activities *in vitro* against different carbapenemase-producing strains, accurate and rapid detection of carbapenemases produced by CRE is of great value for precise dosing of clinical anti-infective therapy and prevention and control of hospital infection (Bassetti et al., 2016; Sheu et al., 2019; Bush and Bradford, 2019). Several phenotypic methods have been developed for the detection and identification of carbapenemases. Modified carbapenem inactivation method (mCIM) and EDTA carbapenem inactivation method (eCIM): mCIM and eCIM tests are simple to perform, do not require special reagents and are of low cost. The disadvantage is that they both require overnight incubation and is time consuming (Pierce et al., 2017; Lutgring et al., 2018). Combination disk testing (CDT) shows high sensitivity and specificity, but its results take 24 hours and the interpretation of the results is sometimes unclear (Giske et al., 2011). The Carba NP test is simple and rapid (4-6 h) and is suitable for all clinical microbiology laboratories. The disadvantages are low

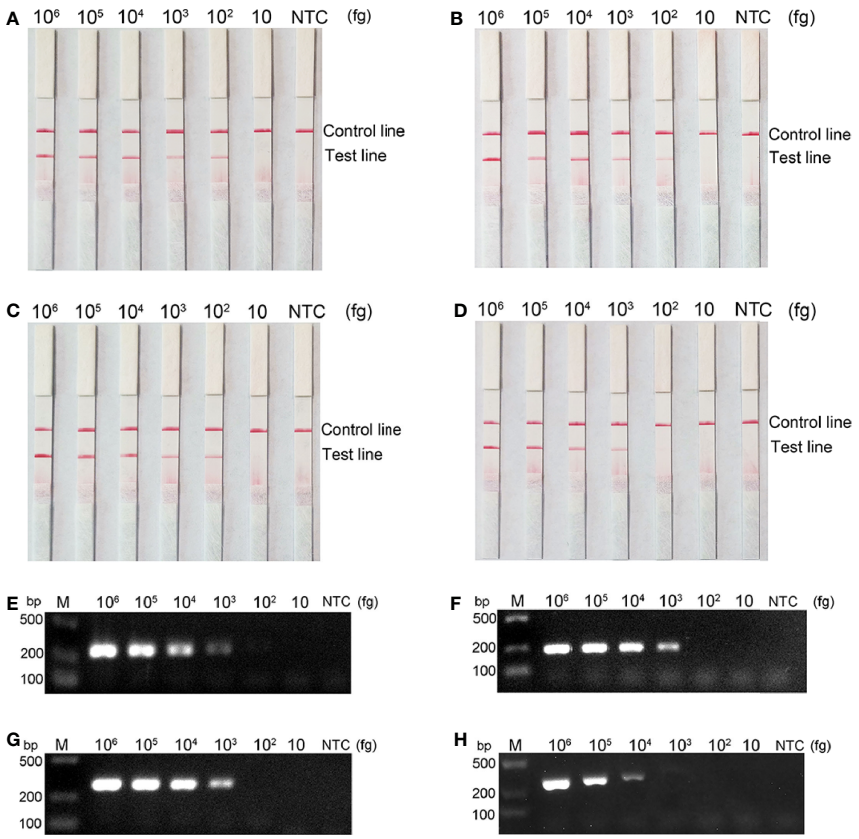

FIGURE 5 | Comparison of the sensitivity between the RPA-LFS reaction and PCR for detection of the four carbapenemase gene families. The amount of template added to each reaction is marked above the corresponding strip. **(A–D)** detection sensitivity of the RPA-LFS assay and **(E–H)** detection sensitivity of the PCR assay, representing bla_{KPC}, bla_{NDM}, $bla_{OXA-48-like}$ and bla_{IMP}, respectively. The NTC strip is the control reaction without a template.

TABLE 3 | Prevalence of carbapenemase genes in 207 strains of *Enterobacterales* using RPA-LFS and PCR.

Method	bla_{KPC}, n (%)	bla_{NDM}, n (%)	$bla_{OXA-48-like}$, n (%)	bla_{IMP}, n (%)	Time (min)
RPA-LFS	134 (64.7)	69 (33.4)	3 (1.5)	1 (0.4)	35
PCR	134 (64.7)	69 (33.4)	3 (1.5)	1 (0.4)	100

N represents number.

sensitivity to $bla_{\text{OXA-48-live}}$ and the fact that a certain percentage (3-5%) of the results are uninterpretable (Cunningham et al., 2017). Xpert® Carba-R is rapid and can clarify the carbapenemase genotype. However, special reagents and equipment are required. False negative results will occur if the gene to be tested is different from the target gene (Mancini et al., 2014; Tato et al., 2016). MALDI-TOF has good sensitivity and specificity, but the cost and the requirement for trained personnel limit their use in under-resourced situations (Yu et al., 2018). Enzyme immunochromatographic techniques have the advantage of the simplicity of operation and easy interpretation of results, but the disadvantage is that they are more expensive (Hopkins et al., 2018; Glupczynski et al., 2019).

To cater to the current situation, carbapenemase genes assays should be less expensive and friendly to carry out for end users. The requirements for reduced cost of consumables and technical complexity led to the development of an isothermal RPA assay for the detection of four major carbapenemase families, namely bla_{KPC}, bla_{NDM}, $bla_{\text{OXA-48-like}}$, and bla_{IMP}-type. This assay could rapidly amplify the target DNA under low isothermal conditions and tolerate unpurified templates in this complex system, being a promising molecular assay that is user-friendly (no trained staff required), excellent performance (high sensitive and specific), and low cost (approximately $9 per reaction compared to $13.50 for the inmunocromatographic technique and $27 for the Xpert Carba-R technique) (Boutal et al., 2018; Yoon et al., 2021). In addition, the chemical labeling of the RPA reaction allows the amplification product to be read using AuNPs-based LFS in a short time, which does not require highly precise readout equipment.

We initially designed five separate pairs of primers during the development of the primer-probe set for the RPA-LFS assay, however, four were discarded because of the presence of primer-dimers and non-specific amplification. In contrast, the optimal pair of amplification primers was selected to design the probe, although it also produced a false-positive signal on the LFS without the DNA template. Therefore, the introduction of base substitutions on the probe and reverse primer eliminated the false-positive signal. Once the primer-probe device was established, the RPA-LFS method showed good performance in detecting the carbapenemase gene (Daher et al., 2015; Liu et al., 2019). All four primer-probe combinations specifically detected the corresponding genes without cross-reactivity.

Our RPA-LFS system for carbapenemase detection retained the advantageous characteristics of both RPA and LFS technologies. The RPA-LFS method was highly sensitive, requiring only 10^2 fg of genomic DNA template from a pure culture of carbapenemase bacteria for detection, and was more sensitive than conventional PCR methods, which is consistent with previous studies. Amplification can be performed at 37°C–42°C, and the entire assay can be completed in less than 30 min. When applied to clinical strain testing, samples do not need to be purified, and the DNA is released by simply boiling over heat and used directly in the assay. The detection accuracy was 100%, and the results were consistent with traditional PCR methods. Thus, our RPA-LFS system provides an experimental basis for the rapid detection of carbapenemase genes in clinical strains, which offers justification for the rational clinical use of antibiotics, especially for individualized anti-infective therapy.

There are two limitations of the study. First, although VIM metallo-B-lactamase is also very common worldwide, the detection rate is low in regions surveyed in this study, so the method does not cover VIM metallo-B-lactamase. The use of the test receives some limitations in geographic areas where VIM metallo-B-lactamase is commonly prevalent (Wang et al., 2018; Han et al., 2020). Second, a major limitation of the RPA-LFS method is that amplification of each carbapenemase gene must be performed individually (i.e., 1 reaction/gene), as it is currently difficult to perform multiplex reactions.

DATA AVAILABILITY STATEMENT

The raw data supporting the conclusions of this article will be made available by the authors, without undue reservation.

ETHICS STATEMENT

The studies involving human participants were reviewed and approved by the Medical Ethics Committee of the Second People's Hospital of Lianyungang City. The patients/participants provided their written informed consent to participate in the study.

AUTHOR CONTRIBUTIONS

FW and WL conceived and designed the experiments. LW, HC, and NL performed the experiments. YW collected the clinical strains. YL analyzed the data. FW wrote the paper. All authors reviewed, revised and approved the final report. All authors contributed to the article and approved the submitted version.

FUNDING

This study was supported by grants from the Natural Science Foundation of Jiangsu Province (grant numbers BK20191210) and the "Project 333" training fund of Jiangsu Province (grant numbers BRA2019248).

ACKNOWLEDGMENTS

We thank Charlesworth Author Services for the professional English language editing and written format amendment targeting to the Journal of Frontiers in Cellular and Infection Microbiology.

SUPPLEMENTARY MATERIAL

The Supplementary Material for this article can be found online at: https://www.frontiersin.org/articles/10.3389/fcimb.2021.772966/full#supplementary-material

REFERENCES

Aguirre-Quiñonero, A., and Martínez-Martínez, L. (2017). Non-Molecular Detection of Carbapenemases in Enterobacteriaceae Clinical Isolates. *J. Infect. Chemother.* 23 (1), 1–11. doi: 10.1016/j.jiac.2016.09.008

Bassetti, M., Pecori, D., and Peghin, M. (2016). The Management of Multidrug-Resistant Enterobacteriaceae. *Curr. Opin. Infect. Dis.* 29 (6), 583–594. doi: 10.1097/QCO.0000000000000314

Bengtsson-Palme, J., Kristiansson, E., and Larsson, D. G. (2018). Environmental Factors Influencing the Development and Spread of Antibiotic Resistance. *FEMS Microbiol. Rev.* 42 (1), 68–80. doi: 10.1093/femsre/fux053

Boutal, H., Vogel, A., Bernabeu, S., Devilliers, K., Creton, E., Cotellon, G., et al. (2018). A Multiplex Lateral Flow Immunoassay for the Rapid Identification of NDM-, KPC-, IMP- and VIM-Type and OXA-48-Like Carbapenemase-Producing Enterobacteriaceae. *J. Antimicrob. Chemother.* 73 (4), 909–915. doi: 10.1093/jac/dkx521

Bush, K., and Bradford, P. J. (2019). Author Correction: Interplay Between β-Lactamases and New β-Lactamase Inhibitors. *Nat. Rev. Microbiol.* 17 (7), 459–460. doi: 10.1038/s41579-019-0221-6

Conlan, S., Thomas, P. J., Deming, C., Park, M., Lau, A. F., Dekker, J. P., et al. (2014). Single-Molecule Sequencing to Track Plasmid Diversity of Hospital-Associated Carbapenemase-Producing *Enterobacteriaceae*. *Sci. Transl. Med.* 6 (254), 254ra126. doi: 10.1126/scitranslmed.3009845

Cunningham, S., Limbago, B., Traczewski, M., Anderson, K., Hackel, M., Hindler, J., et al. (2017). Multicenter Performance Assessment of Carba NP Test. *J. Clin. Microbiol.* 55 (6), 1954–1960. doi: 10.1128/jcm.00244-17

Daher, R. K., Stewart, G., Boissinot, M., Boudreau, D. K., and Bergeron, M. G. (2015). Influence of Sequence Mismatches on the Specificity of Recombinase Polymerase Amplification Technology. *Mol. Cell Probes* 29 (2), 116–121. doi: 10.1016/j.mcp.2014.11.005

Feil, E. J. (2017). *Enterobacteriaceae*: Joining the Dots With Pan-European Epidemiology. *Lancet Infect. Dis.* 17 (2), 118–119. doi: 10.1016/s1473-3099(16)30333-4

Foudraine, D. E., Dekker, L. J. M., Strepis, N., Bexkens, M. L., Klaassen, C. H. W., Luider, T. M., et al. (2019). Accurate Detection of the Four Most Prevalent *Carbapenemases* in E. Coli and K. Pneumoniae by High-Resolution Mass Spectrometry. *Front. Microbiol.* 10, 2760. doi: 10.3389/fmicb.2019.02760

Giske, C., Gezelius, L., Samuelsen, Q., Warner, M., Sundsfjord, A., Woodford, N. J., et al. (2011). A Sensitive and Specific Phenotypic Assay for Detection of Metallo-β-Lactamases and KPC in Klebsiella Pneumoniae With the Use of Meropenem Disks Supplemented With Aminophenylboronic Acid, Dipicolinic Acid and Cloxacillin. *Clin. Microbiol. Infect.* 17 (4), 552–556. doi: 10.1111/j.1469-0691.2010.03294.x

Glupczynski, Y., Evrard, S., Huang, T. D., and Bogaerts, P. (2019). Evaluation of the RESIST-4 K-SeT Assay, a Multiplex Immunochromatographic Assay for the Rapid Detection of OXA-48-Like, KPC, VIM and NDM Carbapenemases. *J. Antimicrob. Chemother.* 74 (5), 1284–1287. doi: 10.1093/jac/dkz031

Glupczynski, Y., Evrard, S., Ote, I., Mertens, P., Huang, T. D., Leclipteux, T., et al. (2016). Evaluation of Two New Commercial Immunochromatographic Assays for the Rapid Detection of OXA-48 and KPC Carbapenemases From Cultured Bacteria. *J. Antimicrob. Chemother.* 71 (5), 1217–1222. doi: 10.1093/jac/dkv472

Hansen, G. T. (2021). Continuous Evolution: Perspective on the Epidemiology of Carbapenemase Resistance Among *Enterobacterales* and Other Gram-Negative Bacteria. *Infect. Dis. Ther.* 10 (1), 75–92. doi: 10.1007/s40121-020-00395-2

Han, R., Shi, Q., Wu, S., Yin, D., Peng, M., Dong, D., et al. (2020). Dissemination of *Carbapenemases* (KPC, NDM, OXA-48, IMP, and VIM) Among Carbapenem-Resistant *Enterobacteriaceae* Isolated From Adult and Children Patients in China. *Front. Cell Infect. Microbiol.* 10, 314. doi: 10.3389/fcimb.2020.00314

Hopkins, K. L., Meunier, D., Naas, T., Volland, H., and Woodford, N. (2018). Evaluation of the NG-Test CARBA 5 Multiplex Immunochromatographic Assay for the Detection of KPC, OXA-48-Like, NDM, VIM and IMP Carbapenemases. *J. Antimicrob. Chemother.* 73 (12), 3523–3526. doi: 10.1093/jac/dky342

Kanahashi, T., Matsumura, Y., Yamamoto, M., Tanaka, M., and Nagao, M. (2021). Comparison of the Xpert Carba-R and NG-Test CARBA5 for the Detection of Carbapenemases in an IMP-Type Carbapenemase Endemic Region in Japan. *J. Infect. Chemother.* 27 (3), 503–506. doi: 10.1016/j.jiac.2020.11.001

Khan, A. U., Ali, A., Danishuddin,, Srivastava, G., and Sharma, A. (2017). Potential Inhibitors Designed Against NDM-1 Type Metallo-β-Lactamases: An Attempt to Enhance Efficacies of Antibiotics Against Multi-Drug-Resistant Bacteria. *Sci. Rep.* 7 (1), 9207. doi: 10.1038/s41598-017-09588-1

Law, I. L. G., Loo, J. F. C., Kwok, H. C., Yeung, H. Y., Leung, C. C. H., Hui, M., et al. (2018). Automated Real-Time Detection of Drug-Resistant Mycobacterium Tuberculosis on a Lab-on-a-Disc by Recombinase Polymerase Amplification. *Anal. Biochem.* 544, 98–107. doi: 10.1016/j.ab.2017.12.031

Lin, D., Chen, K., Guo, J., Ye, L., Li, R., Chan, E. W. C., et al. (2020). Contribution of Biofilm Formation Genetic Locus, pgaABCD, to Antibiotic Resistance Development in Gut Microbiome. *Gut Microbes* 12 (1), 1–12. doi: 10.1080/19490976.2020.1842992

Liu, X., Yan, Q., Huang, J., Chen, J., Guo, Z., Liu, Z., et al. (2019). Influence of Design Probe and Sequence Mismatches on the Efficiency of Fluorescent RPA. *World J. Microbiol. Biotechnol.* 35 (6), 95. doi: 10.1007/s11274-019-2620-2

Lutgring, J., Zhu, W., de Man, T., Avillan, J., Anderson, K., Lonsway, D., et al. (2018). Phenotypic and Genotypic Characterization of Enterobacteriaceae Producing Oxacillinase-48-Like Carbapenemases, United States. *Emerg. Infect. Dis.* 24 (4), 700–709. doi: 10.3201/eid2404.171377

Mancini, N., Infurnari, L., Ghidoli, N., Valzano, G., Clementi, N., Burioni, R., et al. (2014). Potential Impact of a Microarray-Based Nucleic Acid Assay for Rapid Detection of Gram-Negative Bacteria and Resistance Markers in Positive Blood Cultures. *J. Clin. Microbiol.* 52 (4), 1242–1245. doi: 10.1128/jcm.00142-14

Ma, Q., Yao, J., Yuan, S., Liu, H., Wei, N., Zhang, J., et al. (2019). Development of a Lateral Flow Recombinase Polymerase Amplification Assay for Rapid and Visual Detection of Cryptococcus Neoformans/C. Gattii in Cerebral Spinal Fluid. *BMC Infect. Dis.* 19 (1), 108. doi: 10.1186/s12879-019-3744-6

Nordmann, P., Dortet, L., and Poirel, L. (2012). Carbapenem Resistance in *Enterobacteriaceae*: Here Is the Storm. *Trends Mol. Med.* 18 (5), 263–272. doi: 10.1016/j.molmed.2012.03.003

Nordmann, P., Sadek, M., Demord, A., and Poirel, L. (2020). NitroSpeed-Carba NP Test for Rapid Detection and Differentiation Between Different Classes of Carbapenemases in *Enterobacterales*. *J. Clin. Microbiol.* 58 (9), e00932–e00920. doi: 10.1128/jcm.00932-20

Paveenkittiporn, W., Lyman, M., Biedron, C., Chea, N., Bunthi, C., Kolwaite, A., et al. (2021). Molecular Epidemiology of Carbapenem-Resistant Enterobacterales in Thailan-2018. *Antimicrob. Resist. Infect. Control* 10 (1), 88. doi: 10.1186/s13756-021-00950-7

Piepenburg, O., Williams, C. H., Stemple, D. L., and Armes, N. A. (2006). DNA Detection Using Recombination Proteins. *PloS Biol.* 4 (7), e204. doi: 10.1371/journal.pbio.0040204

Pierce, V. M., Simner, P. J., Lonsway, D. R., Roe-Carpenter, D. E., Johnson, J. K., Brasso, W. B., et al. (2017). Modified Carbapenem Inactivation Method for Phenotypic Detection of Carbapenemase Production Among. *Enterobacteriaceae J. Clin. Microbiol.* 55 (8), 2321–2333. doi: 10.1128/jcm.00193-17

Rochford, C., Sridhar, D., Woods, N., Saleh, Z., Hartenstein, L., Ahlawat, H., et al. (2018). Global Governance of Antimicrobial Resistance. *Lancet* 391 (10134), 1976–1978. doi: 10.1016/s0140-6736(18)31117-6

Segagni Lusignani, L., Presterl, E., Zatorska, B., Van den Nest, M., and Diab-Elschahawi, M. (2020). Infection Control and Risk Factors for Acquisition of Carbapenemase-Producing *Enterobacteriaceae.* A 5 Yea-2016) Case-Control Study. *Antimicrob. Resist. Infect. Control* 9 (1), 18. doi: 10.1186/s13756-019-0668-2

Sheu, C., Chang, Y., Lin, S., Chen, Y., and Hsueh, P. J. (2019). *Enterobacteriaceae* Infections Caused by Carbapenem-Resistant: An Update on Therapeutic Options. *Front. Microbiol.* 10, 80. doi: 10.3389/fmicb.2019.00080

Tato, M., Ruiz-Garbajosa, P., Traczewski, M., Dodgson, A., McEwan, A., Humphries, R., et al. (2016). Multisite Evaluation of Cepheid Xpert Carba-R Assay for Detection of Carbapenemase-Producing Organisms in Rectal Swabs. *J. Clin. Microbiol.* 54 (7), 1814–1819. doi: 10.1128/jcm.00341-16

Tsai, Y. M., Wang, S., Chiu, H. C., Kao, C. Y., and Wen, L. L. (2020). Combination of Modified Carbapenem Inactivation Method (mCIM) and EDTA-CIM (eCIM) for Phenotypic Detection of Carbapenemase-Producing *Enterobacteriaceae*. *BMC Microbiol.* 20 (1), 315. doi: 10.1186/s12866-020-02010-3

van Duin, D., and Doi, Y. (2017). The Global Epidemiology of Carbapenemase-Producing *Enterobacteriaceae*. *Virulence* 8 (4), 460–469. doi: 10.1080/21505594.2016.1222343

Vergara, A., Moreno-Morales, J., Roca, I., Pitart, C., Kostyanev, T., Rodriguez-Baño, J., et al. (2020). A Comparative Study Between Real-Time PCR and Loop-Mediated Isothermal Amplification to Detect Carbapenemase and/or ESBL Genes in Enterobacteriaceae Directly From Bronchoalveolar Lavage Fluid Samples. *J. Antimicrob. Chemother.* 75 (6), 1453–1457. doi: 10.1093/jac/dkaa031

Wang, Q., Wang, X., Wang, J., Ouyang, P., Jin, C., Wang, R., et al. (2018). Phenotypic and Genotypic Characterization of Carbapenem-Resistant *Enterobacteriaceae*: Data From a Longitudinal Large-Scale CRE Study in China, (2012-2016). *Clin. Infect. Dis.* 67 (suppl_2), S196–S205. doi: 10.1093/cid/ciy660

Wang, L., Zhao, P., Si, X., Li, J., Dai, X., Zhang, K., et al. (2019). Rapid and Specific Detection of Listeria Monocytogenes With an Isothermal Amplification and Lateral Flow Strip Combined Method That Eliminates False-Positive Signals From Primer-Dimers. *Front. Microbiol.* 10, 2959. doi: 10.3389/fmicb.2019.02959

Xie, J., Yang, X., Duan, L., Chen, K., Liu, P., Zhan, W., et al. (2021). One-Step Reverse-Transcription Recombinase Polymerase Amplification Using Lateral Flow Strips for the Detection of Coxsackievirus A6. *Front. Microbiol.* 12, 629533. doi: 10.3389/fmicb.2021.629533

Yang, A. K., Lu, H., Wu, S. Y., Kwok, H. C., Ho, H. P., Yu, S., et al. (2013). Detection of Panton-Valentine Leukocidin DNA From Methicillin-Resistant *Staphylococcus Aureus* by Resistive Pulse Sensing and Loop-Mediated Isothermal Amplification With Gold Nanoparticles. *Anal. Chim. Acta* 782, 46–53. doi: 10.1016/j.aca.2013.04.004

Yoon, J., Kim, C. H., Yoon, S. Y., Lim, C. S., and Lee, C. K. (2021). Application of a Multiplex Immunochromatographic Assay for Rapid Identification of Carbapenemases in a Clinical Microbiology Laboratory: Performance and Turn-Around-Time Evaluation of NG-Test Carba 5. *BMC Microbiol.* 21 (1), 260. doi: 10.1186/s12866-021-02309-9

Yu, J., Liu, J., Li, Y., Yu, J., Zhu, W., Liu, Y., et al. (2018). Rapid Detection of Carbapenemase Activity of Enterobacteriaceae Isolated From Positive Blood Cultures by MALDI-TOF MS. *Ann. Clin. Microbiol. Antimicrob.* 17 (1), 22. doi: 10.1186/s12941-018-0274-9

Conflict of Interest: The authors declare that the research was conducted in the absence of any commercial or financial relationships that could be construed as a potential conflict of interest.

Publisher's Note: All claims expressed in this article are solely those of the authors and do not necessarily represent those of their affiliated organizations, or those of the publisher, the editors and the reviewers. Any product that may be evaluated in this article, or claim that may be made by its manufacturer, is not guaranteed or endorsed by the publisher.

frontiers in Cellular and Infection Microbiology

REVIEW
published: 03 February 2022
doi: 10.3389/fcimb.2022.807668

Total Laboratory Automation for Rapid Detection and Identification of Microorganisms and Their Antimicrobial Resistance Profiles

Abdessalam Cherkaoui[1]* *and Jacques Schrenzel*[1,2]

[1] Bacteriology Laboratory, Division of Laboratory Medicine, Department of Diagnostics, Geneva University Hospitals, Geneva, Switzerland, [2] Genomic Research Laboratory, Division of Infectious Diseases, Department of Medicine, Faculty of Medicine, Geneva University Hospitals, Geneva, Switzerland

At a time when diagnostic bacteriological testing procedures have become more complex and their associated costs are steadily increasing, the expected benefits of Total laboratory automation (TLA) cannot just be a simple transposition of the traditional manual procedures used to process clinical specimens. In contrast, automation should drive a fundamental change in the laboratory workflow and prompt users to reconsider all the approaches currently used in the diagnostic work-up including the accurate identification of pathogens and the antimicrobial susceptibility testing methods. This review describes the impact of TLA in the laboratory efficiency improvement, as well as a new fully automated solution for AST by disk diffusion testing, and summarizes the evidence that implementing these methods can impact clinical outcomes.

Keywords: total laboratory automation, antimicrobial susceptibility testing, Copan, WASPLab® platform, WASPLab artificial intelligence, Colibri, Radian

OPEN ACCESS

Edited by:
Elena Jordana-Lluch, Balearic Islands Health Research Institute (IdISBa), Spain

Reviewed by:
Haris Antypas, Nanyang Technological University, Singapore
Gino Mongelli, Azienda Sanitaria Provinciale di Catania, Italy

***Correspondence:**
Abdessalam Cherkaoui
abdessalam.cherkaoui@hcuge.ch

Specialty section:
This article was submitted to Clinical Microbiology, a section of the journal Frontiers in Cellular and Infection Microbiology

Received: *02 November 2021*
Accepted: *17 January 2022*
Published: *03 February 2022*

Citation:
Cherkaoui A and Schrenzel J (2022) Total Laboratory Automation for Rapid Detection and Identification of Microorganisms and Their Antimicrobial Resistance Profiles. Front. Cell. Infect. Microbiol. 12:807668. doi: 10.3389/fcimb.2022.807668

INTRODUCTION

The early 19th century was characterized by the development of a large number of industry plants. Improving production performance – and ultimately automating the processes – was a constant motivation in industrial development, mostly for costs issues, but sometimes also for the workers' safety. During the 20th century, the electronics revolution permitted automation to alleviate humans from physically challenging, tedious, and routine handling tasks. Automation then appeared the way for companies to improve their productivity rates without increasing their employee headcounts. Reducing operating costs, improving goods availability, producing with higher reliability and increased performance are the other obvious benefits commonly expected from automation. But despite a broad consensus about those benefits, several pitfalls and a number of obstacles have to be overcome before implementing automated systems, and this holds true across various business area (Dolci et al., 2017). As the automation becomes reality, several issues concerning acceptance by the workers and their relation towards machines are surfacing. A large number of workers consider the implementation of automated systems as a direct threat to their employment (Lippi and Da Rin, 2019). Hence, the success of automation projects lies also on the way to manage staff implication as well as to identify and address their concerns. Nowadays, the

automation is effectively implemented in nearly every business area, including medical laboratories (Burckhardt, 2018).

Clinical bacteriology has always been very manual and labor intensive. Unlike some other disciplines including clinical chemistry, molecular biology, immunology and hematology, total automation in clinical bacteriology is not an easy task. The level of efficiency of an automated system in clinical bacteriology relies heavily on in its potential to deal with the highly heterogeneous clinical specimens, due to various container types as well as complex analytical procedures (Bourbeau and Ledeboer, 2013; Thomson and McElvania, 2019).

The first stand-alone automated systems in clinical bacteriology were launched in the 1970s. They were designed to detect bacterial growth in blood culture specimens using broth-based cultures (the BACTEC™ 225, BACTEC™ 301, and BACTEC™ 460 were released between 1971 and 1974). The major difference between these systems and the manual operations, which were still widely used at this period, was that microbial growth was detected automatically by the BACTEC™ instrument rather than by the visual inspection of the technologist. The automatic detection of microbial growth was initially performed by adding radioactively labeled substrates to the broth. The metabolism of these substrates led to the release of radioactively-labeled carbon dioxide that is specifically detected by the instrument. When the amount of the radioactively-labeled carbon dioxide reaches a pre-defined level, the bottle is considered as suspect of microbial growth. This principle has been perpetuated in most recent blood culture instruments, with the exception that the radioactive-labeling has been replaced by fluorescence (Mitchell and Ryan, 1993; Diekema and Marchesseault, 1999).

The first total laboratory automation (TLA) system for culture-based testing (BD Kiestra™) was installed in a diagnostic laboratory in 2006. Few years after, the Copan Company commercialized another TLA system (WASPLab™) with a first installation in a routine laboratory in 2012 (Croxatto et al., 2016). The two TLA systems consist in a complex integration of robotics, digital imaging and software to pilot instruments and provide data interpretation. They are designed for accessioning and inoculating clinical specimens on a variety of culture plates, moving such media plates to automated incubators and providing high-resolution digital imaging at pre-defined time points of the culture plates. Viewing the digitized images of all plates from the same sample on a screen constitutes one of the most important advantages that automation brings to the technologists who are used to retrieve the plates from the incubators, and manipulate the agar plates to inspect them visually before executing some quick and basic biochemical tests (e.g., oxidase, catalase, Pastorex™ …). The TLA systems now enable the staff to call up the agar plates to the workbench for manual assessment whenever deemed necessary, which effectively enhances the staff's confidence in the digitized images and minimizes handling. The workflow is also impacted by the automation. It allows extended flow processing, more compatible with a 24/7 operation, in contrast to the traditional manual approach of batch reading the plates in the morning and processing them in the afternoon. Since a large number of repetitive tasks are carried out by machines, some staff can be redirected to perform other tasks that typically require their skills and knowledge.

TOTAL LABORATORY AUTOMATION (TLA)

Processing of Clinical Specimens

Enhancing efficiency and specimen traceability is clearly expected from TLA. Upon receipt in the laboratory, all specimens are treated serially, without delay. Applicable culture media are selected and labeled automatically according to the specimen type, and the requested analyses. The inoculation of specimens is accurately carried out using calibrated metallic loops according to a defined streaking pattern. Inoculated media are swiftly transferred to the incubators *via* conveyors. This allows skipping the batch processing of specimens as well as the creation of manual worklists. TLA also increases the safety level of the technologists by massively reducing the handling of the specimens, especially since the inspection of culture plates is performed on screen, through digital images.

Incubation and Imaging of Culture Media Plates

By using TLA, inoculated media are transferred without delay from the processing area to the incubators. The agar plates are incubated under optimal growth conditions, stable temperature and adequate atmosphere, because the incubators' doors are kept closed throughout the incubation process. Microbial growth is monitored through high-resolution digital images taken at pre-defined time points. This enables a more rapid detection of microbial growth while also improving the recovery of slow-growing pathogens. Moreover, TLA uses a software that enables the digital images to be viewed under increased magnification, thus facilitating a consistent assessment of colony morphologies and the detection of mixed cultures. The digital images are interpreted by training technologists, a factor that raises an important challenge as compared to the conventional diagnostic work-up, because the bacterial colonies appear quite different on the screen. Adaptation will be necessary. TLA finally builds a library of images that can be used for training objectives, but also to support and document individual patient's analyses during discussions with infectious disease specialists, whenever needed.

Work-up of Culture Media Plates

To get most out of the imaging, the digital images should be performed at different time points while observing a short lead time to detect significant microbial growth as early as possible (**Figure 1**). The identification of pathogens and AST can therefore be obtained much earlier as compared to the conventional work-up, improving therefore the turnaround-time (TAT). Before the TLA era, in most clinical bacteriology laboratories, the working day starts by distributing all incubated culture plates to the different workbenches according to specimen's type (e.g., blood cultures, urine, non-sterile site specimens, sterile site specimens, respiratory tract specimens, specimens screened for a defined microorganism

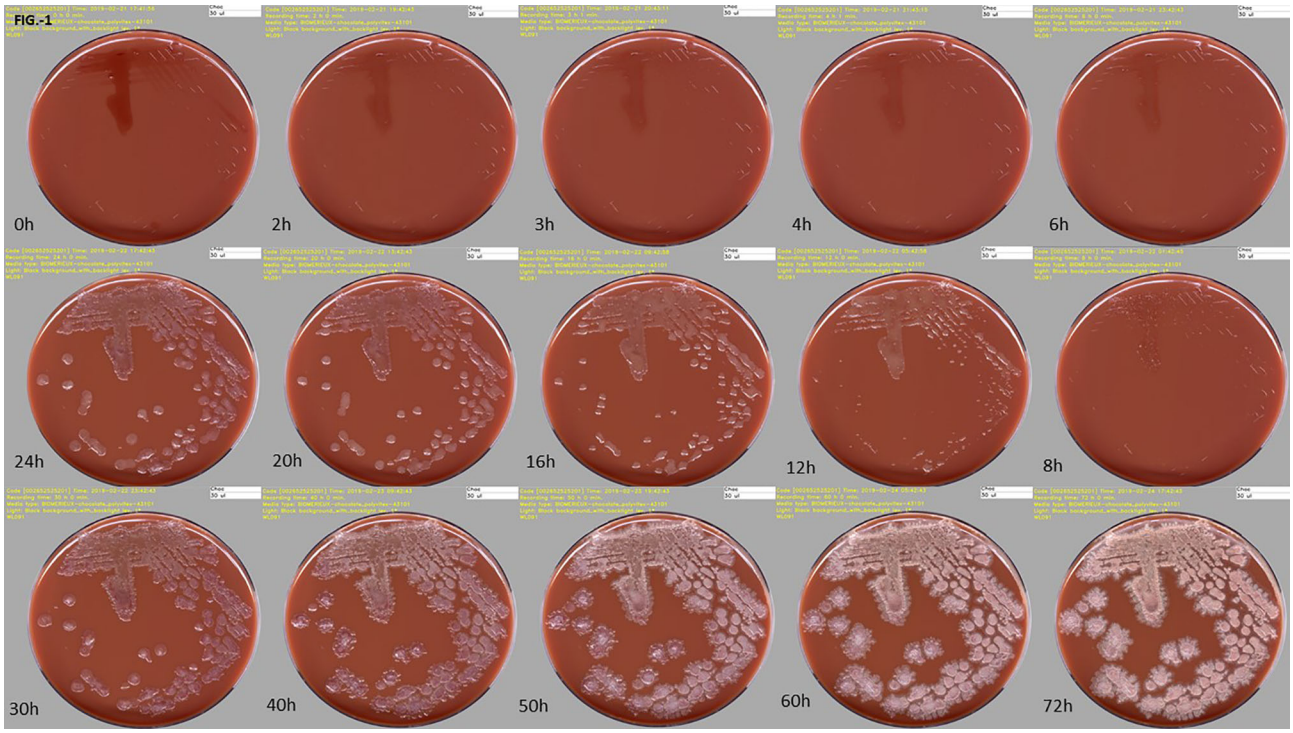

FIGURE 1 | High-resolution digital images of one culture media plate taken at different incubation times on the WASPLab™. Time-series image acquisitions for a clinical specimen positive with *Bacillus* sp., at ascending time points, is depicted here, highlighting the progressive growth of bacterial colonies. Source of all images: A. Cherkaoui, Geneva University Hospitals.

carriage…) or based on patients ID or wards (ICU, ED, etc.). The specimen-based organization allows executing repetitive tasks in a more systematic manner than based on patients ID or wards and permits a better planning and follow-up of the routine activities. However, it also leads to an uneven distribution of work across workbenches, and to the difficulty to get a comprehensive diagnostic picture for an individual patient. Using TLA, each inoculated media plate is incubated for a pre-defined period, so that it becomes available for processing throughout the day and evening. This processing is most efficient and has a beneficial impact on TAT, allowing better management of the workload and of the workflow (**Figure 2**). The assessment and interpretation of culture media plates using digital images are still performed by the technologists who define which colonies of interest have to be isolated and further processed for identification and AST. The current version of TLA cannot replace these skilled activities. However, other automated systems newly introduced on the market (e.g., Copan Colibri™), can prepare the target for microbial identification (ID) by MALDI-TOF and a standardized inoculum for performing the AST (**Figure 3**). The ID and AST results must also be interpreted by skilled technologists, which requires adequate coordination in the staffing of these different activities. To help matching the workload with the level of diagnostic activity, TLA allows to track, at any moment, all specimens throughout their diagnostic pathway. TLA provides also different metrics to evaluate the processes and the team efficiencies, and additional interpretation of patient's results including trends analysis of antimicrobial resistance.

Implementation and Deployment

Clinical microbiology laboratories are nowadays confronted with many different challenges including the needs: i) to enhance efficiency (i.e. to deliver more cost-effective diagnostics), ii) to deliver earlier results (i.e. to shorten the TAT), iii) to comply with the increasingly demanding accreditation requirements (i.e. to provide traceability and documentation to assess the quality of the whole diagnostic process), and iv) to meet the challenges raised by the growing number of multidrug resistant organisms (i.e. to deliver rapidly more comprehensive AST, but whenever needed). Most such challenges can be significantly addressed by TLA. However, successful implementation of TLA requires : i) substantial changes in the traditional workflow, ii) strong leadership skills with smooth teamwork and cooperation of all stakeholders involved in the project, and iii) a customized support of the technical staff throughout the transition period.

IMPROVING TURN-AROUND TIMES (TAT) IN CLINICAL BACTERIOLOGY

During the last two decades, significant resources were allocated by the industry to develop accurate and faster assays to reduce

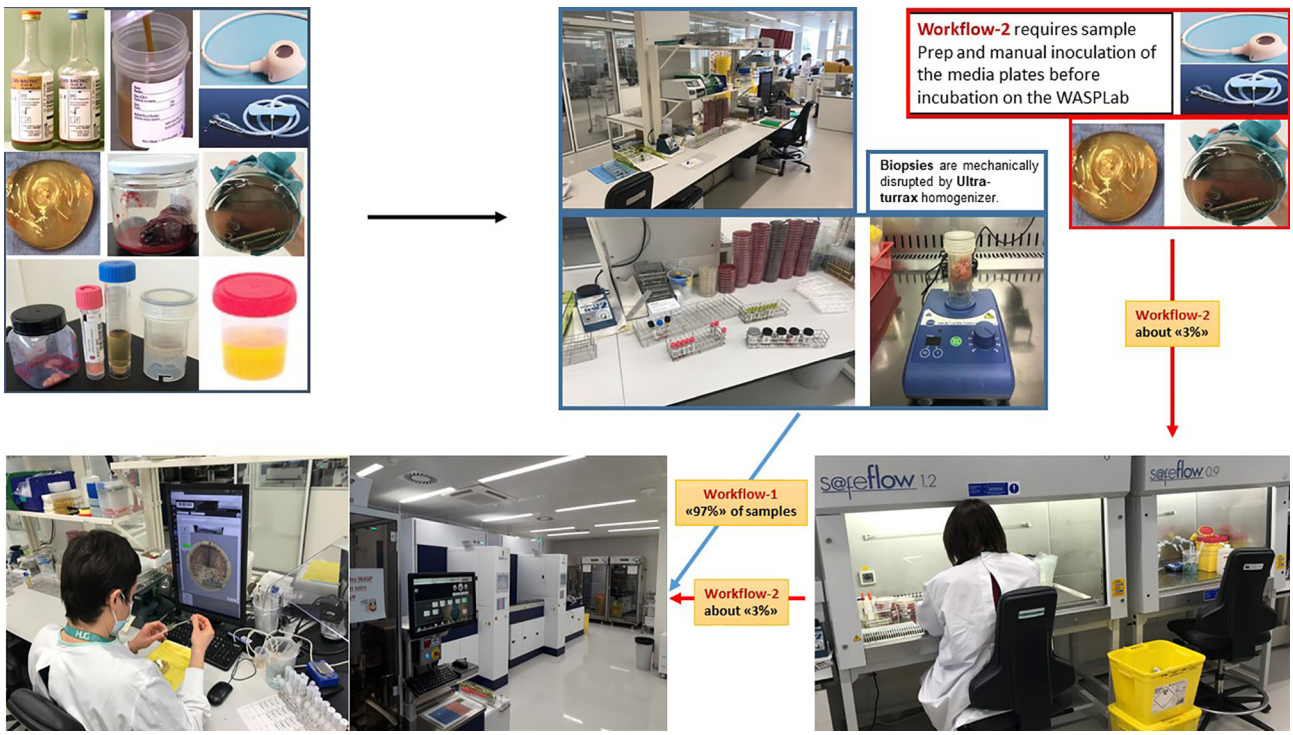

FIGURE 2 | Total Lab automation workflows. A supposed advantage of TLA in microbiology is an improved efficiency by reducing the repetitive tasks with moderate added-value. Automated incubators with digital imaging drastically reduce the number of manipulations of the culture media plates. Currently, 97% of the identified "automatable" specimens are processed by TLA in our lab. The residual 3% corresponds to specimens that require manual sample preparation or manual inoculation of the media plates before incubation on the WASPLab (e.g., catheters, vascular or orthopedic prostheses, and chirurgical devices). Source of all images: A. Cherkaoui, Geneva University Hospitals.

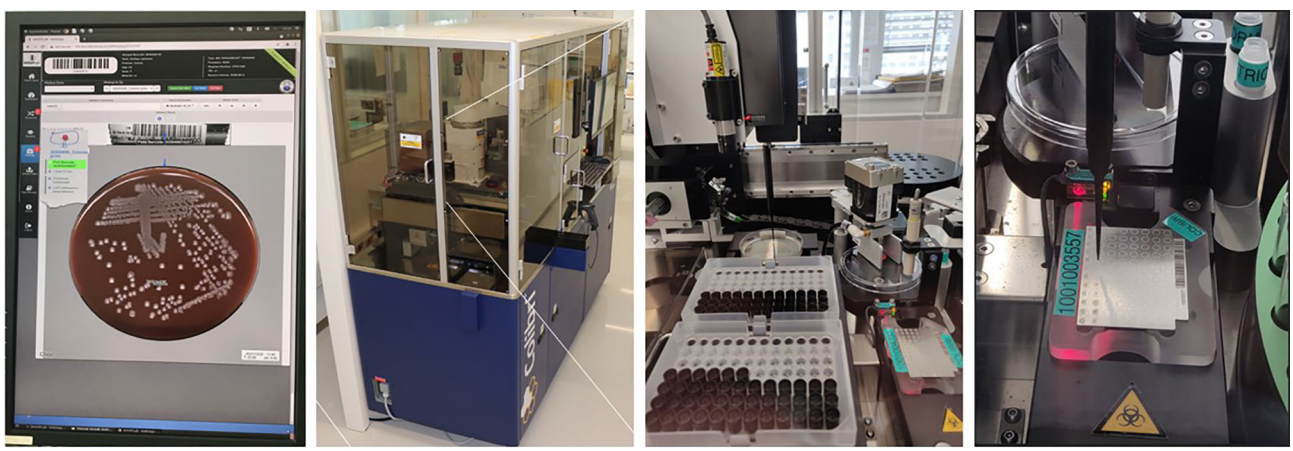

FIGURE 3 | Automated System for Colony Picking and MALDI-TOF Targets Preparation (Copan Colibri™). A pipetting system permits: i) the picking of the specific colonies determined by the technologists during the reading step on the WASPLab screen; ii) the transfer of the microorganisms' cells on the MALDI-target; and iii) the deposition of the matrix. Two protocols are available with (or without) extraction using a formic acid. Source of all images: A. Cherkaoui, Geneva University Hospitals.

TAT in clinical bacteriology. Such timely patient management has become even more critical with the steadily increase of antimicrobial resistance. Before the TLA era, the development of matrix-assisted laser desorption/ionization time-of-flight (MALDI-TOF) mass spectrometry (MS) for the identification of bacteria, mycobacteria, yeasts, and molds has fundamentally replaced the well-established conventional diagnostic methods for identifying microorganisms, which were based essentially on biochemistry testing. In comparison with the conventional phenotype methods or molecular assays used in the identification of microorganisms, MALDI-TOF/MS has several advantages which can be summarized in three points: rapid turnaround time, low specimen volume requirements, and moderate reagent costs (Cherkaoui et al., 2010; Cherkaoui et al., 2011; Gaillot et al., 2011; Kaleta et al., 2011; Tan et al., 2012; Barberis et al., 2014; Verroken et al., 2016; Faron et al., 2017; Chen et al., 2021; Torres-Sangiao et al., 2021). Accurate and rapid identification of microorganisms using MALDI-TOF/MS helped to quickly support treatment decisions, especially when the infecting pathogen was unexpected. Thus, this technology has enabled real improvement in antimicrobial therapy, infection prevention and control measures (**Figures 4A, B**).

AUTOMATION OF ANTIMICROBIAL SUSCEPTIBILITY TESTING (AST) BY DISK DIFFUSION

Success criteria for TLA should be rapidly visible and related to the objectives defined before the initiation of the project. In addition to the measurable indicators exposed in the previous chapters, we considered also the implementation of a fully automated solution for the antimicrobial susceptibility testing as one of the major indicators of success for our automation project. It is even more relevant in our case because we added a second automation line with the specific purpose to automate AST by disk diffusion. Firstly, we performed an important validation study in which we investigated the agreement at the categorical level between the previous version of the automated AST by disk diffusion proposed by Copan against the SIRscan 2000 automatic, which represents a gold standard in our routine diagnostic. A large panels of resistant and susceptible strains were included in this study. The analysis revealed that the overall categorical agreement between the compared methods yielded to 99% (Cherkaoui et al., 2020). Unfortunately, the implementation of this new method, fully automated, was postponed partly owing to recurrent mechanical issues. The most important breakdown of the system was linked to the antibiotic disk dispensers and the heterogenous quality of the springs contained in the dispensers of the antibiotic disk cartridges. To overcome these issues, the manufacturer developed a new module including a carousel that can hold fifty antibiotic cartridges. This new module was developed also with the explicit goal to minimize the workflow bottlenecks on the AST line by adding a second conveyor belt for the media plates. This new fully integrated and automated system permits: to prepare an inoculum suspensions using au minimum four different colonies in order to capture different resistant patterns; to automatically inoculate the suspensions of bacterial cells over the entire surface of the specific media plates; to dispense antibiotic disks according to predefined panels; to transport the culture media to the incubators; to perform a high-quality digitalized images of the media plates at predefined time point; and finally to extract and interpret the inhibition zones diameters for all the antibiotics tested.

The basic rules to be complied when we seek to assess the accuracy of the fully automated solution for the AST by disk diffusion may be summarized in two points: i) To evaluate the ability of this new method to detect the most important resistance mechanisms, a representative number of non-duplicate clinical strains that expressed a resistant patterns to different classes of antibiotics should be included in the study; II) To determine the percentage of the major errors, mistakenly interpreted as resistant, a great number of non-duplicate susceptible clinical strains should be also included in the analysis. In our previous study we determine the agreement at the categorical level between the fully automation solution proposed by Copan for AST by disk diffusion against the Vitek2 system, which represent one of the principal AST methods used in our routine diagnostic. In this study, we included 718 strains comprising *Staphylococcus aureus*, coagulase-negative staphylococci, *Enterococcus faecalis, Enterococcus faecium*, *Pseudomonas aeruginosa*, and different species of Enterobacterales. All these strains were isolates in our laboratory from non-consecutive clinical specimens. The results of this study showed that the overall categorical agreement between the two compared methods was 99.1%. More importantly, this study revealed a great number of very major errors, mistakenly interpreted as susceptible, for *P. aeruginosa* when the AST were performed by Vitek2.

All these very major errors were linked to the hetero-resistant subpopulations within the bacteria cells (Cherkaoui et al., 2021).

ROUTINE AST OF ANAEROBES AND MULTIDRUG RESISTANT GRAM-NEGATIVE BACTERIA

Over the last decade, several reports have highlighted the steadily increase in antibiotic resistance among anaerobic bacteria. The first bacteria species concerned is *Bacteroides fragilis*. In addition, antibiotic resistance is now also detected among different species that were, until recently, spared by this concern (e.g., *Clostridium difficile, Cutibacterium acnes)*. Consequently, clinicians raised concerns regarding the appropriateness of the empirical therapy (Nagy et al., 2011; Boyanova et al., 2015; Kim et al., 2016). Facing such a challenge, it was essential to perform the susceptibility testing of anaerobic bacteria routinely. As a complement to the fully automated disk diffusion, we tested on a large number of clinically relevant anaerobic strains the accuracy of the Thermo Scientific™ Sensititre™ Anaerobe MIC plate by comparing it with the ATB ANA® test (BioMérieux), our current routine method. The overall categorical agreement between both methods reached 95%, allowing us to implement the Thermo

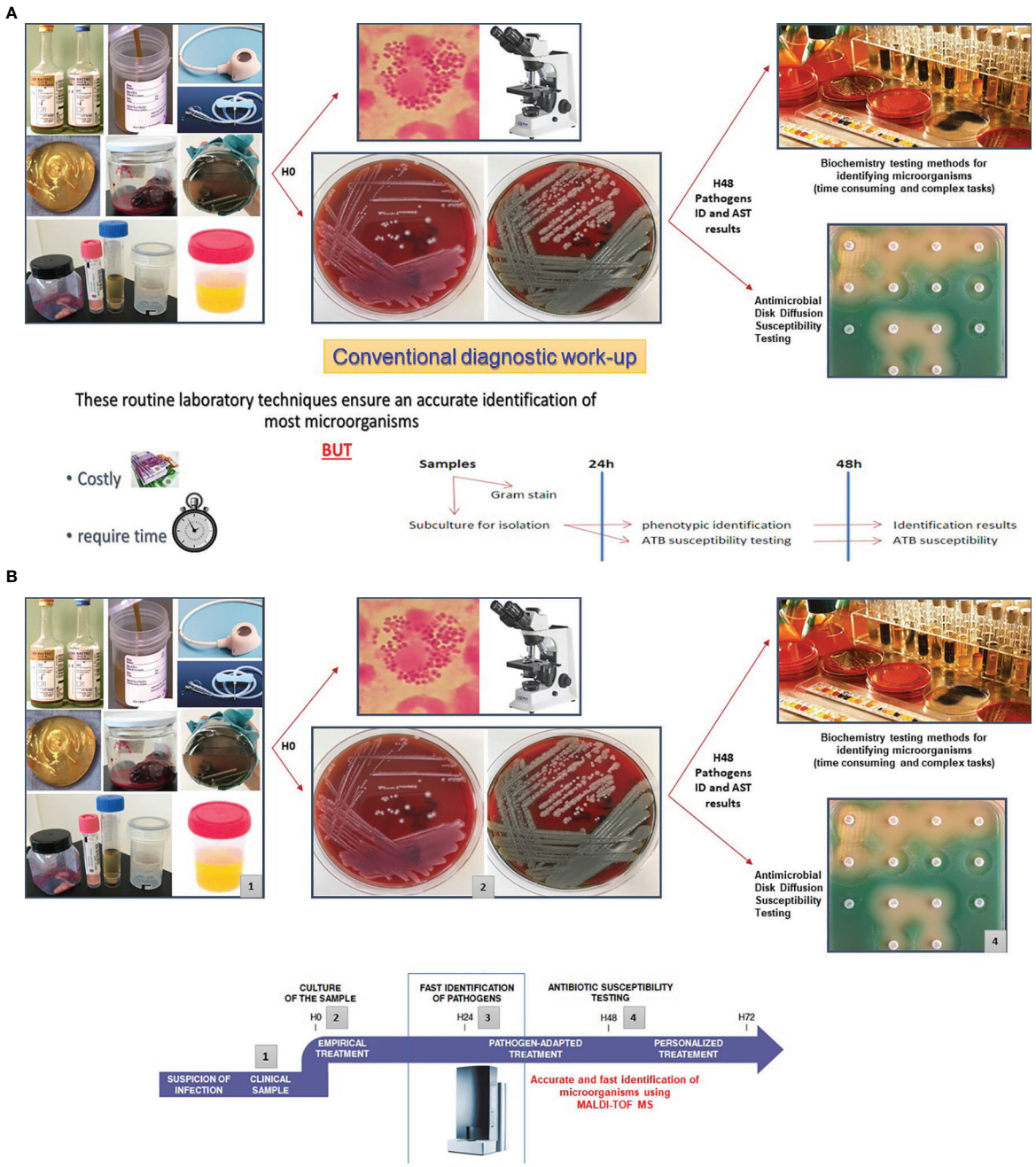

FIGURES 4 | Improving Turn-Around Times (TAT) in clinical bacteriology by MALDI-TOF/MS. Several studies have highlighted that MALDI-TOF/MS is highly accurate to identify bacteria and yeasts isolated from clinical specimens. This approach is efficient, inexpensive, and rapid. The positive impact of the MALDI-TOF/MS in the enhancement of turn-around times (TAT) was assessed in various reports. **(A)** Depicts the traditional workflow using manual inoculation of the culture media plates, identification of the pathogen by traditional phenotypic methods, and manual AST by disk diffusion. **(B)** MALDI-TOF/MS reduces the TATs by an average of 1.45 days in comparison with the traditional phenotypic methods used for identification (Tan et al., 2012). Hence, this approach contributes to swiftly support treatment decisions, especially when the identification of the pathogen is unexpected (Angeletti et al., 2015; Verroken et al., 2016; Theparee et al., 2018). Source of all images: A. Cherkaoui, Geneva University Hospitals.

Scientific™ Sensititre™ Anaerobe MIC plate (Cherkaoui et al., 2018). We then decided to design a new plate for multidrug resistant Gram-negative bacteria by integrating the latest molecules used in targeted therapy (**Figure 5A**). This plate was manufactured by Thermo Scientific™ and validated using reference ATCC strains. This plate is now implemented as our second line testing, whenever AST by disk diffusion has detected defined resistance patterns. This strategy enabled us to effectively

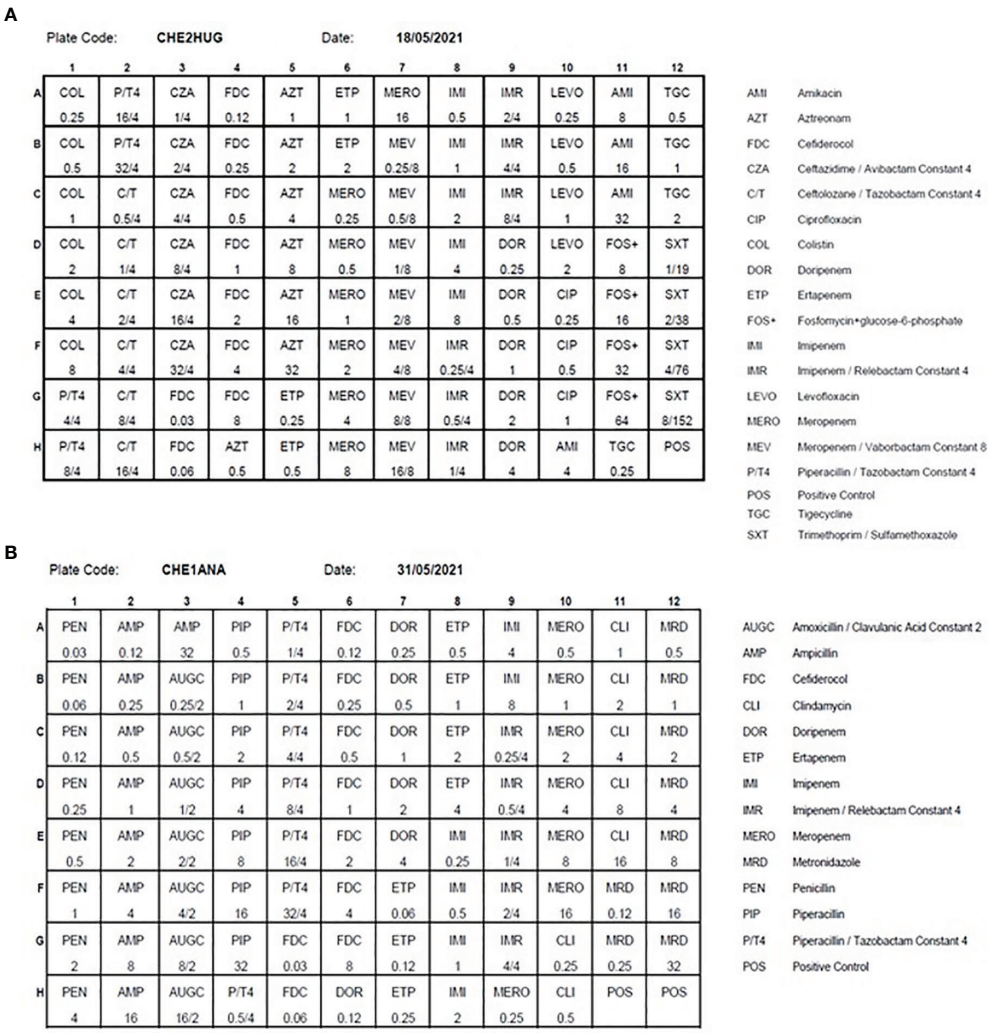

FIGURE 5 | The antibiotics panels of the MDR (CHE2HUG / Panel **A**) and anaerobes (CHE1ANA / Panel **B**) Thermo Scientific™ Sensititre™ plates Source of all images: A. Cherkaoui, Geneva University Hospitals.

monitor antibiotic resistance in our institution at a reasonable cost, by systematically targeting suspect strains, as reported by the automated AST testing. Finally, we also designed a new plate for the routine susceptibility testing of anaerobes, which the antibiotics panel fits better with the treatment guidelines. We included in this panel some new antibiotics, to anticipate the emergence of new resistance mechanisms within this group of bacteria (**Figure 5B**).

The Sensititre® susceptibility system is a micro broth method using dried plate format. Qualitative (susceptible or resistant) and quantitative Minimum Inhibitory Concentration (MIC) results are provided. Dried plates are dosed with serially diluted antimicrobial agents selected for the micro-organisms tested. Strain suspensions are prepared manually and the plates are automatically inoculated using Sensititre AutoInoculator®/ AIM®. After incubation, results are read using the Sensititre® manual viewer. Bacterial growth occurs as turbidity or as a deposit of cells at the bottom of a well. The MIC is defined as the lowest concentration of drug that inhibits visible bacterial growth.

Over the last few decades, multidrug-resistant Gram-negative bacterial infections have become one of the major areas of concern in medicine and global health. To optimize the selection of a successful treatment and to deal with the increasing number of carbapenemase-producing Gram negative bacteria, the additional use of Minimum Inhibitory Concentration (MIC) results for last resource drugs has become essential. This allows targeted AST determinations on MDR strains and, when coupled to therapeutic drug monitoring (TDM), permits to select the most appropriate treatments. As agar disk diffusion does not provide MICs, the Sensititre constitutes an interesting complement to the fully automated AST by disk diffusion when deemed necessary, as in the case of MDR strains or for anaerobic bacteria.

DISCUSSION

All clinical microbiology laboratories around the world express the unmet need for improved quality, productivity, reduced turnaround-time (TAT), rationalization of laboratory technologist labor force, and faster diagnostics to reduce the misuse of antibiotics. Responding to these growing needs will require highly effective strategies. In that sense, the implementation of TLA represents an appealing option, given the fact that the bulk of the workload in culture-based analysis relies in specimen handling, media plate inoculation, incubation, culture reading, pathogen identification and antimicrobial susceptibility testing (ID/AST), all of which remaining highly manual processes.

As discussed in the previous chapters, TLA enables rapid results and significantly reduces TAT. In 2020, about 30'000 urine specimens were processed in our lab. Using TLA, the median TAT for negative reports decreased by almost half from 52.1 h (2017) to 28.3 h (2019) ($p < 0.001$), potentially allowing to stop unnecessary antimicrobial treatments (Cherkaoui et al., 2020). It is important to note that this reduction of TAT was not associated with a loss of analytical sensitivity. Rather, automated processing of urine specimens and optimized incubation periods contributed to higher detection rates for fastidious uropathogens such as *Alloscardovia* spp. and *Aerococcus* spp (Klein et al., 2018; Lainhart and Burnham, 2018; Cherkaoui et al., 2019). It is noteworthy to mention that the benefits of TLA for patient care (including drug de-escalation or antimicrobial therapy adjustments) should be further improved, providing trained technologists are available to analyze the on-screen digital images and to report positive cultures results in real time, which would require 24/7 staffing. This represents a real challenge for many laboratories, in terms of costs but also of attracting trained technologists. This is why artificial intelligence (AI), like automated colony recognition, is making its way towards routine microbiology, as it can be coupled to TLA. These applications compare media plate images at time zero and at defined incubation time points in order to identify potential bacterial growth, but also to differentiate bacterial morphologies and enumerate corresponding colonies (Van et al., 2019; Foschi et al., 2021). After careful validation studies, negative cultures may be automatically processed and the results automatically released without human intervention, which further increases the laboratory efficiency and improves the TAT (Faron et al., 2019; Faron et al., 2020; Ford and McElvania, 2020; Dauwalder et al., 2021).

To face the continual increase of antimicrobial resistance and its dramatic consequences, infection control has become a core activity of clinical microbiology labs. The amount of screening specimens for carbapenemase-producing Enterobacteriaceae (CPE), extended-spectrum β-lactamases (ESBLs), methicillin-resistant *Staphylococcus aureus* (MRSA), and vancomycin-resistant *Enterococcus* VRE carriage sent into the microbiology labs for analysis has increased thoroughly over the last decade.

In our laboratory, we process about 35'000 screening specimens per year. Using TLA, the median TAT for negative reports decreased by almost half for MRSA screening from 50.7 to 26.3 h ($p < 0.001$). The difference in median TAT for negative cultures was less pronounced for screening of ESBLs (50.2 vs. 43.0 h) ($p < 0.001$) and VRE (50.6 vs. 45.7 h) ($p < 0.001$), but remained significant (Cherkaoui et al., 2020). Several recent reports have also highlighted the positive impact of the TLA on the TAT (Cheng et al., 2020; Zhang et al., 2021; Kim et al., 2022).

Upcoming improvements in TLA will enable positive cultures to be automatically released for MRSA or VRE when chromogenic media are used and analyzed by artificial intelligence algorithms. These algorithms permit recognition of characteristically colored colonies, with performances that can be measured and whose cut-offs can be customized by the labs (Faron et al., 2016a; Faron et al., 2016b). Shortening the TAT could prevent the spread of multi-resistant bacteria and reduce nosocomial transmission, by alleviating unnecessary infection control measures or by prompting specific searches whenever appropriate. Yet, despite these major improvements, the real impact of TLA on medical decisions stumbles upon the reactiveness of the medical teams when the results are delivered by the laboratory information system or when pushed to the physicians' cell phones.

In the last few years, many countries have experienced a lack of trained microbiological technologists. This problem is further emphasized in the USA. The direct consequences of this shortage in skilled technologists leads to understaffed diagnostic laboratories, which is reflected in delayed analysis results and increased risks for patients (Culbreath et al., 2021; Zimmermann, 2021). Likewise, laboratories have progressively lost their ability to develop customized diagnostic procedures when facing complex cases, not to mention their capability and delay to detect them. In response to this increasing problem, one approach is to optimize the productivity by increasing the number of clinical specimens handled per FTE without compromising the quality nor overloading the staff. TLA has made this possible. Moreover, TLA is devoted to accommodate the constantly increasing demand for clinical bacteriology analyses and to empower the specialized skills of the laboratory technologists by allowing them (i) to dedicate more of their time to the analysis of complex specimens, (ii) to execute new tasks including system troubleshooting (both the instrument and its software), and (iii) to establish, and validate new protocols.

The economic benefits of the implementation of TLA can be measured throughout the increased productivity accompanied by a reduction of the cost per specimen as reported by Culbreath et al. (2021). In this report, the authors determined the economic benefits of the implementation of TLA in four different-sized clinical microbiology labs in North America. They observed that the productivity increased by up to 90%, while the cost per specimen was reduced by up to 47% by using TLA. These measurable improvements led to annual laboratory savings of up to $1.2 million, depending on the size of the lab operations. The integration of the upcoming artificial intelligence tools will ensure further improvement in the efficiency and the quality of the results (Culbreath et al., 2021).

For several years, before the implementation of more stringent laboratory regulation, the practice of using the positive blood culture broth as the inoculum for AST by disk diffusion and some

semi-automated AST methods was widely used to speed up the AST results from positive blood cultures, with an acceptable accuracy. The important factors in favor of this method were the following: i) when growth is detected in a positive blood culture, the concentration of bacteria approximates a 0.5 McFarland, and ii) the overwhelming majority of positive blood cultures is mono-microbial (Banerjee and Humphries, 2021). Nowadays this practice becomes less frequently carried out in modern microbiology laboratories, largely due to the actual laboratory regulations and the arrival of new EUCAST guidelines for rapid AST directly from positive blood culture bottles. This method enables the reading of the inhibition zones of certain drugs as early as 4, 6 and/or 8 hours. The performance of this method has been widely assessed in different centers. Thus, 70% and 80% of the inhibition zones diameters can be accurately interpreted at 4h and 6h, respectively (Akerlund et al., 2020; Jonasson et al., 2020). Overall, the EUCAST rapid AST directly from positive blood culture method remains time consuming and its interpretation is more error-prone. However, the advent of the fully automated antimicrobial disk diffusion susceptibility testing on TLA should facilitate the implementation of this method by accommodating this continuously increasing activity with a minimal workload and a high traceability.

CONCLUSIONS

TLA has now shown able to accommodate the high diversity and complexity of the procedures required for culture-based testing in clinical microbiology laboratories. Its positive impact on various metrics (clinical challenges, productivity, traceability, quality management, and TAT) have also been thoroughly assessed and published. These advantages have most recently been reinforced by the availability of full automation of AST by disk diffusion.

The implementation of artificial intelligence (AI) to rapidly identify bacterial growth (detection), but also to differentiate bacterial morphologies (segmentation) and enumerate the corresponding colonies (counting) will further enhance the workflow and ensure reproducible and predictable performances. Careful validation studies are now warranted to enable negative cultures to be automatically processed using AI and its results automatically released without human intervention. Finally, TLA systems (using the Colibri coupled to the Radian) will facilitate the implementation of EUCAST rapid AST which can bring several advantages regarding patient outcomes.

AUTHOR CONTRIBUTIONS

AC designed the review and wrote the manuscript. JS revised the manuscript. All authors contributed to the article and approved the submitted version.

FUNDING

This study was supported by internal funding.

REFERENCES

Akerlund, A., Jonasson, E., Matuschek, E., Serrander, L., Sundqvist, M., Kahlmeter, G., et al. (2020). EUCAST Rapid Antimicrobial Susceptibility Testing (RAST) in Blood Cultures: Validation in 55 European Laboratories. *J. Antimicrob. Chemother.* 75, 3230–3238. doi: 10.1093/jac/dkaa333

Angeletti, S., Dicuonzo, G., D'Agostino, A., Avola, A., Crea, F., Palazzo, C., et al. (2015). Turnaround Time of Positive Blood Cultures After the Introduction of Matrix-Assisted Laser Desorption-Ionization Time-of-Flight Mass Spectrometry. *New Microbiol.* 38, 379–386.

Banerjee, R., and Humphries, R. (2021). Rapid Antimicrobial Susceptibility Testing Methods for Blood Cultures and Their Clinical Impact. *Front. Med. (Lausanne)* 8, 635831. doi: 10.3389/fmed.2021.635831

Barberis, C., Almuzara, M., Join-Lambert, O., Ramirez, M. S., Famiglietti, A., and Vay, C. (2014). Comparison of the Bruker MALDI-TOF Mass Spectrometry System and Conventional Phenotypic Methods for Identification of Gram-Positive Rods. *PloS One* 9, e106303. doi: 10.1371/journal.pone.0106303

Bourbeau, P. P., and Ledeboer, N. A. (2013). Automation in Clinical Microbiology. *J. Clin. Microbiol.* 51, 1658–1665. doi: 10.1128/JCM.00301-13

Boyanova, L., Kolarov, R., and Mitov, I. (2015). Recent Evolution of Antibiotic Resistance in the Anaerobes as Compared to Previous Decades. *Anaerobe* 31, 4–10. doi: 10.1016/j.anaerobe.2014.05.004

Burckhardt, I. (2018). Laboratory Automation in Clinical Microbiology. *Bioeng. (Basel)* 5 (4), 102. doi: 10.3390/bioengineering5040102

Cheng, C. W. R., Ong, C. H., and Chan, D. S. G. (2020). Impact of BD Kiestra Inoqula Streaking Patterns on Colony Isolation and Turnaround Time of Methicillin-Resistant Staphylococcus Aureus and Carbapenem-Resistant Enterobacterale Surveillance Samples. *Clin. Microbiol. Infect.* 26, 1201–1206. doi: 10.1016/j.cmi.2020.01.006

Chen, X. F., Hou, X., Xiao, M., Zhang, L., Cheng, J. W., Zhou, M. L., et al. (2021). Matrix-Assisted Laser Desorption/Ionization Time of Flight Mass Spectrometry (MALDI-TOF MS) Analysis for the Identification of Pathogenic Microorganisms: A Review. *Microorganisms* 9 (7), 1536. doi: 10.3390/microorganisms9071536

Cherkaoui, A., Emonet, S., Fernandez, J., Schorderet, D., and Schrenzel, J. (2011). Evaluation of Matrix-Assisted Laser Desorption Ionization-Time of Flight Mass Spectrometry for Rapid Identification of Beta-Hemolytic Streptococci. *J. Clin. Microbiol.* 49, 3004–3005. doi: 10.1128/JCM.00240-11

Cherkaoui, A., Fischer, A., Azam, N., Riat, A., and Schrenzel, J. (2018). A Comparison of Sensititre Anaerobe MIC Plate With ATB ANA(R) Test for the Routine Susceptibility Testing of Common Anaerobe Pathogens. *Eur. J. Clin. Microbiol. Infect. Dis.* 37, 2279–2284. doi: 10.1007/s10096-018-3369-5

Cherkaoui, A., Hibbs, J., Emonet, S., Tangomo, M., Girard, M., Francois, P., et al. (2010). Comparison of Two Matrix-Assisted Laser Desorption Ionization-Time of Flight Mass Spectrometry Methods With Conventional Phenotypic Identification for Routine Identification of Bacteria to the Species Level. *J. Clin. Microbiol.* 48, 1169–1175. doi: 10.1128/JCM.01881-09

Cherkaoui, A., Renzi, G., Fischer, A., Azam, N., Schorderet, D., Vuilleumier, N., et al. (2020). Comparison of the Copan Wasplab Incorporating the Biorad Expert System Against the Sirscan 2000 Automatic for Routine Antimicrobial Disc Diffusion Susceptibility Testing. *Clin. Microbiol. Infect.* 26, 619–625. doi: 10.1016/j.cmi.2019.11.008

Cherkaoui, A., Renzi, G., Martischang, R., Harbarth, S., Vuilleumier, N., and Schrenzel, J. (2020). Impact of Total Laboratory Automation on Turnaround Times for Urine Cultures and Screening Specimens for MRSA, ESBL, and VRE Carriage: Retrospective Comparison With Manual Workflow. *Front. Cell Infect. Microbiol.* 10, 552122. doi: 10.3389/fcimb.2020.552122

Cherkaoui, A., Renzi, G., Vuilleumier, N., and Schrenzel, J. (2019). Copan Wasplab Automation Significantly Reduces Incubation Times and Allows

Earlier Culture Readings. *Clin. Microbiol. Infect.* 25, 1430.e5–1430.e12. doi: 10.1016/j.cmi.2019.04.001

Cherkaoui, A., Renzi, G., Vuilleumier, N., and Schrenzel, J. (2021). Performance of Fully Automated Antimicrobial Disk Diffusion Susceptibility Testing Using Copan WASP Colibri Coupled to the Radian in-Line Carousel and Expert System. *J. Clin. Microbiol.* 59, e0077721. doi: 10.1128/JCM.00777-21

Croxatto, A., Prod'hom, G., Faverjon, F., Rochais, Y., and Greub, G. (2016). Laboratory Automation in Clinical Bacteriology: What System to Choose? *Clin. Microbiol. Infect.* 22, 217–235. doi: 10.1016/j.cmi.2015.09.030

Culbreath, K., Piwonka, H., Korver, J., and Noorbakhsh, M. (2021). Benefits Derived From Full Laboratory Automation in Microbiology: A Tale of Four Laboratories. *J. Clin. Microbiol.* 59 (3), e01969–20. doi: 10.1128/JCM.01969-20

Dauwalder, O., Michel, A., Eymard, C., Santos, K., Chanel, L., Luzzati, A., et al. (2021). Use of Artificial Intelligence for Tailored Routine Urine Analyses. *Clin. Microbiol. Infect.* 27, 1168.e1–1168.e6. doi: 10.1016/j.cmi.2020.09.056

Diekema, D. J., and Marchesseault, A. (1999). Clinical Impact of Changing to an Automated Blood-Culture System at a Small Community Hospital. *Clin. Microbiol. Infect.* 5, 590–593. doi: 10.1111/j.1469-0691.1999.tb00444.x

Dolci, A., Giavarina, D., Pasqualetti, S., Szoke, D., and Panteghini, M. (2017). Total Laboratory Automation: Do Stat Tests Still Matter? *Clin. Biochem.* 50, 605–611. doi: 10.1016/j.clinbiochem.2017.04.002

Faron, M. L., Buchan, B. W., Coon, C., Liebregts, T., van Bree, A., Jansz, A. R., et al. (2016a). Automatic Digital Analysis of Chromogenic Media for Vancomycin-Resistant-Enterococcus Screens Using Copan Wasplab. *J. Clin. Microbiol.* 54, 2464–2469. doi: 10.1128/JCM.01040-16

Faron, M. L., Buchan, B. W., and Ledeboer, N. A. (2017). Matrix-Assisted Laser Desorption Ionization-Time of Flight Mass Spectrometry for Use With Positive Blood Cultures: Methodology, Performance, and Optimization. *J. Clin. Microbiol.* 55, 3328–3338. doi: 10.1128/JCM.00868-17

Faron, M. L., Buchan, B. W., Relich, R. F., Clark, J., and Ledeboer, N. A. (2020). Evaluation of the Wasplab Segregation Software to Automatically Analyze Urine Cultures Using Routine Blood and Macconkey Agars. *J. Clin. Microbiol.* 58 (4), e01683–19. doi: 10.1128/JCM.01683-19

Faron, M. L., Buchan, B. W., Samra, H., and Ledeboer, N. A. (2019). Evaluation of Wasplab Software to Automatically Read Chromid CPS Elite Agar for Reporting of Urine Cultures. *J. Clin. Microbiol.* 58 (1), e00540–19. doi: 10.1128/JCM.00540-19

Faron, M. L., Buchan, B. W., Vismara, C., Lacchini, C., Bielli, A., Gesu, G., et al. (2016b). Automated Scoring of Chromogenic Media for Detection of Methicillin-Resistant Staphylococcus Aureus by Use of Wasplab Image Analysis Software. *J. Clin. Microbiol.* 54, 620–624. doi: 10.1128/JCM.02778-15

Ford, B. A., and McElvania, E. (2020). Machine Learning Takes Laboratory Automation to the Next Level. *J. Clin. Microbiol.* 58 (4), e00012–20. doi: 10.1128/JCM.00012-20

Foschi, C., Turello, G., Lazzarotto, T., and Ambretti, S. (2021). Performance of Phenomatrix for the Detection of Group B Streptococcus From Recto-Vaginal Swabs. *Diagn. Microbiol. Infect. Dis.* 101, 115427. doi: 10.1016/j.diagmicrobio.2021.115427

Gaillot, O., Blondiaux, N., Loiez, C., Wallet, F., Lemaitre, N., Herwegh, S., et al. (2011). Cost-Effectiveness of Switch to Matrix-Assisted Laser Desorption Ionization-Time of Flight Mass Spectrometry for Routine Bacterial Identification. *J. Clin. Microbiol.* 49, 4412. doi: 10.1128/JCM.05429-11

Jonasson, E., Matuschek, E., and Kahlmeter, G. (2020). The EUCAST Rapid Disc Diffusion Method for Antimicrobial Susceptibility Testing Directly From Positive Blood Culture Bottles. *J. Antimicrob. Chemother.* 75, 968–978. doi: 10.1093/jac/dkz548

Kaleta, E. J., Clark, A. E., Cherkaoui, A., Wysocki, V. H., Ingram, E. L., Schrenzel, J., et al. (2011). Comparative Analysis of PCR-Electrospray Ionization/Mass Spectrometry (MS) and MALDI-TOF/MS for the Identification of Bacteria and Yeast From Positive Blood Culture Bottles. *Clin. Chem.* 57, 1057–1067. doi: 10.1373/clinchem.2011.161968

Kim, K., Lee, S. G., Kim, T. H., and Lee, S. G. (2022). Economic Evaluation of Total Laboratory Automation in the Clinical Laboratory of a Tertiary Care Hospital. *Ann. Lab. Med.* 42, 89–95. doi: 10.3343/alm.2022.42.1.89

Kim, J., Lee, Y., Park, Y., Kim, M., Choi, J. Y., Yong, D., et al. (2016). Anaerobic Bacteremia: Impact of Inappropriate Therapy on Mortality. *Infect. Chemother.* 48, 91–98. doi: 10.3947/ic.2016.48.2.91

Klein, S., Nurjadi, D., Horner, S., Heeg, K., Zimmermann, S., and Burckhardt, I. (2018). Significant Increase in Cultivation of Gardnerella Vaginalis, Alloscardovia Omnicolens, Actinotignum Schaalii, and Actinomyces Spp. In Urine Samples With Total Laboratory Automation. *Eur. J. Clin. Microbiol. Infect. Dis.* 37, 1305–1311. doi: 10.1007/s10096-018-3250-6

Lainhart, W., and Burnham, C. A. (2018). Enhanced Recovery of Fastidious Organisms From Urine Culture in the Setting of Total Laboratory Automation. *J. Clin. Microbiol.* 56 (8), e00546–18. doi: 10.1128/JCM.00546-18

Lippi, G., and Da Rin, G. (2019). Advantages and Limitations of Total Laboratory Automation: A Personal Overview. *Clin. Chem. Lab. Med.* 57, 802–811. doi: 10.1515/cclm-2018-1323

Mitchell, R., and Ryan, M. D. (1993). Historical Evolution of Automated Blood Culture Systems. *Clin. Microbiol. Newslett.* 15 (14).

Nagy, E., Urban, E., Nord, C. E.Bacteria ESGoARiA (2011). Antimicrobial Susceptibility of Bacteroides Fragilis Group Isolates in Europe: 20 Years of Experience. *Clin. Microbiol. Infect.* 17, 371–379. doi: 10.1111/j.1469-0691.2010.03256.x

Tan, K. E., Ellis, B. C., Lee, R., Stamper, P. D., Zhang, S. X., and Carroll, K. C. (2012). Prospective Evaluation of a Matrix-Assisted Laser Desorption Ionization-Time of Flight Mass Spectrometry System in a Hospital Clinical Microbiology Laboratory for Identification of Bacteria and Yeasts: A Bench-by-Bench Study for Assessing the Impact on Time to Identification and Cost-Effectiveness. *J. Clin. Microbiol.* 50, 3301–3308. doi: 10.1128/JCM.01405-12

Theparee, T., Das, S., and Thomson, R. B. Jr. (2018). Total Laboratory Automation and Matrix-Assisted Laser Desorption Ionization-Time of Flight Mass Spectrometry Improve Turnaround Times in the Clinical Microbiology Laboratory: A Retrospective Analysis. *J. Clin. Microbiol.* 56 (1), e01242–17. doi: 10.1128/JCM.01242-17

Thomson, R. B. Jr., and McElvania, E. (2019). Total Laboratory Automation: What is Gained, What is Lost, and Who can Afford it? *Clin. Lab. Med.* 39, 371–389.

Torres-Sangiao, E., Leal Rodriguez, C., and Garcia-Riestra, C. (2021). Application and Perspectives of MALDI-TOF Mass Spectrometry in Clinical Microbiology Laboratories. *Microorganisms* 9 (7), 1539. doi: 10.3390/microorganisms9071539

Van, T. T., Mata, K., and Dien Bard, J. (2019). Automated Detection of Streptococcus Pyogenes Pharyngitis by Use of Colorex Strep a Chromagar and Wasplab Artificial Intelligence Chromogenic Detection Module Software. *J. Clin. Microbiol.* 57 (11), e00811–19. doi: 10.1128/JCM.00811-19

Verroken, A., Defourny, L., le Polain de Waroux, O., Belkhir, L., Laterre, P. F., Delmee, M., et al. (2016). Clinical Impact of MALDI-TOF MS Identification and Rapid Susceptibility Testing on Adequate Antimicrobial Treatment in Sepsis With Positive Blood Cultures. *PloS One* 11, e0156299. doi: 10.1371/journal.pone.0156299

Zhang, W., Wu, S., Deng, J., Liao, Q., Liu, Y., Xiong, L., et al. (2021). Total Laboratory Automation and Three Shifts Reduce Turnaround Time of Cerebrospinal Fluid Culture Results in the Chinese Clinical Microbiology Laboratory. *Front. Cell Infect. Microbiol.* 11, 765504. doi: 10.3389/fcimb.2021.765504

Zimmermann, S. (2021). Laboratory Automation in the Microbiology Laboratory: An Ongoing Journey, Not a Tale? *J. Clin. Microbiol.* 59 (3), e02592–20. doi: 10.1128/JCM.02592-20

Conflict of Interest: The authors declare that the research was conducted in the absence of any commercial or financial relationships that could be construed as a potential conflict of interest.

frontiers in Cellular and Infection Microbiology

ORIGINAL RESEARCH
published: 17 February 2022
doi: 10.3389/fcimb.2022.848365

Visual Detection of Duck Tembusu Virus With CRISPR/Cas13: A Sensitive and Specific Point-of-Care Detection

*Dongdong Yin[1], Lei Yin[1], Jieru Wang[1], Xuehuai Shen[1], Xiaocheng Pan[1], Hongyan Hou[1], Ruihong Zhao[1], Xiaomiao Hu[1], Guijun Wang[2], Kezong Qi[2] and Yin Dai[1]**

[1] Institute of Animal Husbandry and Veterinary Science, Anhui Academy of Agricultural Sciences, Livestock and Poultry Epidemic Diseases Research Center of Anhui Province, Anhui Province Key Laboratory of Livestock and Poultry Product Safety Engineering, Hefei, China, [2] Anhui Province Key Laboratory of Veterinary Pathobiology and Disease Control College of Animal Science and Technology, Anhui Agricultural University, Hefei, China

OPEN ACCESS

Edited by:
Elena Jordana-Lluch, Balearic Islands Health Research Institute (IdISBa), Spain

Reviewed by:
Quan Liu, Foshan University, China
Bin Zhou, Nanjing Agricultural University, China

***Correspondence:**
Yin Dai
daiyin2020@163.com

Specialty section:
This article was submitted to Clinical Microbiology, a section of the journal Frontiers in Cellular and Infection Microbiology

Received: *04 January 2022*
Accepted: *28 January 2022*
Published: *17 February 2022*

Citation:
Yin D, Yin L, Wang J, Shen X, Pan X, Hou H, Zhao R, Hu X, Wang G, Qi K and Dai Y (2022) Visual Detection of Duck Tembusu Virus With CRISPR/Cas13: A Sensitive and Specific Point-of-Care Detection. Front. Cell. Infect. Microbiol. 12:848365. doi: 10.3389/fcimb.2022.848365

Duck tembusu virus (DTMUV), which causes huge economic losses for the poultry industries in Southeast Asia and China, was first identified in 2010. DTMUV disease has become an important disease that endangers the duck industry. A sensitive, accurate, and convenient DTMUV detection method is an important means to reduce the occurrence of the disease. In this study, a CRISPR/Cas13a system was combined with recombinase polymerase amplification to develop a convenient diagnostic method to detect DTMUV. The novel method was based on isothermal detection at 37°C, and the detection was used for visual readout or real-time analysis. The assay was highly sensitive and specific, with a detection limit of 1 copy/μL of the target gene and showed no cross-reactivity with other pathogens. The enhanced Cas13a detection worked well with clinical samples. Overall, a visual, sensitive, and specific nucleic acid detection method based on CRISPR/Cas13a proved to be a powerful tool for detecting DTMUV.

Keywords: duck tembusu virus, RPA, CRISPR/Cas13a, lateral flow detection, fluorescence detection

INTRODUCTION

In April 2010, a new epidemic disease erupted in breeding ducks and laying ducks in Fujian, Hebei, Zhejiang, Shandong, and other provinces in China. The disease is characterized by a sharp loss of appetite and a significant decline in egg production, causing huge economic losses to the duck industry (Cao et al., 2011; Li et al., 2013). In-depth study of its etiology revealed that the disease is caused by duck tembusu virus (DTMUV). For ducks with high egg production rates, the egg production rate drops rapidly to 20%–30% 4–5 days after disease onset, and production stops about 7 days after disease onset (Homonnay et al., 2014; Thontiravong et al., 2015). The disease has become an important disease that endangers the poultry industry (Chen et al., 2014; Dai et al., 2015; Ti et al., 2015; Lu et al., 2016; Peng et al., 2020). For the prevention and treatment of the virus, it is necessary to detect the disease as early as possible and take as many measures as possible to prevent

the spread of the virus; therefore, the establishment of a sensitive, accurate, and convenient DTMUV detection method is an important means to reduce the occurrence of DTMUV disease.

At present, the detection of DTMUV is usually based on reverse transcription PCR (RT-PCR), real-time RT-PCR, loop-mediated isothermal amplification (LAMP), and virus isolation (Wang et al., 2011; Jiang et al., 2012; Tang et al., 2012; Yan et al., 2012). These methods are time consuming, labor-intensive, and complicated to operate, and rapid and accurate on-site detection of the virus remains difficult. According to the standards of the World Health Organization, ideal pathogen diagnostic tests are cheap, sensitive, specific, easy to use, and fast, and they can be realized without large-scale equipment (Kosack et al., 2017). Point-of-care testing (POCT) helps to improve efficiency, optimize decision making in a timely manner, and reduce costs, especially in resource-constrained areas (Hansen, 2015; Alp, 2018).

Clustered regularly interspaced short palindromic repeats (CRISPR)/CRISPR-associated protein 13a (CRISPR/Cas13a) is a new type of CRISPR system that only targets RNA. It can specifically cleave single-stranded target RNA under the guidance of CRISPR RNA (crRNA) and has collateral cleavage activity (East-Seletsky et al., 2016; Gootenberg et al., 2017). Zhang and colleagues (Kellner et al., 2019) have developed a diagnostic system called SHERLOCK (specific high-sensitivity enzymatic reporter unlocking) based on CRISPR/Cas13a, which can be used to quickly and easily detect a small amount of RNA in clinical samples. Specifically, the SHERLOCK system is an isothermal amplification system that combines recombinase polymerase amplification (RPA), CRISPR/Cas13a, crRNA, and fluorescent reporter molecules. SHERLOCK can achieve visual readings by combining with lateral flow readout, eliminating the dependence on thermal cyclers (Gootenberg et al., 2018). In recent years, CRISPR/Cas13a-based detection has been successfully applied to detect porcine reproductive and respiratory syndrome virus (PRRSV), Avian influenza A (H7N9) virus, and Ebola virus (EBOV) (Liu et al., 2019; Qin et al., 2019; Chang et al., 2020). In this study, a Cas13a detection method combined with RPA, T7 transcription, and the collateral effect of CRISPR/Cas13a was developed for sensitive, specific, equipment-free, and visual detection of DTMUV targeting the conserved DTMUV *E* gene.

MATERIALS AND METHODS

Viruses and Clinical Samples

The DTMUV AH-F10 strain (Zhao et al., 2011) isolated in 2010 in our laboratory was used in the present study (Accession number: KM102539.1). Novel duck parvovirus (NDPV), muscovy duck reovirus (MDRV), duck plague virus (DPV), goose astrovirus (GoAstV), and fowl adenovirus serotype 4 (FAdV-4) were isolated in our laboratory. Newcastle disease virus (NDV) inactivated vaccine was produced by Shandong Lvdu Bio-Sciences & Technology Co., Ltd. 15 tissue samples were collected from different farms.

RPA Primer Design and crRNA Preparation

The RPA primers were selected in the conserved nucleotide region of the *E* gene. The T7 promoter sequence (GAAATTAATACG ACTCACTATAGGG) was appended to the 5′ end of the RPA forward primer. For crRNA preparation, the DNA templates of crRNA were appended with the T7 promoter sequence and synthesized as primers by General Biological System (Anhui) Co. (**Table 1**). The FAM-N6-BHQ1 probe used in the fluorescent reporter assays was synthesized by General Biological System (Anhui) Co. Two oligonucleotides were annealed to a double-stranded DNA by using Annealing Buffer for DNA Oligos (Beyotime, China). The double-stranded DNA was purified by gel extraction. According to the instructions of the HiScribe T7 Quick High Yield RNA Synthesis kit (NEB, USA), the double-stranded DNA was transcribed to crRNA. Finally, crRNA was purified using NucAway™ Spin Columns (Invitrogen, USA) according to the manufacturer's instructions and stored at −80°C.

Nucleic Acid Preparation

The viral genomic nucleic acids of the DTMUV AH-F10 strain, NDPV, MDRV, DPV, GoAstV, FAdV-4, and NDV were extracted with a TIANamp Virus DNA/RNA Kit (Tiangen, China) according to the manufacturer's instructions and stored at −80°C until use.

Cas13a Nucleic Acid Detection

For RPA, 1 μL of cDNA or DNA was amplified in a 50-μL reaction system for 20 min at 37°C, according to the instructions of the Basic isothermal amplification reagent kit-Powder (Magigen, China). For Cas13a detection with lateral flow detection, the Cas13a reaction system consisted of 50 μL containing 22.5 nM crRNA, 45 nM Cas13a (Magiltd, China), 125 nM FAM-N6-BHQ1 probe, 0.25 μL RNase inhibitor, 2.5 μL NTP Buffer Mix, 0.4 μL T7 RNA Polymerase Mix (NEB, USA), and 1 μL RPA products. Cas13a detection was performed at 37°C for 40 min. The detection products were diluted 10 times with Hybridetect Assay Buffer (Magiltd, China), loaded onto the lateral flow strips (Magigen, China), and placed for 5 min to observe the results. For Cas13a detection with fluorescence detection, the FAM-N6-BHQ1 probe was replaced by the RNA reporter (RNAse Alert v2, Thermo Fisher Scientific, USA) in a 50-μL Cas13a reaction system. Reactions were performed in an ABI StepOnePlus™ (Applied Biosystems, USA) instrument at 37°C for 60 min, and fluorescence intensity kinetics was recorded every 5 min.

TABLE 1 | The crRNA, primers, and probes used in this study.

Primers	Sequences(5'-3')
RPA-F	GAAATTAATACGACTCACTATAGGGGAAGCTGAAAGGAATGACC TACCCGATGT
RPA-R	TGACTGTTATCAAGCGTCCAACTGGTGTC
crRNA-F	GATTTAGACTACCCCAAAAACGAAGGGGACTAAAACCCAAAAAC CTGATGAATGCCTTTCCCAA
crRNA-R	TTGGGAAAGGCATTCATCAGGTTTTTGGGTTTTAGTCCCCTTCGT TTTTGGGGTAGTCTAAATC
Probe	FAM-mArArUrGrGrCmAmArArUrGrGrCmA-Bio

Sensitivity and Specificity of the Cas13a Lateral Flow Detection

The E fragments of DTMUV AH-F10 strain were cloned into the pMD-19T vector. Ten-fold serial dilutions of pMD19T-E (1.0×10^8 to 1.0×10^0 copies/μL) were prepared as a template for Cas13a lateral flow detection, then visually observed. The specificity of lateral flow detection was assessed using the genomic cDNA or DNA of a panel of pathogens, including NDPV, MDRV, DPV, GoAstV, NDV, and FAdV-4.

Sensitivity and Specificity of the Cas13a Fluorescence Detection

Aliquots of the DTMUV standard DNA ranging from 1.0×10^8 to 1.0×10^0 copies/μL were prepared as a template for Cas13a l fluorescence detection. The fluorescence intensity was read to determine the limit of detection to evaluate the sensitivity. The specificity of fluorescence detection was assessed using the genomic cDNA or DNA of a panel of pathogens, including NDPV, MDRV, DPV, GoAstV, NDV, and FAdV-4.

Validation With Clinical Samples

A total of 15 ovarian tissue samples were collected from 2018 to 2021 from farms located in Anhui Province where laying ducks had decreased egg production. All samples were used to confirm the applicability of DTMUV-specific lateral flow and fluorescence assays in clinical diagnosis. Then, the results were compared with those obtained with RT-PCR described previously (Liu et al., 2013), which was run in parallel for the above clinical samples. The studies involving animals were reviewed and approved by the Ethics Committee of Anhui Academy of Agricultural Sciences, and the owners of animals provided written informed consent to participate in this study.

RESULTS

Validation of the Cas13a Detection

We performed RPA combined with CRISPR/Cas13a to detect DTMUV according to the schematic diagram in **Figure 1**. To verify the effectiveness of the designed primers, we performed Cas13a experiments using the RPA products as templates. The experimental group showed that lateral flow detection strips of DTMUV appeared as obvious positive bands (**Figure 2A**). As shown in **Figure 2B**, the fluorescence units of the positive group increased rapidly with time until the peak value, while the negative group had no value. The results indicated that the Cas13a lateral flow and fluorescence detection could be used to detect DTMUV.

Specificity and Sensitivity of the Cas13a Lateral Flow Detection

When the analytical specificity analysis was conducted, the positive band was observed on the lateral flow detection strip of DTMUV, and the lateral flow detection strips of five other viruses had no positive bands (**Figure 3A**). As the analytical sensitivity analysis proceeded, positive bands could be observed in the test line on the strips with 1.0×10^8 to 1.0×10^0 copies of DTMUV standard DNA serving as the template (**Figure 3B**). Thus, the detection limit of the Cas13a lateral flow detection was 1 copy/μL. As mentioned above, these results revealed that the Cas13a lateral flow detection for DTMUV was highly specific and sensitive.

Specificity and Sensitivity of the Cas13a Fluorescence Detection

In the analytical specificity analysis, only DTMUV was amplified with the development of a typical fluorescence curve, and there was no cross-reaction with other viruses (**Figure 4A**),

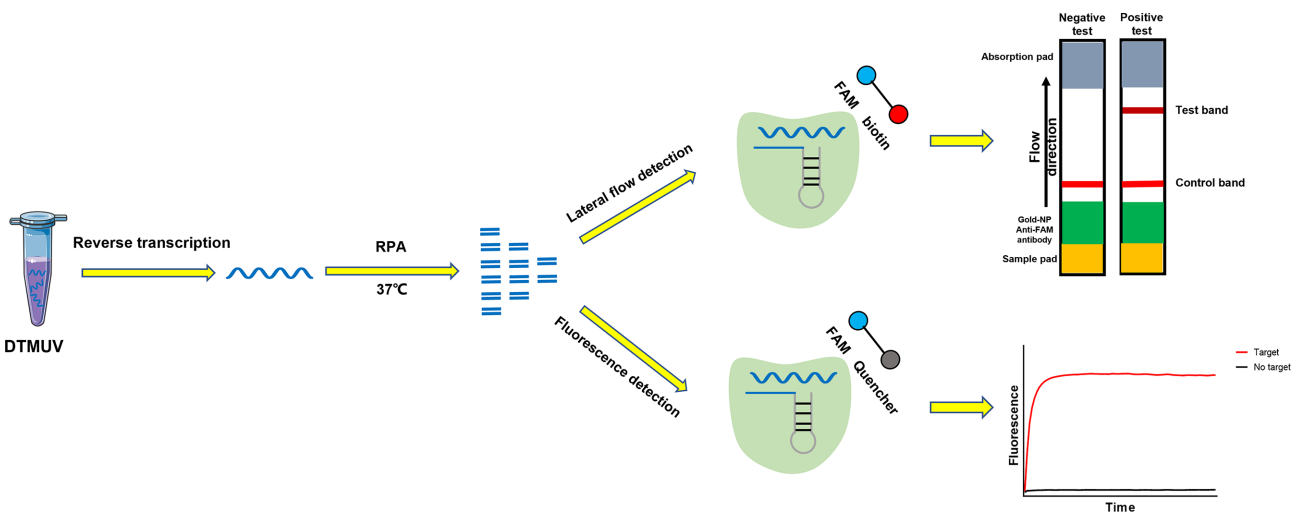

FIGURE 1 | Schematic illustration of the workflow for Cas13a DTMUV testing.

FIGURE 2 | Performance of DTMUV Cas13a lateral flow and fluorescence detection. **(A)** Analysis of DTMUV by Cas13a lateral flow detection. **(B)** Analysis of DTMUV by Cas13a fluorescence detection. *n* = 3 technical replicates; values represent mean ± SEM.

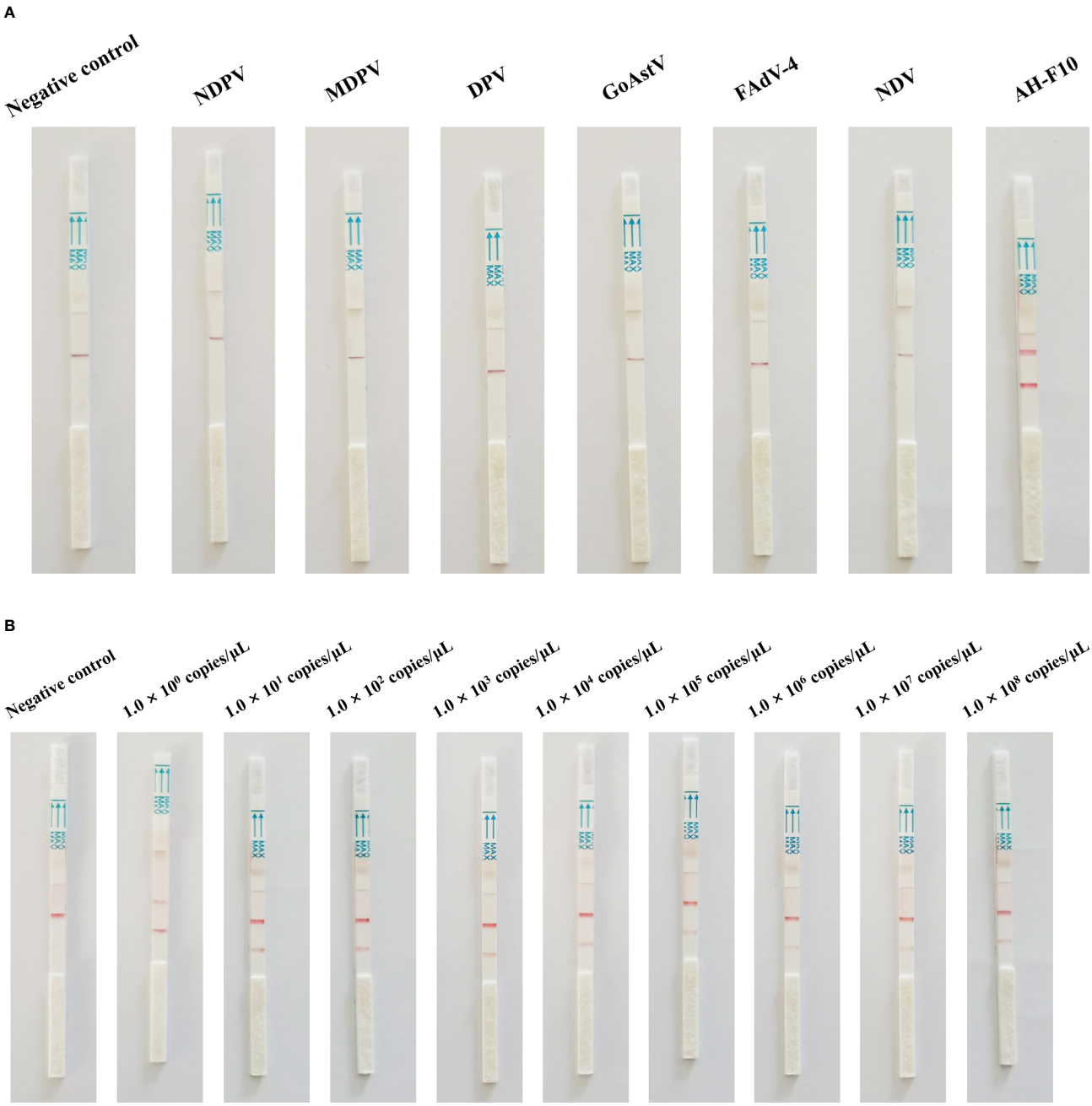

FIGURE 3 | Specificity and sensitivity of Cas13a lateral flow detection. **(A)** Specificity of Cas13a lateral flow detection. **(B)** Sensitivity of Cas13a lateral flow detection.

suggesting that Cas13a fluorescence detection could be used for the specific detection of DTMUV. The sensitivity of the Cas13a fluorescence detection was tested with 10-fold serially diluted template DTMUV standard DNA. As shown in **Figure 4B**, nine orders of magnitude from 1.0×10^8 copies/μL down to 1.0×10^0 copies/μL template could be detected. These data showed that the detection limit of Cas13a fluorescence detection was 1 copy/μL.

Cas13a Detection in Clinical Samples

To verify the application of Cas13a lateral flow and fluorescence detection in clinical samples, 15 tissue samples collected from different farms were detected by Cas13a lateral flow, fluorescence detection, and RT-qPCR. Six tissue samples were DTMUV-positive, and nine samples were DTMUV-negative, as determined by Cas13a lateral flow detection. Cas13a fluorescence detection and RT-qPCR displayed the same results as Cas13a

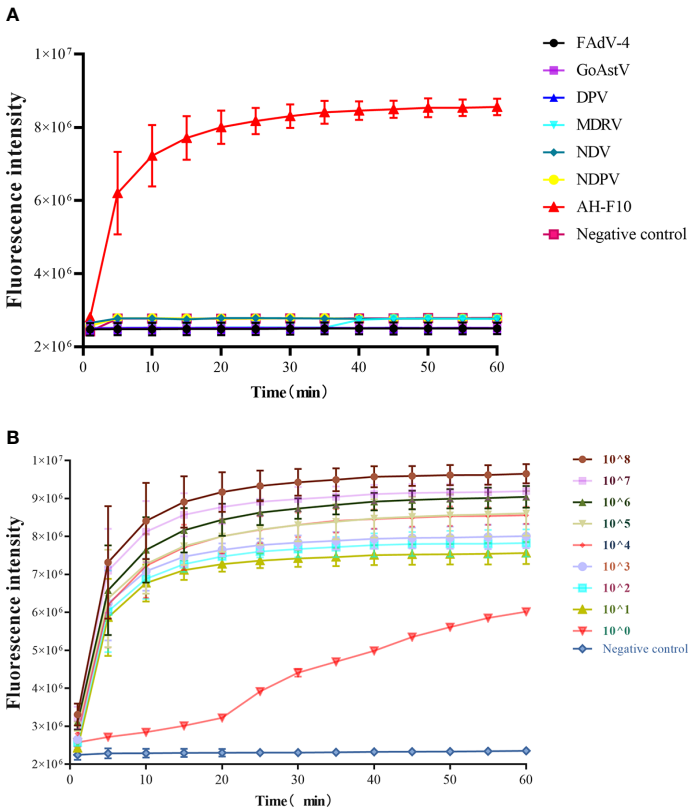

FIGURE 4 | Specificity and sensitivity of Cas13a fluorescence detection. **(A)** Specificity of Cas13a fluorescence detection. **(B)** Sensitivity of Cas13a fluorescence detection. *n* = 3 technical replicates; values represent mean ± SEM.

lateral flow detection in clinical samples (**Table 2**). These data indicated that Cas13a lateral flow and fluorescence detection could be used in clinical samples, and Cas13a lateral flow detection does not require expensive equipment.

DISCUSSION

DTMUV disease was first discovered in parts of southern China in April 2010. DTMUV disease mainly affects ducks in the laying stage (Cao et al., 2011; Li et al., 2013). The disease causes a sharp drop in egg production, resulting in serious economic losses to laying duck farmers, and has a great impact on the breeding industry. Although a DTMUV vaccine has been applied to poultry farms, DTMUV outbreaks still occur in many areas (Lu et al., 2016; Peng et al., 2020; Zhu et al., 2021). Therefore, timely monitoring of DTMUV through diagnosis is essential for early control of the epidemic. At present, most of the available DTMUV detection methods have many shortcomings, such as not being suitable for field detection and low sensitivity. Ideal diagnostic methods are inexpensive, accurate, fast, and easy to operate, and should not require specialized equipment. Therefore, there is an urgent need to develop a specific and sensitive DTMUV detection method with minimal equipment requirements.

In this study, a new method for DTMUV nucleic acid detection based on CRISPR/Cas13a was established, which could detect DTMUV with minimal equipment. In order to determine the appropriate target region, a set of DTMUV genomes were compared and analyzed. According to the comparison results, the RPA primer and crRNA of the DTMUV *E* gene were designed. In Yan et al.'s study, the detection limit of real-time PCR based on a TaqMan probe was 50 copies per reaction (Yan et al., 2012). In Yun et al.'s study, the detection limit of the real-time PCR method based on minor groove binding was 10 copies per reaction (Yun et al., 2012). The RT-PCR method established by Liu et al., (2013) can detect 20 copies per reaction. In addition, the detection limit of the LAMP method established by Tang et al. can reach 10 copies per

TABLE 2 | Detection results of clinical samples in Cas13a lateral flow detection, Cas13a fluorescence detection, and RT-qPCR assays.

Assay	Number of samples	
	Positive	Negative
RT-qPCR	6	9
Cas13a lateral flow detection	6	9
Cas13a fluorescence detection	6	9

reaction, and it does not require much equipment (Tang et al., 2012), but it still has shortcomings such as high target selectivity and cross-contamination, which render the method unsuitable for laboratory research. The method established in this study had a low detection limit of 1 copy/μL for DTMUV and was hence more sensitive than the above method.

Cas13a detection can not only be used for the analysis of fluorescence detection samples but can also be combined with lateral flow detection for visual readout, making it available for use both in the laboratory and in the field. At the same time, the combination of RPA and crRNA-specific sequence identification makes Cas13a detection more specific (Gootenberg et al., 2017). In addition, another important advantage is that Cas13a detection is performed at 37°C, which is convenient for use in poorly equipped laboratories or in the field (Gootenberg et al., 2017; Gootenberg et al., 2018; Myhrvold et al., 2018). The Cas13a detection method has been applied to the detection of other pathogens. Myhrvold et al. utilizes the Cas13-based SHERLOCK platform to detect Zika virus (ZIKV) and dengue virus (DENV) in patient samples at concentrations as low as 1 copy per microliter. Chang et al. used this method to detect PRRSV with specificity and sensitivity, and it was successfully applied to detect clinical specimens from different farms. In conclusion, this method provides a new technical means for the molecular detection of pathogens.

In conclusion, a visual and reliable nucleic acid detection method based on CRISPR/Cas13a was established to identify DTMUV. This is the first report using Cas13a methods to detect DTMUV. The novel method had the advantages of high specificity, high sensitivity, and minimal equipment, particularly in resource-poor settings.

DATA AVAILABILITY STATEMENT

The original contributions presented in the study are included in the article/supplementary material. Further inquiries can be directed to the corresponding author.

AUTHOR CONTRIBUTIONS

DY conceived and designed the experiments. DY, LY, and JW were responsible for sampling and sample testing. HH, XP, and XS analyzed the data. DY, RZ, and XH wrote the paper. GW, KQ, and YD edited the paper. All authors contributed to the article and approved the submitted version.

FUNDING

This study was supported financially by the Major Science and Technology Special Project in Anhui Province (No. 202003a06020012), the Anhui Academy of Agricultural Sciences Platform Project (No. 2021YL065), and the Anhui Province Poultry Industry Technology System (No. AHCYJSTX-06).

REFERENCES

Alp, A. (2018). Advancement in POCT Molecular Testing: The Multiplex PCR POCT Devices for Infectious Diseases. *EJIFCC* 29, 205–209.

Cao, Z., Zhang, C., Liu, Y., Liu, Y., Ye, W., Han, J., et al. (2011). Tembusu Virus in Ducks, China. *Emerg. Infect. Dis.* 17, 1873–1875. doi: 10.3201/eid1710.101890

Chang, Y., Deng, Y., Li, T., Wang, J., Wang, T., Tan, F., et al. (2020). Visual Detection of Porcine Reproductive and Respiratory Syndrome Virus Using CRISPR-Cas13a. *Transbound Emerg. Dis.* 67, 564–571. doi: 10.1111/tbed.13368

Chen, S., Wang, S., Li, Z., Lin, F., Cheng, X., Zhu, X., et al. (2014). Isolation and Characterization of a Chinese Strain of Tembusu Virus From Hy-Line Brown Layers With Acute Egg-Drop Syndrome in Fujian, China. *Arch. Virol.* 159, 1099–1107. doi: 10.1007/s00705-013-1931-0

Dai, L., Li, Z., and Tao, P. (2015). Evolutionary Analysis of Tembusu Virus: Evidence for the Emergence of a Dominant Genotype. *Infect. Genet. Evol.* 32, 124–129. doi: 10.1016/j.meegid.2015.03.004

East-Seletsky, A., O'Connell, M. R., Knight, S. C., Burstein, D., Cate, J. H., Tjian, R., et al. (2016). Two Distinct RNase Activities of CRISPR-C2c2 Enable Guide-RNA Processing and RNA Detection. *Nature* 538, 270–273. doi: 10.1038/nature19802

Gootenberg, J. S., Abudayyeh, O. O., Kellner, M. J., Joung, J., Collins, J. J., and Zhang, F. (2018). Multiplexed and Portable Nucleic Acid Detection Platform With Cas13, Cas12a, and Csm6. *Science* 360, 439–444. doi: 10.1126/science.aaq0179

Gootenberg, J. S., Abudayyeh, O. O., Lee, J. W., Essletzbichler, P., Dy, A. J., Joung, J., et al. (2017). Nucleic Acid Detection With CRISPR-Cas13a/C2c2. *Science* 356, 438–442. doi: 10.1126/science.aam9321

Hansen, G. T. (2015). POCT in Clinical Microbiology May Be a Pathway to Better Patient Care. *MLO Med. Lab. Obs.* 47, 26–27.

Homonnay, Z. G., Kovacs, E. W., Banyai, K., Albert, M., Feher, E., Mato, T., et al. (2014). Tembusu-Like Flavivirus (Perak Virus) as the Cause of Neurological Disease Outbreaks in Young Pekin Ducks. *Avian Pathol.* 43, 552–560. doi: 10.1080/03079457.2014.973832

Jiang, T., Liu, J., Deng, Y. Q., Su, J. L., Xu, L. J., Liu, Z. H., et al. (2012). Development of RT-LAMP and Real-Time RT-PCR Assays for the Rapid Detection of the New Duck Tembusu-Like BYD Virus. *Arch. Virol.* 157, 2273–2280. doi: 10.1007/s00705-012-1431-7

Kellner, M. J., Koob, J. G., Gootenberg, J. S., Abudayyeh, O. O., and Zhang, F. (2019). SHERLOCK: Nucleic Acid Detection With CRISPR Nucleases. *Nat. Protoc.* 14, 2986–3012. doi: 10.1038/s41596-019-0210-2

Kosack, C. S., Page, A. L., and Klatser, P. R. (2017). A Guide to Aid the Selection of Diagnostic Tests. *Bull. World Health Organ* 95, 639–645. doi: 10.2471/BLT.16.187468

Liu, Z., Fu, Y., Ji, Y., Wei, J., Cai, X., and Zhu, Q. (2013). Development and Validation of One-Step SYBR Green Real-Time RT-PCR for the Rapid Detection of Newly Emerged Duck Tembusu Virus. *Avian Dis.* 57, 595–601. doi: 10.1637/10484-010713-Reg.1

Liu, Y., Xu, H., Liu, C., Peng, L., Khan, H., Cui, L., et al. (2019). CRISPR-Cas13a Nanomachine Based Simple Technology for Avian Influenza A (H7N9) Virus on-Site Detection. *J. BioMed. Nanotechnol.* 15, 790–798. doi: 10.1166/jbn.2019.2742

Li, S., Zhang, L., Wang, Y., Wang, S., Sun, H., Su, W., et al. (2013). An Infectious Full-Length cDNA Clone of Duck Tembusu Virus, A Newly Emerging Flavivirus Causing Duck Egg Drop Syndrome in China. *Virus Res.* 171, 238–241. doi: 10.1016/j.virusres.2012.10.019

Lu, Y., Dou, Y., Ti, J., Wang, A., Cheng, B., Zhang, X., et al. (2016). The Effect of Tembusu Virus Infection in Different Week-Old Cherry Valley Breeding Ducks. *Vet. Microbiol.* 192, 167–174. doi: 10.1016/j.vetmic.2016.07.017

Myhrvold, C., Freije, C. A., Gootenberg, J. S., Abudayyeh, O. O., Metsky, H. C., Durbin, A. F., et al. (2018). Field-Deployable Viral Diagnostics Using CRISPR-Cas13. *Science* 360, 444–448. doi: 10.1126/science.aas8836

Peng, S. H., Su, C. L., Chang, M. C., Hu, H. C., Yang, S. L., and Shu, P. Y. (2020). Genome Analysis of a Novel Tembusu Virus in Taiwan. *Viruses* 12, 567. doi: 10.3390/v12050567

Qin, P., Park, M., Alfson, K. J., Tamhankar, M., Carrion, R., Patterson, J. L., et al. (2019). Rapid and Fully Microfluidic Ebola Virus Detection With CRISPR-Cas13a. *ACS Sens.* 4, 1048–1054. doi: 10.1021/acssensors.9b00239

Tang, Y., Diao, Y., Yu, C., Gao, X., Chen, L., and Zhang, D. (2012). Rapid Detection of Tembusu Virus by Reverse-Transcription, Loop-Mediated Isothermal Amplification (RT-LAMP). *Transbound Emerg. Dis.* 59, 208–213. doi: 10.1111/j.1865-1682.2011.01257.x

Thontiravong, A., Ninvilai, P., Tunterak, W., Nonthabenjawan, N., Chaiyavong, S., Angkabkingkaew, K., et al. (2015). Tembusu-Related Flavivirus in Ducks, Thailand. *Emerg. Infect. Dis.* 21, 2164–2167. doi: 10.3201/eid2112.150600

Ti, J., Zhang, L., Li, Z., Zhao, D., Zhang, Y., Li, F., et al. (2015). Effect of Age and Inoculation Route on the Infection of Duck Tembusu Virus in Goslings. *Vet. Microbiol.* 181, 190–197. doi: 10.1016/j.vetmic.2015.10.001

Wang, Y., Yuan, X., Li, Y., Yu, K., Yang, J., Xu, H., et al. (2011). Rapid Detection of Newly Isolated Tembusu-Related Flavivirus by Reverse-Transcription Loop-Mediated Isothermal Amplification Assay. *Virol. J.* 8, 553. doi: 10.1186/1743-422X-8-553

Yan, L., Peng, S., Yan, P., Zhou, J., Teng, Q., Li, G., et al. (2012). Comparison of Real-Time Reverse Transcription Loop-Mediated Isothermal Amplification and Real-Time Reverse Transcription Polymerase Chain Reaction for Duck Tembusu Virus. *J. Virol. Methods* 182, 50–55. doi: 10.1016/j.jviromet.2012.03.007

Yun, T., Ni, Z., Hua, J., Ye, W., Chen, L., Zhang, S., et al. (2012). Development of a One-Step Real-Time RT-PCR Assay Using a Minor-Groove-Binding Probe for the Detection of Duck Tembusu Virus. *J. Virol. Methods* 181, 148–154. doi: 10.1016/j.jviromet.2012.01.019

Zhao, Y., Li, C., Zhu, L., Zhan, S., Wang, H., Wei, J., et al. (2011). Clinical Diagnosis and Pathogenic Identification of Egg Drop-Death Syndrome in Duck. *J. Yangzhou Univ. Agric. Life Sci. Ed.* 32, 11–14. doi: 10.16872/j.cnki.1671-4652.2011.03.004

Zhu, Y., Hu, Z., Lv, X., Huang, R., Gu, X., Zhang, C., et al. (2021). A Novel Tembusu Virus Isolated From Goslings in China Form a New Subgenotype 2.1.1. *Transbound Emerg. Dis.* doi: 10.1111/tbed.14155

Conflict of Interest: The authors declare that the research was conducted in the absence of any commercial or financial relationships that could be construed as a potential conflict of interest.

Publisher's Note: All claims expressed in this article are solely those of the authors and do not necessarily represent those of their affiliated organizations, or those of the publisher, the editors and the reviewers. Any product that may be evaluated in this article, or claim that may be made by its manufacturer, is not guaranteed or endorsed by the publisher.

frontiers in Cellular and Infection Microbiology

REVIEW
published: 16 March 2022
doi: 10.3389/fcimb.2022.859935

Diagnosis and Management of Bloodstream Infections With Rapid, Multiplexed Molecular Assays

Sherry A. Dunbar, Christopher Gardner and Shubhagata Das*

Luminex Corporation, A DiaSorin Company, Austin, TX, United States

Bloodstream infection is a major health concern, responsible for considerable morbidity and mortality across the globe. Prompt identification of the responsible pathogen in the early stages of the disease allows clinicians to implement appropriate antibiotic therapy in a timelier manner. Rapid treatment with the correct antibiotic not only improves the chances of patient survival, but also significantly reduces the length of hospital stay and associated healthcare costs. Although culture has been the gold standard and most common method for diagnosis of bloodstream pathogens, it is being enhanced or supplanted with more advanced methods, including molecular tests that can reduce the turnaround time from several days to a few hours. In this article, we describe two rapid, molecular bloodstream infection panels that identify the most common pathogens and associated genetic determinants of antibiotic resistance – the Luminex® VERIGENE® Gram-Positive Blood Culture Test and the VERIGENE® Gram-Negative Blood Culture Test. We conducted a search on PubMed to retrieve articles describing the performance and impact of these tests in the clinical setting. From a total of 48 articles retrieved, we selected 15 for inclusion in this review based on the type and size of the study and so there would be minimum of three articles describing performance and three articles describing the impact post-implementation for each assay. Here we provide a comprehensive review of these publications illustrating the performance and clinical utility of these assays, demonstrating how genotypic tests can benefit diagnostic and antimicrobial stewardship efforts.

Keywords: bloodstream infection, molecular diagnostics, microarray, antimicrobial stewardship, antibiotic resistance

OPEN ACCESS

Edited by:
Nicasio Mancini,
Vita-Salute San Raffaele University, Italy

Reviewed by:
Gabriel Motoa,
Jackson Health System, United States
M. Jahangir Alam,
University of Houston, United States

****Correspondence:***
Sherry A. Dunbar
sdunbar@luminexcorp.com

Specialty section:
This article was submitted to Clinical Microbiology, a section of the journal Frontiers in Cellular and Infection Microbiology

Received: *22 January 2022*
Accepted: *21 February 2022*
Published: *16 March 2022*

Citation:
Dunbar SA, Gardner C and Das S (2022) Diagnosis and Management of Bloodstream Infections With Rapid, Multiplexed Molecular Assays. Front. Cell. Infect. Microbiol. 12:859935. doi: 10.3389/fcimb.2022.859935

INTRODUCTION

Bloodstream infection (BSI) is a serious, life-threatening illness and a major cause of morbidity and mortality worldwide (Santella et al., 2020; Timsit et al., 2020). Estimates have indicated that BSI affects approximately 30 million people each year, leading to 6 million deaths (Wisplinghoff et al., 2004; Fleischmann et al., 2016). The outcome of BSI can depend on host-specific factors (including age and underlying comorbidities) and microbiological aspects (including the type of the infecting organism and antibiotic susceptibility), but some estimates have indicated that the mortality rate can be as high as 25% to 80% (Kollef et al., 2011; Levy et al., 2014). Prompt initiation of suitable

antimicrobial therapy is vital and can significantly improve patient management and decrease the mortality rate in bacteremic patients (Leibovici et al., 1998; Kumar et al., 2006).

Gram-positive pathogens are involved in >50% of all bacterial bloodstream infections, and coagulase-negative staphylococci (CoNS), *Staphylococcus aureus*, and *Enterococcus* spp. are the most often isolated gram-positive bacteria in blood cultures (Beekmann et al., 2003; Wisplinghoff et al., 2004; Grozdanovski et al., 2012). At least 30% of hospital-acquired BSIs are due to gram-negative bacteria (Gaynes and Edwards, 2005; Diekema et al., 2019). Infections caused by these pathogens, particularly in hospital-acquired infections, have been linked to a 15% to 29% higher mortality as compared to case controls (Wisplinghoff et al., 2003; Al-Hasan et al., 2012). This is especially true for infections with multidrug-resistant organisms, such as those harboring extended-spectrum β-lactamases (ESBLs) or carbapenemases (Schwaber et al., 2006; Patel et al., 2008; Kaye and Pogue, 2015; Kern and Rieg, 2020).

Although culture with biochemical and susceptibility testing has long been the standard method for diagnosis of bloodstream pathogens, it is being enhanced and, in some cases, supplanted with more advanced methods (Idelevich et al., 2018; Lamy et al., 2020). Among these new and more rapid diagnostic methods are molecular tests that can reduce the turnaround time from several days to a few hours. While implementation of these rapid diagnostics tests may add cost to the clinical microbiology laboratory, they can transform the management of BSI patients by providing antimicrobial stewardship teams the opportunity to quickly escalate therapy and improve patient outcomes through prompt organism identification and detection of resistance determinants, and thus provide a net financial benefit to the institution (Walker et al., 2016).

In this article, we describe two of these rapid molecular bloodstream infection panels, the Luminex® VERIGENE® Gram-Positive Blood Culture Test (BC-GP) and the VERIGENE® Gram-Negative Blood Culture Test (BC-GN), and review some of the key publications that demonstrate the performance and clinical utility of these tests which illustrate how genotypic tests can benefit both diagnostic and antimicrobial stewardship programs. For this review, we conducted a literature search in PubMed® (https://pubmed.ncbi.nlm.nih.gov/) on the product name of each panel. We retrieved a total of 48 citations published between 2013 and 2020. Studies were considered for inclusion if they described a performance evaluation, clinical or economic effects post-implementation, conventional methods were used as comparators, and the research was conducted in a clinical laboratory setting. Publications were then ordered based on the study size or number of samples or subjects included, and selected so that there would be a minimum of three publications on performance and three on clinical/economic impact for each assay. Studies were excluded if the comparator was not an IVD-cleared test. A total of fifteen representative studies have been described for this review.

The VERIGENE Blood Culture Nucleic Acid tests are qualitative, multiplexed *in vitro* diagnostic tests for the simultaneous detection and identification of bacteria which may cause BSI (Luminex, 2021a). The tests are performed directly on media from blood culture bottles that have been identified as positive (by a continuous monitoring blood culture system), using the sample-to-answer VERIGENE® System.

The VERIGENE System is a moderately complex sample-to-answer molecular diagnostic instrument for direct or post-PCR detection of specific nucleic acid targets (Luminex, 2021b). The system is comprised of the VERIGENE Reader (reader), the Processor SP (sample processor), and the consumables for the specific assay, which include the VERIGENE Test Cartridge (test cartridge), extraction tray, pipette assembly, and utility/amp tray (**Figure 1**). The reader can be connected to either one or

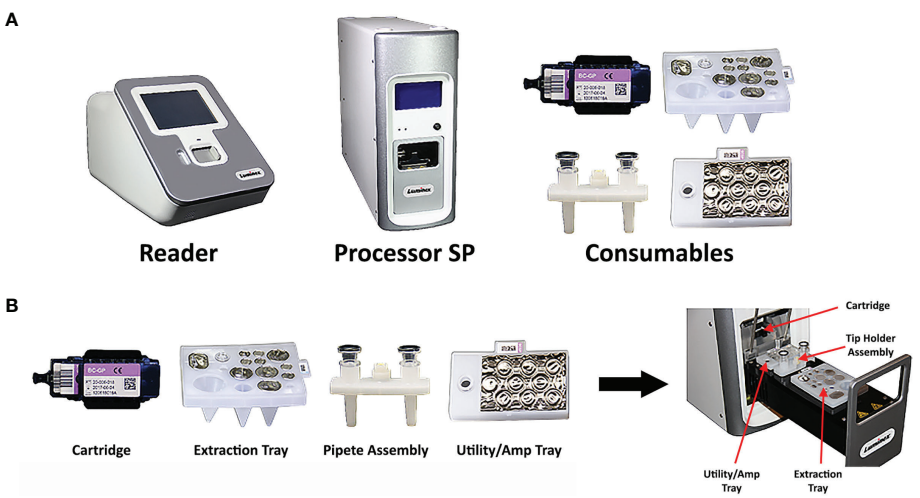

FIGURE 1 | Composition of the VERIGENE® System. **(A)** The VERIGENE System includes the VERIGENE Reader, the Processor SP, and the consumables for the specific assay. **(B)** The VERIGENE test consumables include the VERIGENE Test Cartridge, the extraction tray, the pipette assembly, and the utility/amp tray.

multiple processors. The reader handles sample information, reads the results from test cartridges, and allows the results to be printed, and also provides internal data storage and laboratory information system (LIS) connectivity without the need for an external computer. The processor is a modular, benchtop analysis unit that conducts automated nucleic acid extraction, purification, amplification, and hybridization in each module. The system allows users to run tests as needed in response to testing requirements, without the need for batching, and it is scalable to allow laboratories to customize the throughput to meet their specific needs. The system features a simple user interface and does not require extensive training or specialized facilities. The test cartridges are self-contained, single-use units consisting of a microfluidic cassette containing the hybridization reagents which also captures the waste generated during test processing (the Reagent Pack), and a glass slide as the solid support for the microarray that captures the targeted nucleic acids (the Substrate Holder). Each test cartridge can be used for analysis of one patient sample.

The VERIGENE NanoGrid™ Technology is a novel, proprietary gold nanoparticle probe chemistry that is used for all VERIGENE tests. The gold nanoparticles are 13-20 nanometers (nm) in diameter and can be functionalized with either a defined number of oligonucleotides (oligos) specific for a DNA or RNA target of interest, or a defined number of antibodies specific to a protein of interest. Gold nanoparticle probes can allow for sensitivity that is several orders of magnitude higher as compared to fluorophores (Huang and El-Sayed, 2010). They also enable high specificity for nucleic acid or protein detection and reduce background noise, which creates an enhanced assay signal through an improved signal-to-noise ratio. Gold nanoparticle probes are also stable with a long shelf-life and are non-toxic.

The detection of nucleic acid targets on the VERIGENE System includes: 1) automated nucleic acid extraction and fragmentation (or PCR amplification) from a clinical sample on the processor; 2) automated transfer of the processed nucleic acids into a test cartridge for hybridization; 3) primary hybridization of the target DNA to capture oligos on the microarray; 4) secondary hybridization of specific mediator oligos and gold nanoparticle probes; 5) signal amplification of hybridized probes through silver staining; and 6) automated qualitative reading and analysis of the results on the reader. The time to result from sample input to result is less than two hours. An overview of the workflow as compared to conventional culture methods is shown in **Figure 2**.

Two separate tests are available, for either gram-positive or gram-negative bacteria, and the appropriate test is selected based on the type(s) of bacteria present in the positive blood culture bottle, as determined by Gram stain. The BC-GP and BC-GN tests detect and identify the bacterial species, genera, and resistance markers as shown in **Tables 1** and **2**, respectively. The VERIGENE bloodstream infection tests allow laboratories to quickly identify bacterial pathogens, as well as their resistance markers. Published studies have shown that these assays lower overall hospital costs, shorten a patient's length of hospital stay, and improve patient outcomes by supporting a more targeted treatment plan quicker than traditional methods (Rivard et al., 2017). The assays have also been shown to coordinate well with antimicrobial stewardship programs (ASPs), decrease the use of unnecessary antibiotics, and efficiently help manage infection control. (Box et al., 2015; Rivard et al., 2017). A review on cost-effectiveness of rapid diagnostic tests for BSIs found that implementation of BC-GP and BC-GN with an ASP was associated with lower costs than baseline strategy and is a cost-effective approach, although sensitivity analysis showed that the effectiveness is dependent on the probability of mortality or survival (Pliakos et al., 2018).

PERFORMANCE

The Luminex® VERIGENE® Gram-Positive Blood Culture Test

The clinical performance of the VERIGENE BC-GP test was established in a study conducted at five hospital sites geographically distributed across the United States (Luminex, 2020c). A total of 1642 specimens were included in the

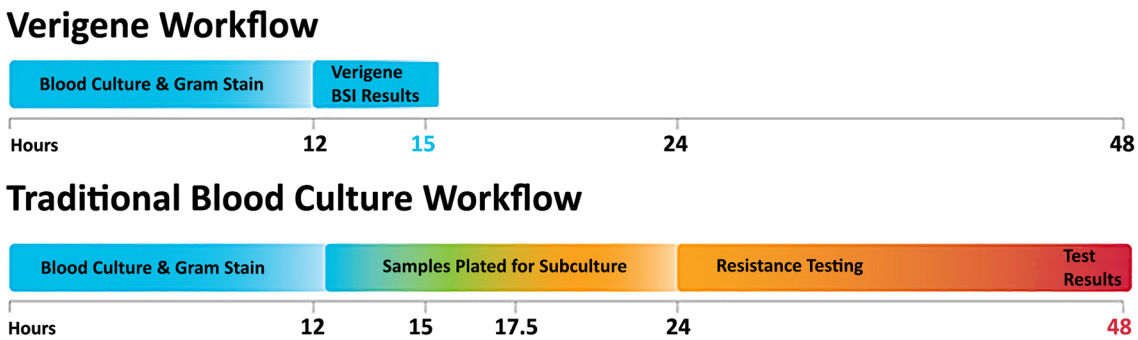

FIGURE 2 | The VERIGENE® workflow as compared to traditional blood culture. Positive blood cultures are evaluated by Gram stain and the appropriate VERIGENE Blood Culture Nucleic Acid Test is selected. Set-up, running the test, and reporting can be easily completed within 3 hours. With traditional culture-based workflows, subculture can add an additional 12 hours, and resistance testing (when required) can add another day so that the final results may not be available for 48 hours.

TABLE 1 | Targets included in the VERIGENE Gram-Positive Blood Culture test.

Species	Genus	Group	Resistance
Staphylococcus aureus	*Staphylococcus* spp.	*Streptococcus anginosus*	*mecA* (methicillin)
Staphylococcus epidermidis	*Streptococcus* spp.		*vanA* (vancomycin)
Staphylococcus lugdunensis	*Micrococcus* spp.[a]		*vanB* (vancomycin)
Streptococcus agalactiae	*Listeria* spp.		
Streptococcus pneumoniae			
Streptococcus pyogenes			
Enterococcus faecalis			
Enterococcus faecium			

[a]*Micrococcus spp. is not IVD-cleared in the United States.*

TABLE 2 | Targets included in the VERIGENE Gram-Negative Blood Culture test.

Species	Genus	Resistance
Escherichia coli[a]	*Acinetobacter* spp.	CTX-M (ESBL)
Klebsiella pneumoniae	*Citrobacter* spp.	IMP (carbapenemase)
Klebsiella oxytoca	*Enterobacter* spp.	KPC (carbapenemase)
Pseudomonas aeruginosa	*Proteus* spp.	NDM (carbapenemase)
Serratia marcescens[b]		OXA (carbapenemase)
		VIM (carbapenemase)

[a]*Test does not distinguish Escherichia coli from Shigella spp. (S. dysenteriae, S. flexneri, S. boydii, and S. sonnei).*
[b]*Serratia marcescens is not IVD-cleared in the United States.*

comparison, comprised of 1426 prospectively collected specimens (1251 fresh and 175 frozen) and 216 simulated specimens utilized for organisms not frequently found in the prospective specimens (i.e., *Streptococcus lugdunensis*, *Streptococcus agalactiae*, *Streptococcus anginosus* group, *Streptococcus pyogenes*, and *Listeria* spp.). The simulated specimens were prepared from glycerol stocks grown on blood agar plates and individual colonies were used to inoculate standard aerobic blood culture media bottles containing whole blood. Blood culture specimens positive by culture using either BACTEC™ Plus Aerobic/F or BacT/ALERT FA FAN® Aerobic blood culture bottles and identified as gram-positive were then processed according to conventional biochemical, culture, and bidirectional sequencing identification methods as the reference comparators. The positive percent agreement (PPA), negative percent agreement (NPA), and the two-sided 95% confidence limits (95% CI) observed for detection of each organism and resistance marker (i.e., *mecA* detection with *Staphylococcus aureus* and *Staphylococcus epidermidis* and *vanA*/*vanB* detection with *Enterococcus faecalis* and *Enterococcus faecium*) are shown in **Table 3**. Other *Staphylococcus* spp. were not tested for methicillin resistance by cefoxitin disk; however, 12 tested positive for *S. epidermidis* and *mecA* by BC-GP and were counted as false positives for *mecA*. Altogether, there were 98 mixed specimens of which 6 were detected by BC-GP only, 25 were detected by the reference method(s) only, and 67 were detected by both. Overall, the test was shown to be highly sensitive and specific with the total PPA ≥93.1% in all cases except for *vanA* linked with *E. faecalis*, which was 85.7%. The total NPA was >98.2% for all targets, with the exceptions of *vanA* linked with *E. faecium* (93.0%) and *mecA* linked with *S. epidermidis* (81.5%).

Subsequently, in 2014, Mestas et al. at the Children's Hospital Los Angeles reported the results of a performance evaluation of the BC-GP assay in 203 pediatric patients, as compared to conventional culture-based identification and susceptibility testing (Mestas et al., 2014). Discordant results were resolved by matrix-assisted laser desorption ionization–time of flight mass spectrometry (MALDI-TOF) or 16S rRNA sequencing. The BC-GP assay demonstrated a concordance of 95.8% (206/215). The targets that are included in the BC-GP test covered 96.4% (215/223) of the recovered isolates. Only 3.0% (6/203) of the blood cultures had invalid results (which were related to the internal processing control) and required repeat testing during the study period, and five of these were correctly identified after one repeat, resulting in an overall correct identification rate of 97.0%. The BC-GP assay showed high accuracy in the detection of the *mecA* gene in *S. aureus* and *S. epidermidis*, and correctly identified 100% of methicillin-resistant *S. aureus* (MRSA) and 98% of methicillin-resistant *S. epidermidis* (MRSE), respectively. All vancomycin-resistant *E. faecium* isolates were also correctly identified but no vancomycin-resistant *E. faecalis* isolates were isolated during the study period. One limitation they describe in the study is that the test is unable to differentiate between monomicrobial or polymicrobial cultures containing *Staphylococcus* spp. other than *S. aureus, S. lugdunensis*, and *S. epidermidis*, or containing *Streptococcus* spp. other than *S. pneumoniae*, *S. pyogenes*, *S. agalactiae*, and *S. anginosus* group. And while multiple organisms could not be determined exclusively from the BC-GP results in 25% of cases, the test was able to correctly detect as least one organism from polymicrobial blood cultures in 93.8% of cases, and accurately identify all targeted bacteria and resistance markers in 81.3% of cases.

TABLE 3 | Summary of clinical performance for the VERIGENE Gram-Positive Blood Culture test.

Target	Fresh		Frozen		Total		Simulated	
	PPA[a] N[b] (95% CI[c])	NPA[d] N (95% CI)	PPA N (95% CI)	NPA N (95% CI)	PPA N (95% CI)	NPA N (95% CI)	PPA N (95% CI)	NPA N (95% CI)
Staphylococcus aureus	99.1% 322/325 (97.3-99.8)	100% 926/926 (99.6-100)	100% 10/10 (69.2-100)	100% 165/165 (97.8-100)	99.1% 332/335 (97.4-99.8)	100% 1091/1091 (99.7-100)	NA[e]	100% 216/216 (98.3-100)
Staphylococcus epidermidis	93.0% 294/316 (89.6-95.6)	98.7% 923/935 (97.8-99.3)	100% 2/2 (15.8-100)	100% 173/173 (97.9-100)	93.1% 296/318 (89.7-95.6)	98.9% 1096/1108 (98.1-99.4)	100% 2/2 (15.8-100)	100% 214/214 (98.3-100)
Staphylococcus lugdunensis	87.5% 7/8 (47.4-99.7)	100% 1243/1243 (99.7-100)	100% 12/12 (73.5-100)	100% 163/163 (97.8-100)	95.0%(h) 19/20 (75.1-99.9)	100% 1406/1406 (99.7-99.9)	100% 20/20 (83.2-100)	99.5% 195/196 (97.2-99.9)
Staphylococcus spp.	97.9% 895/914 (96.8-98.7)	99.4% 335/337 (97.9-99.9)	100% 30/30 (88.4-100)	99.3% 144/145 (96.2-99.9)	98.0% 925/944 (96.9-98.8)	99.4% 479/482 (98.2-99.9)	100% 25/25 (86.3-100)	100% 191/191 (98.1-100)
Listeria spp.	100% 3/3 (29.2-100)	100% 1248/1248 (99.7-100)	NA	100% 175/175 (97.9-100)	100% 3/3 (29.2-100)	100% 1423/1423 (99.7-100)	100% 34/34 (89.7-100)	100% 182/182 (98.0-100)
mecA	94.1% 366/389 (91.2-96.2)	97.8% 843/862 (96.6-98.7)	100% 9/9 (66.4-100)	100% 166/166 (97.8-100)	94.2% 375/398 (91.5-96.3)	98.2% 1009/1028 (97.1-98.9)	NA	100% 216/216 (98.3-100)
mecA linked with *S. aureus*	–	–	–	–	97.5% 157/161 (93.8-99.3)	98.8% 172/174(e) (95.9-99.9)	–	–
mecA linked with *S. epidermidis*	–	–	–	–	92.0% 219/238 (87.8-95.1)	81.5% 75/92 (72.1-88.9)	–	–
Enterococcus faecalis	96.0% 72/75 (88.8-99.2)	99.9% 1175/1176 (99.5-99.9)	100% 21/21 (83.9-100)	100% 154/154 (97.6-100)	96.9% 93/96 (91.1-99.4)	99.9% 1329/1330 (99.6-99.9)	92.3% 12/13 (64.0-99.8)	100% 203/203 (98.2-100)
Enterococcus faecium	94.4% 34/36 (81.3-99.3)	100% 1215/1215 (99.7-100)	100% 32/32 (89.1-100)	100% 143/143 (97.5-100)	97.1% 66/68 (89.8-99.6)	100% 1358/1358 (99.7-100)	100% 46/46 (92.3-100)	99.4% 169/170 (96.8-99.9)
vanA	91.9% 34/37 (78.1-98.3)	100% 1214/1214 (99.7-100)	96.9% 31/32 (83.8-99.9)	97.9% 140/143 (94.0-99.6)	94.2% 65/69 (85.8-98.4)	99.8% 1354/1357 (99.4-99.9)	100% 15/15 (78.2-100)	100% 201/201 (98.2-100)
vanB	–	100% 1251/1251 (99.7-100)	100% 3/3 (29.2-100)	100% 172/172 (97.9-100)	100% 3/3 (29.2-100)	100% 1423/1423 (99.7-100)	97.3% 36/37 (85.8-99.9)	100% 179/179 (98.0-100)
vanA linked with *E. faecalis*	–	–	–	–	85.7% 12/14 (57.2-98.2)	100% 95/95 (96.2-100)	–	–
vanA linked with *E. faecium*	–	–	–	–	97.2% 69/71 (90.2-99.7)	93.0% 40/43 (80.9-98.5)	–	–
vanB linked with *E. faecalis*	–	–	–	–	100% 7/7 (59.0-100)	100% 102/102 (96.5-100)	–	–
vanB linked with *E. faecium*	–	–	–	–	97.0% 32/33 (84.2-99.9)	100% 81/81 (95.6-100)	–	–
S. agalactiae	97.5% 39/40 (86.8-99.9)	100% 1211/1211 (99.7-100)	100% 31/31 (88.8-100)	100% 144/144 (97.5-100)	98.6% 70/71 (92.4-99.9)	100% 1355/1355 (99.7-100)	100% 6/6 (54.1-100)	100% 210/210 (98.3-100)
S. pneumoniae	100% 25/25 (86.3-100)	99.6% 1221/1226 (99.1-99.9)	100% 13/13 (75.3-100)	100% 162/162 (97.8-100)	100% 38/38 (90.8-100)	99.6% 1383/1388 (99.2-99.9)	100% 8/8 (63.1-100)	100% 208/208 (98.2-100)
S. pyogenes	100% 10/10 (69.2-100)	100% 1241/1241 (99.7-100)	92.9% 13/14 (66.1-99.8)	100% 161/161 (97.7-100)	95.8% 23/24 (78.9-99.9)	100% 1402/1402 (99.7-100)	98.2% 53/54 (90.1-99.9)	100% 162/162 (97.8-100)

(Continued)

TABLE 3 | Continued

Target	Fresh		Frozen		Total		Simulated	
	PPA[a] N[b] (95% CI[c])	NPA[d] N (95% CI)	PPA N (95% CI)	NPA N (95% CI)	PPA N (95% CI)	NPA N (95% CI)	PPA N (95% CI)	NPA N (95% CI)
S. anginosus group	100% 9/9 (66.4-100)	99.8% 1239/1242 (99.3-99.9)	100% 3/3 (29.2-100)	100% 172/172 (97.9-100)	100% 12/12 (73.5-100)	99.8% 1411/1414 (99.4-99.9)	100% 23/23 (85.2-100)	99.5% 192/193 (97.2-99.9)

[a]*PPA, Positive Percent Agreement.*
[b]*N, number.*
[c]*95% CI, 95% Confidence Interval.*
[d]*NPA, Negative Percent Agreement.*
[e]*NA, not applicable.*

To evaluate improvements in turnaround time, blood cultures found positive for gram-positive cocci were routinely reflexed to BC-GP testing, which was run 24 hours a day, 7 days a week. The turnaround times for identification of the targeted bacteria were compared in a 4-month pre-implementation period for conventional testing, and a 4-month period post-implementation of BC-GP. Additionally, the turnaround times for reporting susceptibility results for *S. aureus*, *S. epidermidis*, *E. faecalis*, and *E. faecium* compared to detection of resistance genes was conducted for the same time periods. Statistically significant differences in turnaround times between the BC-GP and the conventional methods for identification and resistance detection were calculated using a paired *t* test. Pre-implementation, the average turnaround times for traditional identification and susceptibility reporting were 34.2 hours and 41.4 hours, respectively. After implementation of the BC-GP assay, the average turnaround time was decreased to 4.1 hours for identification and detection of resistance genes. The mean turnaround time for organism identification decreased by 30.1 hours ($P<0.0001$) and by 37.3 hours ($P<0.0001$) for resistance marker detection.

The study by Mestas et al. demonstrates that the BC-GP test is highly accurate for identification of gram-positive bacteria and detection of resistance markers, and strong as compared to the routine laboratory methods. Furthermore, successful integration of the test into the routine workflow of the microbiology laboratory resulted in a marked improvement in turnaround times, especially for identification of MRSA and vancomycin-resistant enterococci (VRE).

The same institution published a more comprehensive study in 2018, which included extensive data describing their results over five years after implementation of the BC-GP test (Vareechon et al., 2018). Within five years, a total of 1636 blood culture bottles positive for a gram-positive organism were tested on the BC-GP panel. BC-GP identified gram-positive organisms in 92.9% (1520/1636) of the blood cultures tested. In positive blood cultures, there was a 96.4% (806/834) agreement of BC-GP to the species level. Compared with conventional antimicrobial susceptibility testing (AST), the PPA for BC-GP was 100% for both MRSA (50) and MRSE (365). The NPA for *mecA* detection in MRSA and MRSE was 99.1% (221/223) and 99.2% (120/121), respectively. The PPA and NPA for vancomycin-resistant *E. faecium* in BC-GP was 100%. None of the 84 blood cultures positive for *E. faecium* were positive for *vanA/B*.

The biggest discrepancy observed was a false-positive rate of 43.1% (25/58) for *Streptococcus pneumoniae*. Most of these were identified as *Streptococcus mitis/oralis* (21/25) by conventional testing and this finding was not unexpected since these species share 99% homology at the sequence level. The authors recommended that identification of *S. pneumoniae* by the BC-GP panel be confirmed by Gram stain plus bile solubility or other test methods. Careful reporting of all *S. pneumoniae* identified by BC-GP as *Streptococcus* spp. when atypical Gram stain morphology was present prevented incorrect reporting in cases of viridans group streptococci. The authors further suggested that incorporating a *S. pneumoniae* antigen test on blood culture broth may complement BC-GP to permit earlier reporting of results for *S. pneumoniae*.

Overall, the results from this five-year retrospective study confirmed that the BC-GP test has outstanding performance, thus allowing clinicians to de-escalate antimicrobial therapy in the absence of detection of a *mecA* and *vanA/B* gene with confidence.

Beckman and coworkers described a study which evaluated the performance of BC-GP on 2115 positive pediatric blood culture specimens (Beckman et al., 2019). The results of BC-GP were compared to the results from conventional culture and susceptibility testing. Of the positive cultures, 1503 were gram-positive by Gram stain and 1231 grew single isolates that were detectable by the BC-GP assay. Out of the 1231 single isolate cultures, 899 were accurately identified to the species level, 282 were identified to the genus, and 50 were not detected by BC-GP. Except for seven organisms, all organisms detected by BC-GP in monomicrobial cultures were also identified as the same organism by traditional methods. There were no differences in the overall agreement for detection of *Enterococcus*, *Streptococcus*, *Staphylococcus* spp., *S. aureus*, *E. faecium*, and *S. agalactiae*. *E. faecalis* was correctly identified in all but 3 of 88 and *S. pyogenes* in all but 1 of 25. The seven isolates with results different than the culture method were correctly identified as *Streptococcus*, but incorrectly as *S. pneumoniae*, instead of *S. mitis/oralis*. Polymicrobial growth of gram-positive organisms was found in 112 cultures. Of these, BC-GP correctly identified all organisms present that were included in the panel in 77 cultures. Exceptional overall agreement was also observed for

antimicrobial resistance markers, with only five samples (1%) showing discordant results. For almost all isolates, the BC-GP assay result was as useful as conventional culture identification, and the detection of antimicrobial resistance markers was highly accurate. Therefore, the data acquired from BC-GP can be confidently used by clinicians to support antimicrobial selection. Based on review of 20 cases where results of BC-GP disagreed with that of the conventional methods, the authors found little to no impact or effect clinically on patients or their management, which was likely due to the maintenance of empiric therapy, and no patients were placed at an increased risk of harm.

The Luminex® VERIGENE® Gram-Negative Blood Culture Test

VERIGENE BC-GN test performance was determined in a clinical study conducted at twelve institutions across the U.S. (Luminex, 2020a). Of the 1434 specimens enrolled in the trial, 73 were invalid on initial testing (5.1%) but gave a valid result upon retesting (final invalid rate of 2.3%). A total of 1412 specimens were included for evaluation, including 876 prospectively collected specimens (604 fresh and 175 frozen), 239 pre-selected frozen specimens, and 297 simulated frozen specimens. The results of BC-GN were compared to reference culture followed by biochemical identification. Results for bacterial resistance markers were compared to results of PCR amplification, followed by bidirectional sequencing. The PPA, NPA, and two-sided 95% CI observed for detection of each organism and resistance marker are shown in **Table 4**. Overall, the PPA was ≥92.2% and the NPA was ≥99.4%. *Serratia marcescens* is not an IVD-cleared target in the U.S. but a separate study conducted at a single site showed a PPA of 88.5% (23/26) (Luminex, 2020b).

The data above were included in a 2015 publication by Ledeboer et al. which described the results from a total of 1,847 blood cultures positive for gram-negative organisms (Ledeboer et al., 2015). The full sample set included 729 fresh, prospective, 781 frozen (prospective or retrospective), and 337 simulated cultures, and represented 7 types of aerobic culture media. Among monomicrobial cultures, the PPA of BC-GN with the reference result ranged from 92.9%-100% for the organism identification targets. The NPA for organism identification ranged from 99.5% to 99.9%. The authors noted that 25/26 cultures containing *Klebsiella pneumoniae* reported as "not detected" by BC-GN were identified as *Klebsiella variicola* by subsequent sequence analysis. The PPA for identification of resistance determinants was ≥94.3% and the NPA was >99.9%. The overall PPA and NPA for the eight organism identification targets was 97.9% and 99.7%, respectively. In polymicrobial specimens (with gram-negative appearance on Gram stain), the BC-GN assay accurately identified a minimum of one organism in 95.4% of the cultures and identified all organisms correctly in 54.5%. The prevalence of genetic resistance determinants was low in the prospective sample set (0.0% to 0.6%), except for CTX-M (5.0%), so performance for these targets was assessed using simulated specimens. The PPA for KPC, VIM, and IMP was 100%. The PPA was 98.9% for CTX-M, 96.2% for NDM, and 94.3% for OXA. The NPA was 100% for all but the simulated OXA specimens (99.6%). Overall, the PPA and NPA were 98.3% and 99.9% for the six genetic resistance markers.

The authors stated that a unique advantage of the BC-GN assay versus other rapid identification methods (e.g., MALDI-TOF MS and peptide nucleic acid fluorescence *in situ* hybridization [PNA FISH]) is the capacity to identify six genetic resistance markers associated with various classes of β-lactam antibiotics. While the frequency of carbapenemases found in this study was low, epidemiology and surveillance data has shown the prevalence steadily increasing over time (Nordmann et al., 2011; van Duin and Doi, 2017). The authors found that the targets included in the BC-GN test enabled identification of the infecting organism in about 90% of the prospective blood culture specimens which contained gram-negative bacilli. They noted that some relatively common gram-negative pathogens, such as *Serratia* spp., *Stenotrophomonas maltophilia*, and non-aeruginosa *Pseudomonas* spp., accounted for 4.4% of the positive cultures but are not included in BC-GN. Additionally, since *K. variicola* may account for up to 10% of all *Klebsiella* spp. isolated from clinical specimens, additional sequencing or biochemical testing may be desirable in the event of a *K. pneumoniae* blood culture identification that was not detected by BC-GN.

As described in the study above, BC-GN identified at least one pathogen in the majority of polymicrobial cultures but could only identify all pathogens present in about half of these cases. Identification of all pathogens present in polymicrobial cultures may be particularly challenging for a technology designed for direct analysis of specimens (e.g., molecular, MALDI-TOF MS, etc.). Use of these tests, such as BC-GN, could be limited in clinical settings due to reduced sensitivity in polymicrobial infections and concomitant concerns for unsuitable antibiotic modification as a result. Although Gram stain is used to confirm the morphology of the organism for appropriate test selection, multiple organisms may have similar appearance by Gram stain. Additionally, when gram-negative organisms are detected in multiple bottles in a set, typically one bottle is prepared for testing and thus the possibility exists that the gram-negative organisms observed in may be different and not all tested using BC-GN. To investigate this potential issue, Claeys and colleagues conducted a retrospective review of 1003 blood culture sets from 2 institutions and found the incidence of missed gram-negative identification to be infrequent at <4% (Claeys et al., 2018a). Since the patient data were not reviewed, a hypothetical analysis was conducted based on assumption that all patients were treated empirically with a gram-negative antibiotic (as directed by their institutional guidelines). Using this analysis, the investigators found that of the missed gram-negative identifications, an adverse impact on patient management could have potentially occurred in <2% of cases. The authors state that it is essential for laboratories to be cognizant of the possibility to miss detection of organisms in polymicrobial cultures so that these cases do not negatively affect stewardship efforts. Even with these known limitations, it is appropriate to trust the BC-GN result in combination with clinical judgment, considering the importance of limiting broad-spectrum antibiotic usage.

TABLE 4 | Summary of clinical performance for the VERIGENE Gram-Negative Blood Culture test.

Target	Fresh		Frozen		Pre-selected		Simulated		Total	
	PPA[a] N[b] (95% CI[c])	NPA[d] N (95% CI)	PPA N (95% CI)	NPA N (95% CI)	PPA N (95% CI)	NPA N (95% CI)	PPA N (95% CI)	NPA N (95% CI)	PPA N (95% CI)	NPA N (95% CI)
Escherichia coli	100% 283/283 (98.7-100)	99.1% 318/321 (97.3-99.8)	99.3% 142/143 (96.2-100)	99.2% 128/129 (95.8-100)	100% 42/42 (91.6-100)	99.5% 196/197 (97.2-100)	100% 50/50 (92.9-100)	100% 247/247 (98.5-100)	99.8% 517/518 (98.9-100)	99.4% 889/894 (98.7-99.8)
Klebsiella pneumoniae	88.0% 88/100 (80.0-93.6)	100% 504/504 (99.3-100)	87.0% 40/46 (73.1-95.1)	100% 226/226 (98.4-100)	94.7% 36/38 (82.3-99.4)	100% 201/201 (98.2-100)	99.2% 121/122 (95.5-100)	100% 175/175 (97.9-100)	93.1% 285/306 (89.7-95.7)	100% 1106/1106 (99.7-100)
Klebsiella oxytoca	95.7& 22/23 (78.1-99.9)	98.2% 576/581 (97.9-100)	100% 9/9 (66.4-100)	99.6% 262/263 (97.9-100)	92.6% 25/27 (75.7-99.1)	100% 212/212 (98.3-100)	60.0% 3/5 (14.7-94.7)	100% 292/292 (98.7-100)	92.2% 59/64 (82.7-97.4)	99.6% 1342/1348 (99.0-99.8)
Pseudomonas aeruginosa	97.1% 67/69 (89.9-99.7)	100% 535/535 (99.3-100)	91.7% 11/12 (61.5-99.8)	100% 260/260 (98.6-100)	100% 19/19 (82.4-100)	100% 220/220 (98.3-100)	100% 27/27 (87.2-100)	100% 270/270 (98.6-100)	97.6% 124/127 (93.3-99.5)	100% 1285/1285 (99.7-100)
Serratia marcescens[e]	–	–	–	–	–	–	–	–	88.5% 23/26 (69.9-97.6)	99.9% 294/297 (97.1-99.8)
Acinetobacter spp.	100% 12/12 (73.5-100)	100% 592/592 (99.4-100)	50% 1/2 (1.3-98.7)	100% 270/270 (98.6-100)	100% 15/15 (78.2-100)	99.6% 223/224 (97.6-100)	100% 27/27 (87.2-100)	100% 270/270 (98.6-100)	98.2% 55/56 (90.5-100)	99.9% 1355/1356 (99.6-100)
Citrobacter spp.	100% 5/5 (47.8-100)	99.8% 598/599 (99.1-100)	100% 1/1 (2.5-100)	100% 271/271 (98.7-100)	100% 13/13 (75.3-100)	100% 226/226 (98.4-100)	100% 30/30 (88.4-100)	100% 267/267 (98.6-100)	100% 49/49 (92.8-100)	99.9% 1362/1363 (99.6-100)
Enterobacter spp.	95.6% 43/45 (84.9-99.5)	100% 559/559 (99.3-100)	95.2% 20/21 (76.2-99.9)	98.4% 247/251 (96.0-99.6)	100% 29/29 (88.1-100)	98.1% 206/210 (95.2-99.5)	100% 28/28 (87.7-100)	100% 269/269 (98.6-100)	97.6% 120/123 (93.0-99.5)	99.4% 1281/1289 (98.8-99.7)
Proteus spp.	100% 20/20 (83.2-100)	100% 584/584 (99.4-100)	100% 12/12 (73.5-100)	100% 260/260 (98.6-100)	100% 24/24 (85.8-100)	99.5% 214/215 (97.4-100)	100% 2/2 (15.8-100)	100% 295/295 (98.8-100)	100% 58/58 (93.8-100)	99.9% 1353/1354 (99.6-100)
CTX-M	97.5% 39/40 (86.8-99.9)	100% 497/497 (99.3-100)	91.2% 11/12 (61.5-99.8)	100% 224/224 (98.4-100)	100% 3/3 (29.2-100)	100% 203/203 (98.2-100)	100% 98/98 (96.3-100)	99.5% 188/189 (97.1-100)	98.7% 151/153 (95.4-99.8)	99.9% 1112/1113 (99.5-100)
IMP	–	100% 537/537 (99.3-100)	–	100% 236/236 (98.5-100)	–	100% 206/206 (98.2-100)	100% 48/48 (92.6-100)	100% 239/239 (98.5-100)	100% 48/48 (92.6-100)	100% 1218/1218 (99.7-100)
KPC	100% 2/2 (15.8-100)	100% 535/535 (99.3-100)	100% 1/1 (2.5-100)	100% 235/235 (985-100)	–	100% 206/206 (98.2-100)	100% 48/48 (92.6-100)	100% 239/239 (98.5-100)	100% 51/51 (93.1-100)	100% 1215/1215 (99.7-100)
NDM	100% 1/1 (2.5-100)	100% 536/536 (99.3-100)	–	100% 236/236 (98.5-100)	–	100% 206/206 (98.2-100)	100% 40/40 (91.2-100)	100% 247/247 (98.5-100)	100% 41/41 (91.4-100)	100% 1225/1225 (99.7-100)
OXA	100% 5/5 (47.8-100)	100% 532/532 (99.3-100)	–	100% 236/236 (98.5-100)	50.0% 2/4 (6.8-93.2)	100% 202/202 (98.2-100)	98.3% 54/55 (90.8-100)	99.6% 231/232 (97.6-100)	95.3% 61/64 (86.9-99.0)	99.9% 1201/1202 (99.5-100)
VIM	–	100% 537/537 (99.3-100)	–	100% 236/236 (98.5-100)	–	100% 206/206 (98.2-100)	100% 41/41 (91.4-100)	100% 246/246 (98.5-100)	100% 41/41 (91.4-100)	100% 1225/1225 (99.7-100)

[a]*PPA, Positive Percent Agreement.*
[b]*N, number.*
[c]*95% CI, 95% Confidence Interval.*
[d]*NPA, Negative Percent Agreement.*
[e]*Serratia marcescens is not IVD-cleared in the United States. Data were collected in a separate study conducted at a single external clinical site.*

While rapid detection of genetic resistance markers in gram-negative BSIs allows quick optimization of empiric antibiotic therapy, how to respond when none are detected is unclear, given the complex nature of gram-negative resistance and the safety of de-escalation in this setting may be unknown. Pogue et al. analyzed the results from 1046 gram-negative blood culture isolates analyzed by the BC-GN test to determine the NPVs of resistance marker absence to predict susceptibility in specific drug-bug combinations at two different sites (Pogue et al., 2018). Except for *Pseudomonas aeruginosa*, the absence of resistance genes detected by BC-GN mostly predicted susceptibility to target antibiotics at both institutions. NPVs for ceftriaxone susceptibility in *Escherichia coli* and *K. pneumoniae* in the absence of either a carbapenemase gene or CTX-M were 93%-94% and 98%, respectively. Similar results were seen for other target bug-drug scenarios, with NPVs of 94% to 100% at both sites, except for *P. aeruginosa*, where the NPVs were poor. This is most likely related to the complexity of antibiotic resistance in this organism. For all other organisms, susceptibility was mainly predicted by the presence or absence of the resistance determinants included in BC-GN. The results of this study showed that clinicians at these institutions could have confidence in antibiotic de-escalation when no resistance determinants are detected and treatment decisions can be based on the results of the BC-GN test (for both escalation and de-escalation). The authors proposed that the methodology they describe could serve as a blueprint for antimicrobial stewardship to assess how BC-GN performs in these scenarios and optimize management of gram-negative bacteremia in their patients.

CLINICAL AND ECONOMIC IMPACT

Gram Positive Bloodstream Infections

Enterococci are a significant cause of BSI in hospitalized patients and there are few antimicrobial treatments due to numerous resistance mechanisms. Sango and coworkers evaluated the impact of rapid organism identification and resistance detection with the BC-GP assay on the clinical and economic outcomes for 74 patients with bacteremia due to *Enterococcus* (Sango et al., 2013). This pre/postintervention study compared non-equivalent groups of inpatients with enterococcal bacteremia over 13 months in a quasi-experimental design. Prior to implementation of BC-GP testing, Gram stain results from positive cultures were called to the patient care area and identification and susceptibility results were reported when available. After the BC-GP assay was implemented, an infectious disease and/or critical care pharmacist was notified of the BC-GP results and appropriate antibiotics were recommended. The preintervention group included 46 patients vs. 28 in the postintervention group, with vancomycin-resistant *Enterococcus* (VRE) bacteremia occurring in 37% and 50%, respectively, which was not significantly different ($P = 0.33$).

The mean time to appropriate antimicrobial therapy was decreased by 23.4 hours in the postintervention group compared to the preintervention group ($P = 0.0054$). The mean time to appropriate therapy for patients with a vancomycin-susceptible *Enterococcus* (VSE) BSI was 18.6 hours in the postintervention group compared to 40.2 hours preintervention, but this decrease was not significant ($P = 0.1145$). However, for patients with VRE bacteremia, the mean time to appropriate antimicrobial therapy was significantly shorter by 31.1 hours in the postintervention group ($P<0.0001$). Also, in the postintervention group, the length of hospital stay was significantly shorter by 21.7 days ($P = 0.0484$) and mean hospital costs were $60,729 lower ($P = 0.02$) than in the preintervention group. There was not a significant difference in the mortality rates in the two groups. The study shows that microarray technology, such as the BC-GP assay, with support from pharmacy and the microbiology laboratory, can substantially decrease the time to suitable antimicrobial therapy, the length of hospital stay, and hospital costs.

A study reported by Box et al. also demonstrated the clinical and economic impact of rapid diagnostics for BSI (Box et al., 2015). The investigators evaluated the effect of implementing the BC-GP test with real-time support from the antibiotic stewardship team (AST) in a community hospital setting. This pre/post, quasi-experimental study was conducted at the five hospitals in the Scripps Healthcare system. Rapid diagnostic testing using BC-GP was performed at the central laboratory for 12 hours each day and pharmacists notified physicians of the results and assisted with antibiotic modifications. Primary outcomes measured were the average time to targeted antibiotic therapy and the difference in antibiotic duration for contaminant organisms. Secondary end points measured included mortality, length of hospital stay, pharmacy costs, and overall hospitalization costs. Of 167 adult patients with a gram-positive BSI, 103 patients (admitted in 2011) were included in the preintervention group and 64 patients (admitted in 2014) were in the postintervention group.

Implementation of rapid identification using BC-GP in combination with AST intervention improved the average time to targeted antibiotic therapy from 61.1 hours to 35.4 hours ($P<0.001$) and decreased the average duration of antibiotic therapy for blood culture contaminants from 42.3 hours to 24.5 hrs ($P = 0.03$). The median length of hospital stay was decreased from 9.1 days to 7.2 days postintervention ($P = 0.04$), and the overall median hospitalization costs were decreased from $17,530 to $10,290 ($P = 0.04$). Median pharmacy costs were similar ($822 vs. $425, $P = 0.11$), as were mortality rates at 9.1% and 9.2% ($P = 0.98$). Rapid identification of gram-positive blood culture isolates with AST intervention has a positive impact on patient outcomes with less time to targeted antibiotic therapy, less time on unnecessary antibiotic therapy, a shorter length of hospital stay, and lower overall hospital costs.

Investigators at Children's Hospital Los Angeles conducted a study to determine the clinical and economic impact of the BC-GP assay on the diagnosis of gram-positive BSIs in pediatric patients (Felsenstein et al., 2016). Data on time to optimization of antibiotics, length of hospitalization, and hospital cost were collected prospectively following implementation of BC-GP testing and were compared with matching preimplementation data. A total of 440 gram-positive BSI episodes from 383 patients were included, with 219 postimplementation and 221 preimplementation. Polymicrobial infections were included

and the pathogens identified were considered when determining appropriate antimicrobial treatment. A pediatric infectious diseases physician and a pharmacist separately assessed the time to antimicrobial optimization, de-escalation, and discontinuation, and the clinical suitability of these decisions. Agreement between the independent assessments was high, and discrepancies were resolved by including another pediatric infectious diseases physician in a third assessment. The overall hospital costs were calculated based on all direct costs incurred within all services during hospitalization, which included lodging, meals, medication, consults, radiology, and laboratory costs.

The time to antimicrobial optimization was shortened by 12.5 hours overall (P = 0.006), and by 11.9 hours specifically for *S. aureus* (P = 0.005) postimplementation. For patients with likely blood-culture contamination by coagulase-negative staphylococci (CoNS), the duration of antibiotics was decreased by 36.9 hours (P<0.001). The median length of hospital stay for patients admitted to a general ward was 1.5 days shorter (P = 0.04), and the median hospital cost was $3,757 less ($P$ = 0.03) after implementation. For *S. aureus* BSIs specifically, the median length of hospital stay and overall costs were decreased by 5.6 days (P = 0.01) and $13,341 ($P$ = 0.03), respectively. Mortality within one month of BSI diagnosis was low, trending toward decreased mortality after implementation, but this difference was not significant (5.7% preimplementation vs. 2.6% postimplementation, P = 0.28). Admission rate to the intensive care unit (ICU) was also not significantly different between the two time periods (40.7% vs. 48.1%, P = 0.24).

Eby and colleagues reported the effect of implementing BC-GP testing together with a triggered, mandatory infectious diseases (ID) consultation, to improve management and outcomes of patients with *S. aureus* bacteremia (Eby et al., 2018). Prior to implementation, *S. aureus* BSI was identified by conventional culture and the results sent to ASP pharmacists. After implementation, *S. aureus* BSI in adult inpatients was identified by BC-GP and the results were paged directly to ID fellows, with immediate initiation of a consultation. The ASP supported management after the initial consultation. Retrospective, pre/postintervention analysis was performed on 106 preintervention and 120 postintervention subjects. The time to a consultation after positive blood culture notification was decreased by 26.0 hours (95% CI, 45.1 hours to 7.1 hours, P < 0.001) postintervention as compared to preintervention. The time to starting targeted antibiotic treatment decreased by 21.2 hours on average (95% CI, 31.4 hours to 11.0 hours, P < 0.001) and the time to targeted antibiotics for methicillin-sensitive *S. aureus* (MSSA) decreased by an average of 40.7 hours (95% CI, 58.0 hours to 23.5 hours, P < 0.001). BC-GP plus intervention also resulted in lower mortality in the hospital (13.2% to 5.8%, P = .047) and a lower 30-day mortality (17.9% to 8.3%, P = .025). A more efficient response to *S. aureus* BSI with BC-GP testing was associated with improved care and outcomes for these patients.

Gram Negative Bloodstream Infections

Walker et al. conducted a retrospective review of gram-negative BSI in hospitalized patients over 6-months before (98 subjects) and 6-months after (97 subjects) implementing the BC-GN test for detection of gram-negative organisms in positive blood cultures (Walker et al., 2016). Antimicrobial stewardship practices were not changed. Patient demographics, the time to organism identification, the time to effective antimicrobial therapy, and some additional clinical parameters were compared. There was no significant difference between the two groups with respect to comorbidities, cause of bacteremia, or admissions to the ICU, as well as use of immunosuppressive therapies, neutropenia, or bacteremia that was due to organisms that were multi-drug resistant. The BC-GN assay resulted an identification in 87% of gram-negative cultures and was correct in 98% (95/97) of the cases, as compared to results from conventional culture. Organism identification was completed faster after BC-GN implementation (mean = 10.9 hours vs. 37.9 hours, P<0.001). Length of ICU stay was 4.2 days shorter (P = 0.033) and the 30-day mortality was 11.1% lower (P = 0.037). The mortality associated with multidrug-resistant organisms occurred in 1 of 8 cases postintervention vs. 12 of 19 cases in the preintervention group (P = 0.033). Implementation of effective therapy was significantly faster in the postintervention cases for extended-spectrum beta-lactamase (ESBL)-producing organisms (P = 0.049), but not significantly faster overall (P = 0.12). The authors estimated the cost per BC-GN test to be $99 but the average net savings per ICU patient would be $11,661. The data show the BC-GN assay was a valuable tool for early identification of gram-negative organisms BSIs and had a significant impact on patient care, especially when genetic resistance markers were detected.

The effect of BC-GN together with an antimicrobial intervention on clinical outcomes was also investigated by Rivard and co-workers in a large pre/post implementation study conducted at The Cleveland Clinic on 877 patients (456 preimplementation and 421 postimplementation) with a gram-negative BSI (Rivard et al., 2017). The main objective was to compare the time from Gram stain to an antimicrobial change. Then the time from Gram stain to effective treatment, the in-hospital mortality rate, and the length of hospital stay were also compared. Prior to implementation of BC-GN, microbiological services were not centralized and blood cultures were processed at regional facilities during two shifts, whereas blood cultures at the academic medical center were processed 24 hours per day. After implementation of BC-GN, an active ASP was utilized with centralized microbiological processing. Both groups had daily audits and feedback on antimicrobial therapy by the ASP pharmacists to identify possible optimization based on the results. An institutional guideline was developed to guide therapy recommendations.

The number and types of antimicrobial changes were similar between the groups. The median time from Gram stain to an antimicrobial change was significantly less in the postimplementation group at 28.6 hours, compared to 44.1 hours in the preimplementation group (P = 0.004). Time to effective therapy for patients on inappropriate therapy at the time of Gram stain was reduced in the postimplementation group (8.8 hours vs. 24.5 hours, P = 0.034). Additionally, the median length of hospital stay was also decreased in the postimplementation

group to 7 days compared to 9 days preimplementation (P = 0.001). The in-hospital mortality rate was similar at 11.6% (preimplementation) vs. 11.4% (postimplementation), P = 0.87. This evaluation supports the incorporation of rapid diagnostic technologies, such as the BC-GN test, into antimicrobial stewardship programs.

A study reported by Claeys et al. investigated the possible impact of an antibiotic treatment algorithm, driven by stewardship and incorporating rapid testing by the BC-GN test into the management of gram-negative bacteremia (Claeys et al., 2018b). This retrospective, observational study of adult patients included a total of 188 patients with gram-negative BSI, of which 144 (76.5%) were positive for organisms targeted by BC-GN. The evaluation employed an AMS-driven treatment algorithm based on data from institution-specific antibiograms with an evidence-based practice for managing drug-resistant gram-negative organisms.

Susceptibility *in vitro* was higher overall with antibiotics recommended by the algorithm as compared with the standard practice for isolates that could be assessed (92.1% versus 77.8%). Among the 144 patients with BC-GN panel organisms, there was a modest level of agreement between reviewers on the suitability of the standard antibiotics (κ = 0.735) but a strong level of agreement for those recommended by the algorithm (κ = 0.855). The algorithm proposed would have allowed 88.4% of cases to receive appropriate antibiotic therapy versus only 78.1% by the standard of care antibiotics (P = .014). The AMS treatment algorithm would have led to a 14.4% appropriate de-escalation, a 4.8% inappropriate de-escalation, a 5.3% appropriate escalation, and a 16.0% unnecessary escalation. The presence of a polymicrobial gram-negative BSI, a central line source for a gram-negative BSI, *Acinetobacter* spp., *Enterobacter* spp., and/or an OXA+ resistance determinant was associated with inappropriate recommendations by the AMS treatment algorithm (P <.05). The authors concluded that the ability to develop a treatment algorithm based on institutional antibiogram data and combined with evidence-based practices and BC-GN results, had the possibility to improve the percentage of gram-negative BSI patients receiving timely appropriate antimicrobial therapy.

CONCLUSION

Technological advances in molecular methods have revolutionized the approach to diagnosis of microbial pathogens in the microbiology laboratory. As these sophisticated methods have become faster, more automated, and simpler to use, they can be easily implemented into the laboratory workflow and have become an integral part of the routine testing repertoire in most diagnostic laboratories.

Although conventional culture techniques remain the foundation for diagnosis of BSIs in most microbiology laboratories, a move toward novel technologies that can identify pathogens and resistance markers directly from blood culture is critically important to optimize treatment and improve patient outcomes. Fortunately, several of these technologies have become available in the last decade to aid in diagnosis of BSIs. Rapid molecular tests, such as the VERIGENE Blood Culture Nucleic Acid Tests, which allow direct identification of bacteria and genetic resistance markers from positive blood cultures, have been shown to perform with extremely high sensitivity and specificity.

It should be noted that there are some limitations to the use of molecular tests for diagnosis of bloodstream pathogens as such tests can only identify those pathogens included in the panels (Lamy et al., 2020). In addition, detection of genetic resistance markers does not preclude phenotypic resistance due to other mechanisms. Identification of the pathogens present in a polymicrobial culture is also difficult and could impact the clinical use of tests such as BC-GN, as a lower sensitivity when multiple pathogens are present could limit the ability to modify antibiotic treatment. And, as reported for BC-GP, differentiation of *S. pneumoniae* from *S. mitis/oralis* is particularly challenging for a molecular test, since the organisms share a 99% sequence homology. Therefore, it would be prudent to confirm *S. pneumoniae* results with additional tests and to refrain from reporting it to the species level.

Altogether, the studies reported in the literature and reviewed here prove the clinical utility of such testing and clearly demonstrate the positive impact on patient outcomes and reduction of overall healthcare costs. Furthermore, the data described here builds the case for these rapid molecular methods as key components in the approach to both diagnostic and antimicrobial stewardship in the healthcare system.

AUTHOR CONTRIBUTIONS

SAD prepared this manuscript. CG and SD prepared the outline, participated in selection of articles to include, and reviewed/edited the manuscript. Final selection of articles to include was conducted by SAD and CG. All authors contributed to the article and approved the submitted version.

REFERENCES

Al-Hasan, M. N., Eckel-Passow, J. E., and Baddour, L. M. (2012). Impact of Healthcare-Associated Acquisition on Community-Onset Gram-Negative Bloodstream Infection: A Population-Based Study: Healthcare-Associated Gram-Negative BSI. *Eur. J. Clin. Microbiol. Infect. Dis.* 31 (6), 1163–1171. doi: 10.1007/s10096-011-1424-6

Beckman, M., Washam, M. C., DeBurger, B., Haslam, D. B., Courter, J. D., Andersen, H., et al. (2019). Reliability of the Verigene System for the Identification for Gram-Positive Bacteria and Detection of Antimicrobial Resistance Markers From Children With Bacteremia. *Diagn. Microbiol. Infect. Dis.* 93 (3), 191–195. doi: 10.1016/j.diagmicrobio.2018.10.005

Beekmann, S. E., Diekema, D. J., Chapin, K. C., and Doern, G. V. (2003). Effects of Rapid Detection of Bloodstream Infections on Length of Hospitalization and Hospital Charges. *J. Clin. Microbiol.* 41 (7), 3119–3125. doi: 10.1128/jcm.41.7.3119-3125.2003

Box, M. J., Sullivan, E. L., Ortwine, K. N., Parmenter, M. A., Quigley, M. M., Aguilar-Higgins, L. M., et al. (2015). Outcomes of Rapid Identification for

Gram-Positive Bacteremia in Combination With Antibiotic Stewardship at a Community-Based Hospital System. *Pharmacotherapy* 35 (3), 269–276. doi: 10.1002/phar.1557

Claeys, K. C., Heil, E. L., Pogue, J. M., Lephart, P. R., and Johnson, J. K. (2018a). The Verigene Dilemma: Gram-Negative Polymicrobial Bloodstream Infections and Clinical Decision Making. *Diagn. Microbiol. Infect. Dis.* 91 (2), 144–146. doi: 10.1016/j.diagmicrobio.2018.01.012

Claeys, K. C., Schlaffer, K. E., Heil, E. L., Leekha, S., and Johnson, J. K. (2018b). Validation of an Antimicrobial Stewardship-Driven Verigene Blood-Culture Gram-Negative Treatment Algorithm to Improve Appropriateness of Antibiotics. *Open Forum Infect. Dis.* 5 (10), ofy233. doi: 10.1093/ofid/ofy233

Diekema, D. J., Hsueh, P. R., Mendes, R. E., Pfaller, M. A., Rolston, K. V., Sader, H. S., et al. (2019). The Microbiology of Bloodstream Infection: 20-Year Trends From the SENTRY Antimicrobial Surveillance Program. *Antimicrob. Agents Chemother.* 63 (7), e00355–19. doi: 10.1128/aac.00355-19

Eby, J. C., Richey, M. M., Platts-Mills, J. A., Mathers, A. J., Novicoff, W. M., and Cox, H. L. (2018). A Healthcare Improvement Intervention Combining Nucleic Acid Microarray Testing With Direct Physician Response for Management of Staphylococcus Aureus Bacteremia. *Clin. Infect. Dis.* 66 (1), 64–71. doi: 10.1093/cid/cix727

Felsenstein, S., Bender, J. M., Sposto, R., Gentry, M., Takemoto, C., and Bard, J. D. (2016). Impact of a Rapid Blood Culture Assay for Gram-Positive Identification and Detection of Resistance Markers in a Pediatric Hospital. *Arch. Pathol. Lab. Med.* 140 (3), 267–275. doi: 10.5858/arpa.2015-0119-OA

Fleischmann, C., Scherag, A., Adhikari, N. K., Hartog, C. S., Tsaganos, T., Schlattmann, P., et al. (2016). Assessment of Global Incidence and Mortality of Hospital-Treated Sepsis. Current Estimates and Limitations. *Am. J. Respir. Crit. Care Med.* 193 (3), 259–272. doi: 10.1164/rccm.201504-0781OC

Gaynes, R., and Edwards, J. R. (2005). Overview of Nosocomial Infections Caused by Gram-Negative Bacilli. *Clin. Infect. Dis.* 41 (6), 848–854. doi: 10.1086/432803

Grozdanovski, K., Milenkovic, Z., Demiri, I., and Spasovska, K. (2012). Prediction of Outcome From Community-Acquired Severe Sepsis and Septic Shock in Tertiary-Care University Hospital in a Developing Country. *Crit. Care Res. Pract.* 2012, 182324. doi: 10.1155/2012/182324

Huang, X., and El-Sayed, M. A. (2010). Gold Nanoparticles: Optical Properties and Implementations in Cancer Diagnosis and Photothermal Therapy. *J. Adv. Res.* 1 (1), 13–28. doi: 10.1016/j.jare.2010.02.002

Idelevich, E. A., Reischl, U., and Becker, K. (2018). New Microbiological Techniques in the Diagnosis of Bloodstream Infections. *Dtsch Arztebl Int.* 115 (49), 822–832. doi: 10.3238/arztebl.2018.0822

Kaye, K. S., and Pogue, J. M. (2015). Infections Caused by Resistant Gram-Negative Bacteria: Epidemiology and Management. *Pharmacotherapy* 35 (10), 949–962. doi: 10.1002/phar.1636

Kern, W. V., and Rieg, S. (2020). Burden of Bacterial Bloodstream Infection-a Brief Update on Epidemiology and Significance of Multidrug-Resistant Pathogens. *Clin. Microbiol. Infect.* 26 (2), 151–157. doi: 10.1016/j.cmi.2019.10.031

Kollef, M. H., Zilberberg, M. D., Shorr, A. F., Vo, L., Schein, J., Micek, S. T., et al. (2011). Epidemiology, Microbiology and Outcomes of Healthcare-Associated and Community-Acquired Bacteremia: A Multicenter Cohort Study. *J. Infect.* 62 (2), 130–135. doi: 10.1016/j.jinf.2010.12.009

Kumar, A., Roberts, D., Wood, K. E., Light, B., Parrillo, J. E., Sharma, S., et al. (2006). Duration of Hypotension Before Initiation of Effective Antimicrobial Therapy Is the Critical Determinant of Survival in Human Septic Shock. *Crit. Care Med.* 34 (6), 1589–1596. doi: 10.1097/01.ccm.0000217961.75225.e9

Lamy, B., Sundqvist, M., and Idelevich, E. A. (2020). Bloodstream Infections - Standard and Progress in Pathogen Diagnostics. *Clin. Microbiol. Infect.* 26 (2), 142–150. doi: 10.1016/j.cmi.2019.11.017

Ledeboer, N. A., Lopansri, B. K., Dhiman, N., Cavagnolo, R., Carroll, K. C., Granato, P., et al. (2015). Identification of Gram-Negative Bacteria and Genetic Resistance Determinants From Positive Blood Culture Broths by Use of the Verigene Gram-Negative Blood Culture Multiplex Microarray-Based Molecular Assay. *J. Clin. Microbiol.* 53 (8), 2460–2472. doi: 10.1128/jcm.00581-15

Leibovici, L., Shraga, I., Drucker, M., Konigsberger, H., Samra, Z., and Pitlik, S. D. (1998). The Benefit of Appropriate Empirical Antibiotic Treatment in Patients With Bloodstream Infection. *J. Intern. Med.* 244 (5), 379–386. doi: 10.1046/j.1365-2796.1998.00379.x

Levy, M. M., Rhodes, A., Phillips, G. S., Townsend, S. R., Schorr, C. A., Beale, R., et al. (2014). Surviving Sepsis Campaign: Association Between Performance Metrics and Outcomes in a 7.5-Year Study. *Intensive Care Med.* 40 (11), 1623–1633. doi: 10.1007/s00134-014-3496-0

Luminex (2020a). *VERIGENE® Gram-Negative Blood Culture Nucleic Acid Test (BC-GN) Package Insert. 89-30000-00-776 (Rev B)*. Austin, TX United States: Luminex Corporation.

Luminex (2020b). *VERIGENE® Gram-Negative Blood Culture Nucleic Acid Test (BC-GN) Package Insert, CE. 89-30000-00-777 (Rev B)*. Austin, TX United States: Luminex Corporation.

Luminex (2020c). *VERIGENE® Gram-Positive Blood Culture Nucleic Acid Test (BC-GP) Package Insert. 89-30000-00-782 (Rev B)*. Austin, TX United States: Luminex Corporation.

Luminex (2021a) *VERIGENE® Bloodstream Infection Testing Panels*. Available at: https://www.luminexcorp.com/bloodstream-infection-tests/#overview (Accessed November 21, 2021).

Luminex (2021b) *The VERIGENE® System*. Available at: https://www.luminexcorp.com/the-verigene-system/#overview (Accessed November 21 2021).

Mestas, J., Polanco, C. M., Felsenstein, S., and Dien Bard, J. (2014). Performance of the Verigene Gram-Positive Blood Culture Assay for Direct Detection of Gram-Positive Organisms and Resistance Markers in a Pediatric Hospital. *J. Clin. Microbiol.* 52 (1), 283–287. doi: 10.1128/JCM.02322-13

Nordmann, P., Naas, T., and Poirel, L. (2011). Global Spread of Carbapenemase-Producing Enterobacteriaceae. *Emerg. Infect. Dis.* 17 (10), 1791–1798. doi: 10.3201/eid1710.110655

Patel, G., Huprikar, S., Factor, S. H., Jenkins, S. G., and Calfee, D. P. (2008). Outcomes of Carbapenem-Resistant Klebsiella Pneumoniae Infection and the Impact of Antimicrobial and Adjunctive Therapies. *Infect. Control Hosp. Epidemiol.* 29 (12), 1099–1106. doi: 10.1086/592412

Pliakos, E. E., Andreatos, N., Shehadeh, F., Ziakas, P. D., and Mylonakis, E. (2018). The Cost-Effectiveness of Rapid Diagnostic Testing for the Diagnosis of Bloodstream Infections With or Without Antimicrobial Stewardship. *Clin. Microbiol. Rev.* 31 (3), e00095–17. doi: 10.1128/cmr.00095-17

Pogue, J. M., Heil, E. L., Lephart, P., Johnson, J. K., Mynatt, R. P., Salimnia, H., et al. (2018). An Antibiotic Stewardship Program Blueprint for Optimizing Verigene BC-GN Within an Institution: A Tale of Two Cities. *Antimicrob. Agents Chemother.* 62 (5), e02538–17. doi: 10.1128/aac.02538-17

Rivard, K. R., Athans, V., Lam, S. W., Gordon, S. M., Procop, G. W., Richter, S. S., et al. (2017). Impact of Antimicrobial Stewardship and Rapid Microarray Testing on Patients With Gram-Negative Bacteremia. *Eur. J. Clin. Microbiol. Infect. Dis.* 36 (10), 1879–1887. doi: 10.1007/s10096-017-3008-6

Sango, A., McCarter, Y. S., Johnson, D., Ferreira, J., Guzman, N., and Jankowski, C. A. (2013). Stewardship Approach for Optimizing Antimicrobial Therapy Through Use of a Rapid Microarray Assay on Blood Cultures Positive for Enterococcus Species. *J. Clin. Microbiol.* 51 (12), 4008–4011. doi: 10.1128/jcm.01951-13

Santella, B., Folliero, V., Pirofalo, G. M., Serretiello, E., Zannella, C., Moccia, G., et al. (2020). Sepsis-A Retrospective Cohort Study of Bloodstream Infections. *Antibiotics (Basel)* 9 (12), 851–862. doi: 10.3390/antibiotics9120851

Schwaber, M. J., Navon-Venezia, S., Kaye, K. S., Ben-Ami, R., Schwartz, D., and Carmeli, Y. (2006). Clinical and Economic Impact of Bacteremia With Extended-Spectrum-Beta-Lactamase-Producing Enterobacteriaceae. *Antimicrob. Agents Chemother.* 50 (4), 1257–1262. doi: 10.1128/aac.50.4.1257-1262.2006

Timsit, J. F., Ruppé, E., Barbier, F., Tabah, A., and Bassetti, M. (2020). Bloodstream Infections in Critically Ill Patients: An Expert Statement. *Intensive Care Med.* 46 (2), 266–284. doi: 10.1007/s00134-020-05950-6

van Duin, D., and Doi, Y. (2017). The Global Epidemiology of Carbapenemase-Producing Enterobacteriaceae. *Virulence* 8 (4), 460–469. doi: 10.1080/21505594.2016.1222343

Vareechon, C., Mestas, J., Polanco, C. M., and Dien Bard, J. (2018). A 5-Year Study of the Performance of the Verigene Gram-Positive Blood Culture Panel in a Pediatric Hospital. *Eur. J. Clin. Microbiol. Infect. Dis.* 37 (11), 2091–2096. doi: 10.1007/s10096-018-3343-2

Walker, T., Dumadag, S., Lee, C. J., Lee, S. H., Bender, J. M., Cupo Abbott, J., et al. (2016). Clinical Impact of Laboratory Implementation of Verigene BC-GN Microarray-Based Assay for Detection of Gram-Negative Bacteria in Positive Blood Cultures. *J. Clin. Microbiol.* 54 (7), 1789–1796. doi: 10.1128/jcm.00376-16

Wisplinghoff, H., Bischoff, T., Tallent, S. M., Seifert, H., Wenzel, R. P., and Edmond, M. B. (2004). Nosocomial Bloodstream Infections in US Hospitals: Analysis of 24,179 Cases From a Prospective Nationwide Surveillance Study. *Clin. Infect. Dis.* 39 (3), 309–317. doi: 10.1086/421946

Wisplinghoff, H., Seifert, H., Tallent, S. M., Bischoff, T., Wenzel, R. P., and Edmond, M. B. (2003). Nosocomial Bloodstream Infections in Pediatric Patients in United States Hospitals: Epidemiology, Clinical Features and Susceptibilities. *Pediatr. Infect. Dis. J.* 22 (8), 686–691. doi: 10.1097/01.inf.0000078159.53132.40

Conflict of Interest: The authors are employees of Luminex, A DiaSorin Company who is the manufacturer of the tests reviewed in this manuscript.

Publisher's Note: All claims expressed in this article are solely those of the authors and do not necessarily represent those of their affiliated organizations, or those of the publisher, the editors and the reviewers. Any product that may be evaluated in this article, or claim that may be made by its manufacturer, is not guaranteed or endorsed by the publisher.

frontiers | Frontiers in Cellular and Infection Microbiology

ORIGINAL RESEARCH
published: 21 April 2022
doi: 10.3389/fcimb.2022.831959

Performance of Metagenomic Next-Generation Sequencing for the Diagnosis of Cryptococcal Meningitis in HIV-Negative Patients

Zhouqing Gan[1†], Jia Liu[1†], Yijie Wang[1], Lu Yang[1], Zheng Lou[2], Han Xia[2], Min Li[1], Zhuolin Chen[1], Ying Jiang[1] and Fuhua Peng[1*]*

[1] Department of Neurology, The Third Affiliated Hospital of Sun Yat-sen University, Guangzhou, China, [2] Department of Scientific Affairs, Hugobiotech Co., Ltd., Beijing, China

OPEN ACCESS

Edited by:
Elena Jordana-Lluch, Balearic Islands Health Research Institute (IdISBa), Spain

Reviewed by:
Daniel Santos, Federal University of Minas Gerais, Brazil
Prashant Gupta, King George's Medical University, India

***Correspondence:**
Ying Jiang
jiangy9@mail.sysu.edu.cn
Fuhua Peng
pengfh@mail.sysu.edu.cn

[†]These authors have contributed equally to this work

Specialty section:
This article was submitted to Clinical Microbiology, a section of the journal Frontiers in Cellular and Infection Microbiology

Received: 09 December 2021
Accepted: 14 March 2022
Published: 21 April 2022

Citation:
Gan Z, Liu J, Wang Y, Yang L, Lou Z, Xia H, Li M, Chen Z, Jiang Y and Peng F (2022) Performance of Metagenomic Next-Generation Sequencing for the Diagnosis of Cryptococcal Meningitis in HIV-Negative Patients. Front. Cell. Infect. Microbiol. 12:831959. doi: 10.3389/fcimb.2022.831959

Objectives: Metagenomic next-generation sequencing (mNGS) has been applied more and more widely for the diagnosis of infectious diseases, but its performance in the diagnosis of cryptococcal meningitis (CM) remains unclear.

Methods: Cerebrospinal fluid (CSF) samples from 197 HIV-negative patients with suspected central nervous system infections were tested simultaneously by mNGS and routine methods [India ink staining, fungal culture, or cryptococcal antigen (CrAg) tests]. The performance of mNGS was evaluated.

Results: Of the 197 enrolled cases, 46 (23.4%) cases were finally diagnosed with CM, including 43 (93.5%) *Cryptococcus neoformans* infections and 3 (6.5%) *Cryptococcus gattii* infections. The sensitivity, specificity, positive predictive value, negative predictive value, and concordance rate of mNGS were 93.5% [95% confidence interval (CI) at 86.4% ~100.0%], 96.0% (95% CI at 92.9%~99.1%), 87.8%, 98.0%, and 95.4%, respectively. Comparing to the conventional diagnostic methods, the sensitivity and concordance rate of mNGS were slightly lower than those of CrAg tests (97.4%) but higher than those of India ink (63.0%) and culture (76.7%). Besides, mNGS had a sensitivity of 100.0% against culture. It should be noted that mNGS could identify *Cryptococcus* at species level; *C. gattii* of the 3 cases was only distinguished by mNGS.

Conclusions: CSF mNGS can be considered as a supplementary test to diagnose CM and directly distinguish *C. gattii* from *C. neoformans* in clinical specimens.

Keywords: metagenomic next-generation sequencing, cerebrospinal fluids, cryptococcal meningitis, diagnosis, *Cryptococcus gattii*

INTRODUCTION

Culture of cerebrospinal fluid (CSF) is the "gold standard" for the diagnosis of cryptococcal meningitis (CM) (Perfect et al., 2010), a serious opportunistic fungal infection caused by *Cryptococcus neoformans* or *Cryptococcus gattii*, with novel cases of *Papiliotrema laurentii* and *Naganishia albida* (Khawcharoenporn et al., 2007; Smith et al., 2017), but it has poor timeliness and low positivity rate for patients receiving antifungal drugs. India ink staining microscopy (India ink) of the CSF is an economical and rapid method, but it has low sensitivity and its performance is affected by the experience of test performers. Cryptococcal capsular polysaccharide antigen (CrAg) test in the CSF is currently the diagnostic assay with the highest sensitivity and specificity (both above 96%) (Boulware et al., 2014), but it cannot determine the presence of infection, detect antigen-deficient strains (Rajasingham et al., 2019), or distinguish specific species. In addition, CrAg antibodies in use are mostly produced by stimulation with *C. neoformans*, which may show low affinity to non-*C. neoformans* strains like *C. gattii* and *P. laurentii*, resulting in decreased sensitivity (99% to 25%) (McMullan et al., 2013; Ragupathi and Reyna, 2015; Smith et al., 2017). Therefore, the method for CM diagnosis is still unsatisfactory. In China, about 40%–66.9% of CM patients are sporadic, HIV-negative, and have no apparent immune deficiency (Lui et al., 2006; Zhu et al., 2010; Liu et al., 2020; Zhang et al., 2020), where it requires more clinical predictions to assign diagnostic tests.

Metagenomic next-generation sequencing (mNGS, also known as high-throughput sequencing) is a genomics-based microbial detection technology developed in recent years (Wilson et al., 2018; Wang et al., 2019; Miller et al., 2019). From 2014 onward, it has been moving gradually from the laboratory toward clinical diagnostic applications, with successful detection of various types of microorganisms such as viruses, bacteria, mycobacteria, fungi, and parasites in clinical samples, showing powerful pathogen detection capabilities. Through alignment to the species-specific sequence of genomes, mNGS can distinguish *C. neoformans* from *C. gattii* and identify coinfections (Xing et al., 2019), which has advantages in identifying strains directly from clinical specimens. Recent studies and case reports with small sample sizes have demonstrated the capability of mNGS to identify fungi like *Cryptococcus* from CSF samples (Wilson et al., 2018; Ramachandran et al., 2019; Wang et al., 2019; Wilson et al., 2019; Xing et al., 2019; Ji et al., 2020; Xing et al., 2020), with preliminarily assessed lower limit of detection (LOD) for *C. neoformans* at about 0.2 CFU/ml (Miller et al., 2019). However, there is yet no systematic evaluation of its performance for the diagnosis of CM, and the clinical significance of mNGS remains unclear.

This study retrospectively recruited HIV-negative patients suspected with acute or subacute central nervous system (CNS) infections whose CSF samples were assigned to both mNGS and routine cryptococcal diagnostic tests (India ink, fungal culture, or CrAg tests) simultaneously in a diagnostic cohort study, with the aim to evaluate the diagnostic performance of mNGS.

METHODS

Study Design and Subjects

This study is approved by the Medical Ethics Committee of the Third Affiliated Hospital of Sun Yat-sen University [approval no (2021). 02-264-01]. The subjects or the guardians of patients with severe cognitive impairment had provided written consent for research and publication.

In this study, data on 207 Chinese Han HIV-negative cases were screened between July 2018 and December 2019 at the Third Affiliated Hospital of Sun Yat-sen University, Guangzhou, China. Among them, 10 cases were excluded due to loss of information or obvious contamination. Finally, we recruited 197 patients. Inclusion criteria are as follows: 1) Suspected with acute or subacute CNS infection (course duration ≤6 months) with at least one or more of the following clinical manifestations: fever (≥38°C), headache, vomiting, convulsions, meningeal irritation, focal neurological deficits, altered consciousness or lethargy; and at least one of the following conditions should be satisfied: A, abnormal CSF: increased white blood cell (WBC) counts (>5 × 10^6 cells/ml) and/or increased total protein levels (>0.5 g/L) and/or decreased glucose levels; B, brain imaging suggesting pathological infection or inflammatory changes; 2) CSF samples had been tested by mNGS together with at least one routine cryptococcal diagnostic tests (India ink, fungal culture, or CrAg tests); 3) Written consents of lumbar puncture and mNGS were obtained; 4) Age ≥14 years old. Exclusion criteria are as follows: 1) Incomplete data or loss of follow-up (follow-up ≤1 month); 2) Puncture bleeding; 3) Risk of obvious contamination: mNGS detected more than 2 similar microorganisms (Miller et al., 2019).

mNGS Procedures and Positivity Standard

A sample of about 2 ml CSF was collected and sealed sterilely and then stored below -20°C or shipped on dry ice to perform PACEseq mNGS test immediately (Hugobiotech, Beijing, China), where technicians had no access to patients' clinical data. Here, 200 μl of CSF specimen was centrifuged at 5,000g at room temperature for 10 min, and DNA was extracted from the supernatant using a TIANamp Micro DNA Kit (DP316, Tiangen Biotech). A "No template" control (NTC) was also included for each run. The sequencing libraries were constructed *via* QIAseq ™ Ultralow Input Library Kit (Illumina) according to manufacturer's recommendations. The library concentration and quality were checked using Qubit (Thermo Fisher) and agarose gel electrophoresis. The qualified libraries with different tags were pooled together and amplified and then sequenced by Nextseq550 system (Illumina) for 150 cycles with the high-output Reagent Kit (Illumina) to generate raw data with 5–10 million total reads per sample (Ji et al., 2020).

High-quality data were generated after filtering out adapters and low-quality, low-complexity, and short (<50 bp) reads, and then the human sequences were excluded by mapping reads to the human reference genome (hg19) using Burrows–Wheeler alignment (Li and Durbin, 2009). Finally, to get the microbial compositions of the sample, the remaining data were aligned to the microbial genome database built locally, downloaded from the National Center for Biotechnology Information

(ftp://ftp.ncbi.nlm.nih.gov/genomes/), containing genomes of tens of thousands of known microorganisms such as bacteria, archaea, mycoplasma, chlamydia, rickettsia, spirochetes, viruses, and fungi. Besides, the sequencing depth, coverage, and species-specific read number (using genus instead if not matched to any specific species) of each microorganism detected were recorded, and the species-specific read number was further normalized to per megabyte of data and defined as reads per million (RPM), referring to the sequence abundance, and the RPM ratio (RPM-r) was calculated (Miller et al., 2019), defined as RPM_{sample}/RPM_{NTC} (if $RPM_{NTC} = 0$, RPM-r = RPM_{sample}).

For *Cryptococcus*, the diagnostic criteria for positive results included the following: 1) The coverage of *Cryptococcus* was in the top 10 of the list of eukaryotes; 2) RPM-r ≥5 [considering the low sequence abundance and low risk of contamination (Bittinger et al., 2014; Schlaberg et al., 2017)] or RPM-r ≥1 (if $RPM_{NTC} = 0$ and *Cryptococcus* not in the local database of common background microorganisms).

Conventional Diagnostic Tests and Etiological Diagnosis

The CSF samples of the enrolled patients all underwent blinded mNGS and traditional cryptococcal diagnostic tests according to the routine diagnostic procedures, including 1) fungal culture (Culture); 2) India ink staining microscopy (India ink); 3) lateral flow immunoassays of CrAg (CrAg-LFAs) (Dynamiker Biotechnology, Tianjin, China).

Etiological diagnoses of cases relied on conventional tests performed together but not mNGS. Patients with positive *Cryptococcus* results by culture or India ink were confirmed with cryptococcal infections [1]. For patients with positive CrAg but negative culture and India ink *Cryptococcus* results, other pieces of clinical evidence, including clinical symptoms, CSF test result, outcomes of antifungal treatment, and the possibility of other infection should be considered.

Statistics and Analysis

Baseline data were collected, and the patients were divided into two groups according to etiological diagnosis: cryptococcal CNS infection and non-cryptococcal infection (viruses, bacteria, immune inflammation, tumor, etc.). The clinical characteristics and the detected *Cryptococcus* species and their RPM levels were compared. The categorical variables were described by the number of cases (percentage). The chi-square test (independent data) was used for comparison between groups. The continuous variables were described in median (lower quartile, upper quartile). The Kruskal–Wallis H test was used for comparison between multiple groups, and the Mann–Whitney U test was used for pairwise comparison. A P-value <0.05 was considered statistically significant. Statistical analysis was performed using SPSS 25.0 software.

RESULTS

Baseline Data and Etiological Diagnosis

In these 197 cases enrolled in this study (**Figure 1**), 46 (23.4%) cases and 151 (76.6%) cases were etiologically diagnosed as cryptococcal CNS infections and non-cryptococcal infections, respectively. Infections of *C. neoformans* and *C. gattii* accounted for 43 (93.5%) and 3 (6.5%), respectively. The baseline information and clinical data of the enrolled cases are shown in **Table S1**.

Cryptococcus Diagnostic Results

The results of the conventional methods (culture, India ink, and CrAg) and mNGS in the 46 cases diagnosed with CM were shown in **Figure 2**. There were 19 cases diagnosed positive by all of the three traditional methods. Fifteen cases were positive by two traditional methods: 4 (culture and India ink) + 8 (culture and CrAg) + 3 (India ink and CrAg). There were 12 cases with positive results by only one conventional method (2 by culture, 3 by India ink, and 7 by CrAg). It should be noted that the 7 patients diagnosed with CM only by CrAg had corresponding symptoms and abnormal CSF results, which were significantly improved after antifungal treatment, and the possibility of other infectious diseases was ruled out.

Evaluation of mNGS Diagnostic Performance on Cryptococcal CNS Infections

The sensitivity, specificity, positive predictive value (PPV), negative predictive value (NPV), and concordance rate of mNGS for the diagnosis of CM using CSF were 93.5% [95% confidence interval (CI) at 86.4%~100.0%], 96.0% (95% CI at 92.9%~99.1%), 87.8% (95% CI at 79.0%~96.6%), 98.0% (95% CI at 95.7%~100.0%), and 95.4%, respectively (**Table 1**). These results showed excellent diagnostic power of mNGS, albeit a few false positives.

The performance of mNGS in diagnosing cryptococcal infections was evaluated by comparing to that of the three conventional methods. The sensitivity, specificity, and concordance rate of the mNGS, India ink, fungal culture, and CrAg methods were shown in **Table 2**. The sensitivity of mNGS was slightly lower than that of CrAg but significantly higher than that of India ink and fungal culture. The specificity of mNGS was not as good as that of the three traditional tests. The concordance rate of mNGS was between that of CrAg and fungal culture.

Culture is considered as the "gold standard" for *Cryptococcus* detection. We further evaluated the mNGS detection results against fungal culture. mNGS reached 100% sensitivity and 100% NPV against culture (**Table 3**), demonstrating its great power in the diagnosis of cryptococcal infections.

DISCUSSION

To the best of our knowledge, this is the first study to evaluate the diagnostic performance of mNGS for CM in HIV-negative patients. In this study, the sensitivity of mNGS for the diagnosis of cryptococcal infections was slightly lower than that of CrAg but higher than those of India ink and culture, and its specificity was slightly lower than that of the traditional methods, with the concordance rate between that of CrAg and culture. Furthermore, when comparing with the "gold standard"

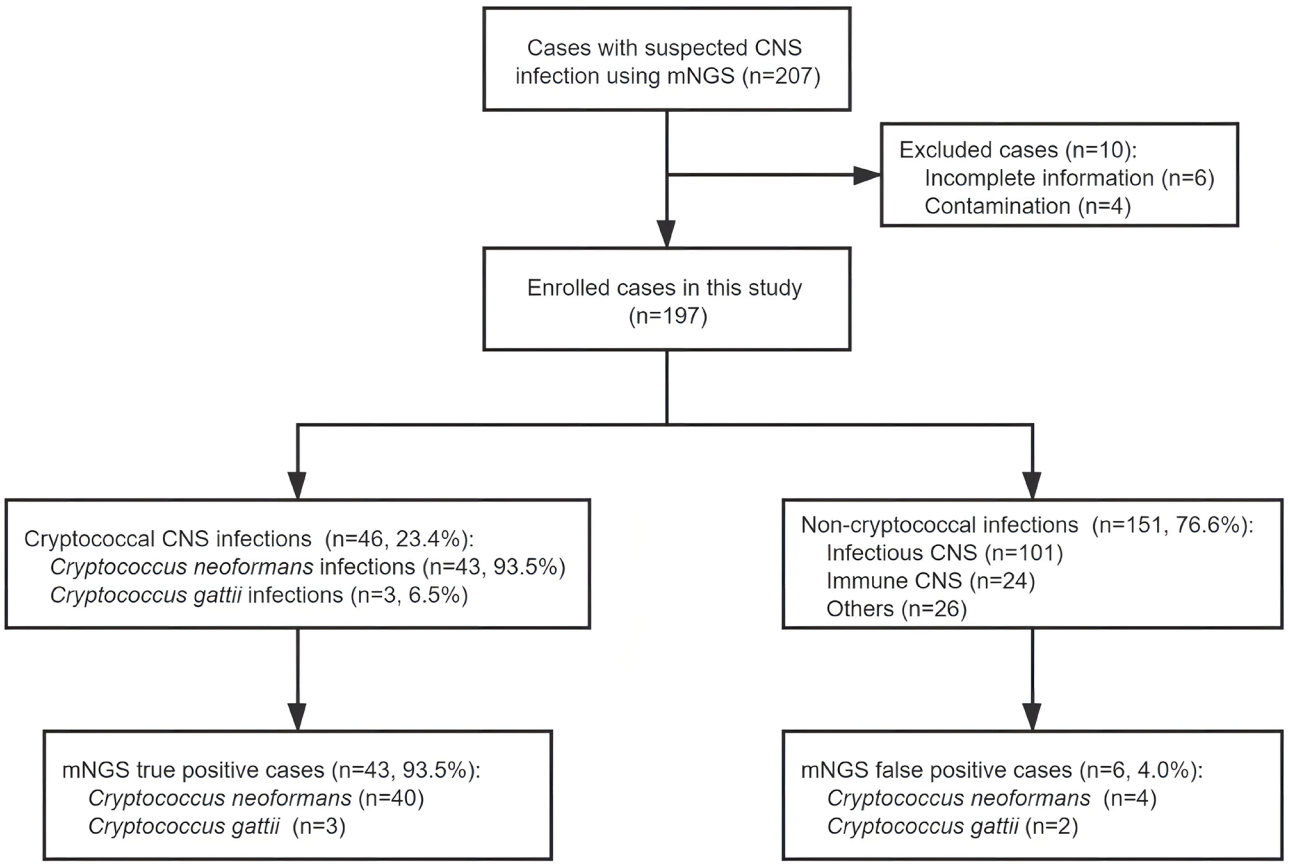

FIGURE 1 | Overview of patient enrollment, metagenomic next-generation sequencing (mNGS) results, and etiological diagnoses. After exclusion of 10 cases, 197 patients with suspected central nervous system (CNS) infection were enrolled in this study. Of these patients, 46 were diagnosed with cryptococcal CNS infection by at least one routine cryptococcal diagnostic test; the other 151 cases were diagnosed with non-cryptococcal infections. The sensitivity and specificity of mNGS in detecting *Cryptococcus* were 93.5% and 96.0%, respectively.

culture method, the sensitivity and NPV of mNGS reached 100.0%, indicating its excellent diagnostic performance. Xing et al. (2019) reported that in 12 cases with India ink- or fungal culture-positive CSF samples, mNGS positivity rate was 75% (9/12), not as good as India ink and fungal culture together (10/12), possibly due to the relatively small sample size.

The false positives of mNGS here were all with very low sequence abundance possibly due to cross-contamination during sampling, as our hospital is a regional CM diagnosis and treatment center in China. It is speculated that false positives would be rare in community hospitals. The false-negative cases were all positive for CrAg assays, and all received antifungal therapies prior to sampling. It could not be excluded that these patients had already cleared the *Cryptococcus* in CSF. After removing the cross-contamination, it was speculated that the sensitivity of mNGS could be comparable to the reported sensitivity (92.9%–96%) of FilmArray (BioMerieux) multiplex PCR for meningitis and encephalitis (Li and Durbin, 2009; Rhein et al., 2016; Liesman et al., 2018), and mNGS could have similar diagnostic value as cryptococcus nucleic acid assays, not just as a screening measure. The sensitivity of mNGS could be improved because the human sequence accounted for more than 95% of the original data, whereas the reads for pathogens were only a small part of it (Simner et al., 2018). To optimize mNGS performance, the next research direction should focus on the efficient removal of human sequences and the enrichment of pathogen sequences (Hasan et al., 2016; Ji et al., 2020). Besides, the collection, transportation, handling of samples, DNA extraction, library construction, procedure standardization, and bioinformatics analysis could all have an impact on the mNGS results (Chiu and Miller, 2019).

mNGS has the following advantages as a diagnosis or screening measure for CM: 1) mNGS has better screening ability and is able to detect mixed infection. mNGS can simultaneously detect a variety of bacteria (including *Mycobacterium tuberculosis*, nontuberculosis mycobacteria) and fungi, without clinical prediction and primer preparation for the presumed pathogens, and it is highly sensitive to *Cryptococcus*. 2) mNGS can assist the diagnosis of atypical cases. In our study, mNGS detected *Cryptococcus* in 7/10 culture-negative samples with India ink or CrAg tests single positive, which offered important support for diagnoses. After

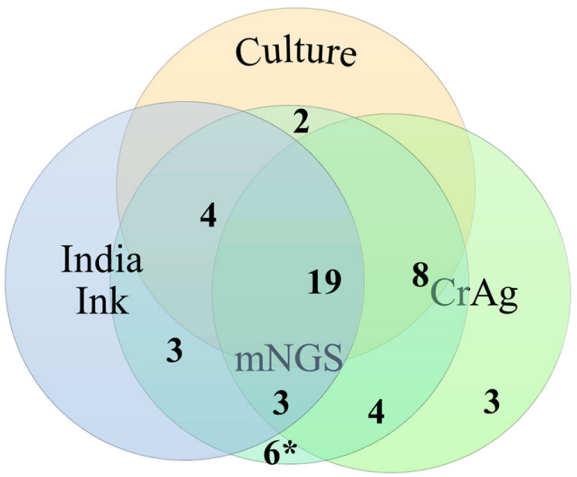

FIGURE 2 | Venn diagram of results of traditional cryptococcal tests and metagenomic next-generation sequencing (mNGS) in 46 patients with cryptococcal central nervous system (CNS) infection. The number of cases detected using culture, India ink, cryptococcal capsular polysaccharide antigen (CrAg), and mNGS was 43, 46, 38, and 46, respectively.*, six mNGS false-positive cases validated by traditional cryptococcal diagnostic tests.

prior antifungal treatment, the decline of cryptococcal load and cryptococcal activity or the deficiency of capsular polysaccharide synthesis may lead to the negative results in fungal culture and India ink staining, which may interfere with clinical judgment. In theory, antifungal drugs killed fungi releasing nucleic acid more into the CSF (Miao et al., 2018). Therefore, mNGS may have the advantages in these cases. Secondly, mNGS also has the advantage in detecting DNA from the capsular polysaccharide antigen-deficient strain and non-*C. neoformans* strains. 3) mNGS can directly distinguish *C. neoformans* from *C. gattii*. In China, *C. neoformans* infection is the most prevalent, while *C. gattii* accounts for only 3.4%–7.0% cases (Dou et al., 2015). However, the disease progression and treatment strategy of *C. gattii* infection is significantly different from that of *C. neoformans* infection, such as the higher possibility of neurological complications, the poorer response to multiple antifungal drugs, and the longer period of antifungal treatment (Dou et al., 2015). The traditional strain identification required a positive culture, but fungal culture has a low positivity rate and is very time-consuming, especially after exposure to antifungal drugs. Therefore, it is difficult to guide clinical decision-making. mNGS distinguishes different fungal species by their nucleic acid sequences, simple and fast, providing useful information for diagnosis and treatment. In theory, it could also identify *Papiliotrema laurentii* and *Naganishia albida*; however, these two strains were not detected in this study.

The current cost for mNGS tests is still very high, and the timeliness is not as good as that of India ink staining or CrAg tests. Furthermore, the antifungal drug resistance analysis is not yet available. mNGS could not replace the traditional diagnostic test for CM and is not recommended for routine use. However, it can be used as a good supplementary test because the results have a high degree of credibility and suggest a present infection. In addition, it has advantages in direct strain identification from clinical specimens, which contributes to clinical decisions.

There are several limitations in our study. Firstly, the *Cryptococcus* nucleic acid assays like PCR were not performed to compare the diagnostic ability. Secondly, quite some cases received antifungal treatment before sampling, which might affect the

TABLE 1 | The performance of mNGS in the diagnosis of cryptococcal CNS infection.

	Cryptococcal CNS infections (case)		Total (case)	Rate (%)
mNGS	Yes	No		
Cryptococcus (RPM ≥1) +	43	6	49	
Cryptococcus (RPM ≥1) –	3	145	148	
Total	46	151	197	
Sensitivity				93.5 ± 3.6
Specificity				96.0 ± 1.6
Positive predictive value (PPV)				87.8 ± 4.5
Negative predictive value (NPV)				98.0 ± 1.2
Concordance rate				95.4

Cryptococcal CNS infections: at least one routine cryptococcal diagnostic test showing positivity.
CNS, central nervous system; mNGS, metagenomic next-generation sequencing; RPM, reads per million.

TABLE 2 | Comparison among mNGS and traditional tests for the diagnosis of cryptococcal CNS infection.

	Sensitivity	Specificity	Concordance rate
mNGS	93.5% (43/46) ± 3.6%	96.0% (145/151) ± 1.6%	95.4% (188/197)
India ink	63.0% (29/46) ± 7.1%	100.0% (148/148) ± 0.0%	91.2% (177/194)
Fungal culture	76.7% (33/43) ± 6.4%	100.0% (127/127) ± 0.0%	94.1% (160/170)
CrAg	97.4% (37/38) ± 2.6%	100.0% (44/44) ± 0.0%	98.8% (81/82)

These assays were compared with the composite etiological diagnosis criteria (at least one routine cryptococcal diagnostic test showing positivity).
CNS, central nervous system; CrAg, cryptococcal capsular polysaccharide antigen; mNGS, metagenomic next-generation sequencing.

TABLE 3 | The performance of mNGS against the "gold standard" culture method.

	Culture (case)		Total (case)	Rate (%)
mNGS	Yes	No		
Cryptococcus (RPM ≥1) +	33	13	46	
Cryptococcus (RPM ≥1) –	0	124	124	
Total	33	137	170	
Sensitivity				100.0 ± 0.0
Specificity				90.5 ± 2.5
Positive predictive value (PPV)				71.7 ± 6.6
Negative predictive value (NPV)				100.0 ± 0.0
Concordance rate				92.4

mNGS, metagenomic next-generation sequencing; RPM, reads per million.

sensitivity to some extent. Furthermore, since the culture for non-*C. neoformans* strains was all negative, we could not assess the accuracy of mNGS to identify *Cryptococcus* strains.

In this study, we evaluated the value of mNGS in the diagnosis of CM in HIV-negative patients. Compared to the conventional methods, mNGS had a higher sensitivity than culture and India ink. The diagnostic ability of mNGS was comparable to that of CrAg method, indicating its excellent diagnostic performance. In addition, mNGS can directly distinguish *C. gattii* from *C. neoformans* in clinical specimens. Our findings indicated that mNGS using CSF can be considered as a supplementary test to diagnose CM.

DATA AVAILABILITY STATEMENT

The datasets presented in this study can be found in online repositories. The names of the repository repositories and accession number(s) can be found below: http://ngdc.cncb.ac.cn, PRJCA008890.

ETHICS STATEMENT

The study was conducted according to the principles expressed in the Declaration of Helsinki and approved by the Medical Ethics Committee of the Third Affiliated Hospital of Sun Yat-sen University. All study participants gave written informed consent for research and publication. The patients/participants provided their written informed consent to participate in this study.

AUTHOR CONTRIBUTIONS

FP and YJ contributed to the conception and design of this study. ZG, JL, YW, LY, ML, and ZC collected and organized the data. ZG, JL, YW, ZL, HX, YJ, and FP analyzed the data. ZG, JL, YW, LY, ZL, HX, ML, ZC, YJ, and FP drafted the article. All the authors read and approved the final article.

FUNDING

This work was supported by the National Science Foundation of Guangdong Province (No. 2015A03013167), the Science and Technology Project of Guangzhou (No. 201510010251), and the Science and Technology Project of Xi'an (No. 21RGSF0013).

SUPPLEMENTARY MATERIAL

The Supplementary Material for this article can be found online at: https://www.frontiersin.org/articles/10.3389/fcimb.2022.831959/full#supplementary-material

REFERENCES

Bittinger K., Charlson E. S., Loy E., Shirley D. J., Haas A. R., Laughlin A., et al. (2014). Improved Characterization of Medically Relevant Fungi in the Human Respiratory Tract Using Next-Generation Sequencing. *Genome Biol.* 15 (10), 487. doi: 10.1186/s13059-014-0487-y

Boulware D. R., Rolfes M. A., Rajasingham R., von Hohenberg M., Qin Z., Taseera K., et al. (2014). Multisite Validation of Cryptococcal Antigen Lateral Flow Assay and Quantification by Laser Thermal Contrast. *Emerg. Infect. Dis.* 20 (1), 45–53. doi: 10.3201/eid2001.130906

Chiu C. Y., Miller S. A. (2019). Clinical Metagenomics. *Nat. Rev. Genet.* 20 (6), 341–355. doi: 10.1038/s41576-019-0113-7

Dou H. T., Xu Y. C., Wang H. Z., Li T. S. (2015). Molecular Epidemiology of Cryptococcus Neoformans and Cryptococcus Gattii in China Between 2007 and 2013 Using Multilocus Sequence Typing and the DiversiLab System. *Eur. J. Clin. Microbiol. Infect. Dis.* 34 (4), 753–762. doi: 10.1007/s10096-014-2289-2

Hasan M. R., Rawat A., Tang P., Jithesh P. V., Thomas E., Tan R., et al. (2016). Depletion of Human DNA in Spiked Clinical Specimens for Improvement of Sensitivity of Pathogen Detection by Next-Generation Sequencing. *J. Clin. Microbiol.* 54 (4), 919–927. doi: 10.1128/JCM.03050-15

Ji X. C., Zhou L. F., Li C. Y., Shi Y. J., Wu M. L., Zhang Y., et al. (2020). Reduction of Human DNA Contamination in Clinical Cerebrospinal Fluid Specimens Improves the Sensitivity of Metagenomic Next-Generation Sequencing. *J. Mol. Neurosci.* 70 (5), 659–666. doi: 10.1007/s12031-019-01472-z

Khawcharoenporn T., Apisarnthanarak A., Mundy L. M. (2007). Non-Neoformans Cryptococcal Infections: A Systematic Review. *Infection* 35 (2), 51–58. doi: 10.1007/s15010-007-6142-8

Li H., Durbin R. (2009). Fast and Accurate Short Read Alignment With Burrows-Wheeler Transform. *Bioinformatics* 25 (14), 1754–1760. doi: 10.1093/bioinformatics/btp324

Liesman R. M., Strasburg A. P., Heitman A. K., Theel E. S., Patel R., Binnicker M. J. (2018). Evaluation of a Commercial Multiplex Molecular Panel for Diagnosis

of Infectious Meningitis and Encephalitis. *J. Clin. Microbiol.* 56 (4), e01927–17. doi: 10.1128/JCM.01927-17

Liu J., Li M., Gan Z. Q., Wang Y. J., Lin C. R., Chen Z. L., et al. (2020). Postinfectious Inflammatory Response Syndrome in HIV-Uninfected and Nontransplant Men After Cryptococcal Meningitis. *Future Microbiol.* 15, 613–621. doi: 10.2217/fmb-2019-0252

Lui G., Lee N., Ip M., Choi K. W., Tso Y. K., Lam E., et al. (2006). Cryptococcosis in Apparently Immunocompetent Patients. *QJM* 99 (3), 143–151. doi: 10.1093/qjmed/hcl014

McMullan B. J., Sorrell T. C., Chen S. C. (2013). Cryptococcus Gattii Infections: Contemporary Aspects of Epidemiology, Clinical Manifestations and Management of Infection. *Future Microbiol.* 8 (12), 1613–1631. doi: 10.2217/fmb.13.123

Miao Q., Ma Y., Wang Q., Pan J., Zhang Y., Jin W., et al. (2018). Microbiological Diagnostic Performance of Metagenomic Next-Generation Sequencing When Applied to Clinical Practice. *Clin. Infect. Dis.* 67 (suppl_2), S231–SS40. doi: 10.1093/cid/ciy693

Miller S., Naccache S. N., Samayoa E., Messacar K., Arevalo S., Federman S., et al. (2019). Laboratory Validation of a Clinical Metagenomic Sequencing Assay for Pathogen Detection in Cerebrospinal Fluid. *Genome Res.* 29 (5), 831–842. doi: 10.1101/gr.238170.118

Perfect J. R., Dismukes W. E., Dromer F., Goldman D. L., Graybill J. R., Hamill R. J., et al. (2010). Clinical Practice Guidelines for the Management of Cryptococcal Disease: 2010 Update by the Infectious Diseases Society of America. *Clin. Infect. Dis.* 50 (3), 291–322. doi: 10.1086/649858

Ragupathi L., Reyna M. (2015). Case Report of Cryptococcus Albidus Peritonitis in a Peritoneal Dialysis Patient and a Review of the Literature. *Perit Dial Int.* 35 (4), 421–427. doi: 10.3747/pdi.2013.00134

Rajasingham R., Wake R. M., Beyene T., Katende A., Letang E., Boulware D. R. (2019). Cryptococcal Meningitis Diagnostics and Screening in the Era of Point-Of-Care Laboratory Testing. *J. Clin. Microbiol.* 57 (1), e01238–18. doi: 10.1128/JCM.01238-18

Ramachandran P. S., Cresswell F. V., Meya D. B., Langelier C., Crawford E. D., DeRisi J. L., et al. (2019). Detection of Cryptococcus DNA by Metagenomic Next-Generation Sequencing in Symptomatic Cryptococcal Antigenemia. *Clin. Infect. Dis.* 68 (11), 1978–1979. doi: 10.1093/cid/ciy1024

Rhein J., Bahr N. C., Hemmert A. C., Cloud J. L., Bellamkonda S., Oswald C., et al. (2016). Diagnostic Performance of a Multiplex PCR Assay for Meningitis in an HIV-Infected Population in Uganda. *Diagn. Microbiol. Infect. Dis.* 84 (3), 268–273. doi: 10.1016/j.diagmicrobio.2015.11.017

Schlaberg R., Chiu C. Y., Miller S., Procop G. W., Weinstock G., Professional Practice C., et al. (2017). Validation of Metagenomic Next-Generation Sequencing Tests for Universal Pathogen Detection. *Arch. Pathol. Lab. Med.* 141 (6), 776–786. doi: 10.5858/arpa.2016-0539-RA

Simner P. J., Miller S., Carroll K. C. (2018). Understanding the Promises and Hurdles of Metagenomic Next-Generation Sequencing as a Diagnostic Tool for Infectious Diseases. *Clin. Infect. Dis.* 66 (5), 778–788. doi: 10.1093/cid/cix881

Smith N., Sehring M., Chambers J., Patel P. (2017). Perspectives on Non-Neoformans Cryptococcal Opportunistic Infections. *J. Community Hosp Intern. Med. Perspect.* 7 (4), 214–217. doi: 10.1080/20009666.2017.1350087

Wang S., Chen Y., Wang D., Wu Y., Zhao D., Zhang J., et al. (2019). The Feasibility of Metagenomic Next-Generation Sequencing to Identify Pathogens Causing Tuberculous Meningitis in Cerebrospinal Fluid. *Front. Microbiol.* 10. doi: 10.3389/fmicb.2019.01993

Wilson M. R., O'Donovan B. D., Gelfand J. M., Sample H. A., Chow F. C., Betjemann J. P., et al. (2018). Chronic Meningitis Investigated *via* Metagenomic Next-Generation Sequencing. *JAMA Neurol.* 75 (8), 947–955. doi: 10.1001/jamaneurol.2018.0463

Wilson M. R., Sample H. A., Zorn K. C., Arevalo S., Yu G., Neuhaus J., et al. (2019). Clinical Metagenomic Sequencing for Diagnosis of Meningitis and Encephalitis. *N Engl. J. Med.* 380 (24), 2327–2340. doi: 10.1056/NEJMoa1803396

Xing X. W., Zhang J. T., Ma Y. B., He M. W., Yao G. E., Wang W., et al. (2020). Metagenomic Next-Generation Sequencing for Diagnosis of Infectious Encephalitis and Meningitis: A Large, Prospective Case Series of 213 Patients. *Front. Cell Infect. Microbiol.* 10. doi: 10.3389/fcimb.2020.00088

Xing X. W., Zhang J. T., Ma Y. B., Zheng N., Yang F., Yu S. Y. (2019). Apparent Performance of Metagenomic Next-Generation Sequencing in the Diagnosis of Cryptococcal Meningitis: A Descriptive Study. *J. Med. Microbiol.* 68 (8), 1204–1210. doi: 10.1099/jmm.0.000994

Zhang C., Tan Z., Tian F. (2020). Impaired Consciousness and Decreased Glucose Concentration of CSF as Prognostic Factors in Immunocompetent Patients With Cryptococcal Meningitis. *BMC Infect. Dis.* 20 (1), 69. doi: 10.1186/s12879-020-4794-5

Zhu L. P., Wu J. Q., Xu B., Ou X. T., Zhang Q. Q., Weng X. H. (2010). Cryptococcal Meningitis in Non-HIV-Infected Patients in a Chinese Tertiary Care Hospital, 1997-2007. *Med. Mycol* 48 (4), 570–579. doi: 10.3109/13693780903437876

Conflict of Interest: ZL and HX are employed by Hugobiotech Co., Ltd.

The remaining authors declare that the research was conducted in the absence of any commercial or financial relationships that could be construed as a potential conflict of interest.

Publisher's Note: All claims expressed in this article are solely those of the authors and do not necessarily represent those of their affiliated organizations, or those of the publisher, the editors and the reviewers. Any product that may be evaluated in this article, or claim that may be made by its manufacturer, is not guaranteed or endorsed by the publisher.

frontiers | Frontiers in Cellular and Infection Microbiology

MINI REVIEW
published: 22 April 2022
doi: 10.3389/fcimb.2022.866463

Raman Spectroscopy—A Novel Method for Identification and Characterization of Microbes on a Single-Cell Level in Clinical Settings

Katarina Rebrosova[1], *Ota Samek*[2], *Martin Kizovsky*[2], *Silvie Bernatova*[2], *Veronika Hola*[1]* *and Filip Ruzicka*[1]

[1] Department of Microbiology, Faculty of Medicine of Masaryk University and St. Anne's University Hospital, Brno, Czechia, [2] Institute of Scientific Instruments of the Czech Academy of Sciences, Brno, Czechia

Rapid and accurate identification of pathogens causing infections is one of the biggest challenges in medicine. Timely identification of causative agents and their antimicrobial resistance profile can significantly improve the management of infection, lower costs for healthcare, mitigate ever-growing antimicrobial resistance and in many cases, save lives. Raman spectroscopy was shown to be a useful—quick, non-invasive, and non-destructive —tool for identifying microbes from solid and liquid media. Modifications of Raman spectroscopy and/or pretreatment of samples allow single-cell analyses and identification of microbes from various samples. It was shown that those non-culture-based approaches could also detect antimicrobial resistance. Moreover, recent studies suggest that a combination of Raman spectroscopy with optical tweezers has the potential to identify microbes directly from human body fluids. This review aims to summarize recent advances in non-culture-based approaches of identification of microbes and their virulence factors, including antimicrobial resistance, using methods based on Raman spectroscopy in the context of possible use in the future point-of-care diagnostic process.

Keywords: Raman spectroscopy, Raman tweezers, identification of microorganisms, antimicrobial resistance, microfluidic devices, magnetic beads, diagnostics

OPEN ACCESS

Edited by:
Nicasio Mancini, Vita-Salute San Raffaele University, Italy

Reviewed by:
Anna Chiara De Luca, National Research Council (CNR), Italy
Jaroslav Hrabak, Charles University, Czechia

***Correspondence:**
Veronika Hola
veronika.hola@fnusa.cz

Specialty section:
This article was submitted to Clinical Microbiology, a section of the journal Frontiers in Cellular and Infection Microbiology

Received: *31 January 2022*
Accepted: *07 March 2022*
Published: *22 April 2022*

Citation:
Rebrosova K, Samek O, Kizovsky M, Bernatova S, Hola V and Ruzicka F (2022) Raman Spectroscopy—A Novel Method for Identification and Characterization of Microbes on a Single-Cell Level in Clinical Settings. Front. Cell. Infect. Microbiol. 12:866463. doi: 10.3389/fcimb.2022.866463

INTRODUCTION

Microorganisms play irreplaceable roles in human existence—we can find them everywhere. In fact, human bodies include more microbial cells than their own cells (Sender et al., 2016). At the same time, it is estimated that approximately 1400 pathogens (including bacteria, fungi, viruses, protozoa, and helminths) can cause infections in humans (Balloux and van Dorp, 2017; Franco-Duarte et al., 2019).

Despite enormous progress in medicine during the last decades, accurate and rapid species-level identification of pathogens causing infections and their virulence factors (including antimicrobial resistance and ability to form biofilms) still poses a challenge. It is important to accent that timely identification and characterization of pathogens is essential for choosing a suitable tailored

antimicrobial treatment and proper management of patients. This, in turn, leads to the shortening of hospital stays, reducing costs and time to adequate treatment, increasing the wellbeing of patients, reducing the spread of antimicrobial resistance, and, above all, saving the lives of many patients.

IDENTIFICATION OF MICROORGANISMS

Basically, we can divide existing identification methods into two groups: culture-based and direct approaches (without cultivation). Major advantages and disadvantages of established methods are summarized in the **Table 1**.

Culture-based approaches are widely used in clinical diagnostics; they could be considered "golden standards". Cultivation provides large amounts of microbial cells for further testing and offers a way to separate different microbes from a mixed culture. This allows the application of various identification and characterization methods separately or in combinations. However, it also makes the culture-based methods relatively time-consuming, expensive, and labor-demanding. Methods commonly used in clinical diagnostics include biochemical testing and mass spectroscopy-based methods. Due to the ever-growing problem of antimicrobial resistance, additional testing of antimicrobial susceptibility (AST) is often required. Conventional AST methods include disk diffusion, gradient diffusion, microdilution, and E-test—all of them require the cultivation step (Khan et al., 2019).

Mass Spectrometry

As an alternative to biochemical testing, matrix-assisted laser desorption/ionization-time-of-flight mass spectrometry (MALDI-TOF MS) has become a revolutionary, widely used tool in numerous clinical diagnostic laboratories. The method is based on the ionization of chemical compounds and measurements of their mass to charge (m/z) ratio. These create a specific microbial fingerprint (a peptide mass fingerprint) allowing identification upon comparison with databases. The whole process takes only minutes and can distinguish even between the most closely related microbial species (Bader et al., 2011; Hendrickx et al., 2011; Lee et al., 2017; Rychert, 2019) and detect antimicrobial resistance (Burckhardt and Zimmermann, 2018; Florio et al., 2020). However, the procedure involves multiple-step-sample preparation and relatively costly consumables. The expensive MALDI-TOF MS device makes the method unaffordable for laboratories in developing countries (Yonetani et al., 2016; Peng et al., 2019).

Direct Methods

Direct methods, besides characterization of microbes and screening, can be used for the identification of microbes in mixed samples as well as for identification of non-culturable microbes (Ramamurthy et al., 2014; Franco-Duarte et al., 2019). They are predominantly based on microscopy, serology, or molecular analyses and do not require cultivation.

Microscopy

Microscopy techniques (bright-field microscopy, dark-field microscopy) can give some indication of the presence of microbes in a sample (Franco-Duarte et al., 2019). A combination of microscopy techniques with other tools/procedures can be used to increase the identification power. Examples include fluorescent dyes (Amann and Fuchs, 2008; Sabnis, 2015), scanning electron microscopy (SEM) (Relucenti et al., 2021), transmission electron microscopy (TEM) (McCutcheon and Southam, 2018), confocal microscopy (CLSM) (Cardinale et al., 2017), and atomic force microscopy (ATM) (James et al., 2016). These methods are also considered valuable in biofilm studies. A disadvantage of direct microscopy methods is an unspecific result not allowing accurate identification unless combined with additional procedure/tools, which makes the process costly and time-demanding.

Serological Methods

Serological methods used in clinical diagnostics include the detection of antigens and antibodies. They are usually highly specific and must be ordered in a goal-directed manner (e.g., confirmation or exclusion of certain infectious agents). The positivity of antibody tests may be delayed due to the dynamics of antibody production in the human body. Besides, the immune response of the hosts usually has polyclonal nature and is influenced by genetic factors as well as environmental

TABLE 1 | Summary of current advantages and disadvantages of Raman spectroscopy in microbiology.

Raman spectroscopy and microbial analyses	
Advantages	**Disadvantages**
rapid	no commercial database for microbial identification
sensitive	
non-destructive	
non-invasive	
microbes remain viable after the analysis and can be used for further testing	need for standardization (data presented in manuscripts are group-specific and custom-tailored)
highly reproducible within a device	
simple sample preparation	
no costly consumables necessary	relatively expensive device
allowing detection of virulence factors	need for trained personnel and possible automatization
allowing single-cell level analyses: applicable for non-culturable microbes, no need for cultivation	cultivation is necessary or can be replaced by separation methods

factors. Therefore, the reaction of a patient´s serum with an analytical system is not precisely predictable and there might be some variations. During the detection of antigens, antigenic variations (leading to different serotypes) might cause problems (Fierz, 2003).

Molecular Methods

The advent of the "genomic era" brought an astounding array of techniques incredibly useful for the characterization of biological materials and organisms, including microbes (Spratt, 2004). The development of polymerase chain reaction (PCR) in 1983 was a real breakthrough in (clinical) microbiology. Later on, real-time PCR (RT-PCR) was developed and brought a new wind into diagnostics improving the speed, sensitivity, and specificity of microbial detection (Mackay, 2004). Also, 16S rRNA, 16S – 23S rRNA (bacteria), and 18S rRNA (eukaryotes) PCR-sequencing can be a useful tool for identifying microorganisms combining PCR amplification of 16S (18S) rRNA gene, which is highly specific to each microbial species, and its subsequent sequencing (Reller et al., 2007; Singhal et al., 2015; Peker et al., 2019). When 16S rRNA gene is identical, species identification could rely on other conserved genes, such as gyrA, gyrB, rpoB, tuf, and heat shock proteins (Franco-Duarte et al., 2019). Although PCR-based methods can detect pathogens at early stages of infection and do not require cultivation, clinical samples often contain low numbers of microbial cells, complicating their capturing. They require preprocessing before the PCR reaction (incl. removal of PCR inhibitors, extraction of maximum microbes from the sample without contamination, isolation of nucleic acids). Furthermore, those methods detect the only presence of nucleic acid (or its part), which can be misleading since the human body contains large amounts of microbial genetic material (Franco-Duarte et al., 2019; Kubina and Dziedzic, 2020).

Modern technologies allow miniaturization and automatization of the methods and building more efficient approaches, such as next-generation sequencing (NGS). NGS allows parallel sequencing of enormous numbers of whole genomes or parts of nucleic acids at once, providing reliable identification of microorganisms at the nucleic acid level (Sabat et al., 2017; Boers et al., 2019). To overcome the low numbers of pathogens present in a sample, PCR amplification can be used. Compared with other widely used methods, disadvantages of using NGS in clinical diagnostics of infections include high costs and lower sensitivity, or more specifically, higher recovery of clinically unimportant microorganisms, and often too general identification (e.g., phylum level) (Lee et al., 2020).

New Approaches

We can conclude that all the methods mentioned above have advantages and disadvantages. Thus, different methods might be suitable or combined for different types of infections/expected causative agents. To shorten the time necessary for identification, many approaches have been proposed. Their main goals include shortening/skipping cultivation, shortening the time and reducing consumables needed for the identification, automatizing the process, and/or adding further information about a sample (e.g., virulence factors). These approaches include but are not limited to certain protocols for MALDI-TOF MS (Drancourt, 2010; Meex et al., 2012; Hoyos-Mallecot et al., 2014; Idelevich et al., 2014; Machen et al., 2014; Verroken et al., 2015; Zhou et al., 2017), infrared spectroscopy (FTIR) (Ojeda and Dittrich, 2012; Zarnowiec et al., 2015; Vogt et al., 2019), nuclear magnetic resonance (NMR) spectroscopy (Romaniuk and Cegelski, 2015; Palama et al., 2016), capillary electrophoresis (incl. capillary isoelectric focusing (Ruzicka et al., 2016; Xu and Sun, 2021), electrical field-flow fractionation (Saenton et al., 2000; Reschiglian et al., 2002), microfluidic devices (Kim et al., 2012; Zhou et al., 2019; Pérez-Rodríguez et al., 2022) and Raman spectroscopy (Franco-Duarte et al., 2019). Recently, Raman spectroscopy has been undergoing a boom in microbiology, as many studies suggest its potential for the identification of microbes, their virulence factors, detection of metabolic changes, and last but not least, single-cell analyses of microbial cells.

RAMAN SPECTROSCOPY

Raman spectroscopy is an optical method based on inelastic scattering of monochromatic light. In general, when a light beam (laser beam) reaches an object (particles), most of the light is scattered elastically (energy after deexcitation is equal to Rayleigh scattering), part of the beam passes through, part of the beam is absorbed. The last tiny part (approximately 10^{-5}%) is inelastically scattered (**Figure 1**)—the energy of photons in the beam changes upon interaction with molecular vibrations in a sample and leads to a momentary distortion of electrons in a bond of a molecule. It means that the molecule has an induced dipole and is temporarily polarized. Upon returning to its normal state, the radiation is reemitted (Raman scattering). If a photon passes a part of its energy on a molecule, its frequency gets lower, and the vibrational energy of the molecule participating in a collision gets higher (Stokes Raman scattering). Thanks to thermal energy, it is also possible that a molecule is in an excited state. Then, a photon can gain energy from the molecule: the energy and the photon's frequency gets higher, the energy of the molecule gets lower (anti-Stokes Raman scattering) (Das and Agrawal, 2011). Therefore, molecular vibrations in a sample play an essential role in Raman scattering: to be Raman active, a molecule must undergo a change in polarizability of an electron cloud around the molecule (a tendency of the electron cloud to be distorted from its original position) during a vibration. The polarizability of molecules decreases with increasing electron density (shorter and stronger bonds). The intensity of the Raman spectrum is dependent on the change of polarizability. Therefore, the most intensive Raman spectra can be acquired from symmetric valence vibrations (Smith and Dent, 2004). To conclude, we can say that the basic principle of Raman spectroscopy is tracking of scattered electrons´ energetic changes against the energy of photons from a source of monochromatic light "mirroring" chemical bonds present in the sample.

This can be useful in various scientific and industrial fields ranging from archeology arts (Ziemann and Madariaga, 2021) and food industry (Weng et al., 2019), pharmacy (Vankeirsbilck et al., 2002), life sciences (McCreery, 2000; Pimenta et al., 2007;

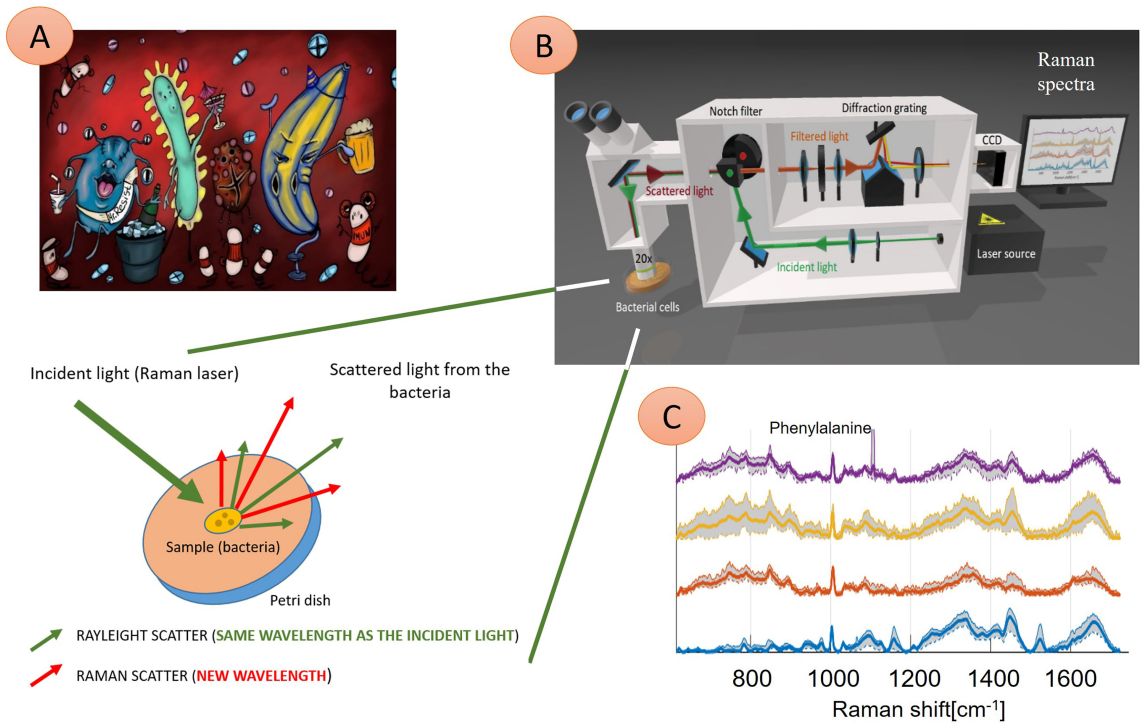

FIGURE 1 | Illustration of four different microbial species interacting with the immune system and their Raman spectra. **(A)** Microbes are present in the human body, causing an infection. These pathogens can be identified using Raman spectroscopy technique **(B)**—here: probing laser (green) is focused on the sample (bacteria), and a small amount of light, which transports the chemical structure of analyzed bacteria, is reflected (red) and in the next step further analyzed. Consequently, four Raman spectra **(C)** show information about molecular bond vibrations of given bacteria, such as phenylalanine at 1005 cm^{-1}. In this example, the naked eye can see differences between the spectra of four samples. Thus, these pathogens can be identified quickly (in minutes) to treat infection with tailored antibiotics. **(C)** Examples of Raman spectra: *Staphylococcus pasteuri* (violet curve), *Staphylococcus warneri* (yellow curve), *Streptococcus oralis* (red curve), *Staphylococcus sciuri* (blue trace).

Butler et al., 2016; Kuhar et al., 2018; Li et al., 2020; Wang et al., 2020; Pezzotti, 2021) to medicine. Examples of medical applications include measurements of inflammatory markers including C-reactive protein (Bergholt and Hassing, 2009; Neugebauer et al., 2014), measurements of blood and urine chemicals (Qi and Berger, 2007), measurements of blood coagulation (Poon et al., 2012), determination oxygen saturation in live tissues (Das and Agrawal, 2011), tissue engineering (Ember et al., 2017), *in vivo* and *in vitro* diagnostics of various cancers (Chan et al., 2008; Harvey et al., 2008; Dochow et al., 2013; Taleb et al., 2013; Kong et al., 2015; Auner et al., 2018), diagnostics of prenatal diseases (Kim et al., 2018), endometriosis (Parlatan et al., 2019), and osteomyelitis (Khalid et al., 2018). Raman spectroscopy also has a plethora of applications in clinical, experimental, environmental, and technical microbiology.

Raman Spectroscopy in Microbiology

Raman spectroscopy appears to be a valuable tool for the identification of microorganisms (Maquelin et al., 2003; Samek et al., 2008; Almarashi et al., 2012; Kastanos et al., 2012; Schie and Huser, 2013; Neugebauer et al., 2015; Pahlow et al., 2015; Read and Whiteley, 2015; Tien et al., 2016; Rebrošová et al., 2017; de Siqueira e Oliveira et al., 2021; Rebrošová et al., 2022), even in mixed samples (Yogesha et al., 2019). The identification can be performed from colonies grown on solid agar plates, microcolonies (Choo-Smith et al., 2001; Mathey et al., 2015), or microorganisms in liquid media (Schuster et al., 2000; Samek et al., 2010; Avci et al., 2015; Kotanen et al., 2016; Nakar et al., 2022; Rebrošová et al., 2022) and microbial spectra are highly reproducible within a device (Mlynáriková et al., 2015). Furthermore, Raman spectroscopy can be used for the characterization of microbial virulence factors, including antimicrobial resistance (Wulf et al., 2012; Bernatová et al., 2013; Dekter et al., 2017; Rousseau et al., 2021; Nakar et al., 2022) and the ability to form a biofilm (Samek et al., 2008; Samek et al., 2014; Liu et al., 2014; Hrubanova et al., 2018; Keleştemur et al., 2018; Rebrošová et al., 2019). There are some Raman studies of phenotypic changes caused by exposure to environmental stimuli, including antibiotics (Athamneh et al., 2014), alcohol (Zu et al., 2016), or metabolic stressors (Tanniche et al., 2020). Raman spectroscopy was successfully used to quantify microbes in a sample, too (Escoriza et al., 2006). To gain a stronger signal, the Raman signal can be amplified using surface-enhanced Raman spectroscopy (SERS), which is widely

used in microbiological studies (Samek et al., 2021). Recently, there was significant progress in single-cell analyzes employing Raman spectroscopy and other variations of Raman spectroscopy, allowing to skip the cultivation step. The most frequently used approaches are summarized below.

Centrifugation

A commonly used method for separating microbes from liquid media/samples is centrifugation. Published works consider centrifugation+Raman spectroscopy to be promising for identification of microbes from human body fluids, namely ascitic fluid (Kloß et al., 2015b), sputum (Kloß et al., 2015a), artificial bronchoalveolar lavage (Wichmann et al., 2021), and urine (Schröder et al., 2015; Rebrošová et al., 2022). Premasiri et al. showed a possibility to combine centrifugation and SERS to identify pathogens and their antimicrobial susceptibility (Premasiri et al., 2017). Together with filtration lysis and SERS, centrifugation was used to identify pathogens from human serum (Kotanen et al., 2016).

Moreover, centrifugation+SERS showed a possibility of identifying *Chlamydia trachomatis* and *Neisseria gonorrhoeae* and characterizing their extra-cellular metabolomics (Chen et al., 2018).

Magnetic Beads

Magnetic beads are widely used for separation and isolation during bioprocessing, especially for the isolation of nucleic acids. However, the mechanism itself allows magnetic separation to be applied on various samples: magnetic separation relies upon forces induced in magnetically susceptible materials by magnetic fields (Schwaminger et al., 2019). In biology, primarily magnetic beads coated with synthetical or biological polymers (including antibodies) capable of capturing the target molecules/cells are used. Target molecules/cells bind to a polymer. Afterward, the whole complex (magnetic carrier with polymer + target molecule/cell) is captured by applying magnetic force (Berensmeier, 2006).

Kusić et al. successfully used magnetic beads coated with *Legionella* spp. specific polyclonal immunoglobulins for isolating single *Legionella* sp. cells from biofilm and subsequently identifying them with Raman spectroscopy (Kusić et al., 2014). Kearns et al. developed a bionanosensor based on magnetic separation and SERS, which can be used to identify microbes in concentrations as low as 10^1 CFU/mL in less than one hour (Kearns et al., 2017). Hu et al. showed a possibility of capturing *Candida* sp. cells from serum and characterizing them using SERS (Hu et al., 2021). Li et al. used polyethyleneimine-modified magnetic microspheres (Fe_3O_4@PEI) and SERS for bacterial identification and antimicrobial resistance determination from 77 blood samples (Li et al., 2019). A combination of SERS and immunomagnetic beads can also be used to detect *Clostridium botulinum* toxins A and B (Kim et al., 2019). Since magnetic separation is commonly used for nucleic acid isolation, Hwang et al. applied this method to isolate bacterial genomic DNA and identify it using SERS and fluorescent assay favoring SERS by means of sensitivity (Hwang et al., 2021). Detection of bacterial DNA by SERS using streptavidin-coated magnetic particles was also proved by Qun et al. with a limit of detection of 5 pM (Qun et al., 2015).

Dielectrophoresis

Dielectrophoresis (DEP) is defined as a movement of dielectric particles through a medium in response to a non-uniform electric field. A particle becomes polarized, and due to the difference in electric field strength on the two sides of the particle, the particle is moved in the electric field gradient region by net dielectrophoretic force (Tay et al., 2009). This effect can be used for the separation of particles (Fernandez et al., 2017) and is widely used for enrichment and isolation of microbial cells before analysis at a single-cell level (Fernandez et al., 2017; Zhang et al., 2019; Sarno et al., 2021; Weber et al., 2021). Some groups recently suggested its possible combination with Raman spectroscopy for single-cell microbial analyses (Neugebauer et al., 2015). Chen et al. showed the efficiency of DEP-based microfluidic chip for Raman detection and measurements of *Shewanella oneidensis* cells in HEPES buffer (Chen et al., 2018). From clinically relevant applications, Cheng et al. used DEP with SERS to isolate and identify bacteria in isotonic solution with human blood cells, proposing rapid detection of microbes in human blood from 12h blood cultures (Cheng et al., 2014). To identify pathogens causing urinary tract infections faster, Schröder et al. proposed using a combination of DEP and Raman spectroscopy to identify *Escherichia coli* and *Enterococcus faecalis* in human urine, providing results in 35 minutes (Schröder et al., 2013).

Optical Tweezers

Optical tweezers—a Nobel price-winning (2018) groundbreaking invention by Alfred Ashkin—use single-beam gradient force to hold particles/micro-objects (incl. microbial cells) in place and manipulate them (Ashkin, 1997; Wu et al., 2017). With an optical trap, living cells suspended in a liquid cultivation medium can be immobilized in a solution using the forces generated by a tightly focused laser beam. Combined with Raman spectroscopy (usually termed Raman tweezers), it has found numerous applications, especially in analytical and physical chemistry. Raman tweezers is currently starting to be applied in cell and molecular biology. It allows single-cell analyses of microbes, for example, direct identification of microbes from liquid samples, including wastewater (Cui et al., 2021) and human urine (Rebrošová et al., 2022), in less than 10 minutes. This combination can also be used to detect antibiotic resistance (Bernatová et. al 2014; Pilát et al., 2018; Bernatová et al., 2021) and an ability to form a biofilm (Samek et al., 2015). Moreover, it was used to describe metabolic changes in microbes (Singh et al., 2006; Huang et al., 2007) and bacterial lysis (Chen et al., 2009).

Challenges

Current advantages and disadvantages of the Raman spectroscopy for microbiology are summarized in the **Table 1**.

Unambiguously, Raman spectroscopy offers a streamlined, fast, non-destructive, and non-invasive approach for identifying

microbes and their virulence factors suitable for clinical diagnostics. Compared to conventional and molecular methods, sample preparation is easy and does not necessarily require expensive consumables. Moreover, multiple methods were proposed to isolate or enrich microbes, allowing their single-cell analyses and non-culture-based detection and identification.

However, getting Raman spectroscopy to clinical laboratories might have a long-time coming. At the moment, there are no commercial and/or well-annotated databases of microbial Raman fingerprints, as discussed by Wang et al. (Wang et al., 2021). To make comparisons of acquired Raman spectra across various instruments, one should consider that the quantum efficiency of the given detector and optical elements depends on a wavelength. Therefore, acquired data should be corrected according to an instrument response profile. Ideally, a spectral sensitivity curve should be used (Rebrošová et al., 2017). Thus, Raman spectra presented in different studies are group-specific and custom-tailored, which makes data standardization complicated (Lorenz et al., 2017). Nonetheless, no large-scale studies were performed to compare microbial Raman spectra from different groups.

Microbial studies often employ the SERS technique. Again, there is a problem with the standardization of SERS microbial detection protocols (Witkowska et al., 2020; Samek et al., 2021). Although SERS provides a stronger signal than conventional Raman spectroscopy, several factors influence the signal enhancement and, consequently, the final spectrum. These may include types of culture media, culturing conditions, sample preparation method, and interactions between SERS substrate and individual microbial cells (Witkowska et al., 2020; Samek et al., 2021).

Other problems are (currently) relatively high input costs, the need for complicated instrumentation, and specialized operators. Automatization and miniaturization would be beneficial for potential future clinical use.

If those problems are solved, Raman spectroscopy-based point-of-care device could start a revolution in clinical diagnostic microbiology in the future. Assuming its broad spectrum of applications in medicine, one device equipped with various diagnostic databases might become a complex diagnostic tool. From a microbiological point of view, Raman spectroscopy could be used for rapid pathogen identification and characterization of its virulence factors, which would, in turn, result in tailored antimicrobial treatment, reduced financial burdens associated with healthcare, and above all, improved patient management and reduced mortality from infections.

SUMMARY

Raman spectroscopy is an elegant optical method that could significantly contribute to rapid clinical diagnostics of infections. It allows the identification of microbes and detection of certain virulence factors, including antimicrobial resistance and biofilm formation. In combination with techniques for isolation/enrichment of microbes from a liquid sample, it could be used for rapid single-cell analyzes of microbial cells, even directly from human body fluids. Therefore, it could provide an effective solution for identifying microbes in the future.

AUTHOR CONTRIBUTIONS

KR, OS, MK participated in conceptualization and writing of the original draft. SB, VH, and FR participated in review and editing. All authors contributed to the article and approved the submitted version.

FUNDING

This work was supported by the Grant Agency of Masaryk University (MUNI/A/1291/2021) and the Czech Health Research Council (NU21-05-00341).

ACKNOWLEDGMENTS

We would like to thank the artist Gabriela Samkova for the beautiful illustration of the bacterial infection she prepared for our manuscript.

REFERENCES

Almarashi, J. F. M., Kapel, N., Wilkinson, T. S., and Telle, H. H. (2012). Raman Spectroscopy of Bacterial Species and Strains Cultivated Under Reproducible Conditions. *Spectroscopy: Int. J.* 27, 361–365. doi: 10.1155/2012/540490

Amann, R., and Fuchs, B. M. (2008). Single-Cell Identification in Microbial Communities by Improved Fluorescence *in Situ* Hybridization Techniques. *Nat. Rev. Microbiol.* 6 (5), 339–348. doi: 10.1038/nrmicro1888

Ashkin, A. (1997). Optical Trapping and Manipulation of Neutral Particles Using Lasers. *Proc. Natl. Acad. Sci.* 94 (10), 4853–4860. doi: 10.1073/pnas.94.10.4853

Athamneh, A. I. M., Alajlouni, R. A., Wallace, R. S., Seleem, M. N., and Senger, R. S. (2014). Phenotypic Profiling of Antibiotic Response Signatures in Escherichia Coli Using Raman Spectroscopy. *Antimicrob. Agents Chemother.* 58 (3), 1302–1314. doi: 10.1128/AAC.02098-13

Auner, G. W., Koya, S. K., Huang, C., Broadbent, B., Trexler, M., Auner, Z., et al. (2018). Applications of Raman Spectroscopy in Cancer Diagnosis. *Cancer Metastasis Rev.* 37 (4), 691–717. doi: 10.1007/s10555-018-9770-9

Avci, E., Kaya, N. S., Ucankus, G., and Culha, M. (2015). Discrimination of Urinary Tract Infection Pathogens by Means of Their Growth Profiles Using Surface Enhanced Raman Scattering. *Anal. Bioanal. Chem.* 407 (27), 8233–8241. doi: 10.1007/s00216-015-8950-5

Bader, O., Weig, M., Taverne-Ghadwal, L., Lugert, R., Groß, U., and Kuhns, M. (2011). Improved Clinical Laboratory Identification of Human Pathogenic Yeasts by Matrix-Assisted Laser Desorption Ionization Time-of-Flight Mass Spectrometry. *Clin. Microbiol. Infect.* 17 (9), 1359–1365. doi: 10.1111/j.1469-0691.2010.03398.x

Balloux, F., and van Dorp, L. (2017). Q&a: What are Pathogens, and What Have They Done to and for Us? *BMC Biol.* 15 (1), 91. doi: 10.1186/s12915-017-0433-z

Berensmeier, S. (2006). Magnetic Particles for the Separation and Purification of Nucleic Acids. *Appl. Microbiol. Biotechnol.* 73 (3), 495–504. doi: 10.1007/s00253-006-0675-0

Bergholt, M. S., and Hassing, S. (2009). Quantification of C-Reactive Protein in Human Blood Plasma Using Near-Infrared Raman Spectroscopy. *Analyst* 134 (10), 2123. doi: 10.1039/b903089a

Bernatová, S., Rebrošová, K., Pilát, Z., Šerý, M., Gjevik, A., Samek, O., et al. (2013). Following the Mechanisms of Bacteriostatic Versus Bactericidal Action Using Raman Spectroscopy. *Molecules* 18 (11), 13188–13199. doi: 10.3390/molecules181113188

Bernatova, S., Samek, O., Pilát, Z., Šerý, M., Ježek, J., Jákl, P., et al. (2014). "Raman Tweezers on Bacteria: Following the Mechanisms of Bacteriostatic Versus Bactericidal Action," in *Spie Photonics Europe*. Ed. J. Popp, et al. (Brussels, Belgium: SPIE), 91291Y. doi: 10.1117/12.2052538

Bernatová, S., Samek, O., Pilat, Z., Sery, M., Jezek, J., Jakl, P., et al. (2021). Rapid Detection of Antibiotic Sensitivity of Staphylococcus Aureus by Raman Tweezers. *Eur. Phys. J. Plus* 136 (2), 233. doi: 10.1140/epjp/s13360-021-01152-1

Boers, S. A., Jansen, R., and Hays, J. P. (2019). Understanding and Overcoming the Pitfalls and Biases of Next-Generation Sequencing (NGS) Methods for Use in the Routine Clinical Microbiological Diagnostic Laboratory. *Eur. J. Clin. Microbiol. Infect. Dis.* 38 (6), 1059–1070. doi: 10.1007/s10096-019-03520-3

Brock, T. D., et al. (2003). 'Brock Biology of Microorganisms', in. *Upper Saddle River NJ: Prentice hall (10)* p, 1019.

Burckhardt, I., and Zimmermann, S. (2018). Susceptibility Testing of Bacteria Using Maldi-Tof Mass Spectrometry. *Front. Microbiol.* 9. doi: 10.3389/fmicb.2018.01744

Butler, H. J., Ashton, L., Bird, B., Cinque, G., Curtis, K., Dorney, J., et al. (2016). Using Raman Spectroscopy to Characterize Biological Materials. *Nat. Protoc.* 11 (4), 664–687. doi: 10.1038/nprot.2016.036

Cardinale, M., Kaiser, D., Lueders, T., Schnell, S., and Egert, M. (2017). Microbiome Analysis and Confocal Microscopy of Used Kitchen Sponges Reveal Massive Colonization by Acinetobacter, Moraxella and Chryseobacterium Species. *Sci. Rep.* 7 (1), 5791. doi: 10.1038/s41598-017-06055-9

Chan, J. W., Taylor, D. S., Lane, S. M., Zwerdling, T., Tuscano, J., and Huser, T. (2008). Nondestructive Identification of Individual Leukemia Cells by Laser Trapping Raman Spectroscopy. *Anal. Chem.* 80 (6), 2180–2187. doi: 10.1021/ac7022348

Chen, D., Chen, T.-Y., Lu, R.-J., and Wu, H.-W. (2009). Laser Tweezers Raman Spectroscopy Potential for Studies of Complex Dynamic Cellular Processes: Single Cell Bacterial Lysis. *Anal. Chem.* 81 (9), 3227–3238. doi: 10.1021/ac8023476

Chen, X., Liang, Z., Li, D., Xiong, Y., Xiong, P., Guan, Y., et al. (2018). Microfluidic Dielectrophoresis Device for Trapping, Counting and Detecting Shewanella Oneidensis at the Cell Level. *Biosensors Bioelectronics* 99, 416–423. doi: 10.1016/j.bios.2017.08.017

Cheng, I.-F., Chen, T.-Y., Lu, R.-J., and Wu, H.-W. (2014). Rapid Identification of Bacteria Utilizing Amplified Dielectrophoretic Force-Assisted Nanoparticle-Induced Surface-Enhanced Raman Spectroscopy. *Nanoscale Res. Lett.* 9 (1), 324. doi: 10.1186/1556-276X-9-324

Chen, Y., Premasiri, W. R., and Ziegler, L. D. (2018). Surface Enhanced Raman Spectroscopy of Chlamydia Trachomatis and Neisseria Gonorrhoeae for Diagnostics, and Extra-Cellular Metabolomics and Biochemical Monitoring. *Sci. Rep.* 8 (1), 5163. doi: 10.1038/s41598-018-23562-5

Choo-Smith, L.-P., Maquelin, K., van Vreeswijk, T., Bruining, H. A., Puppels, G. J., Thi, N. A. N., et al. (2001). Investigating Microbial (Micro)Colony Heterogeneity by Vibrational Spectroscopy. *Appl. Environ. Microbiol.* 67 (4), 1461–1469. doi: 10.1128/AEM.67.4.1461-1469.2001

Cui, L., Li, H.-Z., Yang, K., Zhu, L.-J., Xu, F., and Zhu, Y.-G. (2021). Raman Biosensor and Molecular Tools for Integrated Monitoring of Pathogens and Antimicrobial Resistance in Wastewater. *TrAC Trends Analy. Chem.* 143, 116415. doi: 10.1016/j.trac.2021.116415

Das, R. S., and Agrawal, Y. K. (2011). Raman Spectroscopy: Recent Advancements, Techniques and Applications. *Vibrational Spectrosc.* 57 (2), 163–176. doi: 10.1016/j.vibspec.2011.08.003

Dekter, H. E., Orelio, C. C., Morsink, M. C., Tektas, S., Vis, B., te Witt, R., et al. (2017). Antimicrobial Susceptibility Testing of Gram-Positive and -Negative Bacterial Isolates Directly From Spiked Blood Culture Media With Raman Spectroscopy. *Eur. J. Clin. Microbiol. Infect. Dis.* 36 (1), 81–89. doi: 10.1007/s10096-016-2773-y

de Siqueira e Oliveira, F. S., da Silva, A. M., Pacheco, M. T. T., Giana, H. E., and Silveira, L. (2021). Biochemical Characterization of Pathogenic Bacterial Species Using Raman Spectroscopy and Discrimination Model Based on Selected Spectral Features. *Lasers Med. Sci.* 36 (2), 289–302. doi: 10.1007/s10103-020-03028-9

Dochow, S., Beleites, C., Henkel, T., Mayer, G., Albert, J., Clement, J., et al. (2013). Quartz Microfluidic Chip for Tumour Cell Identification by Raman Spectroscopy in Combination With Optical Traps. *Anal. Bioanal. Chem.* 405 (8), 2743–2746. doi: 10.1007/s00216-013-6726-3

Drancourt, M. (2010). Detection of Microorganisms in Blood Specimens Using Matrix-Assisted Laser Desorption Ionization Time-of-Flight Mass Spectrometry: A Review. *Clin. Microbiol. Infect.* 16 (11), 1620–1625. doi: 10.1111/j.1469-0691.2010.03290.x

Ember, K. J. I., Hoeve, M. A., McAughtrie, S. L., Bergholt, M. S., Dwyer, B. J., Stevens, M. M., et al. (2017). Raman Spectroscopy and Regenerative Medicine: A Review. *NPJ Regenerative Med.* 2 (1), 12. doi: 10.1038/s41536-017-0014-3

Escoriza, M. F., VanBriesen, J. M., Stewart, S., Maier, J., and Treado, P. J. (2006). Raman Spectroscopy and Chemical Imaging for Quantification of Filtered Waterborne Bacteria. *J. Microbiol. Methods* 66 (1), 63–72. doi: 10.1016/j.mimet.2005.10.013

Fernandez, R. E., Rohani, A., Farmehini, V., and Swami, N. S. (2017). Review: Microbial Analysis in Dielectrophoretic Microfluidic Systems. *Analytica Chimica Acta* 966, 11–33. doi: 10.1016/j.aca.2017.02.024

Fierz, W. (2003). "Basic Problems of Serological Laboratory Diagnosis," in *Molecular Diagnosis of Infectious Diseases*. Eds. J. Decker and U. Reischl (New Jersey: Humana Press), 393–428. doi: 10.1385/1-59259-679-7:393

Florio, W., Baldeschi, L., Rizzato, C., Tavanti, A., Ghelardi, E., and Lupetti, A. (2020). Detection of Antibiotic-Resistance by MALDI-TOF Mass Spectrometry: An Expanding Area. *Front. Cell. Infect. Microbiol.* 10. doi: 10.3389/fcimb.2020.572909

Franco-Duarte, R., Černáková, L., Kadam, S., S. Kaushik, K., Salehi, B., Bevilacqua, A., et al. (2019). Advances in Chemical and Biological Methods to Identify Microorganisms—From Past to Present. *Microorganisms* 7 (5), 130. doi: 10.3390/microorganisms7050130

Harvey, T. J., Faria, E. C., Henderson, A., Gazi, E., Ward, A. D., Clarke, N. W., et al. (2008). Spectral Discrimination of Live Prostate and Bladder Cancer Cell Lines Using Raman Optical Tweezers. *J. Biomed. Optics* 13 (6), 064004. doi: 10.1117/1.2999609

Hendrickx, M., Goffinet, J.-S., Swinne, D., and Detandt, M. (2011). Screening of Strains of the Candida Parapsilosis Group of the BCCM/IHEM Collection by MALDI-TOF MS. *Diagn. Microbiol. Infect. Dis.* 70 (4), 544–548. doi: 10.1016/j.diagmicrobio.2011.04.006

Hoyos-Mallecot, Y., Riazzo, C., Miranda-Casas, C., Rojo-Martín, M. D., Gutiérrez-Fernández, J., and Navarro-Marí, J. M. (2014). Rapid Detection and Identification of Strains Carrying Carbapenemases Directly From Positive Blood Cultures Using MALDI-TOF MS. *J. Microbiol. Methods* 105, 98–101. doi: 10.1016/j.mimet.2014.07.016

Hrubanova, K., Krzyzanek, V., Nebesarova, J., Ruzicka, F., Pilat, Z., and Samek, O. (2018). Monitoring Candida Parapsilosis and Staphylococcus Epidermidis Biofilms by a Combination of Scanning Electron Microscopy and Raman Spectroscopy. *Sensors* 18 (12), 4089. doi: 10.3390/s18124089

Huang, S., Chen, D., Pelczar, P. L., Vepachedu, V. R., Setlow, P., and Li, Y. (2007). Levels of Ca2+-Dipicolinic Acid in Individual Bacillus Spores Determined Using Microfluidic Raman Tweezers. *J. Bacteriol.* 189 (13), 4681–4687. doi: 10.1128/JB.00282-07

Hu, S., Kang, H., Gu, F., Wang, C., Cheng, S., Gong, W., et al. (2021). Rapid Detection Method for Pathogenic Candida Captured by Magnetic Nanoparticles and Identified Using SERS *via* Agnps+'. *Int. J. Nanomed.* 16, 941–950. doi: 10.2147/IJN.S285339

Hwang, M. J., Jang, A. S., and Lim, D.-K. (2021). Comparative Study of Fluorescence and Surface-Enhanced Raman Scattering With Magnetic Microparticle-Based Assay for Target Bacterial DNA Detection. *Sensors Actuators B: Chem.* 329, 129134. doi: 10.1016/j.snb.2020.129134

Idelevich, E. A., Schüle, I., Grünastel, B., Wüllenweber, J., Peters, G., and Becker, K. (2014). Rapid Identification of Microorganisms From Positive Blood Cultures by MALDI-TOF Mass Spectrometry Subsequent to Very Short-Term Incubation on Solid Medium. *Clin. Microbiol. Infect.* 20 (10), 1001–1006. doi: 10.1111/1469-0691.12640

James, S. A., Powell, L. C., and Wright, C. J. (2016). "Atomic Force Microscopy of Biofilms—Imaging, Interactions, and Mechanics," in *Microbial Biofilms* -

Importance and Applications. Eds. D. Dhanasekaran and N. Thajuddin (London: InTech). doi: 10.5772/63312

Kastanos, E., Kyriakides, A., Hadjigeorgiou, K., and Pitris, C. (2012). A Novel Method for Bacterial UTI Diagnosis Using Raman Spectroscopy. *Int. J. Spectrosc.* 2012, 1–13. doi: 10.1155/2012/195317

Kearns, H., Goodacre, R., Jamieson, L. E., Graham, D., and Faulds, K. (2017). SERS Detection of Multiple Antimicrobial-Resistant Pathogens Using Nanosensors. *Analytical Chem.* 89 (23), 12666–12673. doi: 10.1021/acs.analchem.7b02653

Keleştemur, S., Avci, E., and Çulha, M. (2018). Raman and Surface-Enhanced Raman Scattering for Biofilm Characterization. *Chemosensors* 6 (1), 5. doi: 10.3390/chemosensors6010005

Khalid, M., Bora, T., Ghaithi, A. A., Thukral, S., and Dutta, J. (2018). Raman Spectroscopy Detects Changes in Bone Mineral Quality and Collagen Cross-Linkage in Staphylococcus Infected Human Bone. *Sci. Rep.* 8 (1), 9417. doi: 10.1038/s41598-018-27752-z

Khan, Z. A., Siddiqui, M. F., and Park, S. (2019). Current and Emerging Methods of Antibiotic Susceptibility Testing. *Diagnostics* 9 (2), 49. doi: 10.3390/diagnostics9020049

Kim, J., Hegde, M., Kim, S. H., Wood, T. K., and Jayaraman, A. (2012). A Microfluidic Device for High Throughput Bacterial Biofilm Studies. *Lab. Chip* 12 (6), 1157. doi: 10.1039/c2lc20800h

Kim, W., Lee, S. H., Kim, J. H., Ahn, Y. J., Kim, Y.-H., Yu, J. S., et al. (2018). Paper-Based Surface-Enhanced Raman Spectroscopy for Diagnosing Prenatal Diseases in Women. *ACS Nano* 12 (7), 7100–7108. doi: 10.1021/acsnano.8b02917

Kim, K., Choi, N., Jeon, J. H., Rhie, G., and Choo, J. (2019). SERS-Based Immunoassays for the Detection of Botulinum Toxins a and B Using Magnetic Beads. *Sensors* 19 (19), 4081. doi: 10.3390/s19194081

Kloß, S., Rösch, P., Pfister, W., Kiehntopf, M., and Popp, J. (2015b). Toward Culture-Free Raman Spectroscopic Identification of Pathogens in Ascitic Fluid. *Anal. Chem.* 87 (2), 937–943. doi: 10.1021/ac503373r

Kloß, S., Lorenz, B., Dees, S., Labugger, I., Rösch, P., and Popp, J. (2015a). Destruction-Free Procedure for the Isolation of Bacteria From Sputum Samples for Raman Spectroscopic Analysis. *Anal. Bioanal. Chem.* 407 (27), 8333–8341. doi: 10.1007/s00216-015-8743-x

Kong, K., Kendall, C., Stone, N., and Notingher, I. (2015). Raman Spectroscopy for Medical Diagnostics — From *in-Vitro* Biofluid Assays to *in-Vivo* Cancer Detection. *Advanced Drug Delivery Rev.* 89, 121–134. doi: 10.1016/j.addr.2015.03.009

Kotanen, C. N., Martinez, L., Alvarez, R., and Simecek, J. W. (2016). Surface Enhanced Raman Scattering Spectroscopy for Detection and Identification of Microbial Pathogens Isolated From Human Serum. *Sens. Bio-Sensing Res.* 8, 20–26. doi: 10.1016/j.sbsr.2016.03.002

Kubina, R., and Dziedzic, A. (2020). Molecular and Serological Tests for COVID-19. A Comparative Review of SARS-Cov-2 Coronavirus Laboratory and Point-of-Care Diagnostics. *Diagnostics 10(6)* p, 434. doi: 10.3390/diagnostics10060434

Kuhar, N., Sil, S., Verma, T., and Umapathy, S. (2018). Challenges in Application of Raman Spectroscopy to Biology and Materials. *RSC Adv.* 8 (46), 25888–25908. doi: 10.1039/C8RA04491K

Kusić, D., Kampe, B., Rösch, P., and Popp, J. (2014). Identification of Water Pathogens by Raman Microspectroscopy. *Water Res.* 48, 179–189. doi: 10.1016/j.watres.2013.09.030

Lee, J., Shin, Y., Kim, S., Rho, K., and Park, K. H. (2017). "SVM Classification Model of Similar Bacteria Species Using Negative Marker: Based on Matrix-Assisted Laser Desorption/Ionization Time-of-Flight Mass Spectrometry," in *2017 IEEE 17th International Conference on Bioinformatics and Bioengineering (BIBE). 2017 IEEE 17th International Conference on Bioinformatics and Bioengineering (BIBE)* (Washington, DC: IEEE), 145–150. doi: 10.1109/BIBE.2017.00-64

Lee, R. A., Al Dhaheri, F., Pollock, N. R., and Sharma, T. S. (2020). Assessment of the Clinical Utility of Plasma Metagenomic Next-Generation Sequencing in a Pediatric Hospital Population. *J. Clin. Microbiol.* 58 (7), e00419–20. doi: 10.1128/JCM.00419-20

Li, J., Wang, C., Shi, L., Shao, L., Fu, P., Wang, K., et al. (2019). Rapid Identification and Antibiotic Susceptibility Test of Pathogens in Blood Based on Magnetic Separation and Surface-Enhanced Raman Scattering. *Microchimica Acta* 186 (7), 475. doi: 10.1007/s00604-019-3571-x

Li, S., Li, Y., Yi, R., Liu, L., and Qu, J. (2020). Coherent Anti-Stokes Raman Scattering Microscopy and its Applications. *Front. Phys.* 8. doi: 10.3389/fphy.2020.598420

Liu, H., Xu, Q., Huo, L., Wei, X., and Ling, J. (2014). Chemical Composition of Enterococcus Faecalis in Biofilm Cells Initiated From Different Physiologic States. *Folia Microbiologica* 59 (5), 447–453. doi: 10.1007/s12223-014-0319-1

Lorenz, B., Wichmann, C., Stöckel, S., Rösch, P., and Popp, J. (2017). Cultivation-Free Raman Spectroscopic Investigations of Bacteria. *Trends Microbiol.* 25 (5), 413–424. doi: 10.1016/j.tim.2017.01.002

Machen, A., Drake, T., and Wang, Y. F. (2014). Same Day Identification and Full Panel Antimicrobial Susceptibility Testing of Bacteria From Positive Blood Culture Bottles Made Possible by a Combined Lysis-Filtration Method With MALDI-TOF VITEK Mass Spectrometry and the VITEK2 System. *PloS One* 9 (2), e87870. doi: 10.1371/journal.pone.0087870. Wayne.

Mackay, I. M. (2004). Real-Time PCR in the Microbiology Laboratory. *Clin. Microbiol. Infect.* 10 (3), 190–212. doi: 10.1111/j.1198-743X.2004.00722.x

Maquelin, K., Kirschner, C., Choo-Smith, L.-P., Ngo-Thi, N. A., van Vreeswijk, T., Stämmler, M., et al. (2003). Prospective Study of the Performance of Vibrational Spectroscopies for Rapid Identification of Bacterial and Fungal Pathogens Recovered From Blood Cultures. *J. Clin. Microbiol.* 41 (1), 324–329. doi: 10.1128/JCM.41.1.324-329.2003

Mathey, R., Dupoy, M., Espagnon, I., Leroux, D., Mallard, F., and Novelli-Rousseau, A. (2015). Viability of 3h Grown Bacterial Micro-Colonies After Direct Raman Identification. *J. Microbiol Methods* 109, 67–73. doi: 10.1016/j.mimet.2014.12.002

McCreery, R. L. (2000). *Raman Spectroscopy for Chemical Analysis: Mccreery/Raman Spectroscopy. Hoboken* (NJ, USA: John Wiley & Sons, Inc). doi: 10.1002/0471721646

McCutcheon, J., and Southam, G. (2018). Advanced Biofilm Staining Techniques for TEM and SEM in Geomicrobiology: Implications for Visualizing EPS Architecture, Mineral Nucleation, and Microfossil Generation. *Chem. Geol.* 498, 115–127. doi: 10.1016/j.chemgeo.2018.09.016

Meex, C., Neuville, F., Descy, J., Huynen, P., Hayette, M.-P., De Mol, P., et al. (2012). Direct Identification of Bacteria From Bact/ALERT Anaerobic Positive Blood Cultures by MALDI-TOF MS: MALDI Sepsityper Kit Versus an in-House Saponin Method for Bacterial Extraction. *J. Med. Microbiol.* 61 (11), 1511–1516. doi: 10.1099/jmm.0.044750-0

Mlynáriková, K., Samek, O., Bernatová, S., Růžička, F., Ježek, J., Hároniková, A., et al. (2015). Influence of Culture Media on Microbial Fingerprints Using Raman Spectroscopy. *Sensors* 15 (11), 29635–29647. doi: 10.3390/s151129635

Nakar, A., Pistiki, A., Ryabchykov, O., Bocklitz, T., Rösch, P., and Popp, J. (2022). Detection of Multi-Resistant Clinical Strains of E. Coli With Raman Spectroscopy. *Anal. Bioanal. Chem.* 18, 1481–1492. doi: 10.1007/s00216-021-03800-y

Neugebauer, U., Rösch, P., and Popp, J. (2014). Fast Differentiation of SIRS and Sepsis From Blood Plasma of ICU Patients Using Raman Spectroscopy: Spectroscopic Differentiation of SIRS and Sepsis From Blood Plasma. *J. Biophotonics* 7 (3–4), 232–240. doi: 10.1002/jbio.201400010

Neugebauer, U., Rösch, P., and Popp, J. (2015). Raman Spectroscopy Towards Clinical Application: Drug Monitoring and Pathogen Identification. *Int. J. Antimicrob. Agents* 46, S35–S39. doi: 10.1016/j.ijantimicag.2015.10.014

Ojeda, J. J., and Dittrich, M. (2012). "Fourier Transform Infrared Spectroscopy for Molecular Analysis of Microbial Cells," in *Microbial Systems Biology*. Ed. A. Navid (Totowa, NJ: Humana Press (Methods in Molecular Biology), 187–211. doi: 10.1007/978-1-61779-827-6_8

Pahlow, S., Meisel, S., Cialla-May, D., Weber, K., Rösch, P., and Popp, J. (2015). Isolation and Identification of Bacteria by Means of Raman Spectroscopy. *Advanced Drug Delivery Rev.* 89, 105–120. doi: 10.1016/j.addr.2015.04.006

Palama, T. L., Canard, I., Rautureau, G. J. P., Mirande, C., Chatellier, S., and Elena-Herrmann, B. (2016). Identification of Bacterial Species by Untargeted NMR Spectroscopy of the Exo-Metabolome. *Analyst* 141 (15), 4558–4561. doi: 10.1039/C6AN00393A

Parlatan, U., Inanc, M. T., Ozgor, B. Y., Oral, E., Bastu, E., Unlu, M. B., et al. (2019). Raman Spectroscopy as a non-Invasive Diagnostic Technique for Endometriosis. *Sci. Rep.* 9 (1), 19795. doi: 10.1038/s41598-019-56308-y

Peker, N., Garcia-Croes, S., Dijkhuizen, B., Wiersma, H. H., van Zanten, E., Wisselink, G., et al. (2019). A Comparison of Three Different Bioinformatics

Analyses of the 16S–23S Rrna Encoding Region for Bacterial Identification. *Front. Microbiol.* 10. doi: 10.3389/fmicb.2019.00620

Peng, Y., Zhang, Q., Xu, C., and Shi, W. (2019). MALDI–TOF MS for the Rapid Identification and Drug Susceptibility Testing of Filamentous Fungi. *Exp. Ther. Med*. 414, 4865–4873 doi: 10.3892/etm.2019.8118

Pérez-Rodríguez, S., García-Aznar, J. M., and Gonzalo-Asensio, J. (2022). Microfluidic Devices for Studying Bacterial Taxis, Drug Testing and Biofilm Formation. *Microbial Biotechnol.* 15, 395–414. doi: 10.1111/1751-7915.13775

Pezzotti, G. (2021). Raman Spectroscopy in Cell Biology and Microbiology. *J. Raman Spectrosc.* 52 (12), 2348–2443. doi: 10.1002/jrs.6204

Pilát, Z., Bernatová, S., Ježek, J., Kirchhoff, J., Tannert, A., Neugebauer, U., et al. (2018). 'Microfluidic Cultivation and Laser Tweezers Raman Spectroscopy of E. *Coli Under Antibiotic Stress' Sensors 18(5)* p, 1623. doi: 10.3390/s18051623

Pimenta, M. A., Dresselhaus, G., Dresselhaus, M. S., Cançado, L. G., Jorio, A., and Saito, R. (2007). Studying Disorder in Graphite-Based Systems by Raman Spectroscopy. *Phys. Chem. Chem. Phys.* 9 (11), 1276–1290. doi: 10.1039/B613962K

Poon, K. W. C., Lyng, F. M., Knief, P., Howe, O., Meade, A. D., Curtin, J. F., et al. (2012). Quantitative Reagent-Free Detection of Fibrinogen Levels in Human Blood Plasma Using Raman Spectroscopy. *Analyst* 137 (8), 1807. doi: 10.1039/c2an35042d

Premasiri, W. R., Chen, Y., Williamson, P. M., Bandarage, D. C., Pyles, C., and Ziegler, L. D. (2017). Rapid Urinary Tract Infection Diagnostics by Surface-Enhanced Raman Spectroscopy (SERS): Identification and Antibiotic Susceptibilities. *Anal. Bioanal. Chem.* 409 (11), 3043–3054. doi: 10.1007/s00216-017-0244-7

Qi, D., and Berger, A. J. (2007). Chemical Concentration Measurement in Blood Serum and Urine Samples Using Liquid-Core Optical Fiber Raman Spectroscopy. *Appl. Optics* 46 (10), 1726. doi: 10.1364/AO.46.001726

Qun, M., Yan-Le, L., Nian-Chun, G., Xi, J., and Shuang-Yan, H. (2015). Surface Enhanced Raman Spectroscopy Sensor Based on Magnetic Beads-Induced Nanoparticles Aggregation for Detection of Bacterial Deoxyribonucleic Acid. *Chin. J. Anal. Chem.* 43 (11), 1676–1681. doi: 10.1016/S1872-2040(15)60876-3

Ramamurthy, T., Ghosh, A., Pazhani, G. P., and Shinoda, S. (2014). Current Perspectives on Viable But non-Culturable (VBNC) Pathogenic Bacteria. *Front. Public Health* 2. doi: 10.3389/fpubh.2014.00103

Read, D. S., and Whiteley, A. S. (2015). Chemical Fixation Methods for Raman Spectroscopy-Based Analysis of Bacteria. *J. Microbiol. Methods* 109, 79–83. doi: 10.1016/j.mimet.2014.12.008

Rebrošová, K., Šiler, M., Samek, O., Růžička, F., Bernatová, S., Holá, V., et al. (2017). Rapid Identification of Staphylococci by Raman Spectroscopy. *Sci. Rep.* 7 (1), 14846. doi: 10.1038/s41598-017-13940-w

Rebrošová, K., Šiler, M., Samek, O., Růžička, F., Bernatová, S., Ježek, J., et al. (2019). Identification of Ability to Form Biofilm in *Candida Parapsilosis* and *Staphylococcus Epidermidis* by Raman Spectroscopy. *Future Microbiol.* 14 (6), 509–517. doi: 10.2217/fmb-2018-0297

Rebrošová, K., Bernatová, S., Šiler, M., Uhlirova, M., Samek, O., Ježek, J., et al. (2022). Raman Spectroscopy—a Tool for Rapid Differentiation Among Microbes Causing Urinary Tract Infections. *Analytica Chimica Acta* 1191, 339292. doi: 10.1016/j.aca.2021.339292

Reller, L. B., Weinstein, M. P., and Petti, C. A. (2007). Detection and Identification of Microorganisms by Gene Amplification and Sequencing. *Clin. Infect. Dis.* 44 (8), 1108–1114. doi: 10.1086/512818

Relucenti, M., Familiari, G., Donfrancesco, O., Taurino, M., Li, X., Chen, R., et al. (2021). Microscopy Methods for Biofilm Imaging: Focus on SEM and VP-SEM Pros and Cons. *Biology* 10 (1), 51. doi: 10.3390/biology10010051

Reschiglian, P., Zattoni, A., Roda, B., Casolari, S., Moon, M. H., Lee, J., et al. (2002). Bacteria Sorting by Field-Flow Fractionation. Application to Whole-Cell *Escherichia Coli* Vaccine Strains. *Anal. Chem.* 74 (19), 4895–4904. doi: 10.1021/ac020199t

Romaniuk, J. A. H., and Cegelski, L. (2015). Bacterial Cell Wall Composition and the Influence of Antibiotics by Cell-Wall and Whole-Cell NMR. *Philos. Trans. R. Soc. B: Biol. Sci.* 370 (1679), 20150024. doi: 10.1098/rstb.2015.0024

Rousseau, A. N., Faure, N., Rol, F., Sedaghat, Z., Le Galudec, J., Mallard, F., et al. (2021). Fast Antibiotic Susceptibility Testing *via* Raman Microspectrometry on Single Bacteria: An MRSA Case Study. *ACS Omega* 6 (25), 16273–16279. doi: 10.1021/acsomega.1c00170

Ruzicka, F., Horka, M., Hola, V., Mlynarikova, K., and Drab, V. (2016). Capillary Isoelectric Focusing—Useful Tool for Detection and Quantification of Lactic Acid Bacteria in Milk. *Food Anal. Methods* 9 (12), 3251–3257. doi: 10.1007/s12161-016-0522-6

Rychert, J. (2019). Benefits and Limitations of MALDI-TOF Mass Spectrometry for the Identification of Microorganisms. *J. Infectiol.* 2 (4), 1–5. doi: 10.29245/2689-9981/2019/4.1142

Sabat, A. J., van Zanten, E., Akkerboom, V., Wisselink, G., van Slochteren, K., de Boer, R. F., et al. (2017). Targeted Next-Generation Sequencing of the 16S-23S Rrna Region for Culture-Independent Bacterial Identification - Increased Discrimination of Closely Related Species. *Sci. Rep.* 7 (1), 3434. doi: 10.1038/s41598-017-03458-6

Sabnis, R. W. (2015). *Handbook of Fluorescent Dyes and Probes. Hoboken* (New Jersey: Wiley).

Saenton, S., Lee, H., Gao, Y.-S., Ranville, J. F., and Williams, S. K. R. (2000). Evaluation of Different Field-Flow Fractionation Techniques for Separating Bacteria. *Separation Sci. Technol.* 35 (11), 1761–1775. doi: 10.1081/SS-100102492

Samek, O., Bernatová, S., and Dohnal, F. (2021). The Potential of SERS as an AST Methodology in Clinical Settings. *Nanophotonics* 10 (10), 2537–2561. doi: 10.1515/nanoph-2021-0095

Samek, O., Telle, H. H., Harris, L. G., Bloomfield, M., and Mack, D. (2008). Raman Spectroscopy for Rapid Discrimination of *Staphylococcus Epidermidis* Clones Related to Medical Device-Associated Infections. *Laser Phys. Lett.* 5 (6), 465–470. doi: 10.1002/lapl.200810011

Samek, O., Jonáš, A., Pilát, Z., Zemánek, P., Nedbal, L., Tříska, J., et al. (2010). Raman Microspectroscopy of Individual Algal Cells: Sensing Unsaturation of Storage Lipids *In Vivo*. *Sensors* 10 (9), 8635–8651. doi: 10.3390/s100908635

Samek, O., Mlynariková, K., Bernatová, S., Ježek, J., Krzyžánek, V., Šiler, M., et al. (2014). Candida Parapsilosis Biofilm Identification by Raman Spectroscopy. *Int. J. Mol. Sci.* 15 (12), 23924–23935. doi: 10.3390/ijms151223924

Samek, O., Bernatová, S., Ježek, J., Šiler, M., Šerý, M., Krzyžánek, V., et al. (2015). Identification of Individual Biofilm-Forming Bacterial Cells Using Raman Tweezers. *J. Biomed. Optics* 20 (5), 51038. doi: 10.1117/1.JBO.20.5.051038

Sarno, B., Heineck, D., Heller, M. J., and Ibsen, S. D. (2021). Dielectrophoresis: Developments and Applications From 2010 to 2020. *ELECTROPHORESIS* 42 (5), 539–564. doi: 10.1002/elps.202000156

Schie, I. W., and Huser, T. (2013). Methods and Applications of Raman Microspectroscopy to Single-Cell Analysis. *Appl. Spectrosc.* 67 (8), 813–828. doi: 10.1366/12-06971

Schröder, U.-C., Ramoji, A., Glaser, U., Sachse, S., Leiterer, C., Csaki, A., et al. (2013). Combined Dielectrophoresis–Raman Setup for the Classification of Pathogens Recovered From the Urinary Tract. *Anal. Chem.* 85 (22), 10717–10724. doi: 10.1021/ac4021616

Schröder, U.-C., Bokeloh, F., O'Sullivan, M., Glaser, U., Wolf, K., Pfister, W., et al. (2015). Rapid, Culture-Independent, Optical Diagnostics of Centrifugally Captured Bacteria From Urine Samples. *Biomicrofluidics* 9 (4), 044118. doi: 10.1063/1.4928070

Schuster, K. C., Urlaub, E., and Gapes, J. R. (2000). Single-Cell Analysis of Bacteria by Raman Microscopy: Spectral Information on the Chemical Composition of Cells and on the Heterogeneity in a Culture. *J. Microbiol. Methods* 42 (1), 29–38. doi: 10.1016/S0167-7012(00)00169-X

Schwaminger, S. P., Fraga-García, P., Eigenfeld, M., Becker, T. M., and Berensmeier, S. (2019). Magnetic Separation in Bioprocessing Beyond the Analytical Scale: From Biotechnology to the Food Industry. *Front. Bioeng. Biotechnol.* 7. doi: 10.3389/fbioe.2019.00233

Sender, R., Fuchs, S., and Milo, R. (2016). Revised Estimates for the Number of Human and Bacteria Cells in the Body. *PloS Biol.* 14 (8), e1002533. doi: 10.1371/journal.pbio.1002533

Singhal, N., Kumar, M., Kanaujia, P. K., and Virdi, J. S. (2015). MALDI-TOF Mass Spectrometry: An Emerging Technology for Microbial Identification and Diagnosis. *Front. Microbiol.* 6. doi: 10.3389/fmicb.2015.00791

Singh, G. P., Volpe, G., Creely, C. M., Grötsch, H., Geli, I. M., and Petrov, D. (2006). The Lag Phase and G1 Phase of a Single Yeast Cell Monitored by Raman Microspectroscopy. *J. Raman Spectrosc.* 37 (8), 858–864. doi: 10.1002/jrs.1520

Smith, E., and Dent, G. (2004). *Modern Raman Spectroscopy - a Practical Approach: Smith/Modern Raman Spectroscopy - a Practical Approach. Chichester* (UK: John Wiley & Sons, Ltd). doi: 10.1002/0470011831

Spratt, D. A. (2004). Significance of Bacterial Identification by Molecular Biology Methods. *Endodontic Topics* 9 (1), 5–14. doi: 10.1111/j.1601-1546.2004.00106.x

Taleb, I., Thiéfin, G., Gobinet, C., Untereiner, V., Bernard-Chabert, B., Heurgué, A., et al. (2013). Diagnosis of Hepatocellular Carcinoma in Cirrhotic Patients: A Proof-of-Concept Study Using Serum Micro-Raman Spectroscopy. *Analyst* 138 (14), 4006. doi: 10.1039/c3an00245d

Tanniche, I., Collakova, E., Denbow, C., and Senger, R. S. (2020). Characterizing Metabolic Stress-Induced Phenotypes of *Synechocystis* PCC6803 With Raman Spectroscopy. *PeerJ* 8, e8535. doi: 10.7717/peerj.8535

Tay, F., Yu, L., and Iliescu, C. (2009). Particle Manipulation by Miniaturised Dielectrophoretic Devices. *Defence Sci. J.* 59 (6), 595–604. doi: 10.14429/dsj.59.1564

Tien, N., Chen, H.-C., Gau, S.-L., Lin, T.-H., Lin, H.-S., You, B.-J., et al. (2016). Diagnosis of Bacterial Pathogens in the Dialysate of Peritoneal Dialysis Patients With Peritonitis Using Surface-Enhanced Raman Spectroscopy. *Clinica Chimica Acta* 461, 69–75. doi: 10.1016/j.cca.2016.07.026

Vankeirsbilck, T., Vercauteren, A., Baeyens, W., van der Weken, G., Verpoort, F., Vergote, G., et al. (2002). Applications of Raman Spectroscopy in Pharmaceutical Analysis. *TrAC Trends Anal. Chem.* 21 (12), 869–877. doi: 10.1016/S0165-9936(02)01208-6

Verroken, A., Defourny, L., Lechgar, L., Magnette, A., Delmée, M., and Glupczynski, Y. (2015). Reducing Time to Identification of Positive Blood Cultures With MALDI-TOF MS Analysis After a 5-H Subculture. *Eur. J. Clin. Microbiol. Infect. Dis.* 34 (2), 405–413. doi: 10.1007/s10096-014-2242-4

Vogt, S., Löffler, K., Dinkelacker, A. G., Bader, B., Autenrieth, I. B., Peter, S., et al. (2019). Fourier-Transform Infrared (FTIR) Spectroscopy for Typing of Clinical Enterobacter Cloacae Complex Isolates. *Front. Microbiol.* 10. doi: 10.3389/fmicb.2019.02582

Wang, X., Huang, S.-C., Hu, S., Yan, S., and Ren, B. (2020). Fundamental Understanding and Applications of Plasmon-Enhanced Raman Spectroscopy. *Nat. Rev. Phys.* 2 (5), 253–271. doi: 10.1038/s42254-020-0171-y

Wang, L., Liu, W., Tang, J.-W., Wang, J.-J., Liu, Q.-H., Wen, P.-B., et al. (2021). Applications of Raman Spectroscopy in Bacterial Infections: Principles, Advantages, and Shortcomings. *Front. Microbiol.* 12. doi: 10.3389/fmicb.2021.683580

Weber, R. E., Petkowski, J. J., Michaels, B., Wisniewski, K., Piela, A., Antoszczyk, S., et al. (2021). Fluid-Screen as a Real Time Dielectrophoretic Method for Universal Microbial Capture. *Sci. Rep.* 11 (1), 22222. doi: 10.1038/s41598-021-01600-z

Weng, S., Zhu, W., Zhang, X., Yuan, H., Zheng, L., Zhao, J., et al. (2019). Recent Advances in Raman Technology With Applications in Agriculture, Food and Biosystems: A Review. *Artif. Intell. Agric.* 3, 1–10. doi: 10.1016/j.aiia.2019.11.001

Wichmann, C., Rösch, P., and Popp, J. (2021). Isolation of Bacteria From Artificial Bronchoalveolar Lavage Fluid Using Density Gradient Centrifugation and Their Accessibility by Raman Spectroscopy. *Anal. Bioanal. Chem.* 413 (20), 5193–5200. doi: 10.1007/s00216-021-03488-0

Witkowska, E., Niciński, K., Korsak, D., Dominiak, B., Waluk, J., and Kamińska, A. (2020). Nanoplasmonic Sensor for Foodborne Pathogens Detection. Towards Development of ISO-SERS Methodology for Taxonomic Affiliation of *Campylobacter* Spp. *J. Biophotonics* 13 (5), e201960227. doi: 10.1002/jbio.201960227

Wu, M., Ling, D., Ling, L., Li, W., and Li, Y. (2017). Stable Optical Trapping and Sensitive Characterization of Nanostructures Using Standing-Wave Raman Tweezers. *Sci. Rep.* 7 (1), 42930. doi: 10.1038/srep42930

Wulf, M. W. H., Willemse-Erix, D., Verduin, C. M., Puppels, G., van Belkum, A., and Maquelin, K. (2012). The Use of Raman Spectroscopy in the Epidemiology of Methicillin-Resistant Staphylococcus Aureus of Human- and Animal-Related Clonal Lineages. *Clin. Microbiol. Infect.* 18 (2), 147–152. doi: 10.1111/j.1469-0691.2011.03517.x

Xu, T., and Sun, L. (2021). A Mini Review on Capillary Isoelectric Focusing-Mass Spectrometry for Top-Down Proteomics. *Front. Chem.* 9. doi: 10.3389/fchem.2021.651757

Yogesha, M., Chawla, K., Bankapur, A., Acharya, M., D'Souza, J. S., and Chidangil, S. (2019). A Micro-Raman and Chemometric Study of Urinary Tract Infection-Causing Bacterial Pathogens in Mixed Cultures. *Anal. Bioanal. Chem.* 411 (14), 3165–3177. doi: 10.1007/s00216-019-01784-4

Yonetani, S., Ohnishi, H., Ohkusu, K., Matsumoto, T., and Watanabe, T. (2016). Direct Identification of Microorganisms From Positive Blood Cultures by MALDI-TOF MS Using an in-House Saponin Method. *Int. J. Infect. Dis.* 52, 37–42. doi: 10.1016/j.ijid.2016.09.014

Zarnowiec, P., Lechowicz, L., Czerwonka, G., and Kaca, W. (2015). Fourier Transform Infrared Spectroscopy (FTIR) as a Tool for the Identification and Differentiation of Pathogenic Bacteria. *Curr. Med. Chem.* 22 (14), 1710–1718. doi: 10.2174/0929867322666150311152800

Zhang, H., Chang, H., and Neuzil, P. (2019). DEP-on-a-Chip: Dielectrophoresis Applied to Microfluidic Platforms. *Micromachines* 10 (6), 423. doi: 10.3390/mi10060423

Zhou, M., Le, J., Chen, Y., Cai, Y., Hong, Z., and Chai, Y. (2017). An Improved in-House MALDI-TOF MS Protocol for Direct Cost-Effective Identification of Pathogens From Blood Cultures. *Front. Microbiol.* 8. doi: 10.3389/fmicb.2017.01824

Zhou, W., Yang, Q., Kudinha, T., Sun, L., Zhang, R., Liu, C., et al. (2019). Recent Advances in Microfluidic Devices for Bacteria and Fungus Research. *TrAC Trends Analy. Chem.* 112, 175–195. doi: 10.1016/j.trac.2018.12.024

Ziemann, M. A., and Madariaga, J. M. (2021). Applications of Raman Spectroscopy in Art and Archaeology. *J. Raman Spectrosc.* 52 (1), 8–14. doi: 10.1002/jrs.6054

Zu, T., Athamneh, A., and Senger, R. (2016). Characterizing the Phenotypic Responses of Escherichia Coli to Multiple 4-Carbon Alcohols With Raman Spectroscopy. *Fermentation* 2 (4), 3. doi: 10.3390/fermentation2010003

Conflict of Interest: The authors declare that the research was conducted in the absence of any commercial or financial relationships that could be construed as a potential conflict of interest.

Publisher's Note: All claims expressed in this article are solely those of the authors and do not necessarily represent those of their affiliated organizations, or those of the publisher, the editors and the reviewers. Any product that may be evaluated in this article, or claim that may be made by its manufacturer, is not guaranteed or endorsed by the publisher.

frontiers | Frontiers in Cellular and Infection Microbiology

ORIGINAL RESEARCH
published: 25 May 2022
doi: 10.3389/fcimb.2022.895261

Fast, Simple, and Highly Specific Molecular Detection of *Porphyromonas gingivalis* Using Isothermal Amplification and Lateral Flow Strip Methods

Duobao Ge, Fang Wang, Yanyan Hu, Bendi Wang, Xuzhu Gao and Zhenxing Chen**

Department of Stomatology, the Second People's Hospital of Lianyungang City (Cancer Hospital of Lianyungang), affiliated to Bengbu Medical College, Lianyungang, China

OPEN ACCESS

Edited by:
Nicasio Mancini, Vita-Salute San Raffaele University, Italy

Reviewed by:
J Christopher Fenno, University of Michigan, United States
Keiji Nagano, Health Sciences University of Hokkaido, Japan

***Correspondence:**
Zhenxing Chen
lygeykqk@163.com
Xuzhu Gao
alexgwan@163.com

Specialty section:
This article was submitted to Clinical Microbiology, a section of the journal Frontiers in Cellular and Infection Microbiology

Received: *13 March 2022*
Accepted: *27 April 2022*
Published: *25 May 2022*

Citation:
Ge D, Wang F, Hu Y, Wang B, Gao X and Chen Z (2022) Fast, Simple, and Highly Specific Molecular Detection of Porphyromonas gingivalis Using Isothermal Amplification and Lateral Flow Strip Methods. Front. Cell. Infect. Microbiol. 12:895261. doi: 10.3389/fcimb.2022.895261

Porphyromonas gingivalis is an important oral pathogen that causes periodontal disease and is difficult to culture under conventional conditions. Therefore, a reliable technique for detecting this pathogenic bacterium is required. Here, isothermal recombinase polymerase amplification (RPA), a new nucleic acid amplification method, was combined with a visualization method based on nanoparticle-based lateral flow strips (LFS) for the rapid detection of *P. gingivalis*. The species-specific 16S rRNA sequence of *P. gingivalis* was used as the target for RPA, and a set of specific primer–probe combinations were designed and screened to amplify the target sequences. As a thermostatic amplification method, the RPA reaction, under optimized conditions, takes only 30 min to complete at a constant temperature (37°C). The amplification reaction products can be detected visually by LFS without any need for special equipment. The RPA-LFS method established for the detection of *P. gingivalis* was shown to be highly specific in distinguishing *P. gingivalis* from other pathogenic organisms by using 20 clinical isolates of *P. gingivalis* and 23 common pathogenic microorganisms. Susceptibility measurements and probit regression analysis were performed with gradient dilutions of *P. gingivalis* genomic DNA. The method was obtained to be highly sensitive, with a detection limit of 9.27 CFU per reaction at 95% probability. By analyzing the gingival sulcus fluid specimens from 130 patients with chronic periodontitis, the results showed that the RPA-LFS method detected 118 positive cases and 12 negative cases of *P. gingivalis*, and the results obtained were consistent with those of a conventional PCR assay. The RPA–LFS method is an efficient, rapid, and convenient diagnostic method that simplifies the tedious process of detecting *P. gingivalis*.

Keywords: periodontal disease, *Porphyromonas gingivalis*, isothermal (DNA) amplification, lateral flow strip, rapid detection

INTRODUCTION

Periodontal disease is a chronic infectious disease that occurs in the periodontal supporting tissues and is currently considered the sixth most prevalent disease in humans due to its high prevalence (Slots, 2017). Plaque microorganisms are known to be the initiating factors in the pathogenesis of periodontal disease, and among them, *Porphyromonas gingivalis* is currently recognized as the main dominant bacterium associated with the development of periodontal disease and is one of the key pathogenic bacteria studied in the field of periodontal microbiology (Olsen et al., 2017). *P. gingivalis* is a Gram-negative anaerobic bacterium that is present in the first complex (red complex) microflora of subgingival plaque in close association with chronic periodontitis (Zhang et al., 2020). As an opportunistic pathogen, *P. gingivalis* is not an aggressor of the inflammatory response, but rather a reciprocal reaction with the host that disrupts the host's immune defense mechanisms, thereby prolonging its survival in the host and triggering the inflammatory response of the organism (Hajishengallis and Diaz, 2020). Previous studies have shown that *P. gingivalis* is closely associated not only with oral diseases such as aggressive periodontitis, periodontal abscesses and periapical inflammation (Mysak et al., 2014), but also with systemic systemic diseases such as atherosclerosis and gastrointestinal malignancies (Qi et al., 2020; Xie et al., 2020). In addition, *P. gingivalis* in periodontal pockets can be used to predict the progression of related diseases, and its number is significantly and positively correlated with the degree of disease (He et al., 2012; Yaseen et al., 2021). Therefore, exploring rapid detection methods for *P. gingivalis* are important guidelines for the diagnosis of oral diseases and related systemic diseases as well as for early intervention.

In the diagnosis of *P. gingivalis* infection, we currently rely on the traditional culture method for its detection, but this culture method requires the isolation, culture, and identification of the microorganism and has the disadvantages of being time-consuming, insensitive, and cumbersome (Atieh, 2008; Fyrestam et al., 2017). With the development of molecular biology techniques, rapid diagnostic studies of *P. gingivalis* have progressed rapidly, including the PCR detection of ribosomal RNA (16S rRNA), fluorescence quantitative PCR, immunochromatography, ionization time-of-flight mass spectrometry, and DNA probe hybridization, which can detect *P. gingivalis* rapidly at the gene or genome level (Rams et al., 2016; Mougeot et al., 2017; O'Brien-Simpson et al., 2017; Marin et al., 2018; Gu et al., 2020). However, these assays rely on trained technicians and sophisticated machines, which limits their application in remote areas and laboratories with limited resources. Therefore, a rapid, specific, sensitive, and device-independent detection method is urgently required (Qin et al., 2016; Alhogail et al., 2018; Ambrosio et al., 2019).

The development of the recombinase polymerase amplification (RPA) technology, which is independent of complex laboratory instrumentation and expertise, has provided a molecular reference tool for the detection of *P. gingivalis* (James and Macdonald, 2015; Li et al., 2018). RPA mimics DNA replication in living organisms and achieves amplification at a constant temperature of 37°C to 42°C and is an alternative technique to PCR amplification (Jiang et al., 2020). In this case, recombinase binds to the primers to form stable nucleoprotein filaments that are used to find sites in the template sequence that are paired with the primer sequence. The double-stranded DNA is opened with the help of single-stranded binding proteins, and finally, the target region on the template is amplified exponentially by replicative extension with the action of Bsu DNA polymerase (Piepenburg et al., 2006; Lobato and O'Sullivan, 2018). The visual detection of labeled RPA amplification products by lateral flow strips (LFS) encapsulated with gold nanoparticles (AuNPs) further simplifies the detection process and allows on-site detection without instruments (**Figure 1**) (Li et al., 2019; Wang et al., 2021a).

In this study, a sensitive method for the rapid detection of *P. gingivalis* was developed using RPA combined with the LFS technology. The method was based on the 16S rRNA gene of *P. gingivalis*, which was used to design the primers and probes, and the assay could be completed for 30 min at 37°C. The specificity of the method was verified by testing 20 clinical isolates of *P. gingivalis* and 23 isolates of other common pathogens. The sensitivity of the RPA–LFS assay was determined in ten independent experiments, and the lowest limit of detection (LOD) was 9.27 colony-forming units (CFU)/reaction. Finally, the established *P. gingivalis* RPA–LFS assay was used to assay clinical specimens, and the results were accurate and consistent with those of the PCR method. In conclusion, in this study, we developed a rapid, sensitive, and specific RPA–LFS assay for *P. gingivalis*, which has promising applications for preliminary medical diagnoses in remote and resource-limited areas.

MATERIALS AND METHODS

Ethical Statement

This study was approved by the Medical Ethics Committee of the Second People's Hospital of Lianyungang City. One hundred and thirty patients with periodontitis in our hospital were enrolled (65 males and 65 females, aged 35–60 years). All subjects gave their written informed consent. Specimens of gingival sulcus fluid were collected with sterile absorbent paper tips inserted into periodontal pockets or gingival sulci and were sent to the laboratory for testing.

Standard Strains and Clinical Isolates

A standard strain of *P. gingivalis* (ATCC 33277) was used to establish the RPA–LFS method for the detection of *P. gingivalis*. Twenty clinical isolates of *P. gingivalis* and 23 other common pathogens were collected. The latter included *Acinetobacter baumannii*, *Aggregatibacter actinomycetemcomitans*, *Bacillus cereus*, *Bacillus mirabilis, Burkholderia cepacia*, *Candida albicans*, *Candida tropicalis*, *Clostridium perfringens*, *Escherichia coli*, *Fusobacterium nucleatum*, *Haemophilus parainfluenzae*, *Klebsiella pneumoniae*, *Morganella morganii*, *Prevotella intermedia*, *Salmonella enterica*, *Serratia marcescens*, *Staphylococcus aureus*, *Stenotrophomonas maltophilia*,

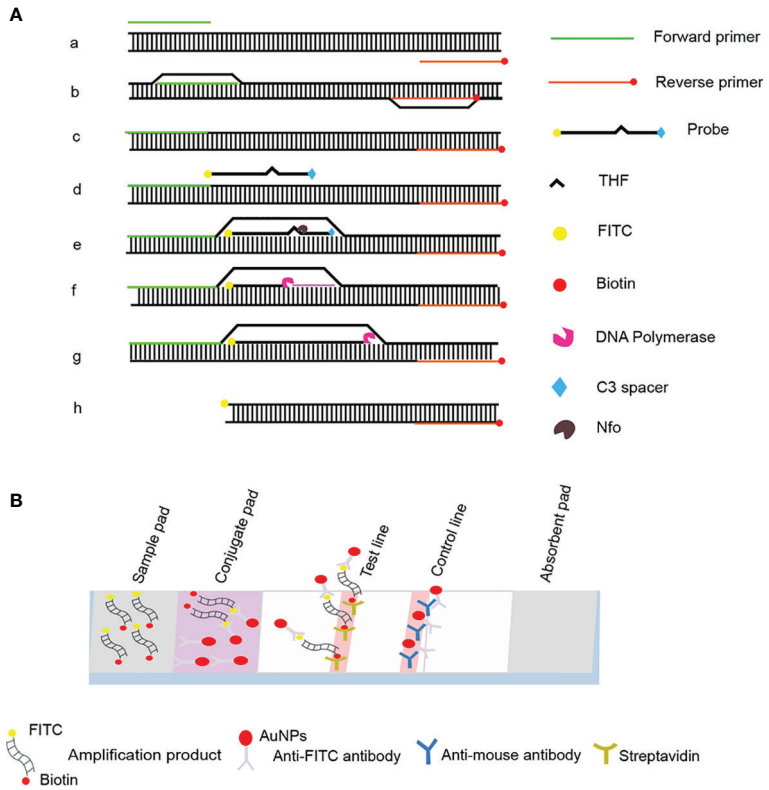

FIGURE 1 | Schematic diagram of the RPA-LFS method. **(A)** Principle of RPA amplification. DNA strands are represented as horizontal lines, and base pairing is represented as short vertical lines between DNA strands. Base pairing is indicated as a short vertical line between DNA strands. **(B)** Schematic representation of the lateral flow strip (LFS) working principle. The shapes and their representative molecules are listed below the graphic.

Streptococcus mutans, *Streptococcus pneumoniae*, *Streptococcus pyogenes*, *Tannerella forsythia*, and *Vibrio parahaemolyticus* were used to verify the specificity of the RPA–LFS method. All strains were provided by the Microbiology Department of the Second People's Hospital of Lianyungang, and the identities of all were confirmed with rRNA sequencing (**Table 1**).

Extraction of Bacterial Genomes

For the reactions that used purified genomic DNA as the template, genomic DNA was extracted with the Bacterial Genomic DNA Extraction Kit (Tiangen Biochemical Technology Co., Ltd, Beijing, China) and stored at −20°C until further processing.

Primer Design for RPA Reaction

Specific RPA primers were designed based on the *P. gingivalis* 16S rRNA gene sequence, using the Primer Premier 5 software. The primer design parameters were: primer size of 30–35 bp, product size of 100–500 bp, GC content of 20%–80%, and melting temperature (T_m) of 50–100°C. All other parameters used were the default settings. Five primer pairs were selected for testing, based on the scores from high to low (General Biosystems Ltd., Anhui, China).

TABLE 1 | Microbial isolates used in this study.

Species	Source	Strain amount
Porphyromonas gingivalis	ATCC 33277	1
Acinetobacter baumannii	Sputum	1
Aggregatibacter actinomycetemcomitans	Gingival sulcus fluid	1
Bacillus cereus	Urine	1
Bacillus mirabilis	Vaginal discharge	1
Burkholderia cepacia	Sputum	1
Candida albicans	Sputum	1
Candida tropicalis	Sputum	1
Clostridium perfringens	Blood	1
Escherichia coli	Sputum	1
Fusobacterium nucleatum	Gingival sulcus fluid	1
Haemophilus parainfluenzae	Sputum	1
Klebsiella pneumoniae	Sputum	1
Morganella morganii	Sputum	1
Prevotella intermedia	Gingival sulcus fluid	1
Salmonella enterica	Feces	1
Serratia marcescens	Sputum	1
Staphylococcus aureus	Sputum	1
Stenotrophomonas maltophilia	Sputum	1
Streptococcus mutans	Sputum	1
Streptococcus pneumoniae	Sputum	1
Streptococcus pyogenes	Sputum	1
Tannerella forsythia	Gingival sulcus fluid	1
Vibrio parahaemolyticus	Feces	1
P. gingivalis	Gingival sulcus fluid	20

RPA Procedure

To initially screen the forward and reverse primers, RPA amplification was performed with the TwistAmp Liquid DNA amplification kit (TwistDx Inc., Maidenhead, UK), according to the manufacturer's instructions. Each 50 μL mixture contained 25 μL of 2 × Reaction buffer, 5 μL of 10 × Basic mix, 2.5 μL of 20 × Core mix, 2.1 μL of forward primers and 2.1 μL of reverse primer (both 10 μM), 1 μL of genomic DNA as template, and 9.8 μL of distilled water. To ensure that all the reaction systems reacted simultaneously, 2.5 μL of 280 mM magnesium acetate was added to the PCR tube cap, and was added to the reaction system simultaneously by transient centrifugation.

The reaction mixture was briefly centrifuged and then incubated in a heater at 37°C for 30 min. Reactions with distilled water as a template were used as negative controls. The amplification products were purified with a DNA purification kit (Tiangen, Beijing, China) and resolved with 1.5% agarose gel electrophoresis.

RPA–LFS Probe Design

The Primer Premier 5 software was used to design specific probes that hybridized to sequences between the forward- and reverse-primer-targeting sequences, which should theoretically avoid, as far as possible, the formation of dimeric structures between the probe and the reverse primer (Daher et al., 2015). The criteria were: (1) probe size of 46–51 bp, GC content of 20%–80%, and T_m of 57–80°C; (2) maximum hairpin fraction set to 9, maximum primer–dimer fraction set to 9, maximum poly-X set to 5′, and all other parameters set to the default values; (3) 5′-end labeled with fluorescein isothiocyanate (FITC), and 3′-end blocked with a C3 spacer; and in the middle of the probe was replaced with a tetrahydrofuran (THF) group, with at least 30 bp before the THF site and at least 15 bp after it; and (4) the 5′-end of the reverse primer was labeled with biotin.

RPA–LFS Procedure

To screen the probe and primer combinations, the RPA–LFS assay was performed with the TwistAmp DNA amplification kit (TwistDx Inc.), according to the manufacturer's instructions. Each 50 μL reaction system contained 29.5 μL of hydration buffer, 2.1 μL each of the RPA forward and reverse primers (both 10 μM), 0.6 μL of RPA probe (10 μM), 11.2 μL of distilled water, 2 μL of genomic DNA, and dried enzyme pellets. To ensure that all the reaction systems started simultaneously, 2.5 μL of 280 mM magnesium acetate was added to the tube cap, transiently centrifuged, and immediately incubated at a constant temperature of 37°C for 30 min. An aliquot (5 μL) of the amplification product was used for visual inspection with LFS (Ustar BioTechnologies Ltd, Hangzhou, China) within 3 min. Two red lines may appear on the LFS, the control line was present in each test to ensure the validity of the LFS, whereas the test line was only observed in a positive reaction. Each sample had two bands, one for the sample itself and the other for the control.

LOD Assay

A 10-fold series of dilutions of the *P. gingivalis* genome corresponding to 6×10^4 CFU/μL to 6×10^{-1} CFU/μL, was prepared for the RPA–LFS assay. The minimum LOD of the method was determined with a probit regression analysis of 10 independent experiments.

Evaluation of the Compliance Rate of RPA–LFS With PCR Method

Clinical specimens were collected from 130 patients with chronic periodontitis in the Department of Stomatology, Lianyungang Second People's Hospital. Specimen collection: Patients were instructed to rinse their mouths with water, rinse with saline to remove food debris, and insert the tip of sterile absorbent paper into the periodontal pocket or gingival sulcus for 30 s. After 30 s, the paper was immediately removed and placed in an EP tube containing 1 mL of PBS (re-collected if blood was present). For DNA extraction, the specimens were centrifuged at 12,000 × g for 2 min, and the supernatant was discarded. 30 μL 5% Chelex-100 (Sigma, United States) was added to the precipitate, which was heat treated at 100°C for 10 min before serving as the templates. The PCR primers were designed according to the 16S rRNA sequence. The compliance rate of the RPA–LFS method used on the clinical specimens was evaluated by comparing the results with those of PCR. The compliance rate between two methods was calculated with the formula: ([number of positive samples detected with both methods + number of negative samples detected with both methods]/total number of samples) × 100%.

RESULTS

Design and Screening of Primer Sets for RPA System

Five primer pairs were designed using the 16S rRNA gene as the target sequence, and genomic DNA was used as the template for the RPA reaction (**Table 2**). All five primer pairs amplified the expected target bands with sizes of 353, 254, 223, 183, and 213 bp (**Figure 2**). Although there were no nonspecific amplified bands in the no-template controls (NTCs), primers 3, 4, and 5 showed primer dimers of < 100 bp. In contrast, primer set #1 and 2 amplified brighter target bands, with fewer primer dimers. Therefore, we selected primer set #1 and 2 for subsequent RPA–LFS probe design.

Modification and Determination of Optimal Primer–Probe Combinations for RPA–LFS

Probes P1 and P2 were designed within the target sequences of primer set #1 and 2, respectively, and RPA–LFS assays were performed to test the amplification performance of the primer–probe combinations primer set #1/probes P1, primer set #2/probes P2, and the corresponding negative controls. Both primer–probe combinations generated the correct positive signals (two visible red bands on both the test and control lines), indicating that both primer–probe combinations performed well. However, the NTCs also showed a visible weaker red band on the test line, indicating a false-positive signal for both primer–probe combinations (**Figure 3**).

TABLE 2 | Primers and probes tested in this study.

Name		Sequence (5'-3')	Length (bp)	Amplicon size (bp)
# 1	Forward	AACGATGATTACTAGGAGTTTGCGATATAC	30	353
	Reverse	CCTTACGACGGCAGTCTCGGTAGAGTCCTCAGC	32	
# 2	Forward	ACCAAGGCGACGATGGGTAGGGGAACTGAG	30	251
	Reverse	GCTGCTGGCACGGAGTTAGCCGATGCTTATTC	32	
# 3	Forward	CCTGGTAGTCCACGCAGTAAACGATGATTA	30	220
	Reverse	TTCACCATCAGTCATCTACATTTCAATCCC	30	
# 4	Forward	CACCAAGGCGACGATGGGTAGGGGAACTGA	30	178
	Reverse	CCCGTATAAAAGAAGTTTACAATCCTTAGGAC	32	
# 5	Forward	CACCAAGGCGACGATGGGTAGGGGAACTGA	30	236
	Reverse	TAGCCGATGCTTATTCTTACGGTACATTCA	30	
P1	Forward	FITC-CCGTGAGGTGTCGGCTTAAGTGCCATAAC G[THF]GCGCAACCCACATCG-/C3-spacer/	46	95
P2	Forward	FITC-GGATTGTAAACTTCTTTTATACGGGAATA A[THF]GGGCGATACGAGTAT-/C3-spacer/	46	97
#1mR	Reverse	Biotin-TACCACGGCAGTCTCGGTAGAGTCCTCA GC	30	354
#2mR	Reverse	Biotin-GCTGCTGGCACGGAGTTAGCCGATGCTTCTTC	32	251
mP1	Forward	FITC-CCGCGATGTGTCGGATTAAGTGCCATAAC G[THF]GCGCAACCCACATCG-/C3-spacer/	46	95
mP2	Forward	FITC-GGATTGTAATCTTCTTTTATACGGGTATA A[THF]GGGCGATACGAGTAT-/C3-spacer/	46	97

Sequences modified with base substitutions. Modified bases are in red.

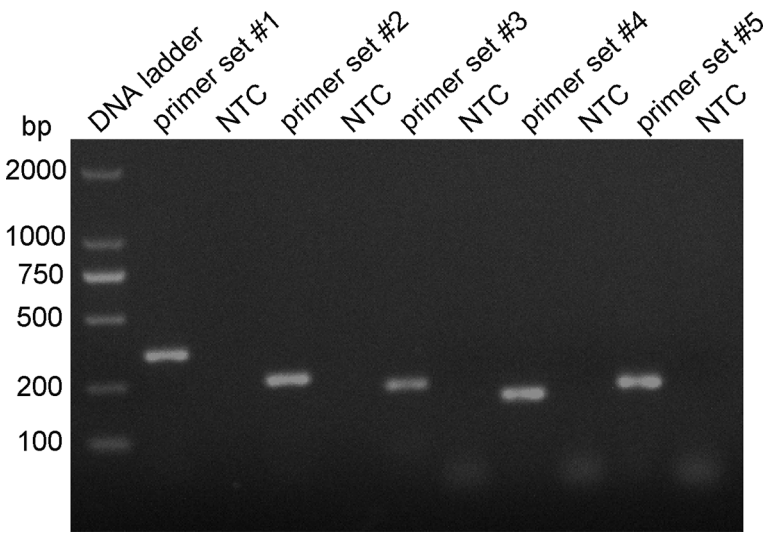

FIGURE 2 | RPA primer set screening. The genomic DNA of the *P. gingivalis* standard strain was used as the template, and amplification with the RPA method was performed with primers set #1–5. The NTC strip is the no-template control for the corresponding RPA reaction, The amplification of the products was confirmed with 1.5% agarose gel electrophoresis.

The pairing between of probe and the reverse primer may have been responsible for the false positive signals (Yang et al., 2021). The formation of a cross dimer between them was analyzed using the Primer Premier 5 software, and the results showed that both primer-probe pairs had multiple consecutive matching bases. Therefore, base substitution was introduced to eliminate consecutive base pairing between the probe and the reverse primer. The principles of this substitution were: (1) break was introduced into for sites with more than four consecutive matches or more than three consecutive matching bases at the 3′ end; and (2) the three bases near the 3′ end could not be replaced. The sequences of the modified reverse primers (mR) and probes (mP) are shown in **Table 2**, and the substituted bases are indicated in red. The RPA–LFS assay was performed using the modified primer and probe sets, but the results still showed a weak signal in the NTC set of the primer set #1/F/mR/mP1 combination. However, the primer set #2/F/mR/mP2 combination eliminated the weak false positive signal while not affecting amplification (**Figure 4A**). Analysis of the RPA amplification products with agarose gel electrophoresis revealed two clear bands for each of the two primer–probe combinations, representing the products of the forward and reverse primers and the probe and reverse primer (**Figure 4B**). Overall, the best primer–probe combination for the RPA–LFS assay of *P. gingivalis* was primer set #2/F/mR/mP2.

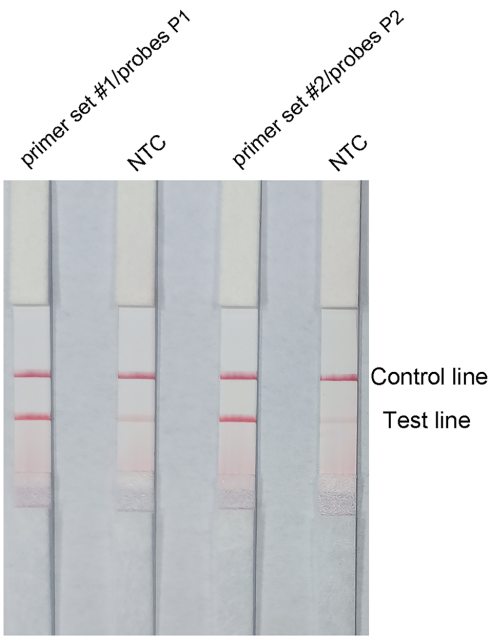

FIGURE 3 | Performance of the primer–probe combinations tested with the RPA–LFS reaction. The results of LFS detection of the RPA amplification products are shown. The name of each primer–probe set is shown on the corresponding strip. The NTC strip is a template-free control for the individual RPA reaction. The reactions were performed for 30 min at 37°C. The positions of the test and control lines are marked on the right side of the bar graph. The image represents the results of three independent experiments.

Analysis of RPA–LFS Assay Specificity

To verify the inclusiveness and specificity of the primer–probe combination, the RPA–LFS assay was used to analyze 20 clinical isolates of *P. gingivalis* and 23 isolates of other pathogenic bacteria. As shown in **Figure 5**, a clear positive signal appeared on the test line when isolated *P. gingivalis* genomic DNA was used as the template, but in contrast, no band appeared on the test line when genomic DNA from the other common pathogens was used as the template. These results demonstrate that the RPA–LFS assay system established is highly specific for *P. gingivalis*, with no cross-reactivity with other pathogens.

Measurement of RPA–LFS Assay LOD

To evaluate the LOD of the RPA–LFS assay, we used it to evaluate 10-fold dilutions of *P. gingivalis* genomic DNA, ranging from 6×10^4 CFU/μL to 6×10^{-1} CFU/μL (1 μL in a 50 μL reaction volume) as the template. There was a clear red band on the test line at 10^4 CFU/μL, and the signal diminished as the template concentration decreased. The signal disappeared in the 6×10^{-1} CFU/μL group (**Figure 6A**). To test whether the system was resistant to interference from human genomes, 10 ng of human DNA were added to the RPA reaction along with dilutions of *P. gingivalis* genomic DNA. The detection sensitivity was not affected by human DNA (**Figure 6B**). In addition, not all assays yielded positive results when strains with concentrations of 6×10^0 CFU/μL (seven positive results from ten samples, 7/10) or 6×10^{-1} CFU/μL (1/10) were used as templates. To more accurately determine

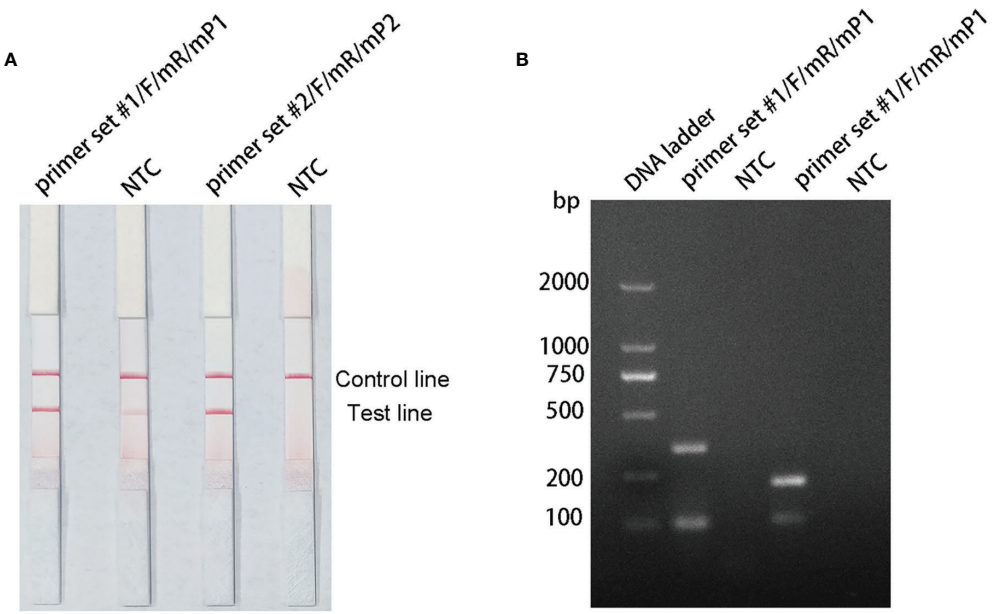

FIGURE 4 | Testing the modified primer–probe combinations with the RPA–LFS reaction. **(A)** Graph shows the LFS results of RPA amplification. **(B)** The RPA amplification products were analyzed with agarose gel electrophoresis. The name of each primer–probe set is shown above the corresponding strip. The NTC strip is the no-template control for the corresponding RPA reaction, on the strip immediately to its left.

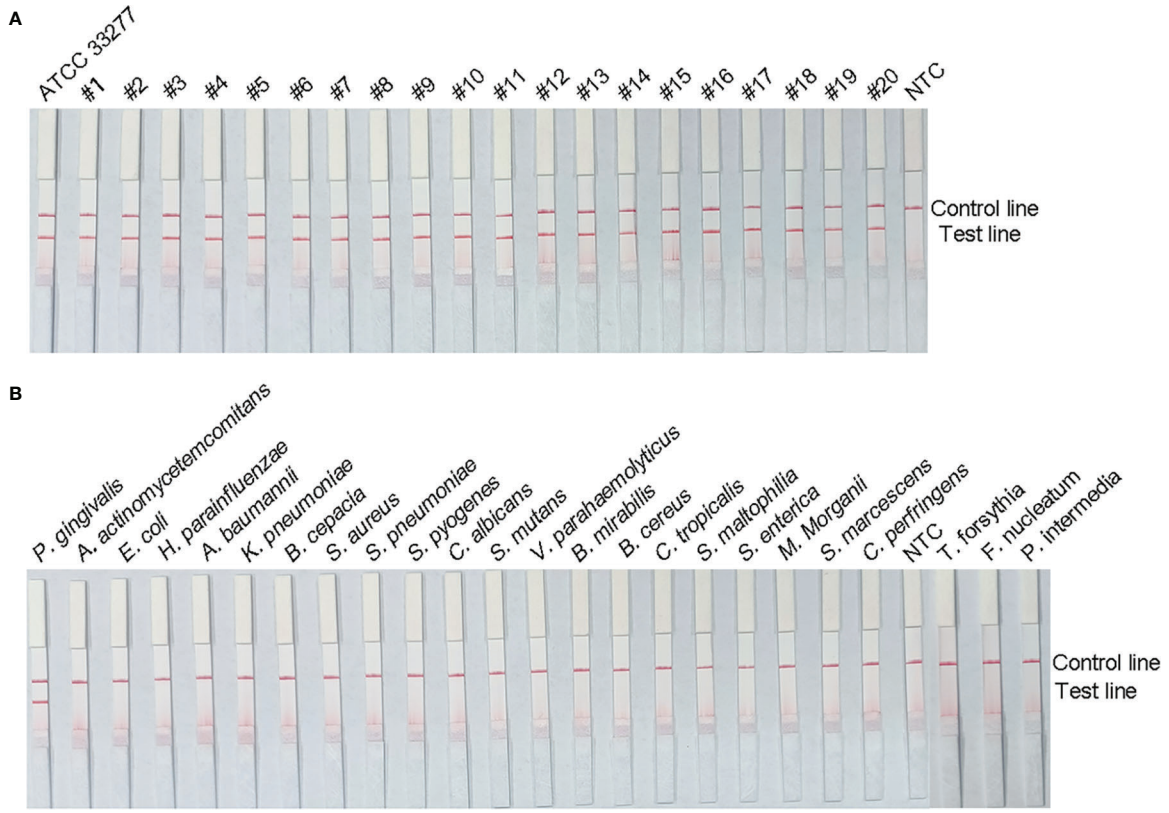

FIGURE 5 | Specificity analysis of the *P. gingivalis* RPA–LFS assay. The specificity of the RPA–LFS assay established for *P. gingivalis* was tested on 20 clinical isolates of *P. gingivalis* **(A)** and genomic DNA extracted from 20 common pathogenic bacteria **(B)**. No-template control (NTC) was used as the negative control and *P. gingivalis* as the positive control. RPA amplification results were detected with LFS, and the samples are labeled at the top of the bar graph.

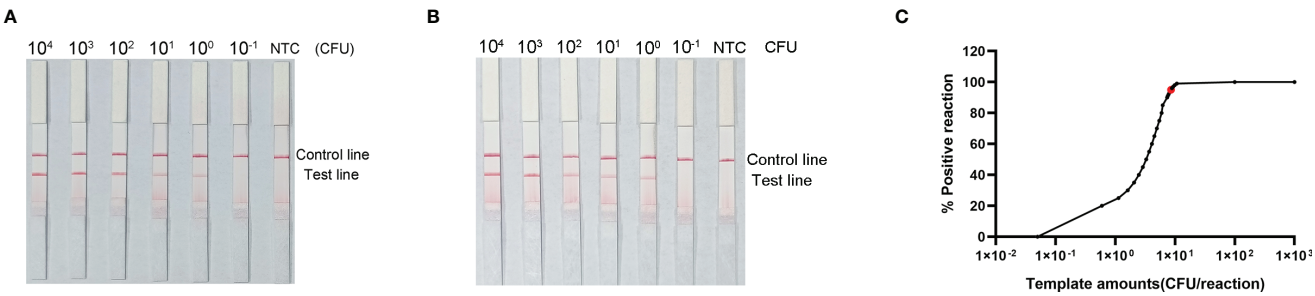

FIGURE 6 | Determination of the limit of detection (LOD) of *P. gingivalis* RPA–LFS. **(A)** The LOD for the *P. gingivalis* RPA-LFS assay system established was determined from 10 independent assays using *P. gingivalis* genomic DNA at serial dilutions from 6×10^4 to 6×10^{-1} CFU/μL. Images show the results of RPA–LFS, with the amount of template shown at the top of the strip. **(B)** The group with 10 ng human genomic DNA added in addition to the *P. gingivalis* genomic DNA. **(C)** Probit regression analysis of data collected from ten replicates, performed with the SPSS software.

the LOD of the RPA–LFS assay, a probit regression analysis was performed on data from ten independent assays; the statistical analysis was performed with SPSS software. With 95% probability, the LOD for the reaction was 9.27 CFU/μL (**Figure 6C**).

Application of *P. gingivalis* RPA–LFS to the Analysis of Clinical Specimens

To evaluate the clinical utility of the established RPA–LFS detection system, gingival sulcus fluid specimens from 130 patients with chronic periodontitis were tested with both the

RPA–LFS method and PCR. As shown in **Table 3**, 118 samples positive for *P. gingivalis* and 12 negative samples were detected with the RPA–LFS method, and the results obtained were in complete agreement with those of the PCR method. These results suggest that the highly specific and sensitive *P. gingivalis* RPA-LFS is feasible and reliable when applied to clinical samples from patients.

DISCUSSION

The isothermal amplification method RPA can rapidly amplify target DNA under low-temperature isothermal conditions with a tolerance for unpurified samples, and is therefore a promising alternative molecular assay for the detection of *P. gingivalis*. The chemical labeling of the RPA reaction allows the products to be read with an AuNP-based LFS, with less reliance on equipment and trained personnel. However, all these simplifications mean that the inherent risk of false-positive signals from primer dimers is not negligible (Miao et al., 2019). It has been reported that the introduction of probes into RPA reactions can reduce primer-dependent artifacts to some extent, but the introduction of probes alone does not guarantee the complete elimination of false-positive signals (Wu et al., 2020). The probe sequence can still pair with the reverse primer to some extent. We took advantage of the fact that the RPA reaction can tolerate some primer-to-template base mismatches and substituted some bases in the probe and reverse primer of RPA–LFS (Wang et al., 2021b). An improved RPA–LFS system was established by rigorously testing the efficacy of these measures, which completely prevented the formation of probe–primer complexes and eliminated false-positive signals.

Increased sensitivity is recognized as a key factor in the development of diagnostic methods. To determine the accurate LOD of the *P. gingivalis* RPA–LFS, we assayed different amounts of *P. gingivalis* genomic DNA template, ranging from 6×10^4 CFU to 6×10^{-1} CFU. According to a probit regression analysis, the LOD of the *P. gingivalis* RPA–LFS was 9.27 CFU per reaction, with 95% probability, which is similar to the LOD of other highly sensitive molecular assays, including multiplex qPCR (50 pg), single PCR with purified DNA (0.5 pg) or crude bacterial cultures (10 CFU), and loop-mediated isothermal amplification (1.4×10^{-1} pg/μL) (Coffey et al., 2016; Su et al., 2019; Rao et al., 2021).

Early chairside microbiological tests used to screen for periodontitis risk included the use of Nbenzoyl-DL-arginine-2-naphthylamide (BANA) tests to determine the level of protease activity in subgingival plaque, agglutination of latex beads and whole-cell bacterial ELISA (Nisengard et al., 1992; Boyer et al., 1996; Loesche et al., 1997). In most of these previous tests, high sensitivity was achieved at the expense of specificity (Hemmings et al., 1997; Eick and Pfister, 2002; Kaman et al., 2012). The immunochromatographic device using A1-adhesin monoclonal antibodies has emerged in recent years, and the sensitivity and specificity of the current assay device are 95.0% and 93.3%, respectively, which is a great improvement compared to the previous ones. However, this method requires ELISA and microbial flow cytometry to screen for specific monoclonal antibodies, and the whole operation is complicated and costly (O'Brien-Simpson et al., 2017). *In vitro* isothermal nucleic acid amplification strategies are important in molecular diagnosis, and loop-mediated isothermal amplification (LAMP) is one of the more widely used ones. Su et al. used LAMP method to detect *P. gingivalis* against specific fragments with a lower limit of detection of 1.4×10^{-1} pg/μl, and the method was non-cross-reactive with other bacterial pathogens (Su et al., 2019). However, LAMP typically has a reaction temperature of 60-65°C and requires three primer pairs, which may lead to primer-primer interactions, thus limiting the reaction.

LFS-based tests are considered the gold standard for point-of-care diagnostics and are portable, rapid, and simple to use. This study was based on the visualization of RPA with the LFS technology, using the 16S rRNA sequence as the target, and the assay was completed within 30 min under isothermal conditions at 37°C. A comparison of clinical isolates of *P. gingivalis* with those of other common pathogenic bacteria demonstrated the excellent specificity of the method. When the RPA–LFS assay was used to test clinical specimens, the samples did not require purification and could be used for the assay after simple processing. The assay showed 100% accuracy, in agreement with the conventional PCR method. In conclusion, in this study, we have established a rapid, specific, and sensitive field assay for *P. gingivalis*. Readable results can be obtained within 1 h with a simple procedure under equipment-free conditions. This may provide a reference for future chairside rapid detection of *P. gingivalis* and other pathogenic microorganisms, and will also contribute to the early diagnosis of related diseases, which is an important guide for early intervention and clinical treatment of oral diseases and systemic diseases.

TABLE 3 | Analysis of gingival sulcus fluid specimens from 130 patients with chronic periodontitis using the RPA–LFS method and PCR.

Method	positive	negative	Amplification time (min)
RPA-LFS	118	12	35
qPCR	118	12	90

DATA AVAILABILITY STATEMENT

The original contributions presented in the study are included in the article/supplementary material. Further inquiries can be directed to the corresponding authors.

ETHICS STATEMENT

This study was approved by the Medical Ethics Committee of the Second People's Hospital of Lianyungang City. One hundred and thirty patients with periodontitis in our hospital were enrolled

(65 males and 65 females, aged 35–60 years). All subjects gave their written informed consent. Specimens of gingival sulcus fluid were collected with sterile absorbent paper tips inserted into periodontal pockets or gingival sulci and were sent to the laboratory for testing.

AUTHOR CONTRIBUTIONS

DG and FW conceived and designed all the experiments and wrote the paper. XG suggested the primer–probe design and directed the experiments. YH collected the clinical specimens, and BW analyzed the data. ZC revised the manuscript, submitted the manuscript, and led all the work. All the authors discussed the results, provided comments, and approved the final version of the manuscript.

FUNDING

This work was funded by the High-level Innovation and Entrepreneurship Talents Introduction Program of Jiangsu Province of China (grant number 2019-30345), the '521 Project' scientific research funding project of Lianyungang City (grant number LYG06521202157), the 'HaiYan Plan' scientific research funding project of Lianyungang City (grant number 2019-QD-008), and the Clinical Medical Science and Technology Development Fund of Jiangsu University (grant number JLY20180020).

REFERENCES

Alhogail, S., Suaifan, G., Bizzarro, S., Kaman, W. E., Bikker, F. J., Weber, K., et al. (2018). On Site Visual Detection of *Porphyromonas Gingivalis* Related Periodontitis by Using a Magnetic-Nanobead Based Assay for Gingipains Protease Biomarkers. *Mikrochim Acta* 185 (2), 149. doi: 10.1007/s00604-018-2677-x

Ambrosio, N., Marín, M. J., Laguna, E., Herrera, D., Sanz, M., and Figuero, E. (2019). Detection and Quantification of *Porphyromonas Gingivalis* and *Aggregatibacter Actinomycetemcomitans* in Bacteremia Induced by Interdental Brushing in Periodontally Healthy and Periodontitis Patients. *Arch. Oral. Biol.* 98, 213–219. doi: 10.1016/j.archoralbio.2018.11.025

Atieh, M. A. (2008). Accuracy of Real-Time Polymerase Chain Reaction Versus Anaerobic Culture in Detection of *Aggregatibacter Actinomycetemcomitans* and *Porphyromonas Gingivalis*: A Meta-Analysis. *J. Periodontol.* 79 (9), 1620–1629. doi: 10.1902/jop.2008.070668

Boyer, B. P., Ryerson, C. C., Reynolds, H. S., Zambon, J. J., Genco, R. J., and Snyder, B. (1996). Colonization by Actinobacillus Actinomycetemcomitans, Porphyromonas Gingivalis and Prevotella Intermedia in Adult Periodontitis Patients as Detected by the Antibody-Based Evalusite Test. *J. Clin. Periodontol* 23 (5), 477–484. doi: 10.1111/j.1600-051x.1996.tb00578.x

Coffey, J., Choudhry, M., Shlossman, M., Makin, I. R. S., and Singh, V. K. (2016). Multiplex Real-Time PCR Detection and Relative Quantification of Periodontal Pathogens. *Clin. Exp. Dent. Res.* 2 (3), 185–192. doi: 10.1002/cre2.37

Daher, R. K., Stewart, G., Boissinot, M., Boudreau, D. K., and Bergeron, M. G. (2015). Influence of Sequence Mismatches on the Specificity of Recombinase Polymerase Amplification Technology. *Mol. Cell Probes* 29 (2), 116–121. doi: 10.1016/j.mcp.2014.11.005

Eick, S., and Pfister, W. (2002). Comparison of Microbial Cultivation and a Commercial PCR Based Method for Detection of Periodontopathogenic Species in Subgingival Plaque Samples. *J. Clin. Periodontol* 29 (7), 638–644. doi: 10.1034/j.1600-051x.2002.290708.x

Fyrestam, J., Bjurshammar, N., Paulsson, E., Mansouri, N., Johannsen, A., and Östman, C. (2017). Influence of Culture Conditions on Porphyrin Production in *Aggregatibacter Actinomycetemcomitans* and *Porphyromonas Gingivalis*. *Photodiagnosis Photodyn Ther.* 17, 115–123. doi: 10.1016/j.pdpdt.2016.11.001

Gu, B. L., Qi, Y. J., Kong, J. Y., Li, Z. T., Wang, J. P., Yuan, X., et al. (2020). An Evaluation of Direct PCR Assays for the Detection and Quantification of *Porphyromonas Gingivalis*. *Epidemiol. Infect.* 148, e107. doi: 10.1017/S0950268820001053

Hajishengallis, G., and Diaz, P. I. (2020). *Porphyromonas Gingivalis*: Immune Subversion Activities and Role in Periodontal Dysbiosis. *Curr. Oral. Health Rep.* 7 (1), 12–21. doi: 10.1007/s40496-020-00249-3

He, J., Huang, W., Pan, Z., Cui, H., Qi, G., Zhou, X., et al. (2012). Quantitative Analysis of Microbiota in Saliva, Supragingival, and Subgingival Plaque of Chinese Adults With Chronic Periodontitis. *Clin. Oral. Investig.* 16 (6), 1579–1588. doi: 10.1007/s00784-011-0654-4

Hemmings, K. W., Griffiths, G. S., and Bulman, J. S. (1997). Detection of Neutral Protease (Periocheck) and BANA Hydrolase (Perioscan) Compared With Traditional Clinical Methods of Diagnosis and Monitoring of Chronic Inflammatory Periodontal Disease. *J. Clin. Periodontol* 24 (2), 110–114. doi: 10.1111/j.1600-051x.1997.tb00475.x

James, A., and Macdonald, J. (2015). Recombinase Polymerase Amplification: Emergence as a Critical Molecular Technology for Rapid, Low-Resource Diagnostics. *Expert Rev. Mol. Diagn.* 15 (11), 1475–1489. doi: 10.1586/14737159.2015.1090877

Jiang, L., Ching, P., Chao, C. C., Dumler, J. S., and Ching, W. M. (2020). Development of a Sensitive and Rapid Recombinase Polymerase Amplification Assay for Detection of Anaplasma Phagocytophilum. *J. Clin. Microbiol.* 58 (5), e01777-19. doi: 10.1128/JCM.01777-19

Kaman, W. E., Galassi, F., de Soet, J. J., Bizzarro, S., Loos, B. G., Veerman, E. C., et al. (2012). Highly Specific Protease-Based Approach for Detection of Porphyromonas Gingivalis in Diagnosis of Periodontitis. *J. Clin. Microbiol.* 50 (1), 104–112. doi: 10.1128/JCM.05313-11

Li, J., Macdonald, J., and von Stetten, F. (2018). Review: A Comprehensive Summary of a Decade Development of the Recombinase Polymerase Amplification. *Analyst* 144 (1), 31–67. doi: 10.1039/c8an01621f

Li, J., Ma, B., Fang, J., Zhi, A., Chen, E., Xu, Y., et al. (2019). Recombinase Polymerase Amplification (RPA) Combined With Lateral Flow Immunoassay for Rapid Detection of Salmonella in Food. *Foods* 9 (1), 27. doi: 10.3390/foods9010027

Lobato, I. M., and O'Sullivan, C. K. (2018). Recombinase Polymerase Amplification: Basics, Applications and Recent Advances. *Trends Analyt Chem.* 98, 19–35. doi: 10.1016/j.trac.2017.10.015

Loesche, W. J., Kazor, C. E., and Taylor, G. W. (1997). The Optimization of the BANA Test as a Screening Instrument for Gingivitis Among Subjects Seeking Dental Treatment. *J. Clin. Periodontol* 24 (10), 718–726. doi: 10.1111/j.1600-051x.1997.tb00188.x

Marin, M. J., Ambrosio, N., Herrera, D., Sanz, M., and Figuero, E. (2018). Validation of a Multiplex qPCR Assay for the Identification and Quantification of Aggregatibacter Actinomycetemcomitans and *Porphyromonas Gingivalis: In Vitro* and Subgingival Plaque Samples. *Arch. Oral. Biol.* 88, 47–53. doi: 10.1016/j.archoralbio.2018.01.012

Miao, F., Zhang, J., Li, N., Chen, T., Wang, L., Zhang, F., et al. (2019). Rapid and Sensitive Recombinase Polymerase Amplification Combined With Lateral Flow Strip for Detecting African Swine Fever Virus. *Front. Microbiol.* 10, 1004. doi: 10.3389/fmicb.2019.01004

Mougeot, J. C., Stevens, C. B., Paster, B. J., Brennan, M. T., Lockhart, P. B., and Mougeot, F. K. (2017). *Porphyromonas Gingivalis* is the Most Abundant Species Detected in Coronary and Femoral Arteries. *J. Oral. Microbiol.* 9 (1), 1281562. doi: 10.1080/20002297.2017.1281562

Mysak, J., Podzimek, S., Sommerova, P., Lyuya-Mi, Y., Bartova, J., Janatova, T., et al. (2014). Porphyromonas Gingivalis: Major Periodontopathic Pathogen Overview. *J. Immunol. Res.* 2014, 476068. doi: 10.1155/2014/476068

Nisengard, R. J., Mikulski, L., McDuffie, D., and Bronson, P. (1992). Development of a Rapid Latex Agglutination Test for Periodontal Pathogens. *J. Periodontol* 63 (7), 611–617. doi: 10.1902/jop.1992.63.7.611

O'Brien-Simpson, N. M., Burgess, K., Lenzo, J. C., Brammar, G. C., Darby, I. B., and Reynolds, E. C. (2017). Rapid Chair-Side Test for Detection of *Porphyromonas Gingivalis*. *J. Dent. Res.* 96 (6), 618–625. doi: 10.1177/0022034517691720

Olsen, I., Lambris, J. D., and Hajishengallis, G. (2017). *Porphyromonas Gingivalis* Disturbs Host-Commensal Homeostasis by Changing Complement Function. *J. Oral. Microbiol.* 9 (1), 1340085. doi: 10.1080/20002297.2017.1340085

Piepenburg, O., Williams, C. H., Stemple, D. L., and Armes, N. A. (2006). DNA Detection Using Recombination Proteins. *PloS Biol.* 4 (7), e204. doi: 10.1371/journal.pbio.0040204

Qi, Y. J., Jiao, Y. L., Chen, P., Kong, J. Y., Gu, B. L., Liu, K., et al. (2020). Porphyromonas Gingivalis Promotes Progression of Esophageal Squamous Cell Cancer *via* Tgfβ-Dependent Smad/YAP/TAZ Signaling. *PloS Biol.* 18 (9), e3000825. doi: 10.1371/journal.pbio.3000825

Qin, W., Zheng, B., Yuan, Y., Li, M., Bai, Y., Chang, J., et al. (2016). Sensitive Detection of *Porphyromonas Gingivalis* Based on Magnetic Capture and Upconversion Fluorescent Identification With Multifunctional Nanospheres. *Eur. J. Oral. Sci.* 124 (4), 334–342. doi: 10.1111/eos.12286

Rams, T. E., Sautter, J. D., Getreu, A., and van Winkelhoff, A. J. (2016). Phenotypic Identification of *Porphyromonas Gingivalis* Validated With Matrix-Assisted Laser Desorption/Ionization Time-of-Flight Mass Spectrometry. *Microb. Pathog.* 94, 112–116. doi: 10.1016/j.micpath.2016.01.021

Rao, A., D'Souza, C., Subramanyam, K., Rai, P., Thomas, B., Gopalakrishnan, M., et al. (2021). Molecular Analysis Shows the Presence of Periodontal Bacterial DNA in Atherosclerotic Plaques From Patients With Coronary Artery Disease. *Indian Heart J.* 73 (2), 218–220. doi: 10.1016/j.ihj.2021.01.011

Slots, J. (2017). Periodontitis: Facts, Fallacies and the Future. *Periodontol 2000* 75 (1), 7–23. doi: 10.1111/prd.12221

Su, Y., Huang, S., Hong, L., Zou, D., Tang, Y., Chao, S., et al. (2019). Establishment of the Molecular Beacon-Loop-Mediated Isothermal Amplification Method for the Rapid Detection of *Porphyromonas Gingivalis*. *J. Microbiol. Methods* 160, 68–72. doi: 10.1016/j.mimet.2019.01.013

Wang, F., Ge, D., Wang, L., Li, N., Chen, H., Zhang, Z., et al. (2021a). Rapid and Sensitive Recombinase Polymerase Amplification Combined With Lateral Flow Strips for Detecting Candida Albicans. *Anal. Biochem.* 633, 114428. doi: 10.1016/j.ab.2021.114428

Wang, F., Wang, L., Chen, H., Li, N., Wang, Y., Li, Y., et al. (2021b). Rapid Detection of Bla (KPC), Bla (NDM), Bla (OXA-48-Like) and Bla (IMP) Carbapenemases in Enterobacterales Using Recombinase Polymerase Amplification Combined With Lateral Flow Strip. *Front. Cell Infect. Microbiol.* 11. doi: 10.3389/fcimb.2021.772966

Wu, H., Zhao, P., Yang, X., Li, J., Zhang, J., Zhang, X., et al. (2020). A Recombinase Polymerase Amplification and Lateral Flow Strip Combined Method That Detects Salmonella Enterica Serotype Typhimurium With No Worry of Primer-Dependent Artifacts. *Front. Microbiol.* 11, 1015. doi: 10.3389/fmicb.2020.01015

Xie, M., Tang, Q., Nie, J., Zhang, C., Zhou, X., Yu, S., et al. (2020). BMAL1-Downregulation Aggravates Porphyromonas Gingivalis-Induced Atherosclerosis by Encouraging Oxidative Stress. *Circ. Res.* 126 (6), e15–e29. doi: 10.1161/CIRCRESAHA.119.315502

Yang, H., Wang, Y., Yang, Q., Fan, H., Wang, L., Zhang, T., et al. (2021). A Rapid and Sensitive Detection Method for Pseudomonas Aeruginosa Using Visualized Recombinase Polymerase Amplification and Lateral Flow Strip Technology. *Front. Cell Infect. Microbiol.* 11. doi: 10.3389/fcimb.2021.698929

Yaseen, A., Mahafzah, A., Dababseh, D., Taim, D., Hamdan, A. A., Al-Fraihat, E., et al. (2021). Oral Colonization by Entamoeba Gingivalis and Trichomonas Tenax: A PCR-Based Study in Health, Gingivitis, and Periodontitis. *Front. Cell Infect. Microbiol.* 11. doi: 10.3389/fcimb.2021.782805

Zhang, Z., Liu, D., Liu, S., Zhang, S., and Pan, Y. (2020). The Role of *Porphyromonas Gingivalis* Outer Membrane Vesicles in Periodontal Disease and Related Systemic Diseases. *Front. Cell Infect. Microbiol.* 10. doi: 10.3389/fcimb.2020.585917

Conflict of Interest: The authors declare that the research was conducted in the absence of any commercial or financial relationships that could be construed as a potential conflict of interest.

Publisher's Note: All claims expressed in this article are solely those of the authors and do not necessarily represent those of their affiliated organizations, or those of the publisher, the editors and the reviewers. Any product that may be evaluated in this article, or claim that may be made by its manufacturer, is not guaranteed or endorsed by the publisher.

frontiers | Frontiers in Cellular and Infection Microbiology

ORIGINAL RESEARCH
published: 02 June 2022
doi: 10.3389/fcimb.2022.878881

Rapid, Simple, and Highly Specific Detection of *Streptococcus pneumoniae* With Visualized Recombinase Polymerase Amplification

Fang Wang[†], *Yan Wang*[†], *Xia Liu*[†], *Lei Wang*, *Kun Wang*, *Chenglai Xu*[*], *Guanhong Huang*[*] *and Xuzhu Gao*[*]

Department of Central Laboratory, The Second People's Hospital of Lianyungang City (Cancer Hospital of Lianyungang), Affiliated to Jiangsu University, Lianyungang, China

Streptococcus pneumoniae is a major pathogen that causes microbiological illness in humans. The introduction of polyvalent vaccines has resulted in a significant decrease in pneumococcal-related mortality. However, pneumococcal infections continue to be a leading cause of death in children under the age of 5 and adults over the age of 65 worldwide. A speedy and highly sensitive diagnostic tool is necessary for routine adoption to adequately manage patients and control the spread of infection. In this study, we investigated a new nucleic acid amplification technique, isothermal recombinase polymerase amplification (RPA), which amplifies DNA at 37°C under isothermal conditions with high specificity, efficiency, and rapidity. Using the autolysin gene *lytA* as the molecular diagnostic target, an RPA primer-probe combination was designed and optimized for the detection of *S. pneumoniae*. This RPA reaction produced amplification products labeled with specific chemical markers, to be detected with gold-nanoparticle-based lateral flow strips (LFS), reducing the reliance on equipment and trained personnel. The high specificity of the RPA-LFS technique was demonstrated with the specific detection of 22 strains of *S. pneumoniae* but not 25 closely related pathogenic bacteria. The assay showed good sensitivity, and detected *S. pneumoniae* down to 3.32 colony-forming units/μL. When used on clinical samples, the assay provided accurate and consistent results compared with PCR. The compliance with the culture-biochemistry method was 98.18% and the kappa index was 0.977. These results reveal that the RPA–LFS test significantly improved *S. pneumoniae* identification, particularly in resource-limited areas.

Keywords: recombinase polymerase amplification, rapid assay, false-positive signal, *Streptococcus pneumoniae*, lateral flow strip

OPEN ACCESS

Edited by:
Onya Opota,
University of Lausanne, Switzerland

Reviewed by:
Diane S. J. Lindsay,
NHS Greater Glasgow and Clyde, United Kingdom
Kenji Sadamasu,
Tokyo Metropolitan Institute of Public Health, Japan

***Correspondence:**
Chenglai Xu
872978918@qq.com
Guanhong Huang
hghlyg0002@sina.cn
Xuzhu Gao
alexgwan@163.com

[†]*These authors have contributed equally to this work and share the first authorship*

Specialty section:
This article was submitted to Clinical Microbiology, a section of the journal Frontiers in Cellular and Infection Microbiology

Received: *18 February 2022*
Accepted: *05 May 2022*
Published: *02 June 2022*

Citation:
Wang F, Wang Y, Liu X, Wang L, Wang K, Xu C, Huang G and Gao X (2022) Rapid, Simple, and Highly Specific Detection of Streptococcus pneumoniae With Visualized Recombinase Polymerase Amplification. Front. Cell. Infect. Microbiol. 12:878881. doi: 10.3389/fcimb.2022.878881

INTRODUCTION

Streptococcus pneumoniae is a Gram-positive, non-flagellated bacterium, often arranged in pairs or short chains of cells (Ye et al., 2018; Paton and Trappetti, 2019). It is widely distributed in nature and often colonizes the mucous membranes of the human upper respiratory organs, mainly targeting immunocompromised people, such as children and the elderly. This bacterium causes pneumonia, meningitis, otitis media, and other invasive diseases after infection, and the annual global morbidity and mortality rates of *S. pneumoniae* infections are very high (Kadioglu et al., 2008; Reynolds et al., 2010; Yu et al., 2019; Zhao et al., 2020). This bacterium is the most common pathogen causing community-acquired pneumonia in clinical practice, and fast and correct pathogenic identification is critical in the selection of clinical therapeutic medications and the construction of treatment strategies (Thummeepak et al., 2015; Arushothy et al., 2020).

The early detection of a clinical infection with a timely and accurate diagnosis in the early stages of the patient's illness allows the appropriate treatment to be administered. However, the current gold standard methods for detecting *S. pneumoniae* are phenotype based, and include culture-based, microscopy-based, and biochemical identification methods (Suárez and Texeira, 2019). Because *S. pneumoniae* growth and identification typically take more than 2 days, positive identification may occur late in the course of infection, and a delayed diagnosis may result in a bad prognosis for individuals infected with this pathogen (Petti et al., 2005). As a result, it is critical to develop and verify a speedy and precise approach to identifying *S. pneumoniae*. Several non-culture methods for detecting *S. pneumoniae* have been developed, including mass spectrometry, immunoassay, PCR, and real-time PCR (El Aila et al., 2010; Park et al., 2010; Lang et al., 2015; Iroh Tam et al., 2018; Kim et al., 2019; Kann et al., 2020). These tests can save considerable time compared with the gold standard culture methods. However, such analyses require skilled technicians and/or sophisticated equipment, which may be unavailable in some situations.

Recombinase polymerase amplification (RPA) is a recombinase-polymerase-mediated amplification technique that mimics DNA replication in living organisms and allows the isothermal amplification of target DNA fragments at room temperature (Piepenburg et al., 2006). The technique relies on three enzymes: the T4-phage-encoded recombinase proteins uvsX and uvsY, the single-stranded binding protein gp32, and the *Bacillus subtilis* (*Bsu*) DNA polymerase. The recombinase proteins bind to the primers to form DNA nucleoprotein microfilaments, which bind to complementary DNA fragments, which then hybridize tightly. With the help of the single-stranded binding protein, the strands of the template DNA begin to separate, and are extended by the *Bsu* DNA polymerase, which exponentially amplifies the target region on the template. The entire process can be completed in 20–30 min at 37–42°C (Wang et al., 2017; Dong et al., 2020). Compared with PCR, the process does not require high temperature denaturation or low temperature annealing, making the reaction simple, fast, and efficient. The labeled amplification products are detected visually by combining RPA with a lateral flow strip (LFS) of encapsulated gold nanoparticles (AuNPs), and the color signal can be observed semiquantitatively on the LFS with the naked eye (Wang et al., 2019). This technique simplifies the detection process and allows the *in situ* detection of the result without instruments. RPA–LFS has been successfully utilized to identify methicillin-resistant *Staphylococcus aureus*, *Mycobacterium tuberculosis*, *Candida albicans*, *Klebsiella pneumoniae*, and other pathogenic microorganisms (**Figure 1**) (Hu et al., 2020; Wang et al., 2020; Wang et al., 2021a; Wang et al., 2021b).

In this study, a rapid and sensitive field assay for *S. pneumoniae* was developed using RPA combined with the LFS technology. The method was based on primers and a probe designed to complement the *S. pneumoniae* autolysin gene (*lytA*) and the experiment was completed in 30 min at 37°C (Kersting et al., 2018). The specificity of the method was verified by testing it against 22 clinical isolates of *S. pneumoniae* and 25 other common pathogenic strains. The sensitivity of the RPA-LFS technique was tested in 10 independent trials, and the limit of detection (LOD) was 3.32 colony-forming units (CFU)/reaction. Finally, the established RPA-LFS assay for *S. pneumoniae* was used to analyze clinical specimens, with accurate results that were consistent with those achieved with PCR. In conclusion, we developed a rapid, specific, and sensitive assay for the detection of *S. pneumoniae* with RPA-LFS, with potential applications in the preliminary medical diagnosis of *S. pneumoniae* in remote and resource-limited areas.

MATERIALS AND METHODS

Standard Strains and Clinical Isolates

A standard strain of *S. pneumoniae* (American Type Culture Collection ATCC 49619) was used to establish the RPA-LFS method for detecting *S. pneumoniae*. Twenty-two clinical isolates of *S. pneumoniae* were obtained from sputum samples from the lower respiratory tract, with serotypes 19F, 19A, 14, 23F, and 6A, respectively. To validate the specificity of the RPA-LFS approach, isolates of 25 other common pathogens (including *Escherichia coli*, *Haemophilus influenzae*, *Acinetobacter baumannii*, *Pseudomonas aeruginosa*, *Enterococcus Faecium*, *Staphylococcus aureus*, *Klebsiella pneumoniae*, *Enterococcus faecalis*, *Serratia marcescens*, *Burkholderia cepacia*, *Candida albicans*, *Candida krusei*, *Vibrio Parahemolyticus*, *Streptococcus lactis*, *Bacillus cereus*, *Salmonella enterica*, *Morganella fulton*, *Coagulase negative Staphylococci*, *Bacillus mirabilis*, *Stenotrophomonas maltophilia*, *Streptcoccus pyogenes*, *Streptcoccus agalactiae*, *Streptcoccus dysgalacitae*, *Streptcoccus mitis*, and *Streptcoccus oralis*) were employed. At the Department of Laboratory of the Second People's Hospital of Lianyungang City, all strains were identified using the reference culture-biochemical approach.

One hundred and ten clinical specimens were collected from patients, including 80 respiratory sputum and 30 invasive specimens (16 blood, 10 cerebrospinal fluid, and 4 peritoneal fluid), which were provided by Lianyungang Second People's Hospital. The positive strains isolated were serotyped by the capsular swelling test and were 19F, 19A, 14, 23F, 9V, 6B, 6A.

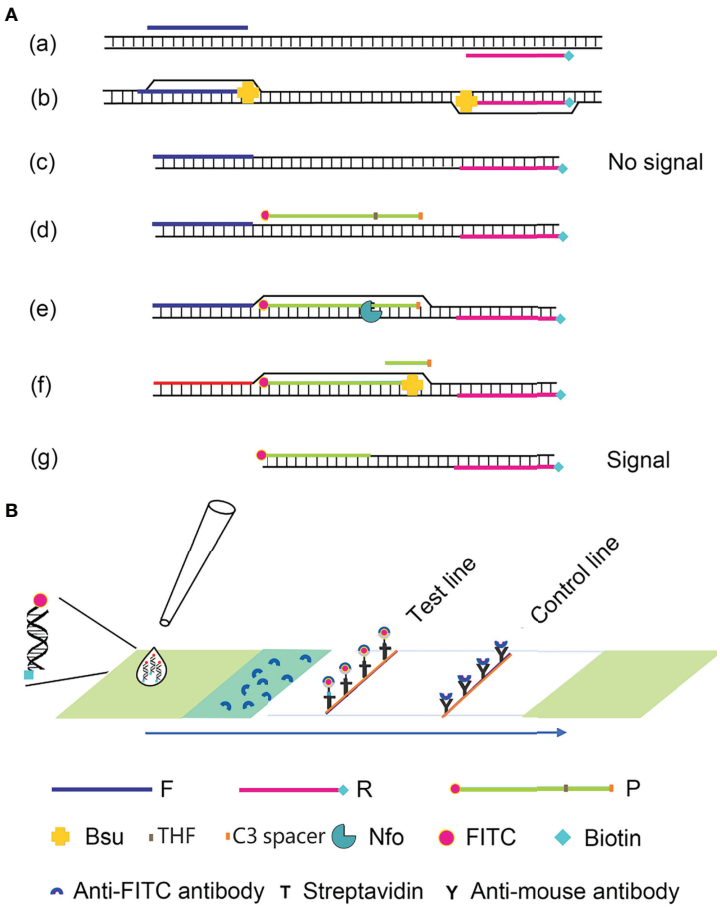

FIGURE 1 | Schematic diagram of the RPA-LFS method. **(A)** The RPA amplification principle. Base pairing is represented as short vertical lines between DNA strands, and DNA strands are represented as horizontal lines. Base pairing is represented by a short vertical line connecting two DNA strands. **(B)** A schematic representation of the lateral flow strip (LFS) operation. The shapes and the molecules that represent them are listed below the graphic.

Extraction of Bacterial Genomes

Genomic DNA was obtained using the Bacterial Genomic DNA Extraction Kit (Tiangen Biochemical Technology Co., Ltd, China) and stored at -20°C as a backup.

Primer Design for RPA Reactions

Specific RPA primers based on the species-specific *S. pneumoniae* autolysin gene (*lytA*) sequence was designed with the Primer-BLAST online design software from the National Center for Biotechnology Information (NCBI). The primer design parameters were: primer size 30–35 bp, product size 100–500 bp, GC content 20%–80%, Tm 50–100°C, and organism *S. pneumoniae*. All other parameters were set to the default values. Five primer pairs were selected (General Biologicals Ltd, Anhui, China) for testing.

RPA Procedure

To screen the best forward and reverse primer pairs, RPA amplification was performed using the TwistAmp Liquid DNA amplification Kit (TwistDx Inc., Maidenhead, United Kingdom). Each 50 μL mixture contained 25 μL of 2× reaction buffer, 5 μL of 10× basic mix, 2.5 μL of 20× core mix, 2.1 μL of forward primers (10 μM), 2.1 μL of reverse primers (10 μM), 9.8 μL of ddH_2O, and 1 μL of the template genome. To ensure that all reaction systems reacted at the same time, 2.5 μL of 280 mM magnesium acetate was added to the PCR tube caps and transiently centrifuged into all reaction tubes. The reaction system was vortexed and immediately incubated at 37°C in a thermostat heater for 30 min. The amplification products were purified using the DNA Purification Kit (Tiangen Biochemical Technology Co., Ltd, Beijing, China) and detected using 1.5 percent agarose gel electrophoresis.

RPA-LFS Probe Design

RPA amplification requires the same pair of forward and reverse primers as PCR amplification. When LFS is used as the endpoint visual readout for an amplified DNA target, a probe must be designed downstream from the forward primer. The 5′ end of the probe was labeled with fluorescein isothiocyanate (FITC), and a tetrahydrofuran (THF) site was included in the middle of the probe which is then closed at the end. When a certain amount of

product accumulated in the reaction system, the probe bound to the product, at which point the nfo enzyme in the reaction system recognized the THF site and cleaved it. Because the *Bsu* polymerase had strand replacement activity, it displaced the DNA strand after the THF site and began amplification. The final product obtained had FITC on one end and biotin on the other (Wang et al., 2018).

We used the Primer Premier 5 software to design specific probes complementary to sites between the sequences targeted by the forward and reverse primers. Theoretically, the formation of a dimeric structure between the probe and the reverse primer should be avoided. The parameters required to do so are: (1) a probe of 46–51 bp, Tm of 57–80°C, and GC content of 20%–80%; (2) The maximum primer dimer fraction is set to nine, the maximum hairpin fraction is set to nine, the maximum poly-X is set to five, and all other parameters are set to their default values. (3) The 5′ end of the probe was tagged with FITC, the 3′ end was blocked with the C3 spacer, and the middle base of the probe was replaced with THF, with at least 30 nucleotides before the THF site and at least 15 nucleotides after it; (4) the reverse primer's 5′ end was labeled with biotin.

RPA-LFS Procedure

To determine the optimal probe and primer combinations, the RPA-LFS assay was done using the TwistAmp DNA Amplification Nfo Kit (TwistDx Inc.). Each 50 μL reaction system included 2.1 μL of RPA forward and reverse primers (10 μM), 0.6 μL of RPA probe (10 μM), 11.2 μL of ddH_2O, 29.5 μL of hydration buffer, 2 μL of genomic DNA, and dried enzyme pellets. 2.5 μL of 280 mM magnesium acetate was added to the tube caps to guarantee that all of the reaction systems started at the same time. The tubes were briefly centrifuged before being incubated for 30 min in a constant-temperature heater set to 37°C. Then, within 5 min, 5 μL of the amplified product was visually evaluated with LFS (Ustar BioTechnologies Ltd, Hangzhou, China). On the LFS, two red lines were displayed: the control line (top) and the test line (bottom). The control line was present in all tests to guarantee the LFS's validity, whereas the test line was only shown in positive reactions.

Specificity Assay

RPA-LFS specificity for *S. pneumoniae* was tested using genomic DNA from 22 clinical isolates of *S. pneumoniae* and 25 common pathogenic bacteria.

Limit of Detection (LOD) Assay

A 10-fold dilution series of the *S. pneumoniae* genome, corresponding to numbers of bacteria ranging from 3×10^4 CFU to 3×10^{-1} CFU was prepared for the RPA-LFS reaction. The LOD of the method was determined with a probit regression analysis of 10 independent experiments.

Polymerase Chain Reaction

PCR primers were designed based on the *S. pneumoniae* autolysin *lytA* gene, and the primer sequences are in **Table 1**. 25 μL of the reaction system was used, including 12.5 μL of PCR Mix (Tiangen Biochemical Technology Co., Ltd., Beijing, China), 0.5 μL (10 μM) each of forward and reverse primers, 1 μL of template, and 10.5 μL of ddH_2O. The cycling procedure was 95°C pre-denaturation for 5 min, followed by 30 cycles including denaturation at 95°C for 30 s, binding at 55°C for 30 s, extension at 72°C for 1 min, and finally extension at 72°C for 5 min. amplification of the products was detected by 1.5% agarose gel electrophoresis.

Examination of Clinical Specimens

The RPA-LFS method was evaluated on clinical specimens to determine its compliance with both traditional culture–biochemical methods and PCR. Clinical specimens were cultured at 37°C for 18–48 hours on selective media, including blood culture bottles and columbia blood plate. Bacterial identification was carried out using the VITEK® 2 system (bioMérieux, Marcy-l'Étoile, France), with further biochemical assays carried out if necessary. For PCR, the

TABLE 1 | Primers and probes tested in this study.

Name	Sequence (5'-3')	Length (bp)	Amplicon size (bp)
lytA-1-F	ACAGAATGAAGCGGATTATCACTGGCGGAAAGA	33	351
lytA-1-R	GGATAAGGGTCAACGTGGTCTGAGTGGTTGTTTG	34	
lytA-2-F	CCGTACAGAATGAAGCGGATTATCACTGGCG	31	355
lytA-2-R	GGATAAGGGTCAACGTGGTCTGAGTGGTTGTTTG	34	
lytA-3-F	CAGAATGAAGCGGATTATCACTGGCGGAAAG	31	369
lytA-3-R	CCATTTAGCAAGATATGGATAAGGGTCAACG	31	
lytA-4-F	CATTGTTGGGAACGGTTGCATCATGCAGGTA	31	281
lytA-4-R	CGTGGTCTGAGTGGTTGTTTGGTTGGTTATTCG	33	
lytA-5-F	GCAGGTTTGCCGAAAACGCTTGATACAGGG	30	154
lytA-5-R	CATGCTTAAACTGCTCACGGCTAATGCCCCAT	32	
P1	FITC-AATCTAGCAGATGAAGCAGGTTTGCCGAAA[THF] CGCTTGATACAGGGA-/C3-spacer/	46	125
P2	FITC-CAATCTAGCAGATGAAGCAGGTTTGCCGAA[THF] ACGCTTGATACAGGG-/C3-spacer/	46	113
lytA-2-mR	Biotin-GGATAAGGGTCAACGTGGTCTGAGTGGTTGGTTG	34	/
lytA-4-mR	Biotin-CGTGGTCTGAGTGGTTGTTTGGTTGGTTAGTCG	33	/
mP1	FITC-AGTCTAGCAGATGAAGCAGGTTTGCCGAAA[THF] CGCTAGATACAGGGA -/C3-spacer/	46	/
mP2	FITC-CAATGTAGCTGATGAAGCAGGTTTGCTGAA[THF] ACGCTTGATACAGGG-/C3-spacer/	46	/
PCR-lytA-F	CAGATTTGCCTCAAGTCGGCGTGC	24	691
PCR-lytA-R	CCTGTAGCCATTTCGCCTGAGTTGTC	26	

Sequences modified with base substitutions. Modified bases are in red. F and R represent forward and reverse primers, respectively.

primers were designed to amplify the *lytA* gene. The compliance rate between the different methods was calculated with the formula: ([number of positive samples detected with both methods + number of negative samples detected with both methods]/total number of samples) × 100%. The kappa index was calculated to evaluate this test.

RESULTS

Design and Screening of Primer Sets for the RPA System

The rational design of primers for detecting *S. pneumoniae* started with a BLAST search with the *lytA* gene sequence. The primers were designed to match the *S. pneumoniae* sequence only. As shown in **Table 1**, five pairs of primers, lytA-1, lytA-2, lytA-3, lytA-4, and lytA-5, were designed to hybridize with the *lytA* gene. The basic RPA reaction was carried out using the genomic DNA of standard *S. pneumoniae* strains as a template, and the products were identified using agarose gel electrophoresis. All five primer sets (lytA-1 to lytA-5) produced distinct target bands with diameters of 456, 456, 456, 275, and 204 bp, respectively, and although there were no nonspecific amplification bands in the NTC, primer dimers of 100 bp were still present (**Figure 2**). However, primer pairs lytA-2 and lytA-4 amplified brighter target bands with fewer primer dimers. Therefore, we selected primer pairs lytA-2 and lytA-4 to design the probes for the RPA–LFS systems.

Modification and Determination of Optimal Primer–Probe Combinations for RPA-LFS

P1 and P2 probes were designed to bind within the sequences amplified by the lytA-2 and lytA-4 primer pairs, respectively, and RPA-LFS tests were performed to determine the amplification performance and false-positive results of the primer–probe combinations lytA-2/F/R/P1 and lytA-4/F/R/P2. **Figure 3A** depicts the results. Both primer-probe combinations produced the expected positive results (visible red bands on both the test and control lines), suggesting that both combinations amplified the target sequence effectively. However, they both also generated a weak red band on the test line in the NTC, indicating false-positive signals for both primer-probe combinations.

The FITC- and biotin-labeled RPA products produced by the probe and reverse primer are particularly recognized by the LFS. Therefore, the RPA-LFS probe should be designed in such a way that the NTC signal is entirely suppressed. Previous research has demonstrated that the RPA reaction can tolerate minor mismatches between primers or probes and the template (Daher et al., 2015). The Primer Premier 5 software was used to examine the potential for probe-reverse primer dimers, and mismatches were inserted at sites with more than five continuous bases or more than three bases at the 3′ end. **Table 1** shows the sequences of the modified reverse primer (mR) and probe (mP), with the replaced bases highlighted in red. The modified probes and primers were then used in the RPA-LFS assay. When the *lytA* gene was amplified from *S. pneumoniae* genomic DNA, both primer-probe pairs showed no signal on the detection line in the NTC group and a significant signal on the detection line in the group containing *S. pneumoniae* genomic DNA (**Figure 3B**). Because the number of mismatched bases in the lyt-2-F/mR/mP1 combination was small, we assumed that this combination performed better. Analysis of the RPA amplification products with agarose gel electrophoresis revealed two clear bands for both primer–probe combinations, representing the amplification products generated with the forward and reverse primers and with the probe and the reverse primer (**Figure 3C**). Overall, the best primer-probe combination for RPA–LFS detection of *S. pneumoniae* was lyt-2-F/mR/mP1.

Specificity Analysis of the RPA-LFS Assay

To verify the inclusiveness and specificity of the primer–probe combination lyt-2-F/mR/mP1, RPA-LFS was used to analyze 22

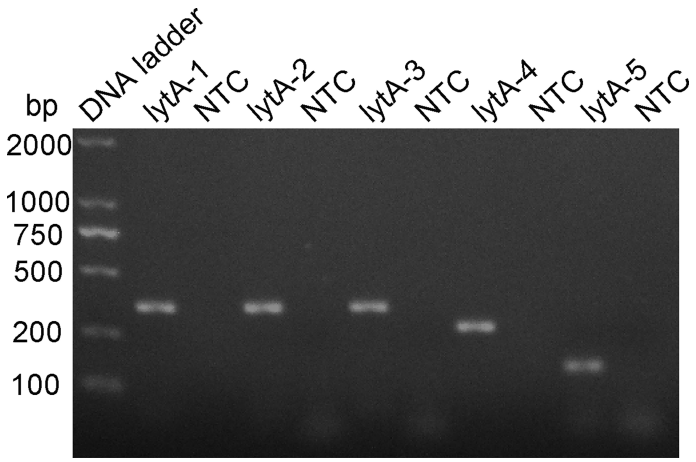

FIGURE 2 | Screening RPA primer sets. The primer pairs lytA-1 to lytA-5 were screened with the RPA method using genomic DNA from standard *S. pneumoniae* strains as the templates. An NTC for each primer set was included as the negative control and 1.5% agarose gel electrophoresis was used to analyze equal volumes (5 μL) of the amplified products.

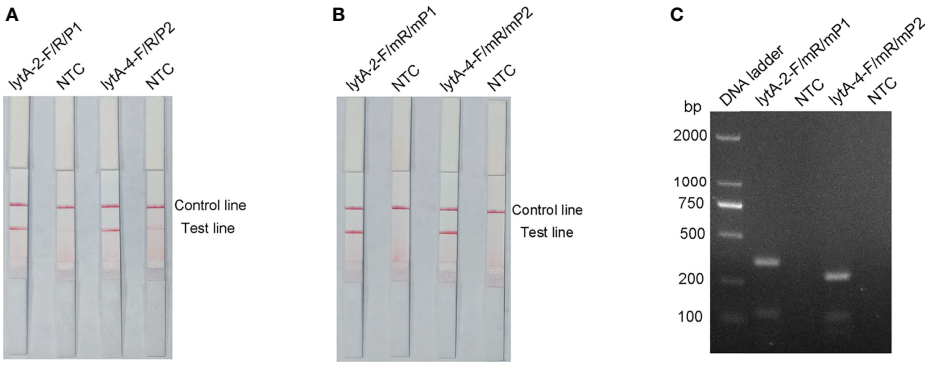

FIGURE 3 | Performance of the primer-probe sets tested with the RPA-LFS system. **(A)** Showing the LFS assay results of RPA amplification products before mismatch. **(B)** Showing the LFS assay results of RPA amplification products after mismatch. **(C)** Agarose gel results. The name of each primer-probe set is shown above the corresponding strip. NTC strip is the no-template control for the corresponding RPA. The positions of the test and control lines are marked on the right side of the bars. Reactions were performed at 37°C for 30 min. This image represents the results of three independent experiments.

clinical isolates of *S. pneumoniae* and 25 other pathogenic bacteria. **Figure 4** shows that when isolated *S. pneumoniae* genomic DNA was used as the template, a clear positive signal appeared on the test line, however no bands showed on the test line when genomic DNA from any other common respiratory infection was used as the template. These results indicated that the RPA-LFS assay system established here was highly specific for *S. pneumoniae* and does not cross-react with other pathogens.

LOD of the RPA-LFS Assay

The detection limit of the RPA-LFS assay was assessed using a 10-fold dilution of inactivated *S. pneumoniae* culture as the template, comparable to bacterial counts ranging from 3×10^4 CFU to 3×10^{-1} CFU (1 μL, reaction volume of 50 μL). A clear red band was visible on the detection line at 3×10^4 CFU, and the signal diminished as the amount of template decreased, disappearing altogether in the 3×10^{-1} CFU sample (**Figure 5A**). To test whether the system was resistant to interference from human genomes, 10 ng of human DNA were added to the RPA reaction along with dilutions of *S. pneumoniae* genomic DNA. The detection sensitivity was not affected by human DNA (**Figure 5B**). Not all assays produced positive results when template equivalent to 3×10^0 CFU (nine positive results in 10 samples) or 3×10^{-1} CFU (one positive results in 10 samples) were used. To confirm the LOD of the RPA–LFS assay more accurately, a probit regression analysis was performed on data from 10 independent assays. The statistical

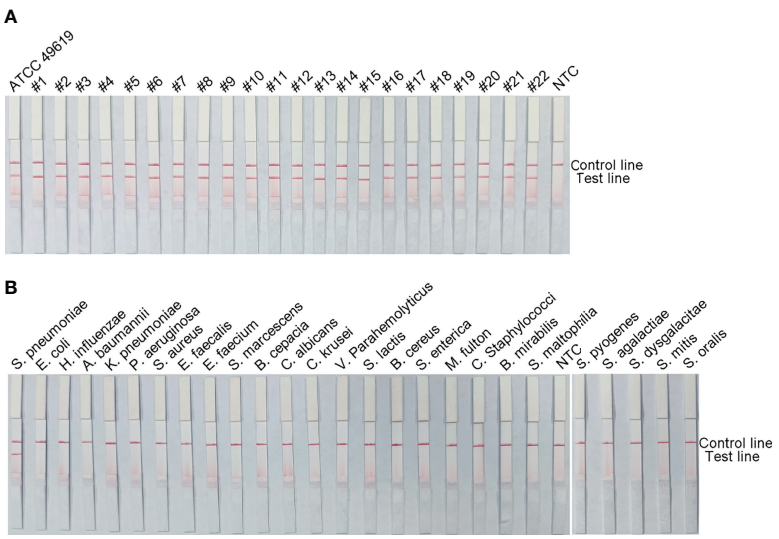

FIGURE 4 | The RPA-LFS assay's specificity. *S. pneumoniae* clinical isolates **(A)** and other common pathogens **(B)** were tested. The positive control was *S. pneumoniae* (ATCC 49619). Each bacterium's species name is shown at the top of each strip. The NTC strip is a no-template control. The reactions were carried out for 30 minutes at 37°C.

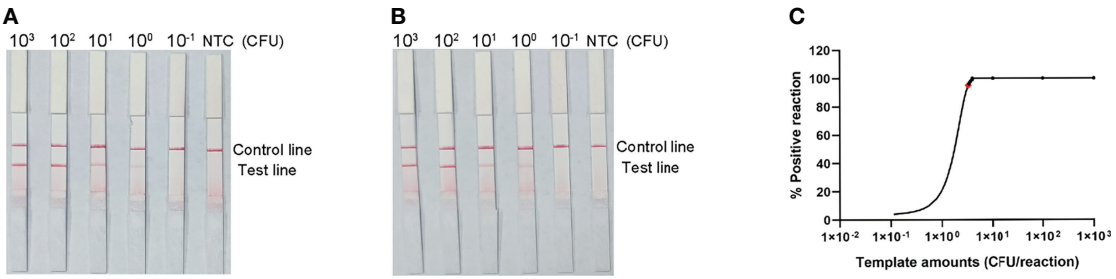

FIGURE 5 | Determination of the limit of detection (LOD) of the *S. pneumoniae* RPA-LFS assay. **(A)** The LOD of the established *S. pneumoniae* RPA-LFS assay was determined from 10 independent assays using the serially diluted genomic DNA of *S. pneumonia*, equivalent to 10^4 to 10^{-1} CFU. Images show the results of the RPA-LFS assays, and the amount of template is indicated at the top of the bar graph. **(B)** The group with 10 ng human genomic DNA added in addition to the P. gingivalis genomic DNA. **(C)** Probit regression analysis was performed on data collected from 10 replicates, using the SPSS software.

analysis was performed with the SPSS software. The LOD for each reaction was 3.32 CFU, with 95% probability (**Figure 5C**).

Application of *S. pneumoniae* RPA-LFS to the Identification of Clinical Specimens

To assess the clinical utility of the established RPA-LFS detection system, 110 clinical specimens were collected from patients and examined with the RPA-LFS method, a PCR method, and a culture-biochemical approach at the Second People's Hospital of Lianyungang. As indicated in **Table 2**, 31 of 110 samples tested positive for *S. pneumoniae* using the RPA-LFS and PCR methods, whereas 30 of 110 tested positive using the culture-biochemistry method. The established RPA-LFS assay was 100 percent compliant with the PCR technique. The RPA-LFS approach had a 98.18% compliance rate with the conventional culture-biochemical method, and the estimated kappa index was 0.977, suggesting that the difference between the two methods was not statistically significant ($p > 0.05$). These results demonstrated the feasibility and reliability of the highly specific and sensitive *S. pneumoniae* RPA-LFS when applied to clinical samples from patients.

DISCUSSION

Streptococcus pneumoniae can be found in the nasopharynx of healthy adults as well as children, and has a wide clinical distribution. It is usually cultured in a medium of blood or serum, where it forms round, grayish-white colonies (Li and Zhang, 2019). It can be spread in airborne droplets and is distributed in greater amounts in places where interpersonal contact rates are high, such as hospitals and military barracks. Infection rates are higher in the elderly, children, and those with low resistance. Consequently, *S. pneumoniae* is the main pathogen causing severe pediatric pneumonia. The early detection and diagnosis of pathogenic clinical infections with timely, effective, and accurate testing in the early stages of a patient's illness allow the correct treatment to be administered (Allan et al., 2016). However, a diagnosis is traditionally made by culturing the bacterium, which is not only time-consuming, but is also susceptible to contamination with other bacteria during the culture process, compromising the accuracy of detection and therefore the diagnosis. In consequence, the choice of treatment plan and the recovery of the patient will be seriously affected. Therefore, a reliable diagnostic method that can rapidly, sensitively, and specifically identify *S. pneumoniae* in a near-patient setting could play an important role in reducing the morbidity and mortality associated with pneumococcal disease, especially in developing countries.

TABLE 2 | Assay performance of the RPA-LFS system, PCR and culture-biochemical method.

Method	positive	negative	Total	Amplification time
RPA-LFS	31	79	110	35 min
qPCR	31	79	110	90 min
Culture-biochemical method	30	80	110	2 d

Because they do not require temperature cycling, *in vitro* isothermal nucleic acid amplification techniques are gaining popularity in molecular diagnostics. Transcription-mediated amplification (TMA), nucleic-acid-sequence-based amplification (NASBA), helicase-dependent amplification (HDA), rolling loop amplification (RCA), loop-mediated isothermal amplification (LAMP), and chain displacement amplification (SDA) are the most common isothermal amplification techniques used today (Walker et al., 1992; Pasternack et al., 1997; Lizardi et al., 1998; Notomi et al., 2000; Deiman et al., 2002; Vincent et al., 2004). Among these methods, TMA, NASBA, RCA, and SDA cannot be considered truly isothermal because they require an initial heating step to denature the target nucleic acid before its amplification. Because no denaturation step is necessary to start amplification, RPA, HDA, and LAMP can be regarded genuinely isothermal. However, LAMP typically requires a reaction temperature of 60–65°C and three primer pairs, which may lead to primer-primer interactions that can limit the reaction. The main advantage of RPA over HAD been its speed, because it can amplify a single copy of nucleic acid to detectable levels in as little as 5–10 min. Furthermore, the use of both primers and a probe in the RPA reaction increases the specificity of the assay. We eliminated primer-dependent artifacts and avoided the formation of false-

positive signals by introducing specific base substitutions into the primer and probe sequences and by rigorously screening and analyzing the formation of primer–probe complexes (Wu et al., 2020). The combination of RPA with the lateral flow immunoassay technique had the advantages of ease of detection, portability, and results that were readable with the naked eye. These advantages make RPA-LFS a method with which nucleic acids can be detected immediately.

Among the molecular targets utilized to identify *S. pneumoniae* were the Spn9802 fragment, the *recA* gene, the 16S rRNA gene, and virulence factor genes such as lysozyme (*ply*). Although these targets have shown beneficial in detecting *S. pneumoniae*, their capacity to identify it clearly remains a challenge. For example, both *ply* and Spn9802 have been associated with false-negative results (Abdeldaim et al., 2008; Carvalho Mda et al., 2007; El Aila et al., 2010; Zbinden et al., 2011). The autolysin gene *lytA* is highly conserved across *S. pneumoniae* strains, with only minor genetic change (0.11 percent–0.32 percent), and is found in practically all clinical isolates. As a result, it was chosen for the identification of *S. pneumoniae* in this case.

This RPA assay was highly specific and all 22 clinical isolates tested positive, whereas all 25 other common pathogens tested negative, indicating that the RPA-LFS established here specifically detected *S. pneumoniae*. A probit regression analysis was used to calculate the LOD (95% confidence level) of the method, which was 3.32 CFU per reaction. This is similar to the LOD of other highly sensitive molecular detection methods (Clancy et al., 2015; Wang et al., 2019).

In conclusion, we developed a sensitive and specific RPA-LFS assay for detecting *S. pneumoniae* in clinical specimens. Using the *lytA* gene as the diagnostic target, specific sets of primer-probe combinations were designed and screened. The detection of *S. pneumoniae* was completed within 30 min at 37°C. This assay had good potential utility for the detection of *S. pneumoniae* in resource-limited areas.

DATA AVAILABILITY STATEMENT

The original contributions presented in the study are included in the article/supplementary material. Further inquiries can be directed to the corresponding authors.

ETHICS STATEMENT

The Medical Ethics Committee of Lianyungang City's Second People's Hospital examined and authorized the human-participant studies. To participate in the study, the patients/participants gave their written informed consent.

AUTHOR CONTRIBUTIONS

XG and GH designed the research. FW, YW, and XL conducted the research. CX, LW, and KW analyzed the data. The manuscript was written by FW and XG. The article was read and approved by all writers.

FUNDING

This work was supported by the Jiangsu Province of China's High-level Innovation and Entrepreneurship Talents Introduction Program (grant number 2019-30345), Lianyungang City's '521 Project' scientific research funding project (grant number LYG06521202157), Lianyungang City's 'HaiYan Plan' scientific research funding project (grant number 2019-QD-008), and Jiangsu University's Clinical Medical Science and Technology Development Fund (grant number JLY20180020).

REFERENCES

Abdeldaim, G. M., Strålin, K., Olcén, P., Blomberg, J., and Herrmann, B. (2008). Toward a Quantitative DNA-Based Definition of Pneumococcal Pneumonia: A Comparison of Streptococcus Pneumoniae Target Genes, With Special Reference to the Spn9802 Fragment. *Diagn. Microbiol. Infect. Dis.* 60 (2), 143–150. doi: 10.1016/j.diagmicrobio.2007.08.010

Allan, R. N., Morgan, S., Brito-Mutunayagam, S., Skipp, P., Feelisch, M., Hayes, S. M., et al. (2016). Low Concentrations of Nitric Oxide Modulate Streptococcus Pneumoniae Biofilm Metabolism and Antibiotic Tolerance. *Antimicrob. Agents Chemother.* 60 (4), 2456–2466. doi: 10.1128/aac.02432-15

Arushothy, R., Ramasamy, H., Hashim, R., Raj, A. S. S., Amran, F., Samsuddin, N., et al. (2020). Multidrug-Resistant *Streptococcus pneumoniae* Causing Invasive Pneumococcal Disease Isolated From a Paediatric Patient. *Int. J. Infect. Dis.* 90, 219–222. doi: 10.1016/j.ijid.2019.10.037

Carvalho Mda, G., Tondella, M. L., McCaustland, K., Weidlich, L., McGee, L., Mayer, L. W., et al. (2007). Evaluation and Improvement of Real-Time PCR Assays Targeting Lyta, Ply, and psaA Genes for Detection of Pneumococcal DNA. *J. Clin. Microbiol.* 45 (8), 2460–2466. doi: 10.1128/jcm.02498-06

Clancy, E., Higgins, O., Forrest, M. S., Boo, T. W., Cormican, M., Barry, T., et al. (2015). Development of a Rapid Recombinase Polymerase Amplification Assay for the Detection of Streptococcus Pneumoniae in Whole Blood. *BMC Infect. Dis.* 15, 481. doi: 10.1186/s12879-015-1212-5

Daher, R. K., Stewart, G., Boissinot, M., Boudreau, D. K., and Bergeron, M. G. (2015). Influence of Sequence Mismatches on the Specificity of Recombinase Polymerase Amplification Technology. *Mol. Cell Probes.* 29 (2), 116–121. doi: 10.1016/j.mcp.2014.11.005

Deiman, B., van Aarle, P., and Sillekens, P. (2002). Characteristics and Applications of Nucleic Acid Sequence-Based Amplification (NASBA). *Mol. Biotechnol.* 20 (2), 163–179. doi: 10.1385/mb:20:2:163

Dong, Y., Zhao, P., Chen, L., Wu, H., Si, X., Shen, X., et al. (2020). Fast, Simple and Highly Specific Molecular Detection of Vibrio Alginolyticus Pathogenic Strains Using a Visualized Isothermal Amplification Method. *BMC Vet. Res.* 16 (1), 76. doi: 10.1186/s12917-020-02297-4

El Aila, N. A., Emler, S., Kaijalainen, T., De Baere, T., Saerens, B., Alkan, E., et al. (2010). The Development of a 16S rRNA Gene Based PCR for the Identification of Streptococcus Pneumoniae and Comparison With Four Other Species Specific PCR Assays. *BMC Infect. Dis.* 10, 104. doi: 10.1186/1471-2334-10-104

Hu, J., Wang, Y., Ding, H., Jiang, C., Geng, Y., Sun, X., et al. (2020). Recombinase Polymerase Amplification With Polymer Flocculation Sedimentation for Rapid Detection of Staphylococcus Aureus in Food Samples. *Int. J. Food Microbiol.* 331, 108691. doi: 10.1016/j.ijfoodmicro.2020.108691

Iroh Tam, P. Y., Hernandez-Alvarado, N., Schleiss, M. R., Yi, A. J., Hassan-Hanga, F., Onuchukwu, C., et al. (2018). Detection of Streptococcus Pneumoniae From Culture-Negative Dried Blood Spots by Real-Time PCR in Nigerian Children

With Acute Febrile Illness. *BMC Res. Notes* 11 (1), 657. doi: 10.1186/s13104-018-3770-2

Kadioglu, A., Weiser, J. N., Paton, J. C., and Andrew, P. W. (2008). The Role of Streptococcus Pneumoniae Virulence Factors in Host Respiratory Colonization and Disease. *Nat. Rev. Microbiol.* 6 (4), 288–301. doi: 10.1038/nrmicro1871

Kann, S., Sao, S., Phoeung, C., By, Y., Bryant, J., Komurian-Pradel, F., et al. (2020). MALDI-TOF Mass Spectrometry for Sub-Typing of Streptococcus Pneumoniae. *BMC Microbiol.* 20 (1), 367. doi: 10.1186/s12866-020-02052-7

Kersting, S., Rausch, V., Bier, F. F., and von Nickisch-Rosenegk, M. (2018). A Recombinase Polymerase Amplification Assay for the Diagnosis of Atypical Pneumonia. *Anal. Biochem.* 550, 54–60. doi: 10.1016/j.ab.2018.04.014

Kim, S. J., Jeong, Y. J., Kim, J. H., Yoon, Y. K., Sohn, J. W., Nahm, M. H., et al. (2019). Development for Clinical Use of a Multiplexed Immunoassay Using Sputum Samples for Streptococcus Pneumoniae: A Non-Culture-Based Approach for Serotype-Specific Detection. *J. Clin. Microbiol.* 57 (10), e01782-18. doi: 10.1128/jcm.01782-18

Lang, A. L. S., McNeil, S. A., Hatchette, T. F., Elsherif, M., Martin, I., and LeBlanc, J. J. (2015). Detection and Prediction of Streptococcus Pneumoniae Serotypes Directly From Nasopharyngeal Swabs Using PCR. *J. Med. Microbiol.* 64 (8), 836–844. doi: 10.1099/jmm.0.000097

Lizardi, P. M., Huang, X., Zhu, Z., Bray-Ward, P., Thomas, D. C., and Ward, D. C. (1998). Mutation Detection and Single-Molecule Counting Using Isothermal Rolling-Circle Amplification. *Nat. Genet.* 19 (3), 225–232. doi: 10.1038/898

Li, J., and Zhang, J. R. (2019). Phase Variation of Streptococcus Pneumoniae. *Microbiol. Spectr.* 7 (1), 268–274. doi: 10.1128/microbiolspec.GPP3-0005-2018

Notomi, T., Okayama, H., Masubuchi, H., Yonekawa, T., Watanabe, K., Amino, N., et al. (2000). Loop-Mediated Isothermal Amplification of DNA. *Nucleic Acids Res.* 28 (12), E63. doi: 10.1093/nar/28.12.e63

Park, H. K., Lee, H. J., and Kim, W. (2010). Real-Time PCR Assays for the Detection and Quantification of Streptococcus Pneumoniae. *FEMS Microbiol. Lett.* 310 (1), 48–53. doi: 10.1111/j.1574-6968.2010.02044.x

Pasternack, R., Vuorinen, P., and Miettinen, A. (1997). Evaluation of the Gen-Probe Chlamydia Trachomatis Transcription-Mediated Amplification Assay With Urine Specimens From Women. *J. Clin. Microbiol.* 35 (3), 676–678. doi: 10.1128/jcm.35.3.676-678.1997

Paton, J. C., and Trappetti, C. (2019). Streptococcus Pneumoniae Capsular Polysaccharide. *Microbiol. Spectr.* 7 (2). doi: 10.1128/microbiolspec.GPP3-0019-2018

Petti, C. A., Woods, C. W., and Reller, L. B. (2005). Streptococcus Pneumoniae Antigen Test Using Positive Blood Culture Bottles as an Alternative Method to Diagnose Pneumococcal Bacteremia. *J. Clin. Microbiol.* 43 (5), 2510–2512. doi: 10.1128/jcm.43.5.2510-2512.2005

Piepenburg, O., Williams, C. H., Stemple, D. L., and Armes, N. A. (2006). DNA Detection Using Recombination Proteins. *PloS Biol.* 4 (7), e204. doi: 10.1371/journal.pbio.0040204

Reynolds, J. H., McDonald, G., Alton, H., and Gordon, S. B. (2010). Pneumonia in the Immunocompetent Patient. *Br. J. Radiol.* 83 (996), 998–1009. doi: 10.1259/bjr/31200593

Suárez, N., and Texeira, E. (2019). Optimal Conditions for Streptococcus Pneumoniae Culture: In Solid and Liquid Media. *Methods Mol. Biol.* 1968, 3–10. doi: 10.1007/978-1-4939-9199-0_1

Thummeepak, R., Leerach, N., Kunthalert, D., Tangchaisuriya, U., Thanwisai, A., and Sitthisak, S. (2015). High Prevalence of Multi-Drug Resistant Streptococcus Pneumoniae Among Healthy Children in Thailand. *J. Infect. Public Health* 8 (3), 274–281. doi: 10.1016/j.jiph.2014.11.002

Vincent, M., Xu, Y., and Kong, H. (2004). Helicase-Dependent Isothermal DNA Amplification. *EMBO Rep.* 5 (8), 795–800. doi: 10.1038/sj.embor.7400200

Walker, G. T., Fraiser, M. S., Schram, J. L., Little, M. C., Nadeau, J. G., and Malinowski, D. P. (1992). Strand Displacement Amplification–an Isothermal, *In Vitro* DNA Amplification Technique. *Nucleic Acids Res.* 20 (7), 1691–1696. doi: 10.1093/nar/20.7.1691

Wang, F., Ge, D., Wang, L., Li, N., Chen, H., Zhang, Z., et al. (2021a). Rapid and Sensitive Recombinase Polymerase Amplification Combined With Lateral Flow Strips for Detecting Candida Albicans. *Anal. Biochem.* 633, 114428. doi: 10.1016/j.ab.2021.114428

Wang, Y., Jiao, W. W., Wang, Y., Wang, Y. C., Shen, C., Qi, H., et al. (2020). Graphene Oxide and Self-Avoiding Molecular Recognition Systems-Assisted Recombinase Polymerase Amplification Coupled With Lateral Flow Bioassay for Nucleic Acid Detection. *Mikrochim. Acta* 187 (12), 667. doi: 10.1007/s00604-020-04637-5

Wang, H., Ma, Z., Qin, J., Shen, Z., Liu, Q., Chen, X., et al. (2019). A Versatile Loop-Mediated Isothermal Amplification Microchip Platform for Streptococcus Pneumoniae and Mycoplasma Pneumoniae Testing at the Point of Care. *Biosens. Bioelectron.* 126, 373–380. doi: 10.1016/j.bios.2018.11.011

Wang, F., Wang, L., Chen, H., Li, N., Wang, Y., Li, Y., et al. (2021b). Rapid Detection of Bla (KPC), Bla (NDM), Bla (OXA-48-Like) and Bla (IMP) Carbapenemases in Enterobacterales Using Recombinase Polymerase Amplification Combined With Lateral Flow Strip. *Front. Cell Infect. Microbiol.* 11, 772966. doi: 10.3389/fcimb.2021.772966

Wang, J., Wang, J., Li, R., Liu, L., and Yuan, W. (2017). Rapid and Sensitive Detection of Canine Distemper Virus by Real-Time Reverse Transcription Recombinase Polymerase Amplification. *BMC Vet. Res.* 13 (1), 241. doi: 10.1186/s12917-017-1180-7

Wang, J., Wang, J., Li, R., Shi, R., Liu, L., and Yuan, W. (2018). Evaluation of an Incubation Instrument-Free Reverse Transcription Recombinase Polymerase Amplification Assay for Rapid and Point-of-Need Detection of Canine Distemper Virus. *J. Virol. Methods* 260, 56–61. doi: 10.1016/j.jviromet.2018.07.007

Wang, L., Zhao, P., Si, X., Li, J., Dai, X., Zhang, K., et al. (2019). Rapid and Specific Detection of Listeria Monocytogenes With an Isothermal Amplification and Lateral Flow Strip Combined Method That Eliminates False-Positive Signals From Primer-Dimers. *Front. Microbiol.* 10, 2959. doi: 10.3389/fmicb.2019.02959

Wu, H., Zhao, P., Yang, X., Li, J., Zhang, J., Zhang, X., et al. (2020). A Recombinase Polymerase Amplification and Lateral Flow Strip Combined Method That Detects Salmonella Enterica Serotype Typhimurium With No Worry of Primer-Dependent Artifacts. *Front. Microbiol.* 11, 1015. doi: 10.3389/fmicb.2020.01015

Ye, W., Zhang, J., Shu, Z., Yin, Y., Zhang, X., and Wu, K. (2018). Pneumococcal LytR Protein Is Required for the Surface Attachment of Both Capsular Polysaccharide and Teichoic Acids: Essential for Pneumococcal Virulence. *Front. Microbiol.* 9, 1199. doi: 10.3389/fmicb.2018.01199

Yu, Y. Y., Xie, X. H., Ren, L., Deng, Y., Gao, Y., Zhang, Y., et al. (2019). Epidemiological Characteristics of Nasopharyngeal Streptococcus Pneumoniae Strains Among Children With Pneumonia in Chongqing, China. *Sci. Rep.* 9 (1), 3324. doi: 10.1038/s41598-019-40088-6

Zbinden, A., Köhler, N., and Bloemberg, G. V. (2011). recA-Based PCR Assay for Accurate Differentiation of Streptococcus Pneumoniae From Other Viridans Streptococci. *J. Clin. Microbiol.* 49 (2), 523–527. doi: 10.1128/jcm.01450-10

Zhao, S., Zhang, Z., Xu, D., Wang, Y., and Li, L. (2020). Selective Loss of Brain-Derived Neurotrophic Factor Exacerbates Brain Injury by Enhancing Neuroinflammation in Experimental Streptococcus Pneumoniae Meningitis. *Front. Immunol.* 11, 1357 doi: 10.3389/fimmu.2020.01357

Conflict of Interest: The authors declare that the research was conducted in the absence of any commercial or financial relationships that could be construed as a potential conflict of interest.

frontiers | Frontiers in Cellular and Infection Microbiology

TYPE Original Research
PUBLISHED 18 August 2022
DOI 10.3389/fcimb.2022.876495

OPEN ACCESS

EDITED BY
Elena Jordana-Lluch,
Balearic Islands Health Research Institute (IdISBa), Spain

REVIEWED BY
Sveva Di Franco,
Università degli Studi della Campania "Luigi Vanvitelli", Italy
Hongsong Chen,
Peking University People's Hospital, China

*CORRESPONDENCE
Zhongjie Hu
huzhongjie@ccmu.edu.cn
Feili Wei
wflcn@126.com

†These authors have contributed equally to this work and share first authorship

SPECIALTY SECTION
This article was submitted to Clinical Microbiology, a section of the journal Frontiers in Cellular and Infection Microbiology

RECEIVED 15 February 2022
ACCEPTED 27 July 2022
PUBLISHED 18 August 2022

CITATION
Wu H-X, Hou W, Zhang W, Wang Z, Guo S, Chen D-X, Li Z, Wei F and Hu Z (2022) Clinical evaluation of bacterial DNA using an improved droplet digital PCR for spontaneous bacterial peritonitis diagnosis.
Front. Cell. Infect. Microbiol. 12:876495.
doi: 10.3389/fcimb.2022.876495

Clinical evaluation of bacterial DNA using an improved droplet digital PCR for spontaneous bacterial peritonitis diagnosis

Hao-Xin Wu[1†], Wei Hou[1†], Wei Zhang[1], Zheng Wang[1], Shan Guo[2], De-Xi Chen[2], Zhen Li[1], Feili Wei[2*] and Zhongjie Hu[1*]

[1]Beijing YouAn Hospital, Capital Medical University, Beijing, China, [2]Beijing Institute of Hepatology, Beijing YouAn Hospital, Capital Medical University, Beijing, China

Objective: Bacterial DNA (bactDNA) detection can be used to quickly identify pathogenic bacteria and has been studied on ascitic fluid. We aimed to retrospectively analyze the diagnostic value and applicational prospect of the bactDNA load in spontaneous bacterial peritonitis (SBP).

Method: We extracted viable bactDNA from ascitic samples of 250 patients with decompensated cirrhosis collected from October 2019 to April 2021 and detected the bactDNA by droplet digital polymerase chain reaction (ddPCR). We used ascitic samples of a baseline cohort of 191 patients to establish diagnostic thresholds for SBP and analyze the patients' diagnostic performance based on ascites polymorphonuclear (PMN) and clinical manifestation. We performed bactDNA quantification analysis on 13 patients with a PMN less than 250 cells/mm^3 but with clinical symptoms. The dynamic changes of the bactDNA load from eight patients (before, during, and after SBP) were analyzed.

Results: After the removal of free DNA, the bactDNA detected by ddPCR was generally decreased (1.75 vs. 1.5 log copies/μl, $P < 0.001$). Compared with the traditional culture and PMN count in the SBP diagnosis, the bactDNA showed that the ddPCR sensitivity was 80.5%, specificity was 95.3%, positive predictive value was 82.5%, and negative predictive value was 94.7%, based on clinical composite criteria. In patients with a PMN less than 250 cells/mm^3, the bactDNA load of 13 patients with symptoms was significantly higher than those without symptoms (2.7 vs. 1.7 log copies/μl, $P < 0.001$). The bactDNA in eight patients had SBP that decreased by 1.6 log copies/μl after 48 h of antibiotic treatment and by 1.0 log copies/μl after 3 days of continued treatment.

Conclusion: BactDNA detection can be used to further enhance the diagnostic efficiency of SBP. Therefore, the application of ddPCR assay not only can be used to discriminate and quantify bacteria but also can be used in the clinical assessment for antibiotics treatment.

KEYWORDS

Peritonitis, BactDNA, diagnosis, bacterascites, viable bacteria

Introduction

Spontaneous bacterial peritonitis (SBP) is an infectious disease caused by pathogenic microorganisms that invade the abdominal cavity and cause obvious damage (European Association for the Study of the Liver., 2018). In people with end-stage liver diseases, the incidence rate of SBP has been shown to reach 40% to 70% (Aithal et al., 2021).. Currently, SBP is defined as an ascites polymorphonuclear (PMN) count greater than 250 cells/mm^3 (European Association for the Study of the Liver., 2018; Aithal et al., 2021; Biggins et al., 2021). However, approximately 60% to 80% of patients with a PMN less than 250 cells/mm^3 have signs and symptoms (Oey et al., 2018; Song and Jiang, 2016); of those patients, 38% develop SBP (Li et al., 2020). However, empirical antibiotic therapy that is based on the patient's clinical symptoms and PMN can lead to the excessive application of antibiotics and the occurrence of multi-drug resistant organisms (Piano et al., 2019; Fernández et al., 2019). Current traditional culture for SBP has insufficient sensitivity to detect samples with bacteria (European Association for the Study of the Liver., 2018), especially those with low bacterial loads. Therefore, it is urgent for researchers and clinicians to introduce more accurate and rapid etiological diagnosis methods.

Recently, ascites bacterial DNA (bactDNA) detection has been expected to replace the general bacterial culture of ascites in the identification of infectious pathogens (Enomoto et al., 2018; Aithal et al., 2021). Droplet digital polymerase chain reaction (ddPCR) is a novel absolute quantitative molecular detection technology that has been developed in recent years with advantages of high sensitivity, simplicity, fastness, and operation without relying on the standard curve (Hussain et al., 2016; Cho et al., 2020). The ddPCR technology produces about 20,000 droplets and enriches target DNA by reducing competition with high-copy templates. After PCR amplification in each droplet, the Poisson algorithm is used to determine the concentration of target DNA from positive and negative droplets. Studies have suggested that the ddPCR technology is able to detect very low amounts of pathogen DNA within 4 h and had been applied in the diagnosis of bloodstream and tuberculosis infections (Cho et al., 2020; Wouters et al., 2020). Those findings provide direction for the application of ddPCR in clinical diagnosis of bacterial infection.

Nevertheless, some previous studies (Zapater et al., 2008; Bruns et al., 2016; Alvarez-silva et al., 2019) have shown that there was no strong correlation between the presence of bactDNA in ascites and SBP; as a result, the diagnosis of SBP by bactDNA has not been readily applied in clinical practice. The possible reasons are as follows: 1) bacterial load plays a very important role in the development of SBP, not just the presence of bactDNA (Bernardi et al., 2020); 2) the large volume of ascites that often occurs in patients with cirrhosis may dilute bacterial products (Akalin et al., 1983); and 3) accumulated evidence indicates (Guarner et al., 2006) that bacteria may translocate either in a viable or non-viable form, and the migration of nucleic acid DNA may potentially obscure any correlation between microbes and clinical parameters.

Therefore, the purpose of our study was to assess the amounts of viable bactDNA in ascites for the diagnostic accuracy of SBP, using an optimized method of ddPCR.

Methods

Study design and population

This study was approved by the ethical committee of Beijing YouAn Hospital, Capital Medical University. The study design was composed of laboratory and clinical studies (Figure 1). Clinical data of the patients enrolled in the study were obtained by medical record review and were analyzed according to clinical course to determine the likelihood of an infection. A total of 250 patients with decompensated cirrhosis and ascites from the Liver Disease Center, Beijing YouAn Hospital, Capital Medical University, between September 2019 and April 2021 were retrospectively collected in the study. Cancerous ascites, secondary peritonitis, and incomplete clinical data were excluded. Ascitic samples of the first baseline cohort from 191 patients were obtained on admission. The SBP diagnosis is based on PMN (2021 practice guideline)

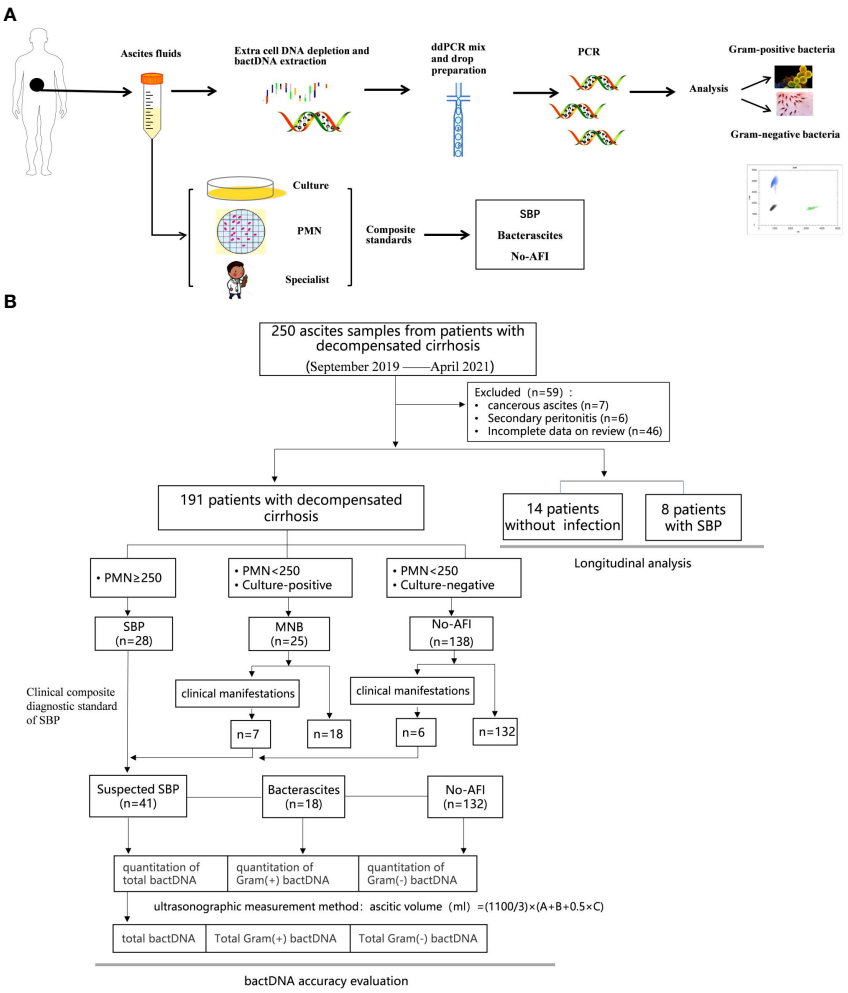

FIGURE 1
Study workflow and sample distribution. **(A)** Schematic of ddPCR ascites analysis workflow. A total of 1.5–2 h were needed for nucleic acid extraction and 2 h for the preparation, amplification, and analysis in ddPCR quantitation detection. **(B)** Overall flow of patients in the study showing patient recruitment and subsequent selection for bactDNA quantitation analysis. ddPCR, droplet digital PCR; PMN, polymorphonuclear; SBP, spontaneous bacterial peritonitis; MNB, monomicrobial non-neutrocytic bacterascites; AFI, ascites fluid infection. Gram(+), Gram-positive; Gram(–), Gram-negative.

(Biggins et al., 2021) and a clinical composite diagnosis (2017 Chinese guidelines) (Chinese Society of Hepatology, Chinese Medical Association, 2017) that incorporated 1) clinical signs or symptoms, 2) laboratory test abnormalities, and 3) adjudication independently by an infectious disease specialist (CLH) and two liver disease experts (YH and WH). Patients were initially classified as either SBP (PMN > 250/mm^3), monomicrobial non-neutrocytic bacterascites (PMN < 250/mm^3 with positive ascites culture), or ascites without infection (no-AFI; PMN < 250/mm^3 with negative ascites culture) (European Association for the Study of the Liver., 2018; Biggins et al., 2021). Patients who had overt clinical symptoms but with a PMN count less than 250/mm^3 were further classified as suspected SBP, bacterascites, and no-AFI (Figure 1B) (Rimola et al., 2000; Campillo et al., 2002; Gu et al., 2021). Subsequently, we selectively enrolled 14 patients without infection to observe an association between a higher baseline bactDNA load and SBP development and eight patients with SBP to analyze the dynamic changes of bactDNA load (before, during, and after antibiotics). The diagnostic standard and the inclusion and exclusion criteria are detailed in the Supplementary Data.

To evaluate and eliminate the influence of ascitic volume on bacterial quantity, we adopted the ultrasonic three-point method from Hirooka et al. (2018); this method is used to calculate the total amount of ascites: total amount (ml) = (1,100/3) × (A + B + 0.5 × C). In this way, the absolute total amount of bacteria could be determined by the total ascitic volume [(ml) × bacterial ddPCR (copies/μl)].

ddPCR methods

Primes and probes

The representative 20 bacteria sequences of primers and probes were adopted and revised from the previous article and synthesized by Sangon Biotech (Shanghai) Co., Ltd (Wouters et al., 2020). The reaction conditions were optimized and screened according to the ddPCR requirements. Then, the performance of primers and probes was verified, which included sensitivity, specificity, linearity, and repeatability.

Sample processing

To deplete the extracellular DNA from the ascitic samples, 1-ml samples were centrifuged at 4°C with 13,000r for 10 min. After discarding the 760-μl supernatant, we added 40.5-μl mixture of buffer and benzonase endonuclease and incubated this mixture at 37°C for 15 min. Next, we added 20 μl of protease K and incubated it at 56°C for 20 min to inactivate the benzonase.

DNA extraction

Approximately 400 μl of 2× DNA/RNA shield (zymo R1200-125) was added into each of the pre-treatment samples. After mixing, the samples were homogenized using a program of 4°C at 60 Hz for 120 s, stopped for 20 s, repeated four times in Tissuelyser (Servicebio, Wuhan, China), and then centrifuged at 10,000r for 2 min. We then individually added 400 μl of DNA/RNA analysis buffer, prep buffer, and wash buffer for repeated DNA washing. Finally, 50 μl of DNase/RNase-free water was added to collect target DNA and stored at −80°C until tested.

Droplet preparation and detection

The ddPCR was performed with the TargetingOne Digital PCR System (TargetingOne, Beijing, China). The master mix for ddPCR included 1× ddPCR supermix for probes, forward and reverse primers at 400 nmol/L, and GRAM+/GRAM− probes at 200 nmol/L; 1-μl sample of DNA and DNase/RNase Free water were mixed together, and the final volume was 30 μl for each well. The droplet was generated according to the manufacturers' protocols.

PCR amplification was performed with the following conditions: 95°C for 10 min followed by 40 cycles of denaturation at 95°C for 10 min; annealing and extension was at 60°C for 1 min. The strip tubes were stored at 4°C until the droplets were analyzed with a TargetingOne chip reader and TargetingOne ddPCR Analyzer 1.0. The threshold between positive and negative droplet populations was manually set using per-plate positive and no-template controls as a guide.

Statistical analysis

The data are presented as a mean ± standard deviation or median with a range. We used the Wilcoxon–Mann–Whitney test for between-group comparisons or the Kruskal-Wallis test with *post hoc* tests for continuous data. The continuous variables were dichotomized according to the maximum approximate index in the receiver operating characteristic (ROC). The statistical analyses were performed using SPSS software, version 24 (IBM, Armonk, NY), and Prism 8 (GraphPad, La Jolla, CA). In the two-sided test, a P-value of <0.05 was considered statistically significant.

Results

Patients' characteristics

Two hundred and fifty patients were enrolled in this study. We excluded seven patients with cancerous ascites, six patients with secondary peritonitis, and 46 patients who had incomplete data. One hundred and ninety-one patients were enrolled, and their ascitic samples were collected. Among them, 155 patients were men (81.2%), with an average age of 58.1 ± 9.1 years. Liver cirrhosis was caused by alcoholic hepatitis in 73 cases (38.2%), hepatitis B in 71 cases (37.2%), hepatitis C in seven cases (3.7%), and other causes in 40 cases (21.0%). There were 41 patients with suspected SBP (21.5%), 18 patients with bacterascites (9.4%), and 132 patients who had no-AFI (69.1%). The demographic data are listed in Table 1 and Supplementary Table S1 and Figure S1.

Analysis and valuation of ddPCR method

Results showed that the clustering effect of ddPCR was best when the primer probe concentration was 400/200 nmol/L and the annealing temperature was 60°C (Supplementary Table S2, Figure S2). Representative Gram-positive and Gram-negative bacteria were selected for a specific probe test, which indicated that the probe could clearly distinguish Gram-positive or Gram-negative bacteria (Figures 2A, B). To determine whether the probe had cross interference in distinguishing Gram-positive and Gram-negative bacteria, we mixed *E. feacium* and *E. coli* in different concentrations (100:1, 1:100, and 1:1) and tested them. The results showed that the corresponding bactDNA loads were 4.3:2.1, 2.0:4.0, and 2.2:2.3 log copies/μl, indicating that reaction systems with different concentrations could be accurately classified and quantified (Figures 2C–E).

To determine the ddPCR detection limit, linearity, and repeatability, nine types of bacteria were spiked in a mixed system and subsequently detected by ddPCR. Serial dilutions of the above bacteria at known concentrations showed a good linearity (R^2 = 0.97–0.99; Supplementary Figure S3), with three replicates at each dilution (1–5 log copies); the ddPCR detection limit was approximately 20–45 copies/μl for bacterial strains. Compared with traditional qPCR methods, the ddPCR showed

TABLE 1 Clinical characteristics of enrolled patients.

	SBP (n = 41)	Bacterascites (n = 18)	no-AFI (n = 132)	P¶
Age (years, mean ± SD)	58.6 ± 8.3	59.4 ± 10.8	57.8 ± 9.2	0.766
Gender (male/female)	37/4	14/4	104/28	0.298
Etiology				
Alcohol	17 (41.5)	9 (50.0)	47 (35.6)	0.934
HBV	15 (37.5)	6 (33.3)	50 (37.9)	
HCV	1 (2.5)	0 (0)	6 (4.5)	
HBV plus alcohol	4 (9.8)	1 (5.6)	9 (6.8)	
Others	4 (9.8)	2 (11.1)	20 (15.2)	
Complications				
Ascites 2/3	24/17	10/8	80/52	0.906
Gastrointestinal bleeding	3 (7.5)	2 (11.1)	12 (9.0)	0.886
Hepatic encephalopathy	4 (10.0)	2 (11.1)	17 (12.9)	0.859
HRS	5 (12.5)	1 (5.6)	22 (16.7)	0.471
Laboratory parameters				
WBC ($\times10^9$/L), median (IQR)	7.6 (5.1, 12.0)	4.9 (3.2, 6.3)	3.7 (2.5, 6.3)	<0.01
neutrophil (%), median (IQR)	81.4 (70.6, 85.4)	73.9 (63.1, 86.7)	68.6 (59.2, 70.7)	<0.01
ALT (IU/L), median (IQR)	18.2 (8.1, 28.3)	17.4 (10.1, 24.3)	19.5 (11.7, 31.6)	0.297
AST(IU/L), median (IQR)	36.5 (18.7, 63.7)	24.2 (15.8, 49.8)	39.6 (24.9, 61.6)	0.147
PCT (ng/L), median (IQR)	0.18 (0.10, 1.84)	0.10 (0.05, 0.42)	0.15 (0.05, 1.82)	<0.01
CRP (mg/L), median (IQR)	17.4 (9.8, 48.8)	10.0 (7.2, 33.2)	10.0 (6.5, 31.9)	0.297
Albumin (g/dl), mean ± SD	30.2 ± 4.7	29.3 ± 4.4	29.7 ± 4.1	0.741
Total bilirubin (μmol/L), median (IQR)	54.8 (15.4, 168.5)	34.4 (21.3, 46.9)	52.3 (26.6, 99.8)	0.282
PTA, mean ± SD	65.7 ± 30.9	59.2 ± 16.8	58.7 ± 18.7	0.231
Serum creatinine (μmol/L), median (IQR)	91.2 (63.8, 179.5)	84.4 (64.8, 134.0)	81.7 (59.5, 120.3)	0.422
Platelets (10^9/L), median (IQR)	91.5 (63.4, 141.3)	53.2 (26.2, 72.7)	79.5 (45.5, 114.8)	0.008
Ascites WBC count ($\times10^6$/L), median (IQR)	1,693 (765, 3620)	220 (92, 322)	200 (130, 620)	<0.01
Ascites PMN count ($\times10^6$/L), median (IQR)	1,437 (1,123, 3,587)	40 (8, 111)	54 (28, 94)	<0.01
Scores				
CTP	10.1 ± 1.8	9.6 ± 1.4	10.0 ± 1.6	0.688
MELD	16.0 ± 9.8	12.7 ± 5.3	14.2 ± 7.9	0.714

SD, standard deviation; IQR, interquartile range; HRS, hepatorenal syndrome; WBC, white blood cell; PCT, procalcitonin; CRP, C-reactive protein; ALT, alanine aminotransferase; AST, aspartate aminotransferase; PTA, prothrombin activity; CTP, Child-Turcotte-Pugh score; MELD, model for end-stage liver disease; PMN, polymorphonuclear neutrophils; AFI, ascitic fluid infection.
¶P-value from the Kruskal–Wallis test for continuous variables or the Fisher's exact test for discrete variables that compares patients with SBP to patients with bacterascites and no-AFI.

better linearity and lower detection limits (Supplementary Figure S4).

Clinical evaluation of an improved ddPCR quantitation method

Benzonase endonuclease digestion was performed on the samples before detection; thus, all detected DNA came from live bacteria. We selected 54 cirrhotic ascites (13 SBP, 15 bacterascites, and 26 no-AFI samples) for validation. The results showed that, compared with the extraction method of none-dependent assay, the benzonase-dependent assay had a significant difference ($P < 0.001$) and even lower bactDNA load (1.75 vs. 1.5 copies/μl; Figures 3A, B); we found that this difference between the two extraction methods was mainly the extraction of Gram-negative bacteria from bacterascites and no-AFI (Figure 3C), which was conducive to distinguishing the interference of cell-free DNA fragments and the real bacterial infection with low loads. After the depletion of DNA fragments, the area under the ROC curve was as follows: bactDNA 0.98 (95% CI, 0.94–1.00), Gram-positive bactDNA 0.91 (95% CI, 0.84–0.99), and Gram-negative bactDNA 0.95 (95% CI, 0.88–1.00; Figure 3D), which indicated that DNA treatment with benzonase may have a better diagnostic value.

We used the ultrasonic three-point method to evaluate and eliminate the influence of ascitic volumes and found that there was no significant variation in bactDNA levels between the concentration and the absolute copies of bactDNA combined with ascitic volumes ($P > 0.53$, Figure 4A). In addition, results

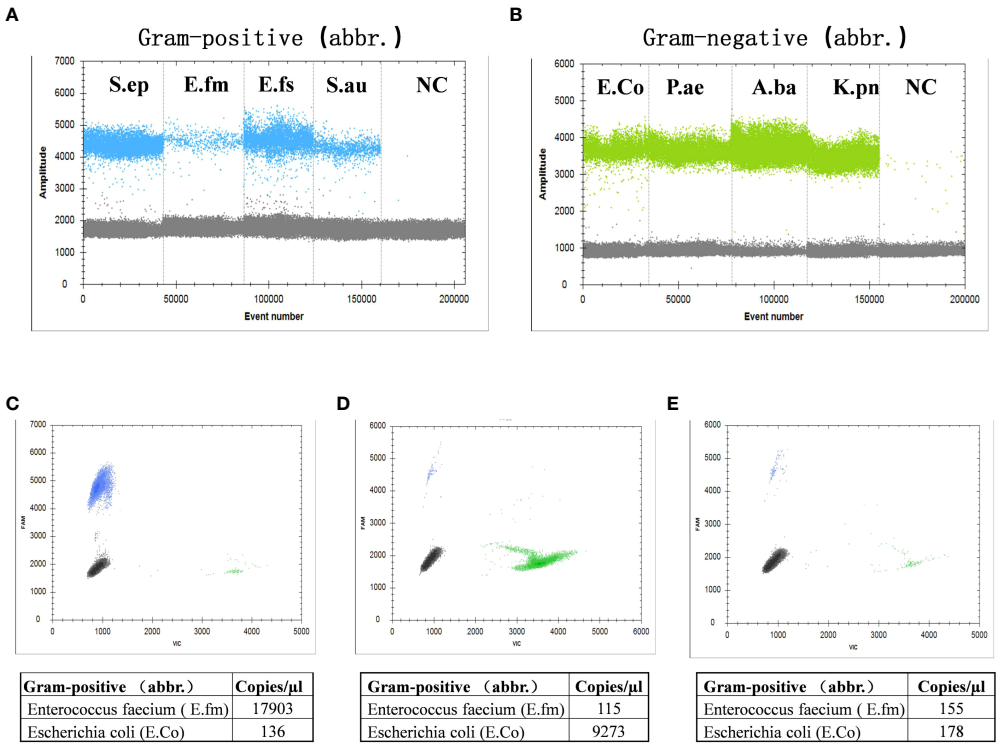

Gram-positive (abbr.)	Copies/μl
Enterococcus faecium (E.fm)	17903
Escherichia coli (E.Co)	136

Gram-positive (abbr.)	Copies/μl
Enterococcus faecium (E.fm)	115
Escherichia coli (E.Co)	9273

Gram-positive (abbr.)	Copies/μl
Enterococcus faecium (E.fm)	155
Escherichia coli (E.Co)	178

FIGURE 2
Detection of Gram-positive bacteria and Gram-negative bacteria using ddPCR. **(A)** Gram-positive bacteria, which included *Staphylococcus epidermidis*, *Enterococcus faecium*, *Enterococcus faecalis*, *Staphylococcus aureus*, and a negative control. **(B)** Gram-negative bacteria, which included *Escherichia coli*, *Pseudomonas aeruginosa*, *Acinetobacter baumannii*, *Klebsiella pneumoniae*, and a negative control. The interference test (different/mixed concentrations) of mixed *E. faecium* and *E. coli*; **(C)** 100:1; **(D)** 1:100; **(E)** 1:1.

showed that bactDNA loads in the ascites of patients with SBP (total of 2.8, Gram-positive of 1.9, and Gram-negative of 2.5 log copies/μl) were significantly higher than that of the patients with bacterascites (1.7, 1.3, and 1.5 log copies/μl) and the patients with no-AFI (2.0, 1.4, and 1.8 log copies/μl; $P < 0.001$; Figure 4A, Supplementary Table S3), whereas there was no significant difference between patients with bacterascites and ascites without infection. Then, we correlated the bactDNA load with the Model for End-Stage Liver Disease (MELD) score and found that bactDNA load in patients with SBP was weakly positively corelated with MELD ($r = 0.321$, $P = 0.052$; Figure 4B), whereas there was no correlation between bactDNA load and MELD in patients with bacterascites and ascites without infection.

The enhanced sensitivity and specificity of bactDNA detection facilitates SBP diagnosis

Subsequently, we plotted ROC curves at varying bactDNA levels that corresponded to the SBP analysis. Results from 191 samples showed that the cutoff value of the bactDNA quantification was 103.2 copies/μl compared with the SBP diagnosis. For patients infected with Gram-positive and Gram-negative bacteria, the cutoff values were 37.3 and 68.6 copies/μl, respectively (Figure 4C).

At the optimal Youden index, which is derived from the ROC curve, the sensitivity and specificity of total bactDNA compared with the composite clinical standard were 80.5% (95% CI, 67.8%–93.2%) and 95.3% (95% CI, 91.1%–98.3%), respectively; the positive predictive agreement (PPA) and negative predictive agreement (NPA) were 82.5% and 94.7%, respectively. The diagnostic test revealed that 72% (95% CI, 53.1%–90.9%) sensitivity, 93.9% (95% CI, 90.3%–97.6%) specificity, 64.3% PPA, and 95.7% NPA of SBP were caused by Gram-positive bacteria; 91.3% (95% CI, 78.8%–100%) sensitivity, 89.3% (95% CI, 84.6%–94.0%) specificity, 53.8% PPA, and 98.6% NPA of SBP were caused by Gram-negative bacteria. In addition, the sensitivity and specificity of traditional culture compared with the composite clinical standard were 53.7% (95% CI, 40.0%–73.5%) and 88.0% (95% CI, 83.2%–93.4%), and PPA and NPA were 55.0% and 87.4% (Figure 4D), respectively. Therefore, as a novel tool, bactDNA based on ddPCR greatly improves microbial diagnosis in SBP.

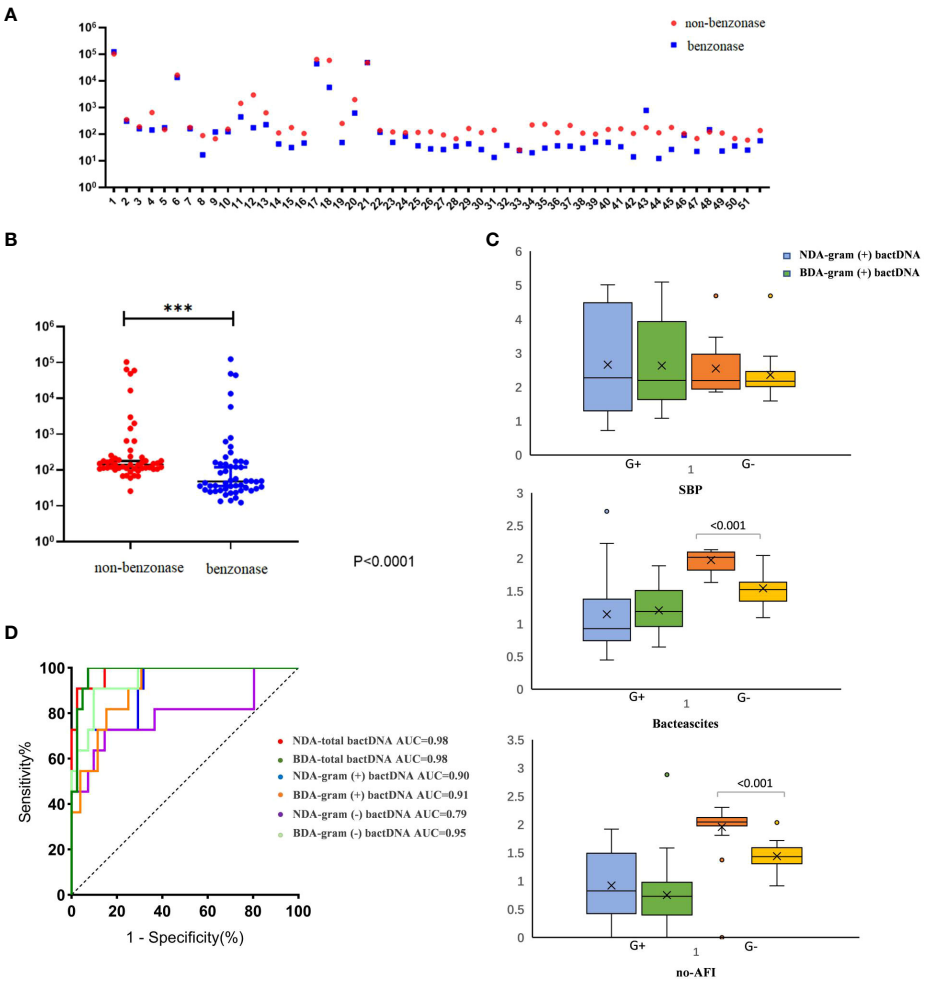

FIGURE 3
Clinical evaluation of an improved ddPCR quantitation method. **(A)** Fifty-four patients were selected in this comparison [SBP, 13; no-SBP, 41 (bacterascites, 15; no-AFI samples, 26)]. **(B)** Comparison between the non-dependent assay (NDA) and benzonase-dependent assay (BDA). **(C)** The results of Gram-positive and Gram-negative bactDNA quantitation of NDA and BDA in patients with SBP, bacteascites, and no-AFI. **(D)** ROC curves stratified by two different methods of NDA and BDA (n = 54 samples in total) based on clinical composite standards. NDA, non-dependent assay; BDA, benzonase-dependent assay; SBP, spontaneous bacterial peritonitis; AFI, ascites fluid infection; ***P < 0.001.

BactDNA levels as indicators of suspected infections in symptomatic patients with a PMN less than 250/mm^3

The data showed that 163 of the 191 samples had PMN less than 250 cells/mm^3, of which 13 patients were consulted by two infectious physicians and one hepatologist to consider SBP diagnosis and were treated with empirical antibiotics (see Supplementary Table S4). After treatment, the patients' symptoms improved, and their diagnosis was clinically confirmed as SBP. Notably, among them, seven patients with culture positive were Gram-positive bacteria (Figure 5A), including *Enterococcus faecalis*, *Enterococcus faecium*, *Staphylococcus haemolyticus*, and *Corynebacterium*, which were consistent with a previous study in bacterascites (Li et al., 2020). In 13 patients with SBP with a PMN less than 250 cells/mm^3, bactDNA amounts in ascites were significantly higher than those in patients with no-SBP (total of 2.7, Gram-positive of of 2.2, and Gram-negative of 2.1 log copies/μl vs. 1.7, 1.1, and 1.5 log copies/μl; P < 0.001; Figure 5B, Supplementary Table S5). According to the diagram of PMN counts, Gram-positive bacterial infections produce lower PMN counts than Gram-negative bacteria infection (Figure 5C). From our data, the cutoff value of PMN count was 192 cells/mm^3 with 73.2% (95% CI, 59.4%–87.2%) sensitivity and 98.6% (95% CI, 97.3%–100%) specificity compared with composite diagnostic standard (Figure 4D). Therefore, we hypothesized that a PMN threshold of 250/mm^3 was too high for the SBP diagnosis, especially for Gram-positive infections.

10.3389/fcimb.2022.876495

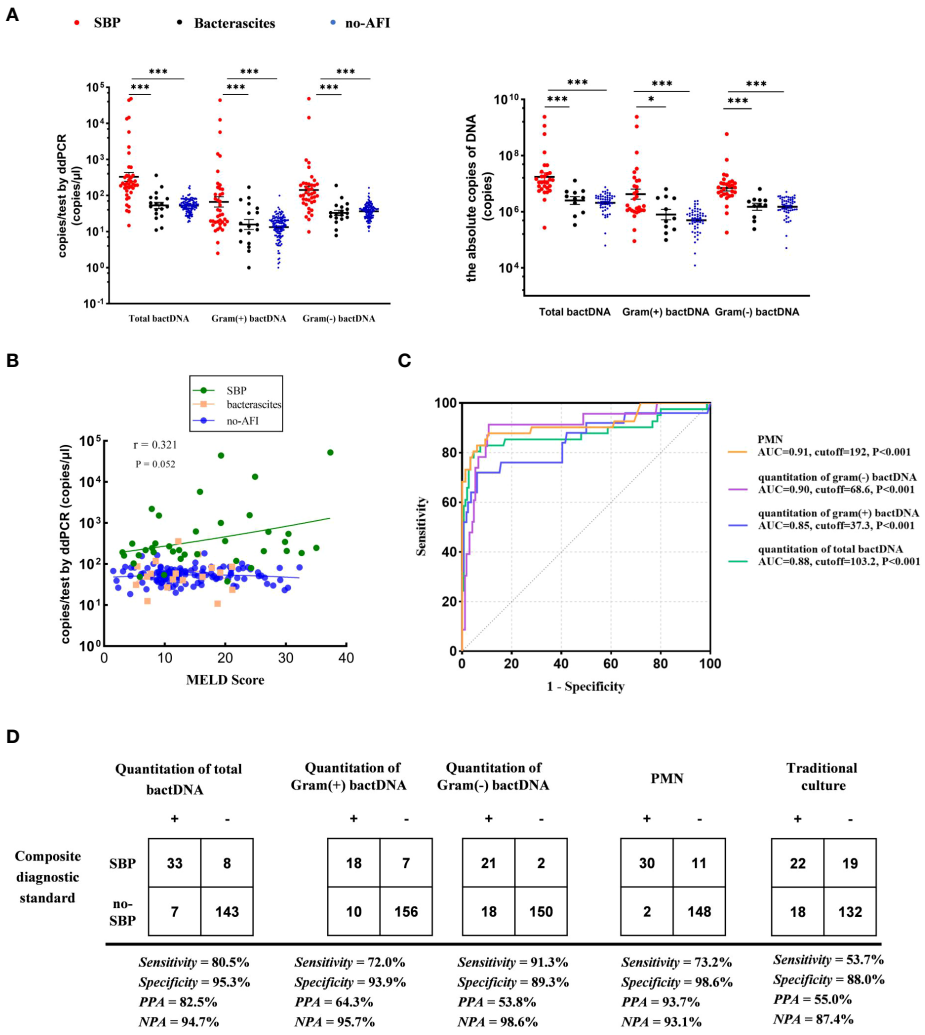

FIGURE 4
Accuracy of ddPCR testing in ascites. **(A)** Samples from 41 patients with SBP, 18 patients with bacterascites, and 132 patients with no-AFI. In the left panels, we compared the concentration of bactDNA. In the right panels, we obtained the absolute copies of bactDNA combined with ascitic volumes using virtual ultrasonography "three-point method". **(B)** Correlation of bactDNA load with MELD. **(C)** ROC curves of bactDNA load from 191 samples based on clinical composite standards. **(D)** The 2 × 2 contingency tables for the validation of the quantification of bactDNA based on a clinical composite standard. MELD, Model for End-Stage Liver Disease; ROC, receiver operating characteristic; PPA, positive predictive agreement; NPA, negative predictive agreement; *P < 0.05, **P < 0.01, and ***P < 0.001.

BactDNA loads assist to predict the development of SBP and monitor antibiotic therapy in clinical practice

We selected 14 patients who developed SBP during hospitalization and collected available consecutive samples for three or more times, and nine ascites without infection on admission that developed SBP during hospitalization, with an average duration of 6 days. Five patients were readmitted due to SBP diagnosis within 3 months (Figure 5D). The results showed that the baseline bactDNA load was higher in patients with SBP development compared with patients without SBP development (55.7 copies/μl vs. 46.7 copies/μl; P = 0.05; Figure 5E), indicating that the bactDNA level was associated with incidence of SBP.

To assess dynamic change in bactDNA load before, during, and after SBP, eight patients with SBP (mean, 4 log copies/μl) were continuously observed before antibacterial treatment, 48 h and 5 days after antibacterial treatment. Results showed that the amount of bactDNA significantly decreased after 48 h of antimicrobial treatment (2.4 log copies/μl) and continued to decline with the use of antibiotics (1.4 log copies/μl; Figure 5F).

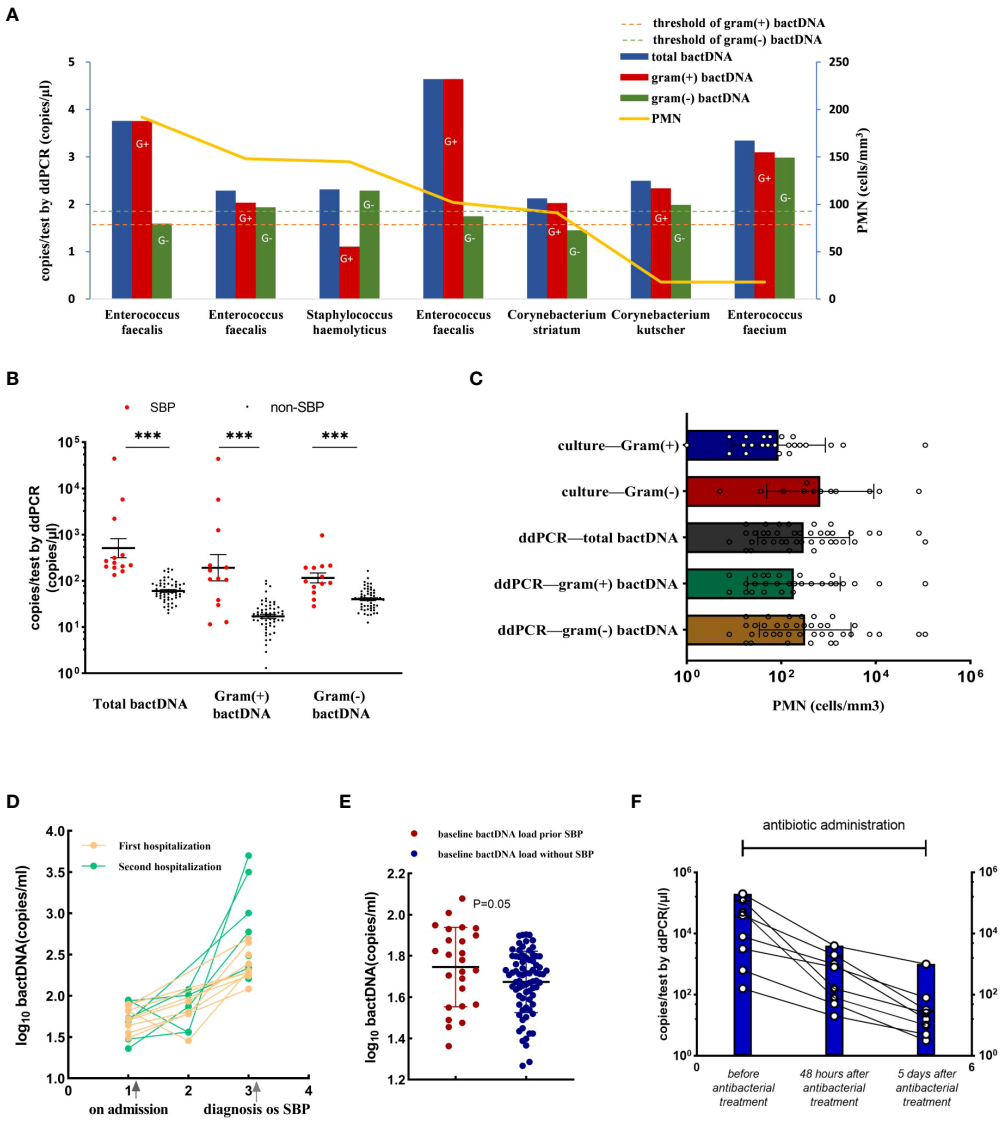

FIGURE 5
Accuracy of ddPCR testing in ascites and the bactDNA quantitation in patients with PMN < 250 cells/mm^3. **(A)** The bactDNA load and PMN counts from seven patients diagnosed as SBP with PMN < 250/mm^3. **(B)** Patients with PMN < 250/mm^3 [SBP (n = 13) and no-SBP (n = 150)]. **(C)** PMN counts of different bacteria species in 191 samples based on culture and ddPCR. **(D)** Nine ascites without infection on admission developed SBP during hospitalization. Five patients were readmitted due to SBP diagnosis within 3 months, and five patients were readmitted due to SBP diagnosis within 3 months. **(E)** Baseline bactDNA load prior and without SBP development. **(F)** Dynamic changes of bactDNA load using ddPCR method in patients with SBP over time precede antibacterial treatment, 48 h and 5 days after antibacterial treatment (n = 8). PMN, polymorphonuclear; SBP, spontaneous bacterial peritonitis. ***P < 0.001.

Discussion

In this study, we described a rapid diagnostic method for bactDNA detection with low loads based on ddPCR to evaluate the bactDNA levels of abdominal infection in a large series of patients with cirrhosis and ascites. To our knowledge, this is the first study reporting detection of vital bacteria using benzonase to improve the SBP diagnosis. In particular, for symptomatic patients with PMN count <250/mm^3, the bactDNA quantitation in ascites can be used to sensitively distinguish patients with suspected infections.

Benzonase has an advantage of removing free DNA fragments without affecting viable bacteria (Amar et al., 2021). Our data showed that, after the removal of free DNA, the concentration of bactDNA had generally decreased, whereas the area under the curve for diagnosing SBP was increased. However, we found that there was a significant decrease in gram-negative bacteria, which we speculated as either the increase of

Gram-negative bactDNA from intestinal translocation to abdominal cavity or the increased destruction of Gram-negative bacteria due to the repeated freeze-thawing of samples during storage of ascitic samples. Notably, considering the effect of abdominal volume, we found that there was no significant variation of bactDNA between the concentration and the absolute copies of bactDNA combined with ascitic volume. Therefore, the abdominal volume dilution may not be a factor in affecting the bacterial absolute amount, which may be due to the high sensitivity of ddPCR detection technology.

Our study showed that the sensitivity and specificity of total bactDNA were 80.5% and 95.3% compared with the SBP diagnosis, which was consistent with the results of the bloodstream infection (Wouters et al., 2020). In addition, the bactDNA load is more likely to predict SBP development and reflect changes in the bacterial number with antibiotic use. The advantage of ddPCR assay is its culture independency and high sensitivity. It is a promising technology that not only performs absolute quantification but also accurately distinguishes Gram-positive and Gram-negative bacteria. Taken together, the bactDNA quantification in ascites by ddPCR is helpful for dynamically monitoring the changes of nucleic acid in pathogens and the effects of antibacterial treatment.

The SBP diagnosis is confirmed when the ascitic neutrophil count is ≥250 cells/mm^3. However, in practice, some patients are symptomatic and have a PMN < 250 cells/mm^3. Results from our data showed that those cases had a significant increase in bactDNA levels about 2–2.5 log copies/μl, indicating that, when PMN counts were not elevated, the bactDNA quantitation improved bacterial detection with low loads. In addition, we further observed that PMN count of 250/mm^3 was probably higher with Gram-positive bacterial infections than with gram-negative bacterial infections. In the future, we will further study the relationship between PMN and the amounts of bacteria combined the bacteria species, thus further improving SBP's diagnostic efficiency.

Some potential limitations of this study should be acknowledged. First, the presence of a small number of false-positive signals in the end data was found using the ddPCR method. Second, the bactDNA was not able to discriminate between bacterial ascites and ascites without infection in our study. The possible reasons are as follows:1) there were only 18 samples in patients with bacterascites, which may cause a statistical difference; 2) due to low positive culture rate of bacteria, there could also be low-load bacteria in non-infectious ascites that had not been detected by conventional method; and 3) because of the limitations of the laboratory environment, there was no significant difference in bactDNA load between the bacterascites and ascites without infection.

In addition, because of the detection time of 4 h and the cost of $5.20 per sample, the ddPCR method has an optimal applicational prospect in future clinical practice. Further prospective studies should be conducted to bactDNA levels on the guidance of clinical medication and its prognostic effect in patients with SBP to truly improve the SBP's diagnostic value. Bacterascites may represent transient and spontaneously reversible colonization of ascites, or they may represent the first step in the development of SBP (European Association for the Study of the Liver., 2018). The bactDNA load in ascitic fluid by ddPCR may help identify the above two scenarios.

In conclusion, our study shows that the ascitic bactDNA quantitation by ddPCR is a promising approach that can be used to improve the SBP's diagnostic accuracy, especially for patients who are symptomatic and have a PMN < 250 cells/mm^3.

Data availability statement

The original contributions presented in the study are included in the article/Supplementary Material. Further inquiries can be directed to the corresponding authors.

Author contributions

HW, WH, and FW conceived the study. FW and ZH contributed to the study design. HW supervised all aspects of the study. WZ, ZW, and ZL were responsible for clinical data collection and verification. DC and SG were responsible for results collection and monitoring in the laboratory. HW and WH wrote the first draft of the manuscript. All authors critically reviewed the manuscript and contributed to writing-editing and approved the final version.

Funding

This work was supported by the Beijing Institute of Hepatology Foundation (grant number Y-2021YS-1), the Clinical Research Special Fund of Wu Jieping Medical Foundation of China (grant number 320.6750.2022-08-1), and the Capital Health Research and Development of Special (grant number 2022-2-2183).

Acknowledgments

The authors would like to thank Hui-Guo Ding and Pei-Zhi Li for their valuable input.

Conflict of interest

The authors declare that the research was conducted in the absence of any commercial or financial relationships that could be construed as a potential conflict of interest.

Publisher's note

All claims expressed in this article are solely those of the authors and do not necessarily represent those of

their affiliated organizations, or those of the publisher, the editors and the reviewers. Any product that may be evaluated in this article, or claim that may be made by its manufacturer, is not guaranteed or endorsed by the publisher.

Supplementary material

The Supplementary Material for this article can be found online at: https://www.frontiersin.org/articles/10.3389/fcimb.2022.876495/full#supplementary-material

References

Aithal, G. P., Palaniyaooan, N., and China, L. (2021). Guidelines on the management of ascites in cirrhosis. *Gut.* 70 (1), 9–29. doi: 10.1136/gutjnl-2020-321790

Akalin, H. E., Laleli, Y., and Telatar, H. (1983). Bactericidal and opsonic activity of ascitic fluid from cirrhotic and noncirrhotic patients. *J. Of Infect. Diseases.* 147 (6), 1011–1017. doi: 10.1093/infdis

Alvarez-silva, C., Schierwagen, R., Pohlmann, A., Magdaleno, F, Uschner, FE, Ryan, P, et al. (2019). Compartmentalization of immune response and microbial translocation in decompensated cirrhosis. *Front. Immunol.* 10. doi: 10.3389/fimmu.2019.00069

Amar, Y., Lagkouvardos, I., Silva, R. L., Ishola, OA, Foesel, BU, Kublik, S, et al. (2021). Pre-digest of unprotected DNA by benzonase improves the representation of living skin bacteria and efficiently depletes host DNA. *Microbiome* 9 (1), 123. doi: 10.1186/s40168-021-01067-0

Bernardi, M., Angeli, P., Claria, J., Moreau, R, Gines, P, Jalan, R, et al. (2020). Albumin in decompensated cirrhosis: new concepts and perspectives. *Gut* 69 (6), 1127–1138. doi: 10.1136/gutjnl-2019-318843

Biggins, S. W., Angeli, P., and Garcia-Tsao, G. (2021). Diagnosis, evaluation, and management of ascites, spontaneous bacterial peritonitis and hepatorenal syndrome: 2021 practice guidance by the American association for the study of liver diseases. *Hepatology* 74 (2), 1014–1048. doi: 10.1002/hep.31884

Bruns, T., Reuken, P. A., Stengel, S., Gerber, L, Appenrodt, B, Schade, JH, et al. (2016). The prognostic significance of bacterial DNA in patients with decompensated cirrhosis and suspected infection. *Liver Int.* 36 (8), 1133–1142. doi: 10.1111/liv.13095

Campillo, B., Richardet, J. P., and Kheo, T. (2002). Nosocomial spontaneous bacterial peritonitis and bacteremia in cirrhotic patients: Impact of isolate type on prognosis and characteristics of infection. *Clin. Infect. Dis.* 35 (1), 1–10. doi: 10.1086/340617

Chinese Society of Hepatology, Chinese Medical Association (2017). Chinese Guidelines on the management of ascites and its related complications in cirrhosis. *J. Clin. Hepatol.* 33 (10), 1847–1863. doi: 10.3969/j.issn.1001-5256.2017.10.003

Cho, S. M., Shin, S., Kim, Y., Song, W, Hong, SG, Jeong, SH, et al. (2020). A novel approach for tuberculosis diagnosis using exosomal DNA and droplet digital PCR. *Clin. Microbiol. Infect.* 26 (7), 942.e1–942.e5. doi: 10.1016/j.cmi.2019.11.012

Enomoto, H., Inoue, S. I., Matsuhisa, A., Iwata, Y, Aizawa, N, Sakai, Y, et al. (2018). Amplification of bacterial genomic DNA from all ascitic fluids with a highly sensitive polymerase chain reaction. *Mol. Med. Rep.* 18 (2), 2117–2123. doi: 10.3892/mmr.2018.9159

European Association for the Study of the Liver. (2018). EASL clinical practice guidelines for the management of patients with decompensated cirrhosis. *J. Hepatol.* 69 (2), 406–460. doi: 10.1016/j.jhep.2018.03.024

Fernández, J., Prado, V., Trebicka, J., Amoros, A, Gustot, T, Wiest, R, et al. (2019). Multidrug-resistant bacterial infections in patients with decompensated cirrhosis and with acute-on-chronic liver failure in Europe. *J. Hepatol.* 70 (3), 398–411. doi: 10.1016/j.jhep.2018.10.027

Guarner, C., Gonzalez-Navajas, J. M., Sanchez, E., Soriando, G, Francés, R, Chiva, M, et al. (2006). The detection of bacterial DNA in blood of rats with CCl (4)-induced cirrhosis with ascites represents episodes of bacterial translocation. *Hepatology* 44 (3), 633–639. doi: 10.1002/hep.21286

Gu, W., Deng, X., Lee, M., Sucu, YD, Arevalo, S, Stryke, D, et al. (2021). Rapid pathogen detection by metagenomic next-generation sequencing of infected body fluids. *Nat. Med.* 27 (1), 115–124. doi: 10.1038/s41591-020-1105-z

Hirooka, M., Koizumi, Y., Imai, Y., Yukimoto, A, Watanabe, T, Yoshida, O, et al. (2018). Validation trial for efficacy of ultrasonographic measurement method to predict ascitic volume using virtual ultrasonography. *J. Med. Ultrasonics* 45 (4), 555–564. doi: 10.1007/s10396-018-0879-9

Hussain, M., Fantuzzo, R., Mercorelli, S., and Cullen, C. (2016). A direct droplet digital PCR method for quantification of residual DNA in protein drugs produced in yeast cells. *J. Pharm. BioMed. Anal.* 123, 128–131. doi: 10.1016/j.jpba.2016.01.050

Li, B. L., Gao, Y. H., Wang, X. B., Meng, Z, and Huang, Y. (2020). Clinical features and outcomes of bacterascites in cirrhotic patients: A retrospective, multicentre study. *Liver Int.* 40 (6), 1447–1456. doi: 10.1111/liv.14418

Oey, R. C., van Buuren, H. R., and de Jong, D. M. (2018). Bacterascites: A study of clinical features, microbiological findings, and clinical significance. *Liver Int.* 38 (12), 2199–2209. doi: 10.1111/liv.13929

Piano, S., Singh, V., Caraceni, P. , Maiwall, R, Alessandria, C, Fernandez, J, et al. (2019). Epidemiology and effects of bacterial infections in patients with cirrhosis worldwide. *Gastroenterology* 156 (5), 1368–1380. doi: 10.1053/j.gastro.2018.12.005

Rimola, A., García-Tsao, G., Navasa, M., Piddock, LJ, Planas, R, Bernard, B, et al. (2000). Diagnosis, treatment and prophylaxis of spontaneous bacterial peritonitis: a consensus document. international ascites club. *J. Hepatol.* 32 (1), 142–153. doi: 10.1016/s0168-8278(00)80201-9

Song, Y. Y., and Jiang, Y. Y. (2016). Research advances in diagnosis and treatment of spontaneous bacterial peritonitis. *J. Clin. Hepatol.* 32 (6), 1188–1191. doi: 103969/j.issn.1001-5256.2016.06.040

Wouters, Y., Dalloyaux, D., Christenhusz, A., Roelofs, HMJ, Wertheim, HF, Bleeker-Rovers, CP, et al. (2020). Droplet digital polymerase chain reaction for rapid broad-spectrum detection of bloodstream infections. *Microb. Biotechnol.* 13 (3), 657–668. doi: 10.1111/1751-7915.13491

Zapater, P., Francés, R., González-Navajas, J. M., de la Hoz, MA, Moreu, R, Pascual, S, et al. (2008). Serum and ascitic fluid bacterial DNA: A new independent prognostic factor in noninfected patients with cirrhosis. *Hepatology* 48 (6), 1924–1931. doi: 10.1002/hep.22564

frontiers | Frontiers in Cellular and Infection Microbiology

TYPE Original Research
PUBLISHED 08 December 2022
DOI 10.3389/fcimb.2022.865637

OPEN ACCESS

EDITED BY
Elena Jordana-Lluch,
Balearic Islands Health Research Institute (IdISBa), Spain

REVIEWED BY
Xiaoming Shu,
China-Japan Friendship Hospital, China
Joseph Paul Myers,
Northeast Ohio Medical University, United States

*CORRESPONDENCE
Yan Du
duyan2014@zju.edu.cn
Jing Xue
jingxue@zju.edu.cn

†These authors have contributed equally to this work and share first authorship

SPECIALTY SECTION
This article was submitted to Clinical Microbiology, a section of the journal Frontiers in Cellular and Infection Microbiology

RECEIVED 30 January 2022
ACCEPTED 16 November 2022
PUBLISHED 08 December 2022

CITATION
Wang H, Shi X, Yang H, Du Y and Xue J (2022) Metagenomic next-generation sequencing shotgun for the diagnosis of infection in connective tissue diseases: A retrospective study.
Front. Cell. Infect. Microbiol. 12:865637.
doi: 10.3389/fcimb.2022.865637

Metagenomic next-generation sequencing shotgun for the diagnosis of infection in connective tissue diseases: A retrospective study

Huyan Wang[1†], Xiaowei Shi[1,2†], Huanhuan Yang[1,3], Yan Du[1*] and Jing Xue[1*]

[1]Department of Rheumatology, the Second Affiliated Hospital of Zhejiang University School of Medicine, Hangzhou, China, [2]Department of Rheumatology and Immunology, Jinhua Hospital of Zhejiang University, Jinhua, China, [3]Department of Nephrology, Affiliated Hangzhou Xixi Hospital of Zhejiang University School of Medicine, Hangzhou, China

Objective: Patients with connective tissue diseases (CTDs) are at high risk of infection due to various reasons. The purpose of the study was to investigate the infection diagnosis value of metagenomic next-generation sequencing (mNGS) shotgun in CTDs to guide the use of anti-infective therapy more quickly and accurately.

Methods: In this retrospective study, a total of 103 patients with CTDs admitted with suspected infection between December 2018 and September 2021 were assessed using mNGS as well as conventional microbiological tests (CMT).

Results: Among these 103 patients, 65 were confirmed to have an infection (Group I) and 38 had no infection (Group II). mNGS reached a sensitivity of 92.31% in diagnosing pathogens in Group I. Moreover, mNGS showed good performance in identifying mixed infection. In all infection types, lung infection was the most common. mNGS also played an important role in detecting *Pneumocystis jirovecii*, which was associated with low CD4+ T-cell counts inextricably.

Conclusion: mNGS is a useful tool with outstanding diagnostic potential in identifying pathogens in patients with CTDs and conduce to provide guidance in clinical practice.

KEYWORDS

metagenomic next-generation sequencing, infection, connective tissue diseases, immunosuppression, diagnosis

Introduction

Connective tissue diseases (CTDs) have significant morbidity and mortality, due in part to concurrent infections (Falagas et al., 2007). The reasons why patients with CTDs show a peculiar vulnerability to infection are diverse: the changes in the intrinsic immune environment, the use of immunosuppressive drugs, and the severity of the disease and complications (Di Franco et al., 2017). One of the major immunological alterations is represented by impairment of the complement system, which is strongly associated to the development of systemic lupus erythematosus (SLE) and to an increased susceptibility to infection (Skattum et al., 2011). Since most patients with CTDs have autoimmune dysfunction, long-term immunosuppressive treatments are inevitable, such as glucocorticoid, conventional disease-modifying anti-rheumatic drugs, and biologics. Although therapeutic agents have improved the symptoms of patients substantially, they are also responsible for a wide spectrum of infections, especially when used in combination (Chiu and Chen, 2020). Infection can also be related to the organ damage due to rheumatic diseases. Some CTDs are more likely to be complicated with interstitial lung disease (ILD), such as systemic sclerosis and dermatomyositis (Kawano-Dourado and Lee, 2021). Thus, underlying lung lesions secondary to CTDs may increase the incidence of respiratory tract infections (Ricci et al., 2021).

It is necessary to identify the correct pathogens quickly, because inaccurate coverage and untimely treatment can give rise to side effects or fail to achieve the desired results. With respect to the diagnosis of bacterial or fungal infections, there are various diagnostic methods. Direct examination and culture are currently the most common procedures. Smear is convenient but the positive rate remained at a relatively low level. As culture is time-consuming, it may delay the optimal treatment time. Furthermore, not all kinds of pathogens are suitable to be cultured and pathogens infecting the immunocompromised host can also be difficult to grow. Moreover, empiric broad-spectrum antimicrobial therapy may contribute to the occurrence of false-negative culture results (Farrell et al., 2013). Viruses are usually tested by nucleic acid-based tests, serologic tests, and immunological tests, which lack specificity to some extent (Vemula et al., 2016). Therefore, there is an urgent need to address the problems of quick and accurate diagnosis.

Recently, it is becoming extremely difficult to ignore the existence of metagenomic next-generation sequencing (mNGS). As a novel technique that has high-throughput capabilities, is unbiased, is accurate, and has a rapid turnaround time, mNGS has proven invaluable for detecting pathogens in clinical samples (Chen et al., 2020). These advantages allow the mNGS test to specify multiple pathogens simultaneously and detect the exit of microbial even with low abundance. mNGS also makes it possible to identify difficult-to-culture microorganisms. Although some studies on the application of mNGS in infectious diseases have been carried out, no previous study has investigated its application in patients with CTDs suspected of infection. The purpose of this study is to evaluate the ability of mNGS to detect pathogens and analyze the characteristics of the distribution of pathogens in CTDs associated with infection.

Methods

Study design

In this retrospective study, we consecutively enrolled 103 patients with CTDs undergoing the mNGS test because of suspected infection who were admitted at the Department of Rheumatology, the Second Affiliated Hospital of Zhejiang University School of Medicine, China, from December 2018 to September 2021. Suspected infection was defined as patients who presented with symptoms, such as fever, cough, weakness, or radiographic involvement. Samples were obtained from sites of suspected infection as clinically indicated, including blood, sputum, joint fluid, bronchoalveolar lavage fluid (BALF), and tissue. Other conventional microbiological tests (CMT) were carried out according to the condition of each subject as clinically indicated, including Gram stain, acid-fast bacilli smear, bacterial culture, fungal smear and culture, T-SPOT.TB test, Epstein–Barr virus and Cytomegalovirus IgM and IgG antibody test, Epstein–Barr virus and Cytomegalovirus nucleic acid detection, (1,3)-β-D-glucan assays (G test), galactomannan assays (GM test), Widal agglutination test, *Cryptococcus neoformans* capsular polysaccharide antigen detection, *Aspergillus* IgG antibody detection, and respiratory microorganism IgM antibody test (*Mycoplasma pneumoniae*, *Chlamydia pneumoniae*, *Legionella pneumophila*, respiratory syncytial virus, influenza virus A, influenza virus B, parainfluenza virus, and adenovirus).

A retrospective-review protocol was approved by the Ethics Committee of the Second Affiliated Hospital of Zhejiang University School of Medicine in China [No. 2021 (1099)]. The ethics committee approved the waiver of informed consent due to the retrospective nature of the study. All research data were anonymously analyzed.

Case definition

Two independent clinicians analyzed an anonymized data file for each patient. Data were collected for each patient including demographic data, types of CTDs, laboratory examinations, glucocorticoid and immunosuppressive treatments, and results of all microbiological tests.

In view of all available documentation, it was determined whether each patient was confirmed to have an infection (Group

I) or an infectious etiology could be excluded (Group II). First, they determined the likelihood of an infectious origin implied by clinical symptoms. Then, they identified pathogens that were potentially responsible for the episode of infection, based on mNGS and other microbiological tests. For non-commonly reported pathogens, unless mNGS results were in accordance with the patient's clinical features, the detected reads were classified as non-pathogenic microbe sequences. Last, an infection-related diagnosis was established.

Sample processing

Low-speed centrifugation (1,500 *g* for 20 min) was performed to remove human cells in the samples including BALF, blood, and cerebrospinal fluid (CSF). For the blood, only the plasma was collected for further testing.

Samples were then homogenized using bead beating followed by DNA or RNA extraction using the IngeniGen DNA or RNA Extraction Kit (IngeniGen XMK Biotechnologies, Inc., Zhejiang, China). Briefly, a 300-µl sample was added to the lysate buffer and mixed thoroughly. The lysates were subsequently incubated for 30 min at 50°C. Then, magnetic beads were added to the mixture and placed stably for 10 min. The magnetic beads were washed with washing buffer 1 and washing buffer 2, respectively. Last, 60 µl of elution buffer, which had been preheated at 65°C to elute the nucleic acids off the beads, was added.

The DNA or RNA libraries were prepared using the IngeniGen DNA or RNA Library Prep Kit according to standard procedures. Briefly, the DNA was fragmented, and the Illumina-compatible adaptors were added to the fragmented DNA simultaneously by a tagment enzyme. The library was purified by magnetic beads and then amplified by 15 PCR cycles. DNase was used to remove residual human DNA and the RNA was fragmented, followed by double-strand cDNA synthesis, end repair, dA tailing, and adapter ligation.

Sequencing was performed on the Illumina MiniSeq (Illumina, San Diego, CA) using 2 × 75 bp chemistry. Sterile nuclease-free water as a negative control was included in each run to detect the background contaminants, involved in the process of nucleic acid extraction, library preparation, and sequencing. A kind of unique marine bacterium (100 CFU/ml) as an internal control was also added to each sample to monitor the whole process. Data analysis was performed using IngeniSeq MG, a proprietary automated shotgun metagenomics analysis platform for pathogen detection. Briefly, all raw reads were quality-filtered using an in-house made program, including filtering adapter contamination and low-quality and low-complexity reads. Next, the human host sequence mapped to the human reference genome (hg19) and other contaminant sequences that were known to be derived from the reagents were removed by using Burrows–Wheeler alignment, and the filtered sequences were de-duplicated and then matched against a curated database consisting of 20,343 microbial reference genomes, including 7,044 bacteria, 2,890 fungi, 9,233 virus, 172 parasites, 139 mycoplasma, and 128 chlamydia. All microbial reference genomes are downloaded from public databases, such as NCBI. The resulting hits were again filtered by a proprietary algorithm that further removed background contaminants that may appear during sampling processing and library preparation. The quality control matrix is briefly presented here: (1) a true-positive result is admitted only when the negative control has corresponding reads <10% compared with the sample; (2) the internal control should have reads >50 for the results to be valid in each sample.

Data analysis

The Mann–Whitney *U* rank sum nonparametric test was utilized to compare the laboratory examination data of two groups. The Chi-square test was applied to assess the pathogen-specific diagnostic performance of mNGS, and kappa statistics were used to evaluate agreements between mNGS and CMT. *p*-values < 0.05 were considered statistically significant. Statistical analysis was performed using the SPSS statistical package 25.0 software. Figure drawings were accomplished by GraphPad Prism 8.0 software.

Results

General characteristics

In the present study, a total of 103 patients were enrolled. The baseline characteristics of the patients are listed in Table 1. Factors include gender, age, maximum body temperature before treatment, course of primary disease, and types of CTDs. Among the 103 patients, 65 were diagnosed with infection by clinical and microbiological evidence (Group I) and 38 were finally confirmed without infection (Group II). The laboratory examinations of the two groups are shown in Table 2, including white blood cell (WBC), neutrophil (N), lymphocyte (Ly), C-reactive protein (CRP), erythrocyte sedimentation rate (ESR), procalcitonin (PCT), ferritin, proportion and absolute CD4+ T-cell counts, and CD4+/CD8+ T-cell count ratio. Patients in Group I showed lymphopenia with a median lymphocyte count of 0.78×10^9/L in peripheral blood and had significantly lower total T-cell proportion ($p = 0.048$), CD4+ T-cell counts ($p < 0.001$), and proportion ($p = 0.007$) compared with Group II, while PCT ($p = 0.017$) and ferritin ($p < 0.001$) were significantly increased compared to Group II.

TABLE 1 Demographics of the enrolled patients with suspected infection.

Characteristics	Group I (*n* = 65)	Group II (*n* = 38)	Overall (*n* = 103)
Gender, female	40 (61.5)	33 (86.8)	73 (68.9)
Age, years	58 (48–66)	55 (42–64.5)	57 (46–66)
Body temperature, °C	38.4 (37.4–39.3)	38.0 (37.2–39.2)	38.4 (37.4–39.2)
Primary disease course, months	12 (5–60)	24 (3.75–120)	18 (5–72)
CTDs			
Dermatomyositis/polymyositis	23	10	33
Rheumatoid arthritis	13	8	21
Systemic lupus erythematosus	11	7	18
Systemic vasculitis	5	5	10
Sjogren's syndrome	3	3	6
Systemic sclerosis	4	0	5
IgG4-related disease	2	1	3
Adult-onset Still's disease	2	1	3
Undifferentiated connective tissue disease	1	1	2
Sarcoidosis	0	1	1
Antiphospholipid antibody syndrome	1	0	1

Continuous variables are presented as median and interquartile range; binary variables are presented as number and percentage. Group I: patients were confirmed with infection. Group II: patients were confirmed without infection. CTDs, connective tissue diseases.

Distribution of clinically relevant pathogens

Sample sources of mNGS from all of the enrolled patients are shown in Table 3, including BALF, blood, and CSF. Among the 65 patients in Group I, distribution of infection sites is shown as follows. The most common site was lung (*n* = 54, 83.08%), followed by blood (*n* = 3, 4.62%), and skin and soft tissue (*n* = 3, 4.62%). Two patients with abdominal infection were diagnosed as subphrenic abscess and bacterial peritonitis. Two patients with brain infection were diagnosed as suppurative meningitis and viral encephalitis. One patient was diagnosed with infectious arthritis. Combined with CMT and mNGS, pathogens can be cleared in 61 patients but remain unknown in 4 patients. According to the results of pathogen distribution, bacteria (*n* = 27, 44.26%) was the most common pathogen identified, followed by fungi (*n* = 14, 22.95%) and virus (*n* = 6, 9.84%). Among the 27 patients infected by bacteria only, Gram-negative bacteria (*n* = 13, 20.00%) was the most frequent type, followed by Gram-positive bacteria (*n* = 8, 12.31%), and then *Mycobacteria* (*n* = 6, 9.23%). As for fungi, it should be noted that *Pneumocystis jirovecii* infected half of the patients. For those identified with *Mycobacteria*, three cases had *Mycobacterium tuberculosis* and there was one case each of *Mycobacterium avium*, *Mycobacterium chelonae*, and

TABLE 2 Laboratory examinations of infection and non-infection patients.

Laboratory examination	Group I (*n* = 65)	Group II (*n* = 38)	*p*-value
WBC, $\times10^9$/L	7.80 (5.05–10.60)	6.91 (4.55–11.75)	0.932
N, $\times10^9$/L	6.74 (3.48–9.19)	4.64 (3.28–9.06)	0.573
Ly, $\times10^9$/L	0.78 (0.48–1.22)	1.35 (0.89–1.83)	**<0.001**
CRP, mg/L	29.70 (11.20–79.90)	18.80 (7.68–51.40)	0.215
ESR, mm/h	48.00 (17.75–72.25)	63.00 (30.00–90.00)	0.072
PCT, ng/ml	0.25 (0.11–0.58)	0.12 (0.05–0.32)	**0.017**
Ferritin, μg/L	651.40 (293.70–1500.00)	183.20 (121.60–446.25)	**<0.001**
Total T-cell proportion, %	68.80 (55.10–79.36)	76.50 (66.23–81.78)	**0.048**
CD4+ T-cell counts,/mm^3	201.16 (131.37–425.13)	492.11 (269.40–798.18)	**<0.001**
CD4+ T-cell proportion, %	33.10 (20.90–42.40)	42.50 (27.55–50.83)	**0.007**
CD8+ T-cell proportion, %	27.60 (22.35–43.75)	29.35 (20.3–37.43)	0.538
CD4+/CD8+ T-cell count ratio	1.16 (0.59–1.77)	1.32 (0.92–2.26)	0.089
Total B-cell proportion, %	11.10 (5.00–20.05)	12.70 (7.91–20.23)	0.486

Data are presented as median and interquartile. Group I: patients were confirmed with infection. Group II: patients were confirmed without infection. WBC, white blood cell; N, neutrophil; Ly, lymphocyte; CRP, C-reaction protein; ESR, erythrocyte sedimentation rate; PCT, procalcitonin. Bold text indicates a statistically significant difference.

TABLE 3 Different sample sources from all of the enrolled patients.

Sample source	Overall (n = 103)
Bronchoalveolar lavage fluid	58
Blood	16
Lung and pleural biopsy	7
Joint fluid	5
Cerebrospinal fluid	4
Pleural effusion	4
Bone marrow	3
Skin and soft tissue	3
Pericardial fluid	1
Sputum	1
Ascites	1

Mycobacterium intracellulare. Mixed infection was not rare and was found in 14 patients, 6 of whom were detected by mNGS only, 1 of whom by culture, and 7 of whom by both mNGS and conventional microbiological tests.

Performance of mNGS

The results of mNGS for the identification of clinically relevant pathogens are presented in Figure 1. The top four pathogens were *P. jirovecii* (n = 12), Cytomegalovirus (n = 7), *Acinetobacter baumannii* (n = 6), and *Pseudomonas aeruginosa* (n = 6). In seven subjects detected with Cytomegalovirus by mNGS, five were tested positive by PCR. Also worth noting was that Epstein–Barr virus was frequent; five subjects were positive for which by mNGS, and PCR confirmed the same results among four of them. Figure 1 also revealed the relationship between the site of sample collection and its legitimate pathogen detected correspondingly. Herein, diagnostic sensitivity and specificity of mNGS were calculated using the clinical composite diagnosis as reference standard. As shown in Table 4A, mNGS showed a good sensitivity of 92.31%. The specificity of mNGS was 71.05%. NPV and PPV were 84.38% and 84.51%, respectively. The results of mNGS and the causative pathogens in the final diagnosis were concordant for 56 of the 65 patients for the analyses performed on samples in Group I, with a coincidence rate of 86.15%. The comparison of the diagnostic results of mNGS with the method of culture and CMT for 103 patients is shown in Table 4B. mNGS had an agreement rate of 42.7% with culture (κ = 0.102) and 54.4% with CMT (κ = 0.212). Additionally, mNGS increased the positive rate of diagnosis compared with CMT (p = 0.003). For nine subjects with discordance results in Table 5, mNGS reported five false-negative cases, three of whom were detected pathogens by other microbiological tests but the rest could not be identified by the pathogen yet. Among the remaining four subjects, mNGS results were different from other microbiological tests and were not considered as causative pathogens combined with clinical manifestations.

For the 38 cases with no evidence of infection in Group II, mNGS detected pathogens in specimens from 11 patients, as shown in Supplementary Table 1. The microbes identified in the 11 cases by mNGS were present at relatively low abundance or considered as colonizing bacteria.

Lymphocyte subsets and their association with mNGS results

The absolute value of CD4+ T lymphocyte counts indicates the strength of immune function. CD4+ T-cell counts > 500/μl are generally considered as normal immune function. A cutoff of 200 CD4+ T cells/μl is defined as the key threshold to predict immune deficiency as usual (Freiwald et al., 2020). We investigated the pathogen type and frequency identified by mNGS with different degrees of CD4+ T-cell counts as in a

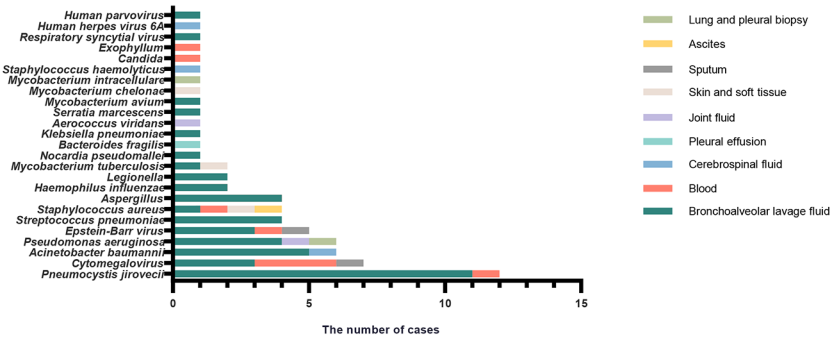

FIGURE 1
The correspondence between the sites of sample collection and frequency of different infection pathogens identified by mNGS in patients with confirmed infection (Group I).

TABLE 4A mNGS value for evaluating infection in CTDs patients.

Group	mNGS-positive	mNGS-negative
Confirmed infection	60	5
Excluded infection	11	27

mNGS, metagenomic next-generation sequencing. CTDs, connective tissue diseases. Sensitivity: 92.31%, specificity: 71.05%, positive predictive value (PPV): 84.38%, negative predictive value (NPV): 84.51%.

TABLE 4B Diagnostic performance of mNGS compared with that of conventional methods.

Group	mNGS-positive	mNGS-negative	Agreement	*p*-value	Kappa
Culture-positive	13	1	42.7%	0.077	0.102
Culture-negative	58	31			
CMT-positive	27	3	54.4%	0.003	0.212
CMT-negative	44	29			

mNGS, metagenomic next-generation sequencing. CMT, conventional microbiologic tests, including testing mentioned in the study design section.

prior study (Bordoni et al., 2019). Analysis of the subgroups based on the CD4+ T-cell counts is shown in Figure 2. In the CD4+ T cells<200/μl subgroup, *P. jirovecii* (n = 7) was the most detected pathogen, followed by Cytomegalovirus (n = 6).

Discussion

Almost all patients with CTDs inevitably use immunosuppressive drugs to control the disease activity, which greatly increases the risk of infection (Wolfe and Peacock, 2017). Precise and timely microbial diagnosis of infection is essential for the clinical care of those immunocompromised patients. Some previous studies have reported about the mNGS diagnostic performance of infection in immunocompromised patients (Parize et al., 2017; Jiang et al., 2021). To our knowledge, this is the first study to evaluate the potential clinical relevance of mNGS involving different sites of specimen for the investigation of infection in a cohort of CTDs.

In our study, mNGS has a high sensitivity in identifying microorganisms and detecting a wide range of pathogens commonly and infrequently. This demonstrated that our study was capable of reflecting a variety of types of infectious diseases in adults admitted with suspected infection in a rheumatology unit. In the confirmed infection group (Group I), there were 19 patients suffering from dermatomyositis (DM)/polymyositis (PM), which ranked first in the enrolled CTDs. Six patients had anti-synthase antibody syndrome and five patients had anti-MDA5 positive dermatomyositis. A study confirmed the high mortality rate in Chinese DM/PM patients, with infection as the leading cause of death (Yang et al., 2020). Therefore, it is recommended to perform mNGS detection if we highly suspect infection in DM/PM patients.

It is noteworthy that for samples from 14 patients diagnosed with mixed infections, mNGS was able to detect pathogens in 13 of them. The diagnostic accuracy of mNGS was 92.86%. Wang et al. in their study found that the sensitivity of diagnosing mixed pulmonary infection by conventional diagnostic testing was 13.9%, which suggests that mixed infection is hard to detect (Wang et al., 2019). We suggest the timely use of mNGS when mixed infection or rare pathogens are suspected.

Lung infection was the most common in our study (54/65), identified by different samples. Forty-two were from BALF, seven from blood, two from lung and pleural biopsy, two from pleural effusion, and one from sputum. Clinicians tend to send BALF for examination, because it is generally accepted that BALF is the most direct sample to confirm whether patients suffer from lung infection (Zhang et al., 2014). In CTD-ILD, BAL has major clinical utility in excluding infections and in the diagnosis of specific patterns of lung damage. A retrospective study reviewing patients with DM-ILD undergoing bronchoscopy demonstrated that BAL can increase the diagnosis of infection in DM-ILD, and 22.1% patients commenced or changed antibiotic therapy on the basis of bronchoscopy results (He et al., 2021). Richter et al. found that pathogens were commonly grown from BALF of patients with granulomatosis polyangiitis (GPA) compared to those with idiopathic pulmonary fibrosis, and *Staphylococcus aureus* was particularly associated with patients with GPA (Richter et al., 2009). Bronchoscopy is a safe procedure in the general population, but as an invasive operation, there is no guarantee that it can be completely free from complications; serious adverse events could sometimes be observed in critically ill patients (Tomassetti et al., 2021). Thus, when patients in critical condition cannot tolerate bronchoscopy, it is more convenient to use blood samples. If it is possible, it will make great sense to design a prospective study to collect BALF and blood samples simultaneously to compare the accuracy of mNGS in identifying microorganisms in the future.

Our study clearly demonstrated that mNGS showed great potential to identify *P. jirovecii*. Similarly, Jiang et al. also reported that mNGS reached a sensitivity of 100% in

TABLE 5 Discordance results of different microbial detection tests in Group I.

Patient ID	Rheumatic disease	Infection clinical diagnosis	Sample	NGS result [reads]	Culture results	Other microbiological diagnostic testing results
29	Dermatomyositis	Pulmonary infection	BALF	*Haemophilus influenzae* [7513], *Moraxella catarrhalis* [169]	*Pseudomonas aeruginosa*	Sputum culture: *Aspergillus fumigatus*, G test (+), GM test (+)
30	Polymyositis	Pulmonary infection	BALF	Cytomegalovirus [92], Epstein–Barr virus [3]	*Staphylococcus aureus*	Negative
31	Polymyositis	Pulmonary infection	BALF	Negative	*Candida albicans*	Negative
32	Dermatomyositis	Pulmonary infection	BALF	Negative	Negative	Respiratory pathogen series antibodies: *Legionella pneumophila* IgM (+)
34	Systemic vasculitis	Pulmonary infection	Plasma	Negative	Negative	TSPOT (+)
48	Adult-onset Still's disease	Pulmonary infection	Plasma	*Enterococcus casseliflavus* [46]	Negative	G test (+)
60	Undifferentiated connective tissue disease	Pulmonary infection	BALF	Negative	Negative	Sputum culture: *Burkholderia cepacia*
61	Sjögren's syndrome	Pulmonary infection	Plasma	Negative	Negative	Sputum culture: *Candida albicans*, G test (+)
62	Overlap syndrome	Pulmonary infection	BALF	*Prevotella melaninogenica* [202397], *Veillonella parvula* [25988], *Rothia mucilaginosa* [25152], Epstein–Barr virus [48], Human betaherpesvirus 7 [9], Human betaherpesvirus *6B* [4]	Negative	G test (+)

BALF, bronchoalveolar lavage fluid.

diagnosing *P. jirovecii* pneumonia (PJP), which was remarkably higher than Gomori methenamine silver staining in non-HIV-infected patients (Jiang et al., 2021). In our study, mNGS figured out 12 cases with *P. jirovecii* infection, of which four subjects tested positive and eight subjects tested negative by G test. The diagnosis of PJP was based on the results of mNGS, combined with imaging manifestations in pulmonary and clinical symptoms such as decreasing oxygenation and dyspnea. Furthermore, subgroup analysis of CD4+ T-cell counts indicated that patients with low lymphocytes were vulnerable to *P. jirovecii* infection. Low CD4+ T-cell counts, attributable to glucocorticoid and immunosuppressant exposure to a certain extent, are identified as a significant risk factor for higher infection rate (Guillen et al., 2019). PJP is an opportunistic infection with high mortality among patients with underlying CTD conditions (Tadros et al., 2017). However, *P. jirovecii* cannot be cultured, and the sensitivity of conventional staining is low (Procop et al., 2004). Hence, the appearance of mNGS is utterly meaningful to detect *P. jirovecii*, especially on the condition of low CD4+ T-cell counts.

We can see that the rate of false-positive results had been high in patients who were confirmed without infection. Contamination is a probable factor, because of the various sample types, and the lack of a standard sample collecting method and site could affect the mNGS results. In addition, we can find that some of the microorganisms are the normal flora of the human oral cavity and upper respiratory tract, which are considered to be human symbiotic bacteria or colonizing bacteria, such as *Prevotella melaninogenica* and *Rothia mucilaginosa*. It is difficult to distinguish colonized pathogens from infection because there are no widely accepted quantitative cutoffs or threshold values for mNGS. Therefore, the definite diagnosis must be based on the comprehensive analysis of clinical characteristics, laboratory examinations, radiologic findings, and other microbiologic proofs rather than mNGS alone.

It should be mentioned that a recent Chinese study has attracted our attention (Su et al., 2022) because it was partially similar to our study. What separates them from us is that they only analyzed whole blood while our samples were collected from diverse sites and BALF was predominant. Types of CTDs with the highest incidence of infection were also slightly different; SLE and DM/PM ranked first and second in their results, whereas DM/PM and rheumatoid arthritis were more common in our study. Moreover, in their study, virus was the most common infection type, with Cytomegalovirus and Epstein–Barr virus being the highest, which showed a discrepancy with our findings, since our data showed that fungus such as *P. jirovecii* was observed the most. Distinctively, the pathogens of mixed infection were further

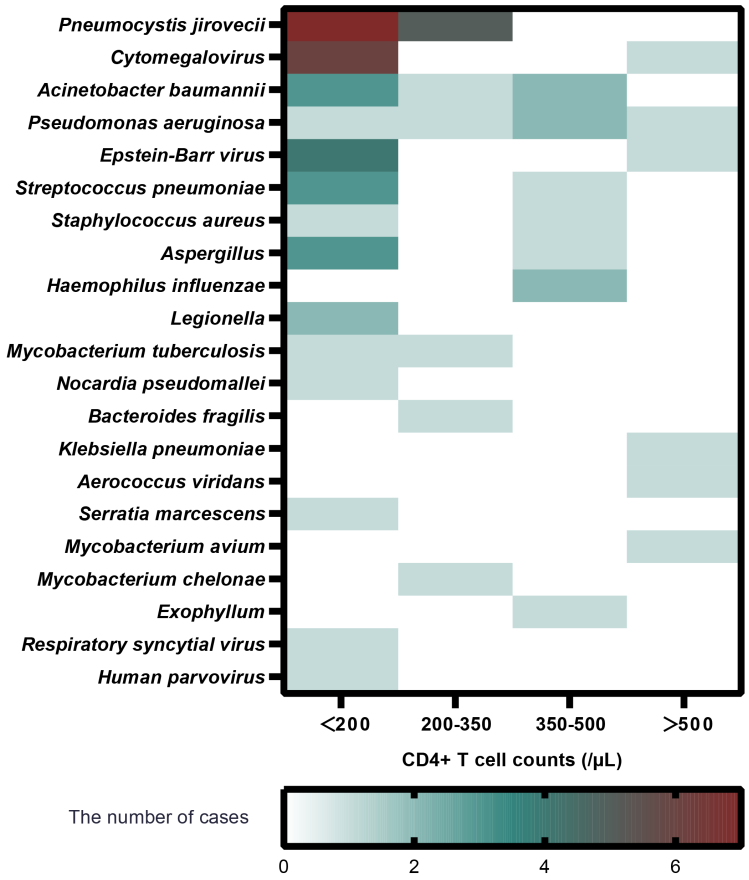

FIGURE 2
The relationship between pathogen type, infection frequency, and absolute value of CD4+ T-cell in patients with confirmed infection (Group I).

classified in their results. Above all, both our results agree that mNGS had a higher detection rate than CMT.

This study had limitations. First, this was a retrospective study in a single center and the sample size was limited, which might have affected the accuracy of the evaluation of mNGS. Second, a negative control population of healthy individuals was not included in this study. Third, due to the complexity of infection, the sources of mNGS samples collected might not correspond to the infection site finally found through other microbial detection methods in a few patients. It may lead to a slight deviation in the results because we excluded these cases in advance during the study. Most importantly, we did not validate the diagnosis of some specific pathogens by quantitative real-time PCR (qPCR), such as *P. jirovecii*, *Mycobacterium tuberculosis*, and *Aspergillus*. qPCR as a molecular diagnostic method is applied widely and is highly sensitive for the analysis of species and abundance of microorganisms. However, because our study is a retrospective analysis, it would not be possible to verify the diagnosis of those samples by qPCR. We are convinced that it is of significance to conduct a comparison of the diagnostic efficiency of mNGS with qPCR in future research. To further evaluate the application of mNGS in the diagnosis of infections, multicenter prospective studies with a larger number of participants are encouraged. In addition, the sample collection method on mNGS performance needs further improvement.

Conclusion

Although there are some limitations, our study indicated that mNGS has opened a new avenue for its clinical application in terms of detection of infectious pathogens for patients with CTDs. It has a high sensitivity in identifying microorganisms, especially *P.* jirovecii, and outperforms other methods in detecting mixed infections.

Data availability statement

The datasets presented in this study can be found in online repositories. The names of the repository/repositories and accession number(s) can be found below: China National Genebank, CNP0003551.

Ethics statement

The studies involving human participants were reviewed and approved by Ethics Committee of the Second Affiliated Hospital of Zhejiang University School of Medicine in China. Written informed consent for participation was not required for this study in accordance with the national legislation and the institutional requirements. Written informed consent was not obtained from the individual(s) for the publication of any potentially identifiable images or data included in this article.

Author contributions

JX and YD contributed to the research design and revision of the manuscript. HW drafted the research protocol, analyzed the results, and drafted the manuscript. XS conducted data analysis and assisted in writing the manuscript. HY and XS contributed to the data acquisition. All authors approved the submitted version and agreed to be responsible for all aspects.

Funding

This work was supported by the National Natural Science Foundation of China (No. 81501388 and 82271817) and the Natural Science Foundation of Zhejiang Province (No. LY20H100007 and LY22H100004).

Conflict of interest

The authors declare that the research was conducted in the absence of any commercial or financial relationships that could be construed as a potential conflict of interest.

Publisher's note

All claims expressed in this article are solely those of the authors and do not necessarily represent those of their affiliated organizations, or those of the publisher, the editors and the reviewers. Any product that may be evaluated in this article, or claim that may be made by its manufacturer, is not guaranteed or endorsed by the publisher.

Supplementary material

The Supplementary Material for this article can be found online at: https://www.frontiersin.org/articles/10.3389/fcimb.2022.865637/full#supplementary-material

References

Bordoni, V., Brando, B., Piselli, P., Forini, O., Perna, F. E., Atripaldi, U., et al. (2019). Naive/Effector CD4 T cell ratio as a useful predictive marker of immune reconstitution in late presenter HIV patients: A multicenter study. *PloS One* 14 (12), e0225415. doi: 10.1371/journal.pone.0225415

Chen, P., Sun, W., and He, Y. (2020). Comparison of the next-generation sequencing (NGS) technology with culture methods in the diagnosis of bacterial and fungal infections. *J. Thorac. Dis.* 12 (9), 4924–4929. doi: 10.21037/jtd-20-930

Chiu, Y. M., and Chen, D. Y. (2020). Infection risk in patients undergoing treatment for inflammatory arthritis: non-biologics versus biologics. *Expert Rev. Clin. Immunol.* 16 (2), 207–228. doi: 10.1080/1744666X.2019.1705785

Di Franco, M., Lucchino, B., Spaziante, M., Iannuccelli, C., Valesini, G., and Iaiani, G. (2017). Lung infections in systemic rheumatic disease: Focus on opportunistic infections. *Int. J. Mol. Sci.* 18 (2), 293. doi: 10.3390/ijms18020293

Falagas, M. E., Manta, K. G., Betsi, G. I., and Pappas, G. (2007). Infection-related morbidity and mortality in patients with connective tissue diseases: a systematic review. *Clin. Rheumatol* 26 (5), 663–670. doi: 10.1007/s10067-006-0441-9

Farrell, J. J., Sampath, R., Ecker, D. J., and Bonomo, R. A. (2013). "Salvage microbiology": detection of bacteria directly from clinical specimens following initiation of antimicrobial treatment. *PloS One* 8 (6), e66349. doi: 10.1371/journal.pone.0066349

Freiwald, T., Buttner, S., Cheru, N. T., Avaniadi, D., Martin, S. S., Stephan, C., et al. (2020). CD4(+) T cell lymphopenia predicts mortality from pneumocystis pneumonia in kidney transplant patients. *Clin. Transplant.* 34 (9), e13877. doi: 10.1111/ctr.13877

Guillen, Y., Noguera-Julian, M., Rivera, J., Casadella, M., Zevin, A. S., Rocafort, M., et al. (2019). Low nadir CD4+ T-cell counts predict gut dysbiosis in HIV-1 infection. *Mucosal Immunol.* 12 (1), 232–246. doi: 10.1038/s41385-018-0083-7

He, L., Ge, Y., Li, S., Huang, K., Liu, X., Chen, F., et al. (2021). Clinical role of bronchoalveolar lavage in dermatomyositis-associated interstitial lung disease. *Rheumatol. (Oxford)* 61 (1), 345–354. doi: 10.1093/rheumatology/keab586

Jiang, J., Bai, L., Yang, W., Peng, W., An, J., Wu, Y., et al. (2021). Metagenomic next-generation sequencing for the diagnosis of pneumocystis jirovecii pneumonia in non-HIV-Infected patients: A retrospective study. *Infect. Dis. Ther.* 10 (3), 1733–1745. doi: 10.1007/s40121-021-00482-y

Kawano-Dourado, L., and Lee, J. S. (2021). Management of connective tissue disease-associated interstitial lung disease. *Clin. Chest Med.* 42 (2), 295–310. doi: 10.1016/j.ccm.2021.03.010

Parize, P., Muth, E., Richaud, C., Gratigny, M., Pilmis, B., Lamamy, A., et al. (2017). Untargeted next-generation sequencing-based first-line diagnosis of infection in immunocompromised adults: a multicentre, blinded, prospective study. *Clin. Microbiol. Infect.* 23 (8), 574 e571–574 e576. doi: 10.1016/j.cmi.2017.02.006

Procop, G. W., Haddad, S., Quinn, J., Wilson, M. L., Henshaw, N. G., Reller, L. B., et al. (2004). Detection of pneumocystis jiroveci in respiratory specimens by four staining methods. *J. Clin. Microbiol.* 42 (7), 3333–3335. doi: 10.1128/JCM.42.7.3333-3335.2004

Ricci, A., Pagliuca, A., Vermi, M., Pizzirusso, D., Innammorato, M., Sglavo, R., et al. (2021). The role of lung colonization in connective tissue disease-associated interstitial lung disease. *Microorganisms* 9 (5), 932. doi: 10.3390/microorganisms9050932

Richter, A. G., Stockley, R. A., Harper, L., and Thickett, D. R. (2009). Pulmonary infection in wegener granulomatosis and idiopathic pulmonary fibrosis. *Thorax* 64 (8), 692–697. doi: 10.1136/thx.2008.110445

Skattum, L., van Deuren, M., van der Poll, T., and Truedsson, L. (2011). Complement deficiency states and associated infections. *Mol. Immunol.* 48 (14), 1643–1655. doi: 10.1016/j.molimm.2011.05.001

Su, R., Yan, H., Li, N., Ding, T., Li, B., Xie, Y., et al. (2022). Application value of blood metagenomic next-generation sequencing in patients with connective tissue diseases. *Front. Immunol.* 13. doi: 10.3389/fimmu.2022.939057

Tadros, S., Teichtahl, A. J., Ciciriello, S., and Wicks, I. P. (2017). Pneumocystis jirovecii pneumonia in systemic autoimmune rheumatic disease: A case-control study. *Semin. Arthritis Rheum* 46 (6), 804–809. doi: 10.1016/j.semarthrit.2016.09.009

Tomassetti, S., Colby, T. V., Wells, A. U., Poletti, V., Costabel, U., and Matucci-Cerinic, M. (2021). Bronchoalveolar lavage and lung biopsy in connective tissue diseases, to do or not to do? *Ther. Adv. Musculoskelet Dis.* 13, 1759720X211059605. doi: 10.1177/1759720X211059605

Vemula, S. V., Zhao, J., Liu, J., Wang, X., Biswas, S., and Hewlett, I. (2016). Current approaches for diagnosis of influenza virus infections in humans. *Viruses* 8 (4), 96. doi: 10.3390/v8040096

Wang, J., Han, Y., and Feng, J. (2019). Metagenomic next-generation sequencing for mixed pulmonary infection diagnosis. *BMC Pulm Med.* 19 (1), 252. doi: 10.1186/s12890-019-1022-4

Wolfe, R. M., and Peacock, J. E.Jr. (2017). Pneumocystis pneumonia and the rheumatologist: Which patients are At risk and how can PCP be prevented? *Curr. Rheumatol Rep.* 19 (6), 35. doi: 10.1007/s11926-017-0664-6

Yang, X., Hao, Y., Zhang, X., Geng, Y., Ji, L., Li, G., et al. (2020). Mortality of Chinese patients with polymyositis and dermatomyositis. *Clin. Rheumatol* 39 (5), 1569–1579. doi: 10.1007/s10067-019-04910-w

Zhang, Y., Chen, Y., Chen, Z., Zhou, Y., Sheng, Y., Xu, D., et al. (2014). Effects of bronchoalveolar lavage on refractory mycoplasma pneumoniae pneumonia. *Respir. Care* 59 (9), 1433–1439. doi: 10.4187/respcare.03032

Frontiers in
Cellular and Infection Microbiology

Investigates how microorganisms interact with their hosts

Explores bacteria, fungi, parasites, viruses, endosymbionts, prions and all microbial pathogens as well as the microbiota and its effect on health and disease in various hosts.

Discover the latest Research Topics

See more →

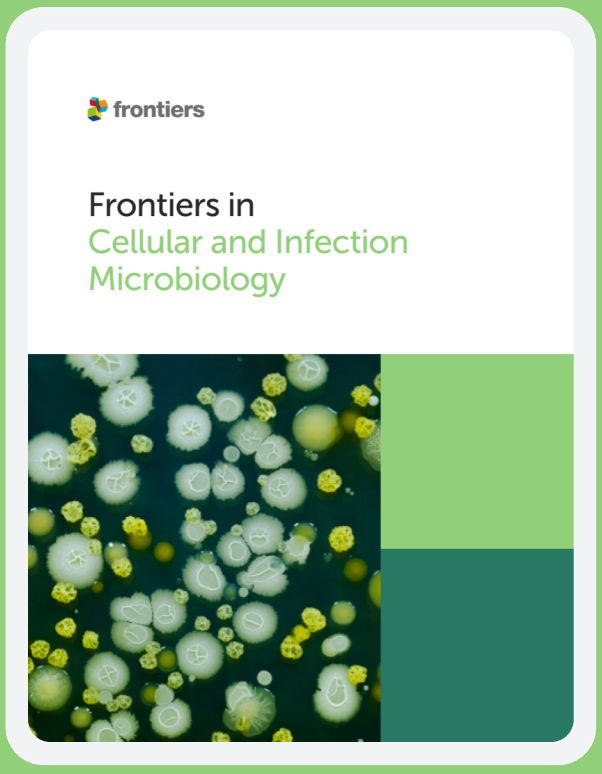

Frontiers

Avenue du Tribunal-Fédéral 34
1005 Lausanne, Switzerland
frontiersin.org

Contact us

+41 (0)21 510 17 00
frontiersin.org/about/contact